

# AERODYNAMICS

17BTAR401

**OBJECTIVES:**

To understand the behavior of airflow over bodies with particular emphasis on airfoil sections in the incompressible flow regime.

**UNIT - I      REVIEW OF FLUID MECHANICS**

Review of Vector Relations – Coordinate systems, Line, surface and Volume Integrals. System and Control volume approach, Continuity, Momentum and Energy equations Circulation and Vorticity, Green's Lemma and Stoke's Theorem, Barotropic Flow, Kelvin's theorem, Streamline, Stream Function, Irrotational flow, Potential Function

**UNIT - II      TWO DIMENSIONAL FLOWS**

Basic flows – Source, Sink, Free and Forced vortex, Uniform parallel flow. Their combinations, Pressure and Velocity distributions on bodies with and without circulation in ideal and real fluid flows. D'Alembert's Paradox, Magnus effect, Kutta Joukowski's theorem

**UNIT - III      CONFORMAL TRANSFORMATION**

Conformal transformation, Kutta-Joukowski transformation and its applications. Joukowski Profiles, Karman - Trefftz Profiles, Kutta condition.

**UNIT - IV      AIRFOIL AND WING THEORY**

Thin aerofoil theory and its applications. Vortex filament, Horse shoe vortex, Downwash and induced drag; Biot-Savart Law and Helmholtz's Theorems, Prandtl's classical lifting line theory, Limitations of Prandtl's lifting line theory.

**UNIT - V      THEORY OF PROPELLERS AND INTERFERENCE EFFECTS**

Axial momentum theory – influence of wake rotation – blade-element theory – combined blade element and momentum theories- tip correction – performance of propellers. wing – body interference- effect of propeller on wings and bodies and tail unit – flow over airplane as a whole.

**TEXT BOOKS:**

S.No.	AUTHOR(S)	TITLE OF THE BOOK	PUBLISHER	YEAR OF PUBLICATION
1.	Anderson J.D	Fundamentals of Aerodynamics	McGraw-Hill Book Co, New York.	2016
2.	EthirajanRathakrishnan	Theoretical Aerodynamics	John Wiley & Sons New York.	2013

**REFERENCE BOOKS:**

S.No.	AUTHOR(S)	TITLE OF THE BOOK	PUBLISHER	YEAR OF PUBLICATION
1.	Edward Lewis Houghton, Steven H. Collicott, P. W. Carpenter, Daniel T. Valentine	Aerodynamics for Engineering students	Edward Arnold Publishers Ltd., London.	2016
2.	John J. Bertin, Russell M. Cummings	Aerodynamics for Engineers	Pearson	2013
3.	Theodore A. Talay	NASA's Flight Aerodynamics Introduction (Annotated and Illustrated)	Seea Publishing, New York.	2013
4.	Milne Thomson L.M	Theoretical aerodynamics	Dover Publications New York	2012
5.	Clancey L.J	Aerodynamics	Sterling Book House Mumbai	2006

**WEB REFERENCE:**

- [www.beknowledge.com/.../review-of-basic-fluid-mechanics-concepts](http://www.beknowledge.com/.../review-of-basic-fluid-mechanics-concepts)
- [www.nasa.gov/audience/forstudents/.../what-is-aerodynamics-k4.html](http://www.nasa.gov/audience/forstudents/.../what-is-aerodynamics-k4.html)  
[www.ims.nus.edu.sg/Programs/wbfst/files/siva1.pdf](http://www.ims.nus.edu.sg/Programs/wbfst/files/siva1.pdf)
- [www.dynamicflight.com/aerodynamics/](http://www.dynamicflight.com/aerodynamics/)
- [www.scientistsandfriends.com/aerodynamics.html](http://www.scientistsandfriends.com/aerodynamics.html)

# KARPAGAM ACADEMY OF HIGHER EDUCATION

(Deemed to be University Established Under Section 3 of UGC Act 1956)

## Faculty of Engineering

### DEPARTMENT OF MECHANICAL ENGINEERING (AEROSPACE)

### LESSON PLAN

**Subject Name** : AERODYNAMICS  
**Subject Code** : 17BTAR401 (Credits - 3)  
**Name of the Faculty** : ARUN PRAKSASH J  
**Designation** : ASSISTANT PROFESSOR  
**Year/Semester/Section** : II/IV SEM  
**Branch** : B.Tech Aerospace Engineering

Sl. No.	No. of Periods	Topics to be Covered	Support Materials
1.	1	<b>Introduction and Fundamentals for the Course</b>	
<b>UNIT – I : REVIEW OF FLUID MECHANICS</b>			
2.	1	Review of Vector Relations, Coordinate systems, Line, surface and Volume Integrals	T [1] , R [1] ,R [2]
3.	1	System and Control volume approach	T [1] , R [1] ,R [2]
4.	1	Continuity and Momentum Equations	T [1] , R [1] ,R [2]
5.	1	Energy equation	T [1] , R [1] ,R [2]
6.	1	Circulation and Vorticity, Green's Lemma and Stoke's Theorem,	T [1] , R [1] ,R [2]
7.	1	Barotropic Flow,	T [1] , R [1] ,R [2]
8.	1	Kelvin's theorem,	T [1] , R [1] ,R [2]
9.	1	Streamline, Stream Function,	T [1] , R [1] ,R [2]
10.	1	Irrotational flow, Potential Function	T [1] , R [1] ,R [2]
11.	1	Tutorial – Continuity, Momentum and Energy Equations	T [1] , R [1] ,R [2]
<b>Total No. of Hours Planned for Unit - I</b>			<b>11</b>

Sl. No.	No. of Periods	Topics to be Covered	Support Materials
<b>UNIT – II TWO DIMENSIONAL FLOWS</b>			
12.	1	Basic flows – Source and Sink	T [1] , R [1] ,R [2]
13.	1	Free and Forced vortex and uniform parallel flow	T [1] , R [1] ,R [2]

14.	1	Combinations of Basic Flows	T [1] , R [1] ,R [2]
15.	1	Pressure and velocity distributions on bodies with circulation in ideal and real fluid flows	T [1] , R [1] ,R [2]
16.	1	Pressure and velocity distributions on bodies without circulation in ideal and real fluid flows	T [1] , R [1] ,R [2]
17.	1	D'Alembert's Paradox	T [1] , R [1] ,R [2]
18.	1	Magnus effect	T [1] , R [1] ,R [2]
19.	1	Kutta Joukowski's theorem	T [1] , R [1] ,R [2]
20.	1	Problems on Kutta Joukowski's theorem	T [1] , R [1] ,R [2]
21.	1	Tutorial – Basic flows and Problems	T [1] , R [1] ,R [2]
<b>Total No. of Hours Planned for Unit - II</b>			<b>10</b>

Sl. No.	No. of Periods	Topics to be Covered	Support Materials
<b>UNIT – III CONFORMAL TRANSFORMATION</b>			
22.	1	Conformal transformation	T [2] , R [1] ,R [2]
23.	1	Kutta-Joukowski transformation	T [2] , R [1] ,R [2]
24.	1	Joukowski Profiles	T [2] , R [1] ,R [2]
25.	1	Application of Joukowski transformation in fluid flow problems (Line and Circle)	T [2] , R [1] ,R [2]
26.	1	Joukowski transformation Problems(Ellipse and Circle)	T [2] , R [1] ,R [2]
27.	1	Application of Joukowski transformation in fluid flow problems.(Cylinder)	T [2] , R [1] ,R [2]
28.	1	Application of Joukowski transformation in fluid flow problems.(Airfoil)	T [2] , R [1] ,R [2]
29.	1	Karman - Trefftz Profiles	T [2] , R [1] ,R [2]
30.	1	Kutta condition	T [2] , R [1] ,R [2]
31.	1	Tutorial - Transformation Problems	T [2] , R [1] ,R [2]
<b>Total No. of Hours Planned for Unit - III</b>			<b>10</b>
Sl. No.	No. of Periods	Topics to be Covered	Support Materials
<b>UNIT – IV AIRFOIL AND WING THEORY</b>			
32.	1	Thin aerofoil theory	T [1] , R [1] ,R [2]
33.	1	Thin aerofoil theory - applications	T [1] , R [1] ,R [2]
34.	1	Vortex filament	T [1] , R [1] ,R [2]
35.	1	Horse shoe vortex	T [1] , R [1] ,R [2]
36.	1	Downwash and induced drag	T [1] , R [1] ,R [2]
37.	1	Biot-Savart Law	T [1] , R [1] ,R [2]
38.	1	Helmholtz's Theorems	T [1] , R [1] ,R [2]

39.	1	Prandtl's classical lifting line theory	T [1] , R [1] ,R [2]
40.	1	Limitations of Prandtl's lifting line theory	T [1] , R [1] ,R [2]
41.	1	Tutorial – Problems on Wing theory	
<b>Total No. of Hours Planned for Unit - IV</b>			<b>10</b>

Sl. No.	No. of Periods	Topics to be Covered	Support Materials
<b>UNIT – V : THEORY OF PROPELLERS AND INTERFERENCE EFFECTS</b>			
42.	1	Axial momentum theory	T [1] , R [1] ,R [2]
43.	1	Influence of wake rotation in Propellers	T [1] , R [1] ,R [2]
44.	1	Blade-element theory	T [1] , R [1] ,R [2]
45.	1	Combined blade element and momentum theories	T [1] , R [1] ,R [2]
46.	1	Tip correction in propellers	T [1] , R [1] ,R [2]
47.	1	Performance of propellers and wing	T [1] , R [1] ,R [2]
48.	1	Body interference effects of propeller on wings	T [1] , R [1] ,R [2]
49.	1	Body interference effects of propeller on bodies and tail unit	T [1] , R [1] ,R [2]
50.	1	Body interference effects on Flow over airplane as a whole body	T [1] , R [1] ,R [2]
51.	1	Tutorial – Problems on propellers	T [1] , R [1] ,R [2]
52.	1	<b>Discussion on University previous year questions</b>	
<b>Total No. of Hours Planned for Unit - V</b>			<b>10+1</b>

**TOTAL PERIODS : 52**

#### TEXT BOOKS

- T [1] – Fundamentals of Aerodynamics by Anderson J.D , McGraw-Hill Book Co,2016.  
T [2] – Theoretical Aerodynamics by Ethirajan Rathakrishnan, John Wiley & Sons,2013.

#### REFERENCES

- R [1] - Aerodynamics for Engineering students by Edward Lewis Houghton, Edward Arnold Publishers,2016.  
R [2] - Aerodynamics by Clancey L.J ,Sterling Book House,2006.

#### WEBSITES

- W [1] - nptel.in/  
W [2] - www.nasa.gov  
W [3] - www.dynamicflight.com/aerodynamics

#### JOURNALS

- J [1] - International Journal of Aerodynamics - Inderscience  
J [2] – Fluid Dynamics Research - IOP Publishing  
J [3] – Journal of Experiments in Fluid Mechanics - China Aerodynamics Research Society

UNIT	Total No. of Periods Planned	Lecture Periods	Tutorial Periods
I	11	9+1	1
II	10	9	1
III	10	9	1
IV	10	9	1
V	10+1	9+1	1
TOTAL	52	45+2	5

I.	CONTINUOUS INTERNAL ASSESSMENT	: 40 Marks
	(Internal Assessment Tests: 25, Attendance: 5, Assignment 5, Seminar 5)	
II.	END SEMESTER EXAMINATION	: 60 Marks
	TOTAL	: 100 Marks

FACULTY

HOD / MECH

DEAN / FOE

## UNIT I

# REVIEW OF BASIC FLUID MECHANICS



Review of Vector Relations – Coordinate systems, Scalar and vector fields, Scalar and vector Products, Gradient of a Scalar Field and Divergence of a Vector field

Curl, Line, surface and Volume Integrals. System and Control volume approach, Fundamentals for Aerodynamics Coordinate System Continuity, momentum and energy equations..





## Concept of Control Volume:

Models of the fluid: control volumes and fluid elements

Aerodynamics is a fundamental science, steeped in physical observation. As you proceed through this book, make every effort to gradually develop a “physical feel” for the material. An important virtue of all successful aerodynamicists (indeed, of all successful engineers and scientists) is that they have good “physical intuition,” based on thought and experience, which allows them to make reasonable judgments on difficult problems. Although this chapter is full of equations and (seemingly) esoteric concepts, now is the time for you to start developing this physical feel.

With this section, we begin to build the basic equations of aerodynamics. There is a certain philosophical procedure involved with the development of these equations, as follows:

Invoke three fundamental physical principles that are deeply entrenched in our macroscopic observations of nature, namely,

Mass is conserved (i.e., mass can be neither created nor destroyed).

Newton’s second law:  $\text{force} = \text{mass} \times \text{acceleration}$ .

Energy is conserved; it can only change from one form to another.

Determine a suitable model of the fluid. Remember that a fluid is a squishy substance, and therefore it is usually more difficult to describe than a well-defined solid body. Hence, we have to adopt a reasonable model of the fluid to which we can apply the fundamental principles stated in item 1.

Apply the fundamental physical principles listed in item 1 to the model of the fluid determined in item 2 in order to obtain mathematical equations which properly describe the physics of the flow. In turn, use these fundamental equations to analyze any particular aerodynamic flow problem of interest.

In this section, we concentrate on item 2; namely, we ask the question: What is a suitable model of the fluid? How do we visualize this squishy

substance in order to apply the three fundamental physical principles to it? There is no single throughout the modern evolution of aerodynamics. They are (1) finite control volume, (2) infinitesimal fluid element, and (3) molecular. Let us examine what these models involve and how they are applied.

## Finite Control volume Approach

Consider a general flow field as represented by the streamlines in Figure. Let us imagine a closed volume drawn within a finite region of the flow.

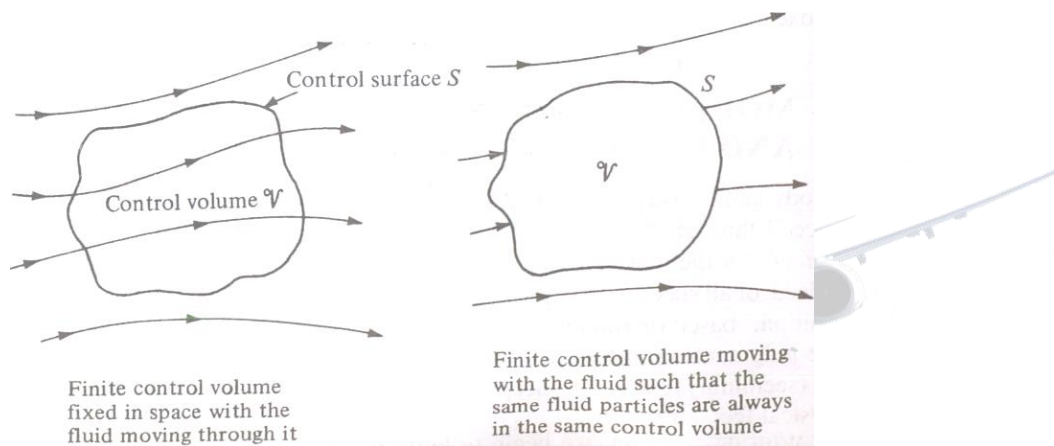


Figure: Finite control volume approach

This volume defines a control volume  $V$ , and a control surface  $S$  is defined as the closed surface which bounds the control volume. The control volume may be fixed in space with the fluid moving through it, as shown at the left of Figure. Alternatively, the control volume may be moving with the fluid such that the same fluid particles are always inside it, as shown at the right of Figure. In either case, the control volume is a reasonably large, finite region of the flow. The fundamental physical principles are applied to the fluid inside the control volume, and to the fluid crossing the control surface (if the control volume is fixed in space). Therefore, instead of looking at the whole flow field at once, with the control volume model we limit our attention to just the fluid in the finite region of the volume itself.

## Infinitesimal Fluid Element Approach

Consider a general flow field as represented by the streamlines in figure. Let us imagine an infinitesimally small fluid element in the flow, with a differential volume  $dV$ . The fluid element is infinitesimal in the same sense as differential calculus; however, it is large enough to contain a huge number of molecules so that it can be viewed as a continuous medium. The fluid element may be fixed in space with the fluid moving through it, as shown at the left of Figure. Alternatively, it may be moving along a streamline with velocity  $V$  equal to the flow velocity at each point. Again, instead of looking at the whole flow field at once, the fundamental physical principles are applied to just the fluid element itself.

### Molecular Approach

In actuality, of course, the motion of a fluid is a ramification of the mean motion of its atoms and molecules. Therefore, a third model of the flow can be a microscopic approach wherein the fundamental laws of nature are applied directly to the atoms and molecules, using suitable statistical averaging to define the resulting fluid properties. This approach is in the purview of kinetic theory, which is a very elegant method with many advantages in the long run. However, it is beyond the scope of the present book.

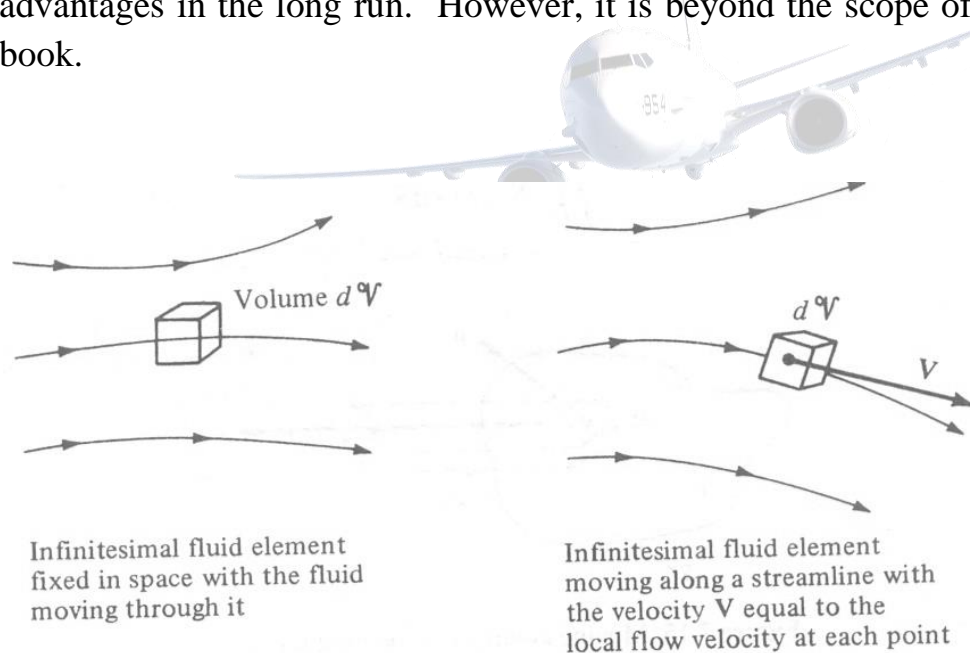


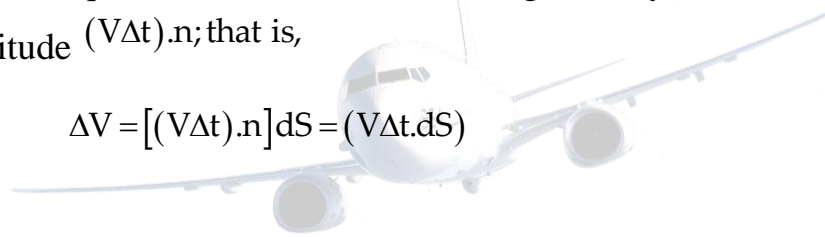
Figure: Infinitesimal fluid element approach

In summary, although many variations on the theme can be found in different texts for the derivation of the general equations of fluid flow, the flow model can usually be categorized under one of the approaches described above.

## Physical Meaning of the Divergence of Velocity

In the equations of flow, the divergence of velocity,  $\nabla \cdot \mathbf{V}$ , occurs frequently. Before  $\nabla \cdot \mathbf{V}$  is physically the time rate of change of the volume of a moving fluid element of fixed mass per unit volume of that element. Consider a control volume moving with the fluid (the case shown of the right of Figure). This control volume is always made up of the same fluid particles as it moves with the flow; hence, its mass is fixed, invariant with time. However, its volume  $V$  and control surface  $S$  are changing with time as it moves to different regions of the flow where different values of  $p$  exist. That is, this moving control volume of fixed mass is constantly increasing or decreasing its volume and is changing its shape, depending on the characteristics of the flow. This control volume is shown in figure at some instant in time. Consider an infinitesimal element of the surface  $dS$  moving at the local velocity  $\mathbf{V}$ , as shown in figure. The change in the volume of the control volume  $\Delta V$ , due to just the movement of  $dS$  over a time increment  $\Delta t$ , is from figure, equal to the volume of the long, thin cylinder with base area  $dS$  and altitude  $(\mathbf{V} \Delta t) \cdot \mathbf{n}$ ; that is,

$$\Delta V = [(\mathbf{V} \Delta t) \cdot \mathbf{n}] dS = (\mathbf{V} \Delta t \cdot d\mathbf{S})$$



Over the time increment  $\Delta t$ , the total change in volume of the whole control volume is equal to the summation of Equation over the total control surface. In the limit as  $dS \rightarrow 0$ , the sum becomes the surface integral

$$\oint_S (\mathbf{V} \Delta t) \cdot d\mathbf{S}$$

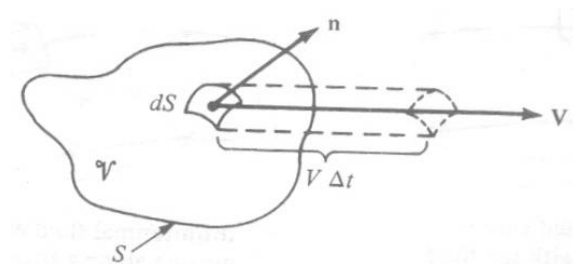


Figure: Moving control volume used for the physical interpretation of the divergence of velocity.

If this integral is divided by  $\Delta t$ , the result is physically the time rate of the change of the control volume, denoted by  $DV/Dt$ ; that is,

$$\frac{DV}{Dt} = \frac{1}{\Delta t} \iiint_S (V \Delta t) \cdot dS = \iiint_S V \cdot dS$$

(The significance of the notation  $D/Dt$  is revealed in Section.) Applying the divergence theorem, Equation, to the right side of Equation, we have

$$\frac{DV}{Dt} = \iiint_{\delta V} (\nabla \cdot V) dV$$

Assume that  $\delta V$  is small enough such that  $\nabla \cdot V$  is essentially the same value throughout  $\delta V$ . Then the integral in Equation can be approximated as  $(\nabla \cdot V) \delta V$ . From Equation, we have

$$\frac{D(\delta V)}{Dt} = (\nabla \cdot V) \delta V$$

or

$$\boxed{\nabla \cdot V = \frac{1}{\delta V} \frac{D(\delta V)}{Dt}}$$

Examine Equation. It states that  $\nabla \cdot V$  is physically the time rate of change of the volume of a moving fluid element, per unit volume. Hence, the interpretation of  $\nabla \cdot V$ , first given in section, Divergence of a Vector Field, is now proved.

### Specification of the Flow Field

In Section we defined both scalar and vector fields. We now apply this concept of a field more directly to an aerodynamic flow. One of the most straightforward ways of describing the details of an aerodynamic flow is simply to visualize the flow in three-dimensional space, and to write the variation of the aerodynamic properties as a function of space and time. For example, in cartesian coordinates the equations.

$$\begin{aligned}
 p &= p(x, y, z, t) && \rightarrow (a) \\
 \rho &= \rho(x, y, z, t) && \rightarrow (b) \\
 T &= T(x, y, z, t) && \rightarrow (c) \\
 \text{and} \quad V &= ui + vj + wk && \rightarrow (d)
 \end{aligned}$$

Where  $u = u(x, y, z, t)$  (b)

$v = v(x, y, z, t)$  (c)

$w = w(x, y, z, t)$

Represent the flow field. Equations (a-c) give the variation of the scalar flow field variables pressure, density, and temperature, respectively. (In equilibrium thermodynamics, the specification of two state variables, such as  $p$  and  $\rho$ , uniquely defines the values of all other state variables, such as  $T$ . In this case, one of Equations can be considered redundant.) Equations (a-d) give the variation of the vector flow field variable velocity  $V$ , where the scalar components of  $V$  in the  $x$ ,  $y$ , and  $z$  directions are  $u$ ,  $v$ , and  $w$ , respectively.

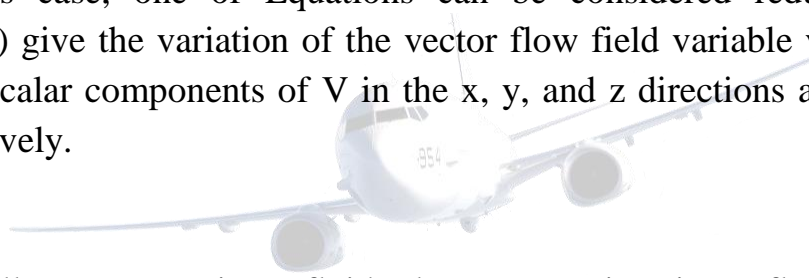


Figure illustrates a given fluid element moving in a flow field specified by Equations and. At the time  $t_1$ , the fluid element is at point 1, located at  $(x_1, y_1, z_1)$  as shown in figure.

At this instant, its velocity is  $V_1$  and its pressure is given by

$$p = p(x_1, y_1, z_1, t_1)$$

and similarly for its other flow variables.

By definition, an unsteady flow is one where the flow field variables at any given point are changing with time. for example, if you lock your eyes on point 1 in figure, and keep them fixed on point 1, if the flow is unsteady you will observe  $p$ ,  $\rho$ , etc. fluctuating with time. Equations and describe an unsteady flow field because time  $t$  is included as one of the independent variables. In contrast, a steady flow is one where the flow field variables at any given point are invariant with time, that is, if you lock your

eyes on point 1 you will continuously observe the same constant values for  $p$ ,  $\rho$ ,  $V$  etc. for all time. A steady flow field is specified by the relations.

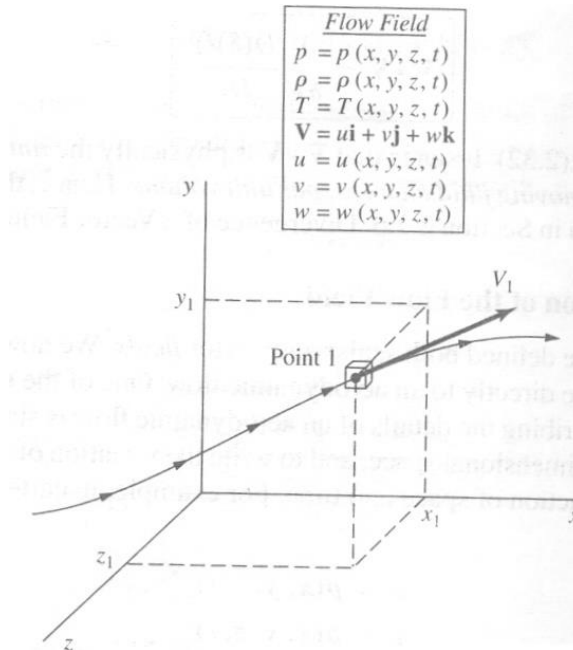


Figure: A fluid element passing through point 1 in a flow field.



$$p = p(x, y, z)$$

$$\rho = \rho(x, y, z)$$

etc.

The concept of the flow field, and a specified fluid element moving through it as illustrated in figure, will be revisited in Section where we define and discuss the concept of the substantial derivative.

The subsonic compressible flow over a cosine-shaped (Wavy) wall is illustrated in Figure. The wavelength and amplitude of the wall are  $I$  and  $h$ , respectively, as shown in figure. The streamlines exhibit the same qualitative shape as the wall, but with diminishing amplitude as distance above the wall increases. Finally, as  $y \rightarrow \infty$ , the

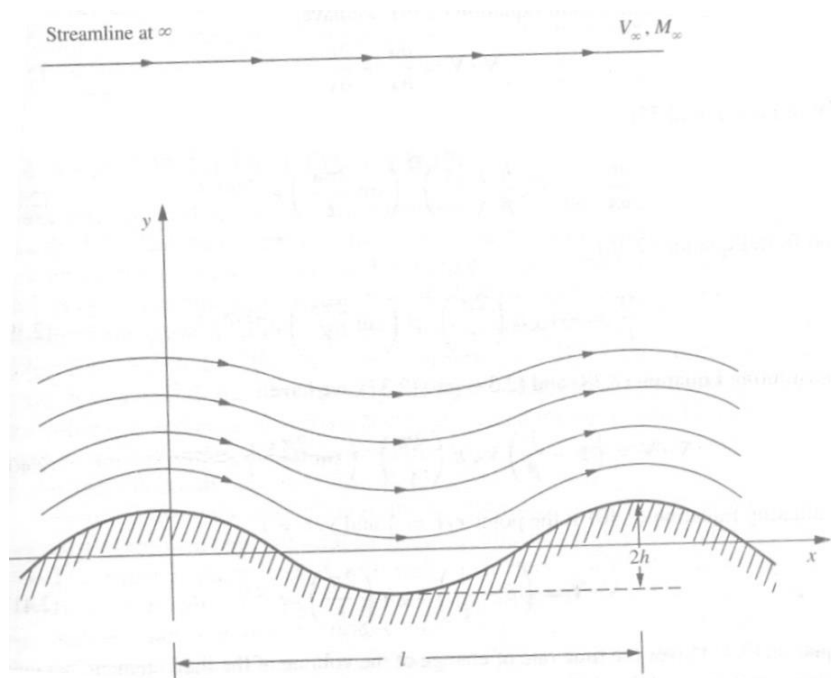


Figure: Subsonic compressible flow over a wavy wall; the streamline pattern becomes straight. Along this straight streamline, the freestream velocity and Mach number are  $V_\infty$  and  $M_\infty$ , respectively. The velocity field in Cartesian coordinates is given by

$$u = V_\infty \left[ 1 + \frac{h2\pi}{\beta l} \right] \left( \cos \frac{2\pi x}{l} \right) e^{-2\pi\beta y/l}$$

and

$$v = -V_\infty h \frac{2\pi}{l} \left( \sin \frac{2\pi x}{l} \right) e^{-2\pi\beta y/l}$$

where  $\beta = \sqrt{1 - M_\infty^2}$

consider the particular flow that exists for the case where  $l = 1.0\text{m}$ ,  $h = 0.01\text{ m}$ ,  $V_\infty = 240\text{ m/s}$ , and  $M_\infty = 0.7$ . Also, consider a fluid element of fixed mass moving along a streamline in the flow field. The fluid element passes through the point  $(x/l, y/l) = \left(\frac{1}{4}, 1\right)$ . At this point, calculate the time rate of change of the volume of the fluid element, per unit volume.

**Solution:**

From section we know that the time rate of change of the volume of a moving fluid element of fixed mass, per unit volume, is given by the



divergence of the velocity  $\nabla \cdot \mathbf{V}$ . In Cartesian coordinates, from Equation, we have

$$\nabla \cdot \mathbf{V} = \frac{\partial u}{\partial x} + \frac{\partial v}{\partial y}$$

From Equation,

$$\frac{\partial u}{\partial x} = -V_{\infty} \frac{h}{\beta} \left( \frac{2\pi}{l} \right)^2 \left( \sin \frac{2\pi x}{l} \right) e^{-2\pi\beta y/l}$$

and from Equation,

$$\frac{\partial v}{\partial y} = -V_{\infty} h \left( \frac{2\pi}{l} \right)^2 \beta \left( \sin \frac{2\pi x}{l} \right) e^{-2\pi\beta y/l}$$

Substituting Equation and into we have

$$\nabla \cdot \mathbf{V} = \left( \beta - \frac{1}{\beta} \right) V_{\infty} h \left( \frac{2\pi}{l} \right)^2 \left( \sin \frac{2\pi x}{l} \right) e^{-2\pi\beta y/l}$$

Evaluating Equation at the point  $x/l = \frac{1}{4}$  and  $y/l = 1$ ,

$$\nabla \cdot \mathbf{V} = \left( \beta - \frac{1}{\beta} \right) V_{\infty} h \left( \frac{2\pi}{l} \right)^2 e^{-2\pi\beta}$$

Equation gives the time rate of change of the volume of the fluid element, per unit volume, as it passes through the point  $(x/l, y/l) = \left( \frac{1}{4}, 1 \right)$ .

Note that it is a finite (nonzero) value; the volume of the fluid element is changing as it moves along the streamline. This is consistent with the definition of a compressible flow, where the density is a variable and hence

the volume of a fixed mass must also be variable. Note from Equation that  $\nabla \cdot V = 0$  only along vertical lines denoted by  $x/l = 0, \frac{1}{2}, 1, 1\frac{1}{2}, \dots$ , where the  $\sin(2\pi x/l)$  goes to zero,.. This is a peculiarity associated with the cyclical nature of the flow field over the cosine-shaped wall. For the particular flow considered here, where  $l=1.0\text{m}$ ,  $h=0.01\text{ m}$ ,  $V_\infty = 240\text{ m/s}$ , and  $M_\infty = 0.7$ , where

$$\beta = \sqrt{1 - M_\infty^2} = \sqrt{1 - (0.7)^2} = 0.714$$

Equation yields

$$\nabla \cdot V = \left(0.714 - \frac{1}{0.714}\right)(240)(0.01)\left(\frac{2\pi}{1}\right)e^{-2\pi(0.714)} = \boxed{-0.7327\text{s}^{-1}}$$

The physical significance of this result is that, as the fluid element is passing through the point  $\left(\frac{1}{4}, 1\right)$  in the flow, it is experiencing a 73 percent rate of decrease of volume per second (the negative quantity denotes a decrease in volume). That is, the density of the fluid element is increasing.

Hence, the point  $\left(\frac{1}{4}, 1\right)$  is in a compression region of the flow, where the fluid element will experience an increase in density. Expansion regions are defined by values of  $x/l$  which yield negative values of the sine function in Equation, which in turn yields a positive value for  $\nabla \cdot V$ . This gives an increase in volume of the fluid element, hence a decrease in density. Clearly, as the fluid element continues its path through this flow field, it experiences cyclical increases and decreases in density, as well as the other flow field properties.

## Continuity Equation

A continuity equation in physics is an equation that describes the transport of a conserved quantity. Since mass, energy, momentum, electric charge and other natural quantities are conserved under their respective appropriate conditions; a variety of physical phenomena may be described using continuity equations.

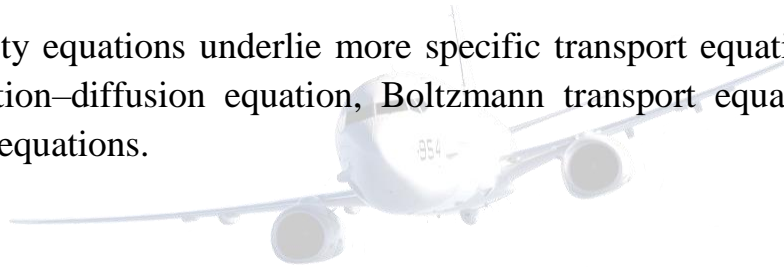
Continuity equations are a stronger, local form of conservation laws. For example, it is true that "the total energy in the universe is conserved". But this statement does not immediately rule out the possibility that energy could disappear from Earth while simultaneously appearing in another

galaxy. A stronger statement is that energy is locally conserved: Energy can neither be created nor destroyed, nor can it "teleport" from one place to another—it can only move by a continuous flow. A continuity equation is the mathematical way to express this kind of statement.

Continuity equations more generally can include "source" and "sink" terms, which allow them to describe quantities that are often but not always conserved, such as the density of a molecular species which can be created or destroyed by chemical reactions. In an everyday example, there is a continuity equation for the number of living humans; it has a "source term" to account for people giving birth, and a "sink term" to account for people dying.

Any continuity equation can be expressed in an "integral form" (in terms of a flux integral), which applies to any finite region, or in a "differential form" (in terms of the divergence operator) which applies at a point.

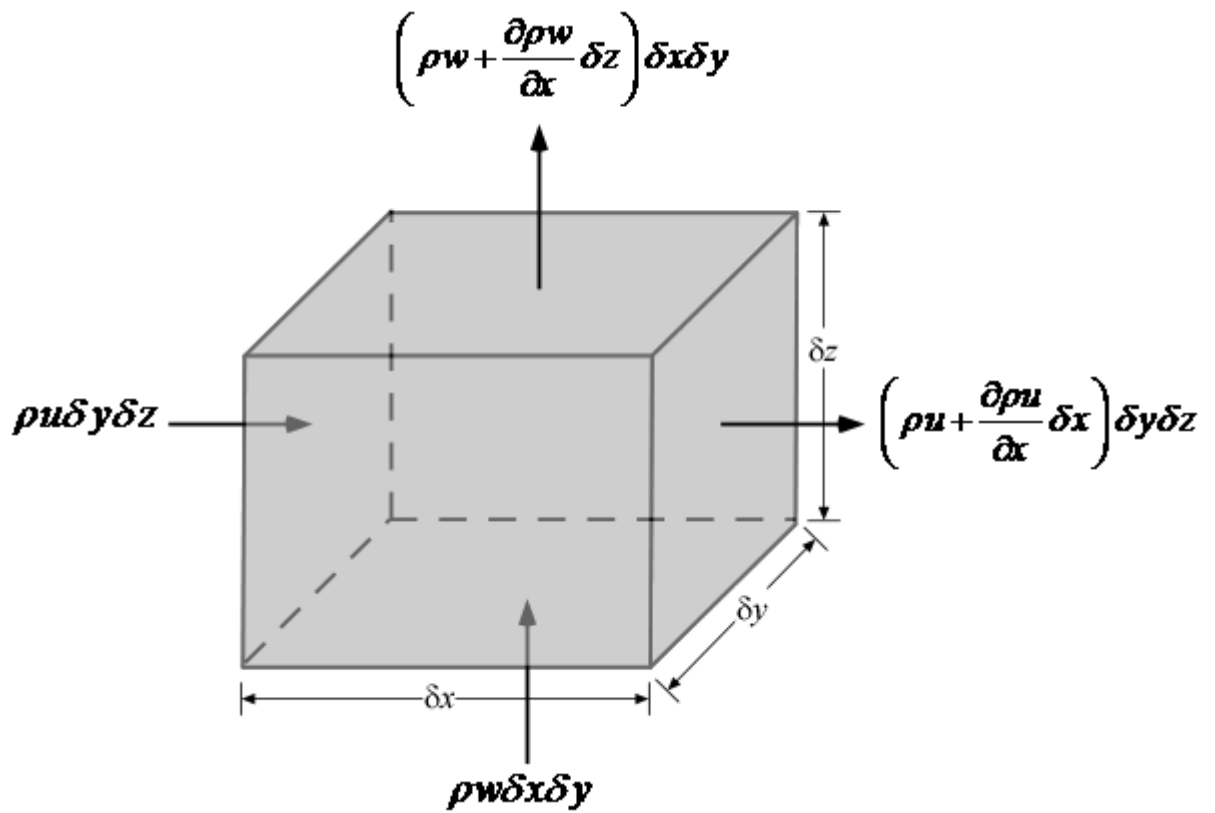
Continuity equations underlie more specific transport equations such as the convection–diffusion equation, Boltzmann transport equation, and Navier-Stokes equations.



## Continuity Equation in Cartesian Coordinates

The continuity equation is an expression of a fundamental conservation principle, namely, that of mass conservation. It is a statement that fluid mass is conserved: all fluid particles that flow into any fluid region must flow out. To obtain this equation, we consider a cubical control volume inside a fluid. Mass conservation requires that the net flow through the control volume is zero. In other words, all fluid that is accumulated inside the control volume (due to compressibility for example) + all fluid that is flowing into the control volume must be equal to the amount of fluid flowing out of the control volume.

$$\text{Accumulation} + \text{Flow In} = \text{Flow Out}$$



The mass of the control volume at some time  $t$  is

$$\mathcal{M}_t = \rho \delta x \delta y \delta z$$

The time rate of change of mass in the control volume is

$$\frac{\partial \rho}{\partial t} \delta x \delta y \delta z$$



Now we can compute the net flow through the control volume faces. Starting with the  $x$  direction, the net flow is

$$\left( \rho u + \frac{\partial \rho u}{\partial x} \delta x \right) \delta y \delta z - \rho u \delta y \delta z = \frac{\partial \rho u}{\partial x} \delta x \delta y \delta z$$

Similarly, the net flow through the  $y$  faces is

$$\frac{\partial \rho v}{\partial y} \delta x \delta y \delta z$$

while that through the  $z$  faces is

$$\frac{\partial \rho w}{\partial z} \delta x \delta y \delta z$$

Upon adding up the resulting net flow and dividing by the volume of the fluid element (i.e.  $\delta x \delta y \delta z$ ), we get the continuity equation in Cartesian coordinates

$$\frac{\partial \rho}{\partial t} + \frac{\partial \rho u}{\partial x} + \frac{\partial \rho v}{\partial y} + \frac{\partial \rho w}{\partial z} = 0$$

# Continuity Equation in Cylindrical Coordinate System

## Cylindrical Coordinate System

A **cylindrical coordinate system** is a three-dimensional coordinate system that specifies point positions by the distance from a chosen reference axis, the direction from the axis relative to a chosen reference direction, and the distance from a chosen reference plane perpendicular to the axis.

To Cartesian:

$$x = \rho \cos \varphi$$

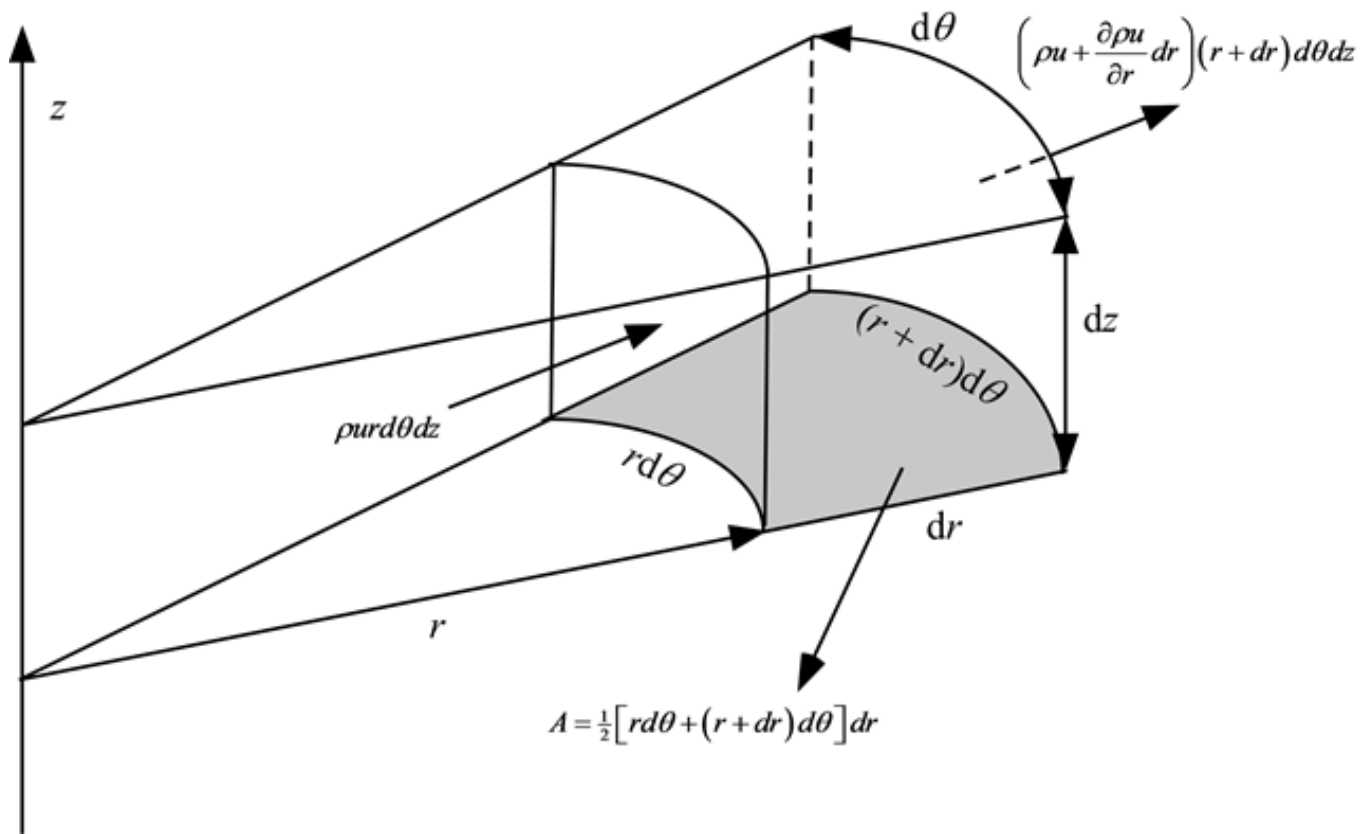
$$y = \rho \sin \varphi$$

$$\rho = \sqrt{x^2 + y^2}$$

$$\varphi = \begin{cases} 0 & \text{if } x = 0 \text{ and } y = 0 \\ \arcsin\left(\frac{y}{\rho}\right) & \text{if } x \geq 0 \\ -\arcsin\left(\frac{y}{\rho}\right) + \pi & \text{if } x < 0 \end{cases}$$

## Derivation

First have to start by selecting a convenient control volume. The idea here is to pick a volume whose sides are parallel per say to the coordinates. For cylindrical coordinates, one may choose the following control volume.



Rate of Rate of Flow In = Accumulation + Rate of Flow Out

Accumulation + Flow Out - Flow In = 0

By construction, the volume of the differential control volume is

$$dV = r dr d\theta dz$$

The mass of fluid in the control volume is

$$dM = \rho dV$$

For the net flow through the control volume, we deal with it one face at a time. Starting with the  $r$  faces, the net inflow is

$$\dot{m}_{r,in} = \rho u r d\theta dz$$

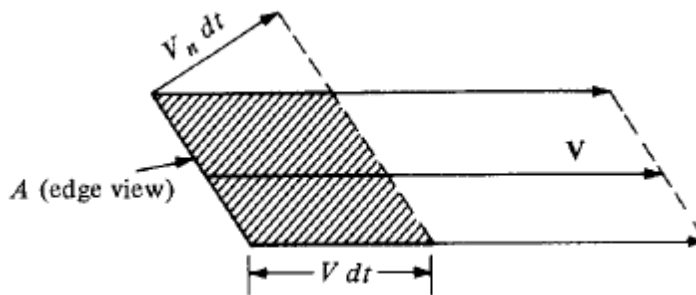
While the outflow in the  $r$  direction is

$$\dot{m}_{r,out} = \left( \rho u + \frac{\partial \rho u}{\partial r} dr \right) (r + dr) d\theta dz$$

$$\dot{m}_{r,out} - \dot{m}_{r,in} = \frac{1}{r} \rho u dV + \frac{\partial \rho u}{\partial r} dV + O(dr^2)$$

Follow the same for theta direction and z direction.

## Continuity Equation in Integral Form/Control Volume Approach



Let  $A$  be small enough such that the flow velocity  $V$  is uniform across  $A$ . Consider the fluid elements with velocity  $V$  that pass through  $A$ . In time  $dt$  after crossing  $A$ , they have moved a distance  $V dt$  and have swept out the shaded volume shown in Figure. This volume is equal to the base area  $A$  times the height of the cylinder  $V_n dt$ , where  $V_n$  is the component of velocity normal to  $A$ ; i.e.,

$$\text{Volume} = (V_n dt) A$$

The mass inside the shaded volume is therefore

$$\text{Mass} = \rho (V_n dt) A$$

This is the mass that has swept past  $A$  in time  $dt$ . By definition, the mass flow through  $A$  is the mass crossing  $A$  per second (e.g., kilograms per second, slugs per second).

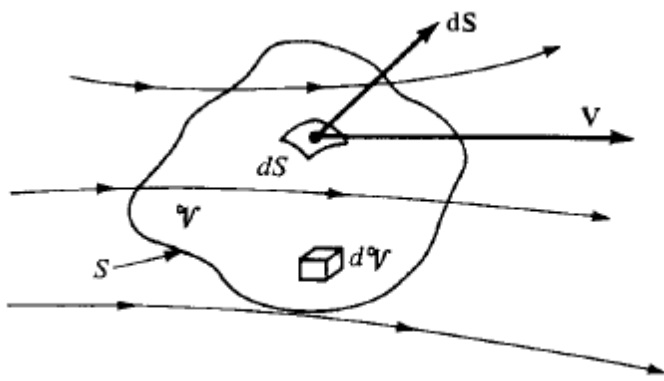
Let  $\dot{m}$  denote mass flow. From Equation

$$\dot{m} = \frac{\rho (V_n dt) A}{dt}$$

$$\boxed{\dot{m} = \rho V_n A}$$

Apply physical principle to a finite control volume fixed in space.

**Physical principle** Mass can be neither created nor destroyed



### Finite control volume fixed in space

Consider a flow field wherein all properties vary with spatial location and time, e.g.,  $p = p(x, y, z, t)$ . In this flow field, consider the fixed finite control volume shown. At a point on the control surface, the flow velocity is  $V$  and the vector elemental surface area is  $dS$ . Also  $dV$  is an elemental volume inside the control volume. Applied to this control volume, the above physical principle means

Net mass flow out of control volume through surface  $S$  = time rate of decrease of mass inside control volume  $V$

i.e.

$$B = C$$

Where  $B$  and  $C$  are just convenient symbols for the left and right sides, respectively, of Equation.

let us obtain an expression for  $B$  in terms of the quantities shown in Figure. the elemental mass flow across the area  $dS$  is

$$\rho V_n dS = \rho \mathbf{V} \cdot d\mathbf{S}$$

The net mass flow out of the entire control surface  $S$  is the summation over  $S$  of the elemental mass flows. In the limit, this becomes a surface integral, which is physically the left side of Equation,

$$B = \oint_S \rho \mathbf{V} \cdot d\mathbf{S}$$

Now consider the right side of Equations, the mass contained within the elemental volume  $dV$  is

$$\rho dV$$

Hence, the total mass inside the control volume is



$$\iiint_V \rho dV$$

The time rate of increase of mass inside V is then

$$\frac{\partial}{\partial t} \iiint_V \rho dV$$

the time rate of decrease of mass inside V is the negative of the above

$$-\frac{\partial}{\partial t} \iiint_V \rho dV = C$$

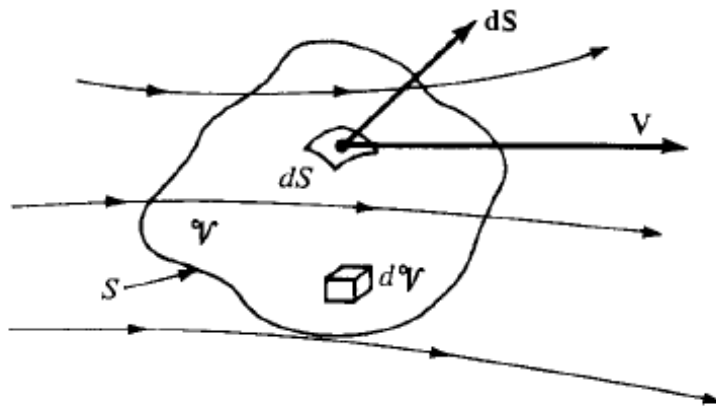
Substituting all the equations we get

$$\oiint_S \rho \mathbf{V} \cdot d\mathbf{S} = -\frac{\partial}{\partial t} \iiint_V \rho dV$$

$$\frac{\partial}{\partial t} \iiint_V \rho dV + \oiint_S \rho \mathbf{V} \cdot d\mathbf{S} = 0$$

This equation is the final result of applying the physical principle of the conservation of mass to a finite control volume fixed in space. It is called the continuity equation. It is one of the most fundamental equations of fluid dynamics.

## Momentum Equation in Integral Form/Control Volume Approach



Finite control volume fixed in space.

Newton's second law is frequently written as

$$\mathbf{F} = m\mathbf{a}$$

Where  $\mathbf{F}$  is the force exerted on a body of mass  $m$  and  $\mathbf{a}$  is the acceleration.

General form of this Equation is

$$\mathbf{F} = \frac{d}{dt}(m\mathbf{V})$$

**Physical principle** Force = time rate of change of momentum

Our objective is to obtain expressions for the left and right sides of Equation in terms of the familiar flow-field variables  $P, \rho, V$ , etc

First, let us concentrate on the left side of Equation i.e., obtain an expression for  $\mathbf{F}$ , which is the force exerted on the fluid as it flows through the control volume. This force comes from two sources:

1. **Body forces:** gravity, electromagnetic forces, or any other forces which "act at a distance" on the fluid inside  $V$ .
2. **Surface forces:** pressure and shear stress acting on the control surface  $S$ .

Let  $\mathbf{f}$  represent the net body force per unit mass exerted on the fluid inside  $V$ . The body force on the elemental volume  $dV$  is

$$\rho \mathbf{f} dV$$

and the total body force exerted on the fluid in the control volume is the summation of the above over the volume  $V$

$$\text{Body force} = \iiint_V \rho \mathbf{f} dV$$

The elemental surface force due to pressure acting on the element of area  $dS$  is

$$-p \, dS$$

Where the negative sign indicates that the force is in the direction opposite of  $dS$ . That is, the control surface is experiencing a pressure force which is directed into the control volume and which is due to the pressure from the surroundings.

The complete pressure force is the summation of the elemental forces over the entire control surface

$$\text{Pressure force} = -\oint_S p \, dS$$

In a viscous flow, the shear and normal viscous stresses also exert a surface force. A detailed evaluation of these viscous stresses is not warranted at this stage of our discussion. Let us simply recognize this effect by letting  $F_{\text{viscous}}$  denote the total viscous force exerted on the control surface.

Now the total force experienced by the fluid is

$$\mathbf{F} = \iiint_V \rho \mathbf{f} \, dV - \oint_S p \, dS + \mathbf{F}_{\text{viscous}}$$

Now consider the right side of Equation. The time rate of change of momentum of the fluid as it sweeps through the fixed control volume is the sum of two terms:

$$\begin{aligned} &\text{Net flow of momentum out} \\ &\text{of control volume across surface } S \equiv \mathbf{G} \end{aligned}$$

and

$$\begin{aligned} &\text{Time rate of change of momentum due to} \\ &\text{unsteady fluctuations of flow properties inside } V \equiv \mathbf{H} \end{aligned}$$

Consider the term denoted by  $G$  in Equation. The flow has a certain momentum as it enters the control volume and, in general, it has a different momentum as it leaves the control volume (due in part to the force  $F$  that is exerted on the fluid as it is sweeping through  $V$ ). The *net* flow of momentum *out* of the control volume across the surface  $S$  is simply this out flow minus the inflow of momentum across the control surface. This change in momentum is denoted by  $G$ , as noted above. To obtain an expression for  $G$ , recall that the mass flow across the elemental area  $dS$  is  $(\rho \mathbf{V} \cdot dS)$ ; hence, the flow of momentum per second across  $dS$  is

$$(\rho \mathbf{V} \cdot d\mathbf{S}) \mathbf{V}$$

The net flow of momentum out of the control volume through S is the summation of the above elemental contributions, i.e.

$$\mathbf{G} = \oint_S (\rho \mathbf{V} \cdot d\mathbf{S}) \mathbf{V}$$

Positive values of  $(p, V, dS)$  represent mass flow out of the control volume, and negative values represent mass flow into the control volume.

The integral over the whole control surface is a combination of positive contributions (outflow of momentum) and negative contributions (inflow of momentum), with the resulting value of the integral representing the net outflow of momentum. If G has a positive value, there is more momentum flowing out of the control volume per second than flowing in; conversely, if G has a negative value, there is more momentum flowing into the control volume per second than flowing out.

Now consider H from Equation, the momentum of the fluid in the elemental volume  $dV$

$$(\rho dV) \mathbf{V}$$

The momentum contained at any instant inside the control volume is therefore

$$\iiint_V \rho \mathbf{V} dV$$



and its time rate of change due to unsteady flow fluctuations is

$$\mathbf{H} = \frac{\partial}{\partial t} \iiint_V \rho \mathbf{V} dV$$

Combining Equations

$$\frac{d}{dt} (m\mathbf{V}) = \mathbf{G} + \mathbf{H} = \oint_S (\rho \mathbf{V} \cdot d\mathbf{S}) \mathbf{V} + \frac{\partial}{\partial t} \iiint_V \rho \mathbf{V} dV$$

Hence, from Newton's second law,

$$\frac{d}{dt} (m\mathbf{V}) = \mathbf{F}$$

Applied to a fluid flow is

$$\frac{\partial}{\partial t} \iiint_V \rho \mathbf{V} dV + \oint_S (\rho \mathbf{V} \cdot d\mathbf{S}) \mathbf{V} = - \oint_S p d\mathbf{S} + \iiint_V \rho \mathbf{f} dV + \mathbf{F}_{\text{viscous}}$$

This equation is the Momentum equation in integral form

## Application of momentum Equation.

### An Application of the momentum Equation: Drag of a Two-Dimensional body

We briefly interrupt our orderly development of the fundamental equations of fluid dynamics in order to examine an important application of the integral form of the momentum equation. During the 1930s and 1940s, the National Advisory Committee for Aeronautics (NACA) measured the lift and drag characteristics of a series of systematically designed airfoil shapes (discussed in detail in chapter). These measurements were carried out in a specially designed wind tunnel where the wing models spanned the entire test section (i.e., the wing tips were butted against both sidewalls of the wind tunnel). This was done in order to establish two dimensional (rather than three-dimensional) flow over the wing, thus allowing the properties of an airfoil (rather than a finite wing) to be measured. The distinction between the aerodynamics of airfoils and that of finite wings is made in chapters and. The important point here is that because the wings were mounted against both sidewalls of the wind tunnel, the NACA did not use a conventional force balance to measure the lift and drag. Rather, the lift was obtained from the pressure distributions on the ceiling from the pressure distributions on the ceiling and floor of the tunnel (above and below the wing), of the wing. These measurements may appear to be a strange way to measure the aerodynamic force on a wing. Indeed, how are these measurements related to lift and drag? What is going on here? The answers to these questions are addressed in this section; they involve an application of the fundamental momentum equation in integral form, and they illustrate a basic technique that is frequently used in aerodynamics.

Consider a two-dimensional body in a flow, as sketched in Figure a. A control volume is drawn around this body, as given by the dashed lines in Figure a. The control volume is bounded by:

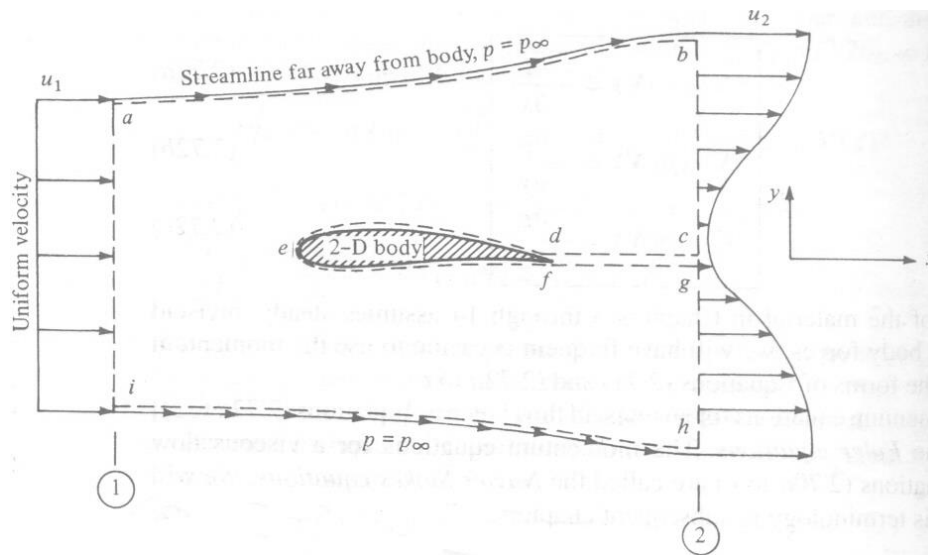


Figure: (a)

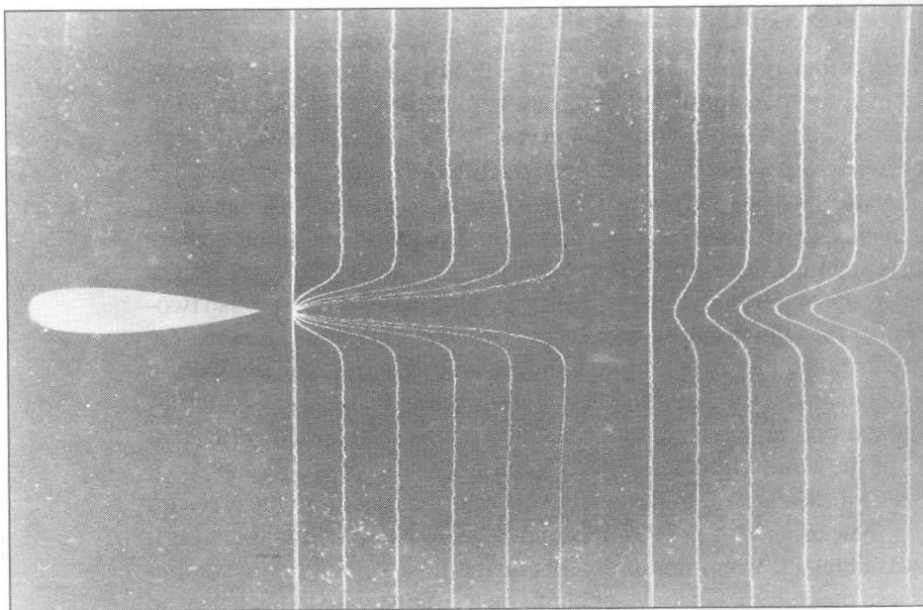


Figure: (b)

Figure: (a) Control volume for obtaining drag on a two-dimensional body. (b) Photograph of the velocity profiles downstream of an airfoil. The profiles are made visible in water flow by pulsing a voltage through a straight wire perpendicular to the flow, thus creating small bubbles of hydrogen that subsequently move downstream with the flow. (Courtesy of Yasuki Nakayama, Tokai University, Japan.)

The upper and lower streamline far above and below the body (asb and hi, respectively),

Lines perpendicular to the flow velocity far ahead of and behind the body (ai and bh, respectively).

A cut that surrounds and wraps the surface of the body (cdefg).

The entire control volume is abcdefghia. The width of the control volume in the z direction (perpendicular to the page) is unity. Stations 1 and 2 are inflow and outflow stations, respectively.

Assume that the control abhi is far enough from the body such that the pressure is everywhere the same on abhi and equal to the freestream pressure  $p = p_\infty$ . Also, assume that the inflow velocity  $u_1$  is uniform across ai (as it would be in a freestream, or a test section of a wind tunnel). The outflow velocity  $u_2$  is not uniform across bh, because the presence of the body has created a wake at the outflow station. However, assume that both  $u_1$  and  $u_2$  are in the x direction; hence,  $u_1 = \text{constant}$  and  $u_2 = f(y)$ .

An actual photograph of the velocity profiles in a wake downstream of an airfoil is shown in figure b.

Consider the surface forces on the control volume shown in figure a. They stem from two contributions:

The pressure distribution over the surface

$$-\iint_{abhi} p dS$$

The surface force on de is created by the presence of the body

In the above list, the surface shear stress on ab and hi has been neglected. Also, note that in Figure a the cuts cd and fg are taken adjacent to each other; hence, any shear stress or pressure distribution on one is equal and opposite to that on the other (i.e., the surface forces on cd and fg cancel each other). Also, note that the surface force on def is the equal and opposite reaction to the shear stress and pressure distribution created by the flow over the surface of the body. To see this more clearly, examine Figure. On the left is shown the flow over the body. As explained in Section the moving fluid exerts pressure and shear stress distributions over the body surface which created a resultant aerodynamic force per unit span  $R'$  on the body. In turn, by Newton's third law, the body exerts equal and opposite pressure and shear stress distributions on the flow (i.e., on the part of the control surface bounded by def). Hence, the body exerts a force  $-R'$  on the control surface, as shown on the right of Figure. With the above in mind, the total surface force on the entire control volume is



$$\text{Surface force} = \iint_{abhi} p dS - R'$$

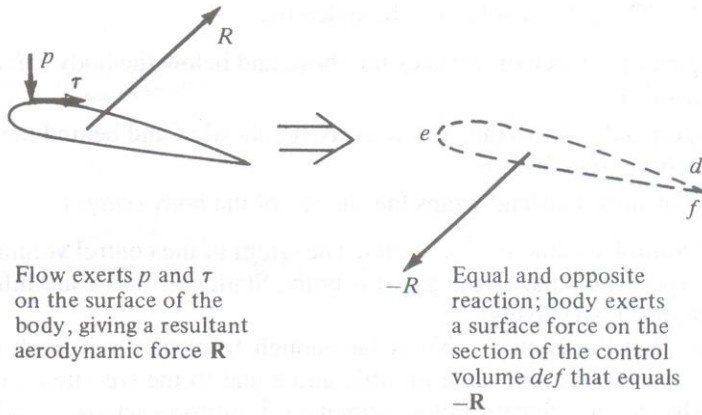


Figure: Equal and opposite reactions on a body and adjacent section of control surface.

Moreover, this is the total force on the control volume shown in figure a because the volumetric body force is negligible.

Consider the integral form of the momentum equation as given by Equation. The right-hand side of this equation is physically the force on the fluid moving through the control volume. For the control volume in figure a, this force is simply the expression given by Equation. Hence, using Equation with the right-hand side given by Equation, we have

$$\frac{\partial}{\partial t} \iiint_V \rho V dv + \iint_S (\rho V \cdot dS) V = - \iint_{abhi} p dS - R'$$

Assuming steady flow, Equation becomes

$$R' = - \iint_S (\rho V \cdot dS) V - \iint_{abhi} p dS$$

Equation is a vector equation. Consider again the control volume in figure a. Take the x component of Equation, noting that the inflow and outflow velocities  $u_1$  and  $u_2$  are in the x direction and the x component of  $R'$  is the aerodynamic drag per unit span  $D'$ .

$$D' = - \iint_S (\rho V \cdot dS) u - \iint_{abhi} (p dS)_x$$



In Equation, the last term is the component of the pressure force in the x direction. [The expression  $(pdS)_x$  is the x component of the pressure force exerted on the elemental and  $dS$  of the control surface.] Recall that the boundaries of the control volume abhi are chosen far enough from the body such that  $p$  is constant along these boundaries. For a constant pressure.

$$\iint_{abhi} (pdS)_x = 0$$

Because, looking along the x direction in figure a, the pressure force on abhi pushing toward the right exactly balances the pressure force pushing toward the left. This is true no matter what the shape of abhi is, as long as  $p$  is constant along the surface (for proof of this statement, see problem). Therefore, substituting Equation into, we obtain

$$D' = -\iiint_S (\rho V \cdot dS)u$$

Evaluating the surface integral in Equation, we note from Figure a that:

The section ab, hi, and def are streamlines of the flow. Since by definition  $V$  is parallel to the streamlines and  $dS$  is perpendicular to the control surface, along these sections  $V$  and  $dS$  are perpendicular vectors, and hence  $V \cdot dS = 0$ . As a result, the contributions of ab, hi, and def to the integral in Equation are zero.

The cuts cd and fg are adjacent to each other. The mass flux out of one is identically the mass flux into the other. Hence, the contributions of cd and fg the integral in Equation cancel each other.

As a result, the only contributions to the integral in Equation come from sections ai and bh. These sections are oriented in the y direction. Also, the control volume has unit depth in the z direction (perpendicular to the page). Hence, for these sections,  $dS = dy(1)$ . The integral in Equation becomes

$$\iint_S (\rho V \cdot dS)u = -\int_i^a \rho_1 u_1^2 dy + \int_h^b \rho_2 u_2^2 dy$$

Note that the minus sign in front of the first term on the right-hand side of Equation is due to  $V$  and  $dS$  being in opposite directions along ai (station 1 is an inflow boundary); in contrast,  $V$  and  $dS$  are in the same direction over

hb (station 2 an outflow boundary), and hence the second term has a positive sign.

Before going further with Equation, consider the integral form of the continuity equation for steady flow, Equation. Applied to the control volume in figure, Equation becomes

$$-\int_i^a \rho_1 u_1 dy + \int_h^b \rho_2 u_2 dy = 0$$

or 
$$\int_i^a \rho_1 u_1 dy = \int_h^b \rho_2 u_2 dy$$

Multiplying Equation by  $u_1$ , which is a constant, we obtain

$$\int_i^a \rho_1 u_1^2 dy = \int_h^b \rho_2 u_2 u_1 dy$$

Substituting Equation into Equation, we have

$$\iint_S (\rho V \cdot dS) u = -\int_h^b \rho_2 u_2 u_1 dy + \int_h^b \rho_2 u_2^2 dy$$

or

$$\iint_S (\rho V \cdot dS) u = -\int_h^b \rho_2 u_2 (u_1 - u_2) dy$$

Substituting Equation into Equation yields

$$\boxed{D' = \int_h^b \rho_2 u_2 (u_1 - u_2) dy}$$

Equation is the desired result of this section; it expresses the drag of a body in terms of the known freestream velocity  $u_1$  and the flow-field properties  $\rho_2$  and  $u_2$ , across a vertical station downstream of the body. These downstream properties can be measured in a wind tunnel, and the drag per unit span of the body  $D'$  can be obtained by evaluating the integral in Equation numerically, using the measured data for  $\rho_2$  and  $u_2$  as a function of  $y$ .

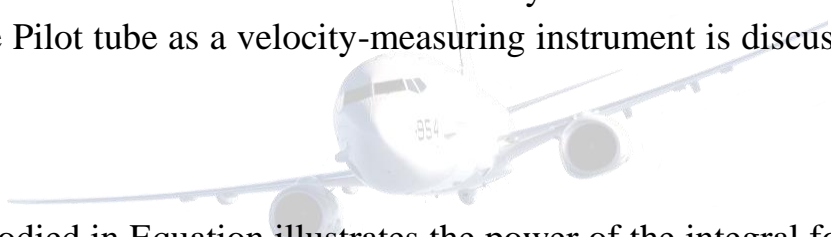
Examine Equation more closely. The quantity  $u_1 - u_2$  is the velocity decrement at a given  $y$  location. In this wake, there is a loss in flow velocity  $u_1 - u_2$ . The quantity  $\rho_2 u_2$  is simply the mass flux; when multiplied by  $u_1$

–  $u_2$ , it gives the decrement in momentum. Therefore, the integral in Equation is physically the decrement in momentum flow that exists across the wake, and from Equation, this wake momentum decrement is equal to the drag on the body.

For incompressible flow,  $\rho = \text{constant}$  and is known. For this case, Equation becomes

$$D' = \rho \int_h^b u_2 (u_1 - u_2) dy$$

Equation is the answer to the questions posed at the beginning of this section. It shows how a measurement of the velocity distribution across the wake of a body can yield the drag. These velocity distributions are conventionally measured with a Pitot rake, such as shown in figure. This is nothing more than a series of Pitot tubes attached to a common stem, which allows the simultaneous measurement of velocity across the wake. (The principle of the Pitot tube as a velocity-measuring instrument is discussed in chapter.



The result embodied in Equation illustrates the power of the integral form of the momentum equation; it relates drag on a body located at some position in the flow to the flow-field variables at a completely different location.

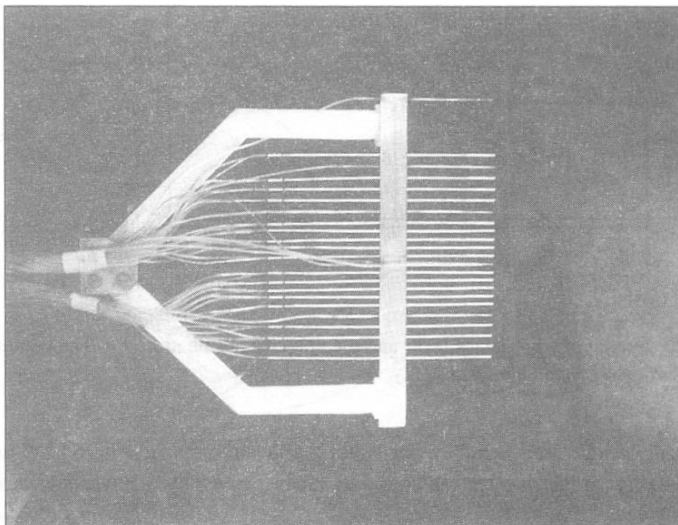


Figure: A Pitot rake for wake surveys. (Courtesy of the University of Maryland Aerodynamic Laboratory.)

At the beginning of this section, it was mentioned that lift on a two-dimensional body can be obtained by measuring the pressures on the ceiling and floor of a wind tunnel, above and below the body. This relation can be established from the integral form of the momentum equation in a manner analogous to that used to establish the drag relation; the derivation is left as a homework problem.

Consider an incompressible flow, laminar boundary layer growing along the surface of a flat plate, with chord length  $c$ , as sketched in figure. The definition of a boundary layer was discussed in section and. For an incompressible, laminar, flat plate boundary layer thickness  $\delta$  at the trailing edge of the plate is

$$\frac{\delta}{c} = \frac{5}{\sqrt{Re_c}}$$

and the skin friction drag coefficient for the plate is

$$C_f \equiv \frac{D'}{q_\infty c(1)} = \frac{1.328}{\sqrt{Re_c}}$$

where the Reynolds number is based on chord length

$$Re_c = \frac{\rho_\infty V_\infty c}{\mu_\infty}$$

[Note: Both  $\delta/c$  and  $C_f$  are functions of the Reynolds number-just another demonstration of the power of the similarity parameters. Since we are dealing with a low-speed,

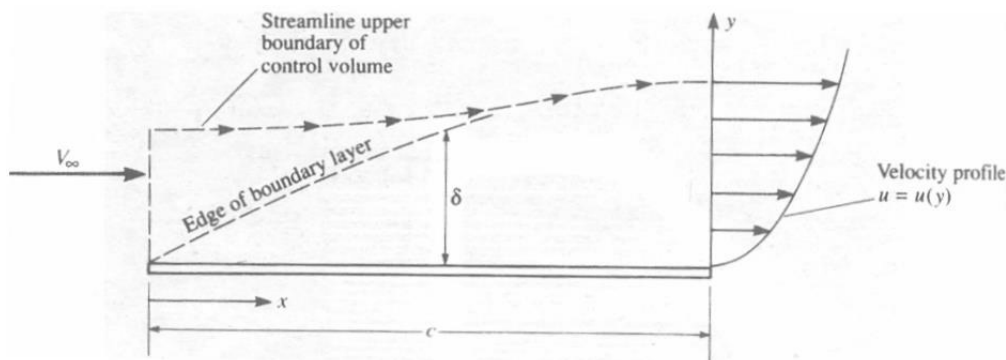


Figure: Sketch of a boundary layer and the velocity profile at  $x = c$ . the boundary-layer thickness  $\delta$  is exaggerated here for clarity.

incompressible flow, the Mach number is not a relevant parameter here.] Let us assume that the velocity profile through the boundary layer is given by a power-law variation

$$u = V_{\infty} \left( \frac{y}{\delta} \right)^n$$

Calculate the value of  $n$ , consistent with the information given above.

Solution

From Equation

$$C_f = \frac{D'}{q_{\infty} c} = \frac{\rho_{\infty}}{\frac{1}{2} \rho_{\infty} V_{\infty}^2 c} \int_0^{\delta} u_2 (u_1 - u_2) dy$$

where the integral is evaluated at the trailing edge of the plate. Hence,

$$C_f = 2 \int_0^{\delta/c} \frac{u_2}{V_{\infty}} \left( \frac{u_1}{V_{\infty}} - \frac{u_2}{V_{\infty}} \right) d\left(\frac{y}{c}\right)$$

However, in equation, applied to the control volume in figure,  $u_1 = V_{\infty}$ .

Thus

$$C_f = 2 \int_0^{\delta/c} \frac{u_2}{V_{\infty}} \left( 1 - \frac{u_2}{V_{\infty}} \right) d\left(\frac{y}{c}\right)$$

Inserting the laminar Boundary-layer result for  $C_f$  as well as the assumed variation of velocity, both given above, we can write this integral as

$$\frac{1.328}{\sqrt{Re_c}} = 2 \int_0^{\delta/c} \left[ \left( \frac{y/c}{\delta/c} \right)^n - \left( \frac{y/c}{\delta/c} \right)^{2n} \right] d \left( \frac{y}{c} \right)$$

Carrying out the integration, we obtain

$$\frac{1.328}{\sqrt{Re_c}} = \frac{2}{n+1} \left( \frac{\delta}{c} \right) - \frac{2}{2n+1} \left( \frac{\delta}{c} \right)$$

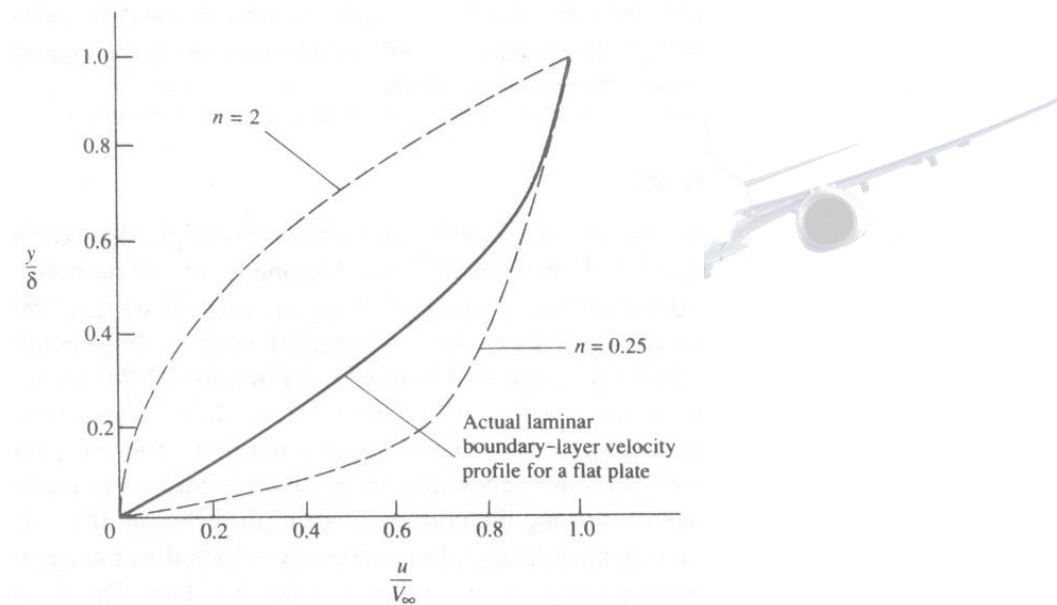


Figure: Comparison of the actual laminar boundary-layer profile with those calculated from Example.

Since  $\delta/c = 5/\sqrt{Re_c}$ , then

$$\frac{1.328}{\sqrt{Re_c}} = \frac{10}{n+1} \left( \frac{1}{\sqrt{Re_c}} \right) - \frac{10}{2n+1} \left( \frac{1}{\sqrt{Re_c}} \right)$$

$$\text{or} \quad \frac{1}{n+1} - \frac{1}{2n+1} = \frac{1.328}{10}$$

$$\text{or} \quad 0.265n - 0.6016n + 0.1328 = 0$$

using the quadratic formula, we have

$$n = 2 \text{ or } 0.25$$

By assuming a power-law velocity profile in the form of  $u/V_\infty = (y/\delta)^n$ , we have found two different velocity profiles that satisfy the momentum principle applied to a finite control volume. Both of these profiles are shown in figure and are compared with an exact velocity profile obtained by means of a solution of the incompressible, laminar boundary-layer equations for a flat plate. (This boundary-layer solution is discussed in Chapter). Note that the result  $n = 2$  gives a concave velocity profile that is essentially nonphysical when compared to the convex profiles always observed in boundary layers. The result  $n = 0.25$  gives a convex velocity profile that is qualitatively physically correct. However, this profile is quantitatively inaccurate, as can be seen in comparison to the exact profile. Hence, our original assumption of a power-law velocity profile for the laminar boundary layer in the form of  $u/V_\infty = (y/\delta)^n$  is not very good, in spite of the fact that when  $n = 2$  or  $0.25$ , this assumed velocity profile does satisfy the momentum principle, applied over a large, finite control volume.

## Energy Equation in Integral Form/Control Volume Approach

### Physical principle

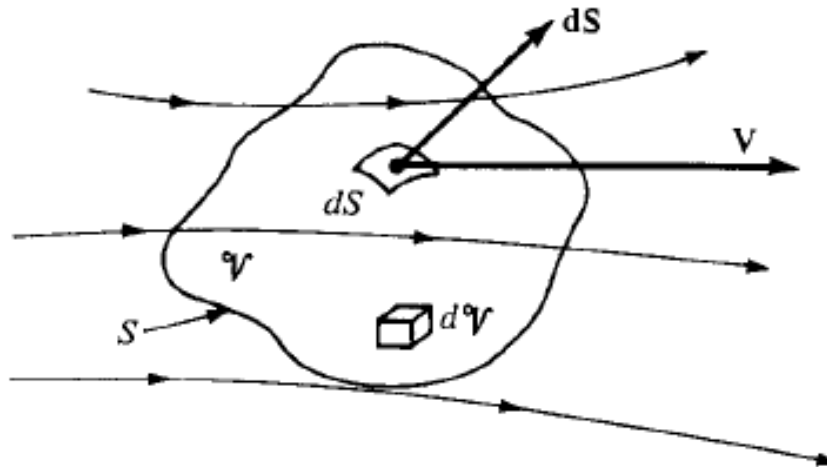
Energy can be neither created nor destroyed;  
it can only change in form.

Consider a fixed amount of matter contained within a closed boundary. This matter defines the system. Because the molecules and atoms within the system are constantly in motion, the system contains a certain amount of energy. For simplicity, let the system contain a unit mass; in turn, denote the internal energy per unit mass by  $e$ .

The region outside the system defines the surroundings. Let an incremental amount of heat  $\delta q$  be added to the system from the surroundings. Also, let  $\delta W$  be the work done on the system by the surroundings.

Both heat and work are forms of energy, and when added to the system, they change the amount of internal energy in the system. Denote this change of internal energy by  $de$ . From our physical principle that energy is conserved, we have for the system

$$\delta q + \delta w = de$$



Finite control volume fixed in space.

Equation is a statement of the first law of thermodynamics.

Let us apply the first law to the fluid flowing through the fixed control volume shown in Figure

Let

$B_1$  = rate of heat added to fluid inside control volume from surroundings

$B_2$  = rate of work done on fluid inside control volume

$B_3$  = rate of change of energy of fluid as it flows through control volume

From the first law,

$$B_1 + B_2 = B_3$$

### Expression for $B_1$

Examining Figure, the mass contained within an elemental volume is  $\rho dV$ ; hence, the rate of heat addition to this mass is  $q(\rho dV)$ . Summing over the complete control volume, we obtain

$$\text{Rate of volumetric heating} = \iiint_V \dot{q} \rho dV$$



In addition, if the flow is viscous, heat can be transferred into the control volume by means of thermal conduction and mass diffusion across the control surface. So the equation becomes,

$$B_1 = \iiint_V \dot{q} \rho dV + \dot{Q}_{\text{viscous}}$$

### **Expression for B2**

Consider the elemental area  $dS$  of the control surface in Figure. The pressure force on this elemental area is  $-\rho dS$ . From the above result, the rate of work done on the fluid passing through  $dS$  with velocity  $\mathbf{V}$  is  $(-\rho dS) \cdot \mathbf{V}$ . Hence, summing over the complete control surface

$$\text{Rate of work done on fluid inside } V \text{ due to pressure force on } S = - \oint_S (p \mathbf{dS}) \cdot \mathbf{V}$$

In addition, consider an elemental volume  $dV$  inside the control volume, Recalling that  $\mathbf{f}$  is the body force per unit mass, the rate of work done on the elemental volume due to the body force is  $(\rho \mathbf{f} dV) \cdot \mathbf{V}$ . Summing over the complete control volume, we obtain

$$\text{Rate of work done on fluid inside } V \text{ due to body forces} = \iiint_V (\rho \mathbf{f} dV) \cdot \mathbf{V}$$

If the flow is viscous, the shear stress on the control surface will also perform work on the fluid as it passes across the surface.

$$B_2 = - \oint_S p \mathbf{V} \cdot \mathbf{dS} + \iiint_V \rho (\mathbf{f} \cdot \mathbf{V}) dV + \dot{W}_{\text{viscous}}$$

### **Expression for B3**

The rate of change of total energy of the fluid as it flows through the control volume. The elemental mass flow across  $dS$  is  $\rho \mathbf{V} dS$ , and therefore the elemental flow of total energy across  $dS$  is

$$(\rho \mathbf{V} \cdot \mathbf{dS}) (e + V^2/2).$$

$$\text{Net rate of flow of total energy across control surface} = \oint_S (\rho \mathbf{V} \cdot \mathbf{dS}) \left( e + \frac{V^2}{2} \right)$$

In addition, if the flow is unsteady, there is a time rate of change of total energy inside the control volume due to the transient fluctuations of the flow-field variables. The total energy contained in the  $\rho (e + V^2/2) dV$  elemental volume  $dV$  is

and hence the total energy inside the complete control volume at any instant in time is

$$\iiint_V \rho \left( e + \frac{V^2}{2} \right) dV$$

Therefore,  
Time rate of change of total energy  
inside  $V$  due to transient variations  
of flow-field variables

$$= \frac{\partial}{\partial t} \iiint_V \rho \left( e + \frac{V^2}{2} \right) dV$$

In turn,  $B_3$  is the sum of Equations

$$B_3 = \frac{\partial}{\partial t} \iiint_V \rho \left( e + \frac{V^2}{2} \right) dV + \iint_{\mathcal{S}} (\rho \mathbf{V} \cdot \mathbf{dS}) \left( e + \frac{V^2}{2} \right)$$

Combining  $B_1, B_2$  and  $B_3$  we get

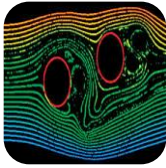
$$\begin{aligned} \iiint_V \dot{q} \rho dV + \dot{Q}_{\text{viscous}} - \iint_S p \mathbf{V} \cdot \mathbf{dS} + \iiint_V \rho (\mathbf{f} \cdot \mathbf{V}) dV + \dot{W}_{\text{viscous}} \\ = \frac{\partial}{\partial t} \iiint_V \rho \left( e + \frac{V^2}{2} \right) dV + \iint_S \rho \left( e + \frac{V^2}{2} \right) \mathbf{V} \cdot \mathbf{dS} \end{aligned}$$

Equation is the energy equation in integral form; it is essentially the first law of thermodynamics applied to a fluid flow.

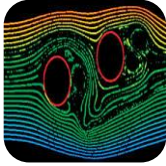


## UNIT II

# TWO DIMENSIONAL FLOWS



Basic flows – Source, Sink, Free and Forced vortex, uniform parallel flow. Their combinations, Pressure and velocity distributions on bodies with and without circulation in ideal and real fluid flows.



Kutta Joukowski's theorem.



## Introduction

**Pathlines, streamlines, and streaklines of a flow**

In addition to knowing the density, pressure temperature, and velocity fields, in aerodynamics we like to draw pictures of “where the flow is going.” To accomplish this, we construct diagrams of pathlines and/or streamlines of the flow. The distinction between pathlines and streamlines is described in this section.

Consider an unsteady flow with a velocity field given by  $V = V(x, y, z, t)$ . Also, consider an infinitesimal fluid element moving through the flow field, say, element A as shown in figure. Element A passes through point 1. Let us trace the path of element A as it moves downstream from point 1, as given by the dashed line in figure a. Such a path is defined as the pathline for element A. Now, trace the path of another fluid element, say, element B as shown in Figure b. Assume that element B also passes through point 1, but at some different time from element A. The pathline of element B is given by the dashed line in figure b. Because the flow is unsteady, the velocity at point 1 (and at all other points of the flow) change with time. hence, the pathline of elements A and B are different curves in figure a and b. In general, for unsteady flow, the pathline for different fluid elements passing through the same point are not the same.

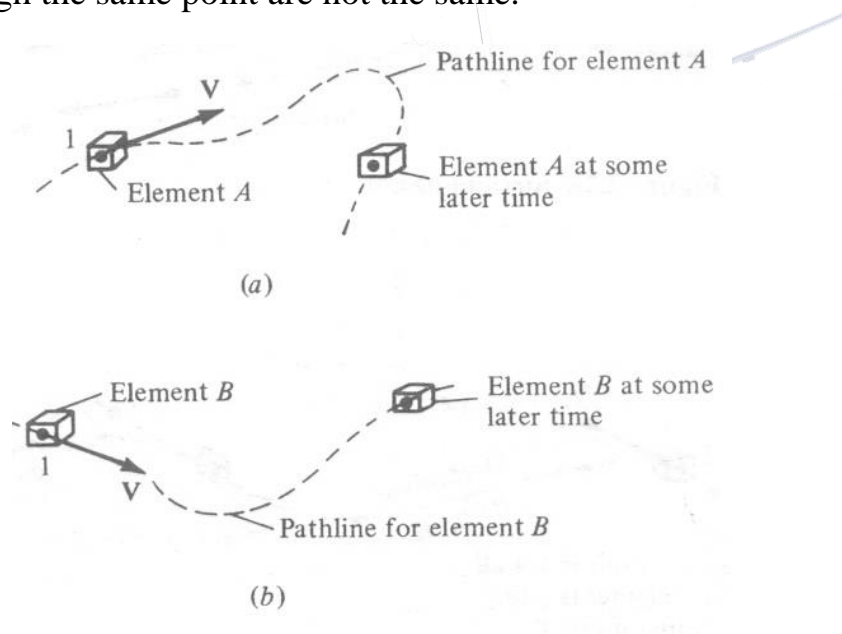


Figure: Pathlines for two different fluid elements passing through the same point in space: unsteady flow.

In section, the concept of a streamline was introduced in a somewhat heuristic manner. Let us be more precise here. By definition, a streamline is a curve whose tangent at any point is in the direction of the velocity vector at that point. Streamlines are illustrated in Figure. The streamlines are drawn such that their tangents at every point along the streamline are in the same

direction as the velocity vectors at those points. If the flow is unsteady, the streamline pattern is different at different times because the velocity vectors are fluctuating with time in both magnitude and direction.

In general, streamlines are different from pathlines. You can visualize a pathline as a time-exposure photograph of a given fluid element, whereas a streamline pattern is like a single frame of a motion picture of the flow. In an unsteady flow, the streamline pattern changes; hence, each “frame” of the motion picture is different.

However, for the case of steady flow (which applies to most of the applications in this book), the magnitude and direction of the velocity vectors at all points are fixed, invariant with time. Hence, the pathlines for different fluid elements going through the same point are the same. Moreover, the pathlines and streamlines are identical. Therefore, in steady flow, there is no distinction between pathlines and streamlines; they are the same curves in space. This fact is reinforced in figure, which illustrates the fixed, time-invariant streamline (pathline) through

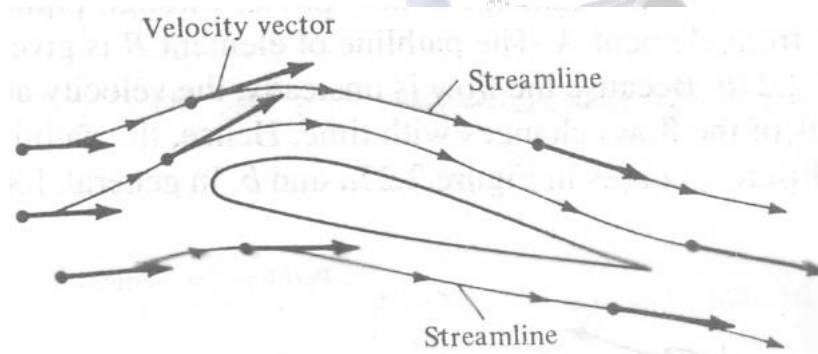


Figure: Streamlines.

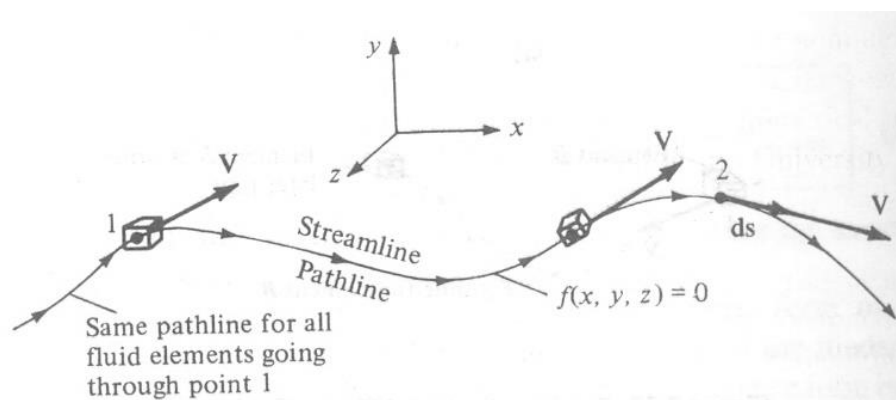


Figure: For steady flow, streamlines and pathlines are the same.

Point 1. Figure , a given fluid element passing through point 1 traces a pathline downstream. All subsequent fluid elements passing through point 1 at later times trace the same pathline. Since the velocity vector is tangent to the pathline at all points on the pathline for all times, the pathline is also a streamline. For the remainder of this book, we deal mainly with the concept of streamlines rather than pathlines; however, always keep in mind the distinction described above.

Question: Given the velocity field of a flow, how can we obtain the mathematical equation for a streamline? Obviously, the streamline illustrated in figure is a curve in space, and hence it can be described by the equation  $f(x, y, z) = 0$ . How can we obtain this equation? To answer this question, let  $ds$  be a directed element of the streamline, such as shown at point 2 in figure. Thus velocity at point 2 is  $V$ , and by definition of a streamline,  $V$  is parallel to  $ds$ . Hence, from the definition of the vector cross product.

$$\boxed{ds \times V = 0}$$

Equation is a valid equation for a streamline. To put it in a more recognizable form, expand Equation in Cartesian coordinates:

$$ds = dx\mathbf{i} + dy\mathbf{j} + dz\mathbf{k}$$

$$V = u\mathbf{i} + v\mathbf{j} + w\mathbf{k}$$

$$ds \times V = \begin{vmatrix} \mathbf{i} & \mathbf{j} & \mathbf{k} \\ dx & dy & dz \\ u & v & w \end{vmatrix}$$

$$= \mathbf{i}(w dy - v dz) + \mathbf{j}(u dz - w dx) + \mathbf{k}(v dx - u dy) = 0$$

Since the vector given by Equation is zero, its components must each be zero.

$$\boxed{\begin{aligned} w dy - v dz &= 0 \\ u dz - w dx &= 0 \\ v dx - u dy &= 0 \end{aligned}}$$

Equations a to c are differential equations for the streamline. Knowing  $u$ ,  $v$ , and  $w$  as functions of  $x$ ,  $y$ , and  $z$ , Equations a to c can be integrated to yield the equation for the streamline:  $f(x, y, z) = 0$ .

To reinforce the physical meaning of Equations a to c, consider a streamline in two dimensions, as sketched in figure a. The equation of this streamline is  $y = f(x)$ . Hence, at point 1 on the streamline, the slope is  $dy/dx$ . However,  $V$  with  $x$  and  $y$  components  $u$  and  $v$ , respectively, is tangent to the streamline at point 1. Thus, the slope of the streamline is also given by  $v/u$ , as shown in figure. Therefore,

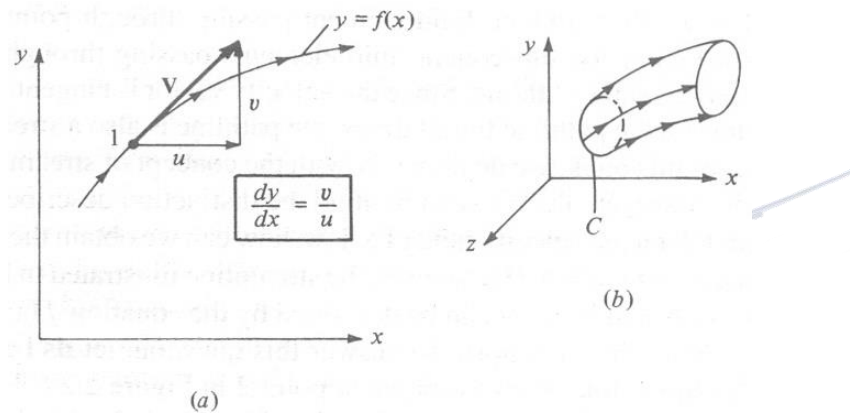


Figure: (a) Equation of a stream in two-dimensional Cartesian space. (b) Sketch of a streamtube in three-dimensional space.

$$\boxed{\frac{dy}{dx} = \frac{v}{u}}$$

Equation is a differential equation for a streamline in two dimensions. From Equation,

$$vdx - udy = 0$$

which is precisely Equation. Therefore, Equation a to c and simply state mathematically that the velocity vector is tangent to the streamline.

A concept related to streamlines is that of a stream tube. Consider an arbitrary closed curve  $C$  in three-dimensional space, as shown in figure b. Consider the streamlines which pass through all points on  $C$ . These streamlines form a tube in space as sketched in Figure b; such a tube is called a streamtube. For example, the walls of an ordinary garden hose form a streamtube for the water flowing through the hose. For a steady flow, a direct application of the integral form of the continuity equation proves that the mass flow across all cross sections of a streamtube is constant. (Prove this yourself).

## Circulation

You are reminded again that this is a tool-building chapter. Taken individually, each aerodynamic tool we have developed so far may not be particularly exciting. However, taken collectively, these tools allow us to obtain solutions for some very practical and exciting aerodynamic problems.

In this section, we introduce a tool that is fundamental to the calculation of aerodynamic lift, namely, circulation. This tool was used independently by Frederick Lanchester (1878-1946) in Russia to create a breakthrough in the theory of aerodynamic lift at the turn of the twentieth century. The relationship between circulation and lift and the historical circumstances surrounding this breakthrough are discussed in chapter. The purpose of this section is only to define circulation and relate it to vorticity.

Consider a closed curve  $C$  in a flow field, as sketched in figure. Let  $V$  and  $ds$  be the velocity and directed line segment, respectively, at a point on  $C$ .



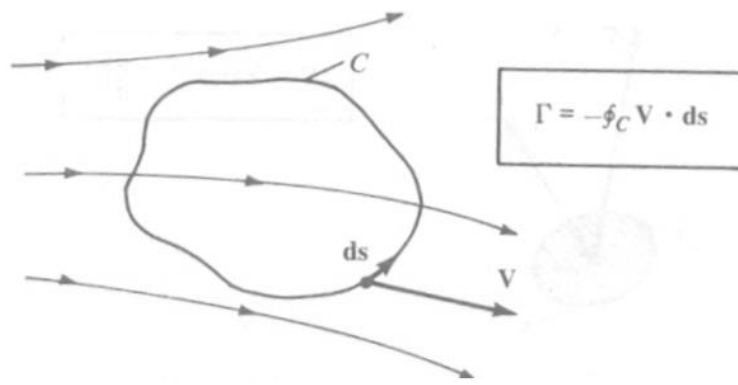


Figure: Definition of circulation.

The circulation, denoted by  $\Gamma$ , is define as

$$\Gamma \equiv -\oint_C \mathbf{V} \cdot d\mathbf{s}$$

The circulation is simply the negative of the line integral of velocity around a closed curve in the flow; it is a kinematic property depending only on the velocity field and the choice of the curve  $C$ . As discussed in section, Line Integrals, by mathematical convention the positive sense of the line integral is counterclockwise. However, in aerodynamics, it is convenient to consider a positive circulation as being clockwise. Hence, a minus sign appears in the definition given by Equation to account for the positive-counterclockwise sense of the integral and the positive-clockwise sense of circulation.<sup>1</sup>

The use of the word circulation to label the integral in Equation may be somewhat misleading because it leaves a general impression of something moving around in a loop. Indeed, according to the American Heritage Dictionary of the English Language, the first definition given to the word “circulation” is “movement in a circle or circuit”. However, in aerodynamics, circulation has a very precise technical meaning, namely, Equation. It does not necessarily mean that the fluid elements are moving around in circles within this flow field—a common early misconception of new students of aerodynamics. Rather, when circulation exists in a flow, it simply means that the line integral in Equation is finite. For example, if the airfoil in Figure is generating lift, the circulation taken around a closed curve enclosing the airfoil will be finite, although the fluid elements are by no

mean executing circles around the airfoil (as clearly seen from the streamlines sketched in figure).

Circulation is also related to vorticity as follows. Refer back which shows an open surface bounded by the closed curve C. Assume that the surface is in a flow field and the velocity at point P is V, where P is any point on the surface (including any point on curve C). From Stokes' theorem Equations.

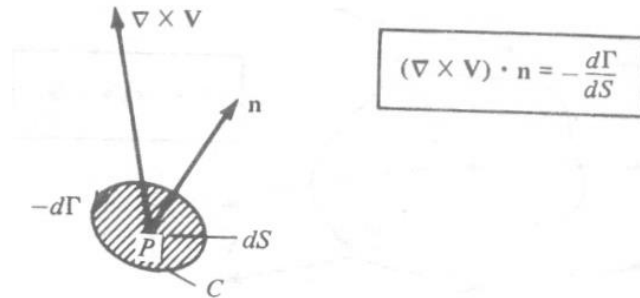


Figure: Relation between vorticity and circulation.

$$\Gamma \equiv -\oint_C \mathbf{V} \cdot d\mathbf{s} = -\iint_S (\nabla \times \mathbf{V}) \cdot d\mathbf{S}$$

Hence, the circulation about a curve C is equal to the vorticity integrated over any open surface bounded by C. This leads to the immediate result that if the flow is irrotational everywhere within the contour of integration (i.e., if  $\nabla \times \mathbf{V} = 0$  over any surface bounded by C), then  $\Gamma = 0$ . A related result is obtained by letting the curve C shrink to an infinitesimal size, and denoting the circulation around this infinitesimally small curve by  $d\Gamma$ . Then, in the limit as C becomes infinitesimally small, Equation yields

$$d\Gamma = -(\nabla \times \mathbf{V}) \cdot d\mathbf{S} = -(\nabla \times \mathbf{V}) \cdot \mathbf{n} dS$$

or

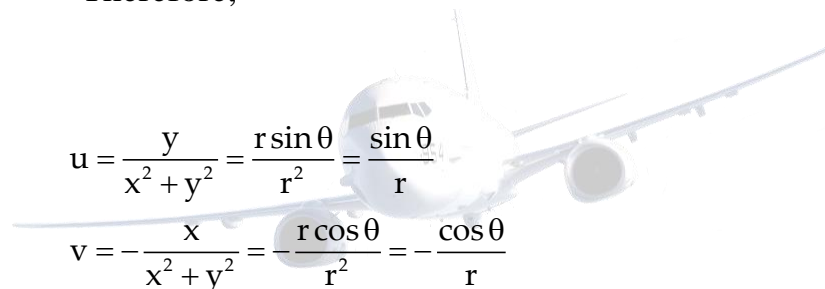
$$(\nabla \times \mathbf{V}) \cdot \mathbf{n} = -\frac{d\Gamma}{dS}$$

where  $dS$  is the infinitesimal area enclosed by the infinitesimal curve  $C$ . Referring to figure, Equation states that at a point  $P$  in a flow, the component of vorticity normal to  $dS$  is equal to the negative of the “circulation per unit area”, where the circulation is taken around the boundary of  $dS$ .

For the velocity field given in example, calculate the circulation around a circular path of radius 5m. Assume that  $u$  and  $v$  given in Example are in units of meters per second.

**Solution**

Since we are dealing with a circular path, it is easier to work this problem in polar coordinates, where  $x = r \cos \theta$ ,  $x^2 + y^2 = r^2$ ,  $V_r = u \cos \theta + v \sin \theta$ , and  $V_\theta = -u \sin \theta + v \cos \theta$ . Therefore,



$$u = \frac{y}{x^2 + y^2} = \frac{r \sin \theta}{r^2} = \frac{\sin \theta}{r}$$

$$v = -\frac{x}{x^2 + y^2} = -\frac{r \cos \theta}{r^2} = -\frac{\cos \theta}{r}$$

$$V_r = \frac{\sin \theta}{r} \cos \theta + \left(-\frac{\cos \theta}{r}\right) \sin \theta = 0$$

$$V_\theta = -\frac{\sin \theta}{r} \sin \theta + \left(-\frac{\cos \theta}{r}\right) \cos \theta = -\frac{1}{r}$$

$$V \cdot ds = (V_r e_r + V_\theta e_\theta) \cdot (dr e_r + r d\theta e_\theta)$$

$$= V_r dr + r V_\theta d\theta = 0 + r \left(-\frac{1}{r}\right) d\theta = -d\theta$$

Hence,

$$\Gamma = -\oint_C V \cdot ds = -\int_0^{2\pi} -d\theta = \boxed{2\pi \text{ m}^2/\text{s}}$$

Note that we never used the 5-m diameter of the circular path; in this case, the value of  $\Gamma$  is independent of the diameter of the path.

**Stream Function:**

In this section, we consider two-dimensional steady flow. Recall from section that the differential equation for a streamline in such a flow is given by Equation repeated below

$$\frac{dy}{dx} = \frac{v}{u}$$

If  $u$  and  $v$  are known functions of  $x$  and  $y$ , then equation can be integrated to yield the algebraic equation for a streamline:

$$f(x, y) = c$$

where  $c$  is an arbitrary constant of integration, with different values for different streamlines. In Equation, denote the function of  $x$  and  $y$  by the symbol  $\bar{\psi}$ . Hence, Equation is written as  $\bar{\psi}(x, y) = c$

The function  $\bar{\psi}(x, y)$  is called the stream function. From Equation we see that the equation for a streamline is given by setting the stream function equal to a constant (i.e.,  $c_1, c_2, c_3$ , etc). Two different streamlines are illustrated in Figure, streamlines  $ab$  and  $cd$  are given by  $\bar{\psi} = c_1$   $\bar{\psi} = c_2$ , respectively.

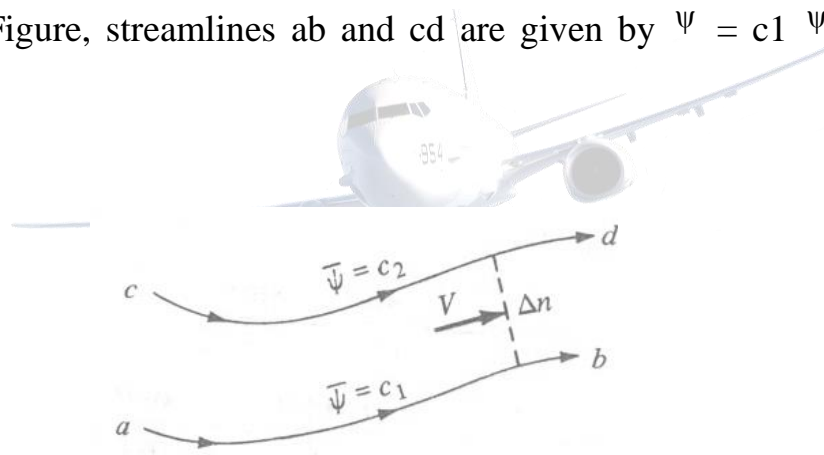


Figure: Different streamlines are given by different values of the stream function.

There is a certain arbitrariness in Equations and via the arbitrary constant of integration  $c$ . Let us define the stream function more precisely in order to reduce this arbitrariness. Referring to figure, let us define the numerical value of  $\bar{\psi}$  such that the difference  $\Delta\bar{\psi}$  between  $\bar{\psi} = c_2$  for streamline  $cd$  and  $\bar{\psi} = c_1$  for streamline  $ab$  is equal to the mass flow between the two streamlines. Since figure is a two-dimensional flow, the mass flow between two streamlines is defined per unit depth perpendicular to the page. That is, in figure, we are considering the mass flow inside a streamtube bounded by streamlines  $ab$  and  $cd$ , with a rectangular cross-

sectional area equal to  $\Delta n$  times a unit depth perpendicular to the page. Here,  $\Delta n$  is the normal distance between  $ab$  and  $cd$ , as shown in figure. Hence, mass flow between streamlines  $ab$  and  $cd$  per unit depth perpendicular to the page is

$$\Delta \bar{\Psi} = c_2 - c_1$$

The above definition does not completely remove the arbitrariness of the constant of integration in Equations and, but it does make things a bit more precise. For example, consider a given two-dimensional flow field. Choose one streamline of the flow, and give it an arbitrary value of the stream function, say,  $\bar{\Psi} = c_1$ . Then, the value of the stream function for any other streamline in the flow, say,  $\bar{\Psi} = c_2$ , is fixed by the definition given in equation. Which streamline you choose to designate as  $\bar{\Psi} = c_1$  and what numerical value you give  $c_1$  usually depend on the geometry of the given flow field.

The equivalence between  $\bar{\Psi} = \text{constant}$  designating a streamline, and  $\Delta \bar{\Psi}$  equaling mass flow (per unit depth) between streamlines, is natural. For a steady flow, the mass flow inside a given streamtube is constant along the tube; the mass flow across any cross section of the tube is the same. Since by definition  $\Delta \bar{\Psi}$  is equal to this mass flow, then  $\Delta \bar{\Psi}$  itself is constant for a given streamtube. In figure, if  $\bar{\Psi}_1 = c_1$  designates the streamline on the bottom of the streamtube, then  $\bar{\Psi}_2 = c_2 = c_1 + \Delta \bar{\Psi}$  is also constant along the top of the streamtube. Since by definition of a streamtube the upper boundary of the streamtube is a streamline itself, then  $\bar{\Psi}_2 = c_2 = \text{constant}$  must designate this streamline.

We have yet to develop the most important property of the stream function, namely, derivatives of  $\bar{\Psi}$  yield the flow-field velocities. To obtain this relationship, consider again the streamlines  $ab$  and  $cd$  in Figure. Assume that these streamlines are close together (i.e., assume  $\Delta n$  is small), such that the flow velocity  $V$  is a constant value across  $\Delta n$ . The mass flow through the streamtube per unit depth perpendicular to the page is

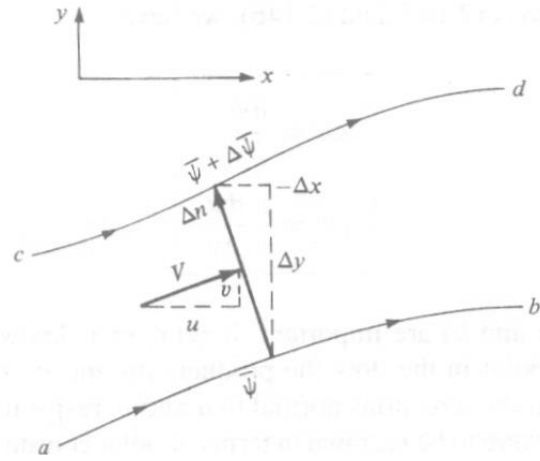


Figure: Mass flow through  $\Delta n$  is the sum of the mass flow through  $\Delta y$  and  $-\Delta x$ .

$$\Delta \bar{\psi} \equiv \rho V \Delta n (1)$$

Or

$$\frac{\Delta \bar{\psi}}{\Delta n} = \rho V$$



Consider the limit of Equation as  $\Delta n \rightarrow 0$ :

$$\rho V = \lim_{\Delta n \rightarrow 0} \frac{\Delta \bar{\psi}}{\Delta n} \equiv \frac{\partial \bar{\psi}}{\partial n}$$

Equation states that if we know  $\bar{\psi}$ , then we can obtain the product  $(\rho V)$  by differentiating  $\bar{\psi}$  in the direction normal to  $V$ . To obtain a practical form of Equation for Cartesian coordinates, consider Figure. Notice that the directed normal distance  $\Delta n$  is equivalent first to moving upward in the  $y$  direction by the amount  $\Delta y$  and then to the left in the negative  $x$  direction by the amount  $-\Delta x$ . Due to conservation of mass, the mass flow through  $\Delta n$  (per unit depth) is equal to the sum of the mass flows through  $\Delta y$  and  $-\Delta x$  (per unit depth):

$$\text{Mass flow} = \Delta \bar{\psi} = \rho V \Delta n = \rho u \Delta y + \rho v (-\Delta x)$$

Letting cd approach ab, Equation becomes in the limit

$$d\bar{\psi} = \rho u dy - \rho v dx$$

However, since  $\bar{\psi} = \bar{\psi}(x, y)$ , the chain rule of calculus states

$$d\bar{\psi} = \frac{\partial \bar{\psi}}{\partial x} dx + \frac{\partial \bar{\psi}}{\partial y} dy$$

Comparing Equation and, we have

$$\begin{aligned} \rho u &= \frac{\partial \bar{\psi}}{\partial y} \\ \rho v &= -\frac{\partial \bar{\psi}}{\partial x} \end{aligned}$$

Equation (a and b) are important. If  $\bar{\psi}(x, y)$  is known for a given flow field, then at any point in the flow the product  $\rho u$  and  $\rho v$  can be obtained by differentiating  $\bar{\psi}$  in the directions normal to  $u$  and  $v$ , respectively.

If Figure were to be redrawn in terms of polar coordinates, then a similar derivation yields

$$\begin{aligned} \rho V_r &= \frac{1}{r} \frac{\partial \bar{\psi}}{\partial \theta} \\ \rho V_\theta &= -\frac{\partial \bar{\psi}}{\partial r} \end{aligned}$$

Such a derivation is left as a homework problem.

Note that the dimensions of  $\bar{\Psi}$  are equal to mass flow per unit depth perpendicular to the page. That is, in SI units  $\bar{\Psi}$  is in terms of kilograms per second per meter perpendicular to the page, or simply kg/(s.m).

The stream function  $\bar{\Psi}$  defined above applies to both compressible and incompressible flow. Now consider the case of incompressible flow only, where  $\rho = \text{constant}$ . Equation can be written as

$$V = \frac{\partial(\bar{\Psi}/\rho)}{\partial n}$$

We define a new stream function, for incompressible flow only, as  $\bar{\Psi}/\rho$ . Then Equation becomes

$$V = \frac{\partial \psi}{\partial n}$$

and Equation and become

$$u = \frac{\partial \psi}{\partial y}$$

$$v = -\frac{\partial \psi}{\partial x}$$



and

$$V_r = \frac{1}{r} \frac{\partial \psi}{\partial \theta}$$

$$V_\theta = -\frac{\partial \psi}{\partial r}$$

The incompressible stream function  $\psi$  has characteristics analogous to its more general compressible counterpart  $\bar{\Psi}$ . For example, since  $\bar{\Psi}(x,y) = c$  is the equation of a streamline, and since  $\rho$  is a constant for incompressible flow, then  $\psi(x,y) \equiv \bar{\Psi}/\rho = \text{constant}$  is also the equation for a streamline (for incompressible flow only). In addition, since  $\Delta \bar{\Psi}$  is mass flow between two streamlines (per unit depth perpendicular to the page), and since  $\rho$  is mass per unit volume, then physically  $\Delta \psi = \Delta \bar{\Psi}/\rho$  represents the volume flow (per unit depth) between two streamlines. In SI units,  $\Delta \psi$  is expressed as cubic meters per second per meter perpendicular to the page, or simply m<sup>2</sup>/s.



In summary, the concept of the stream function is a powerful tool in aerodynamics, for two primary reasons. Assuming that  $\bar{\psi}(x,y)$  [or  $\psi(x,y)$ ] is known through the two-dimensional flow, then:

1.  $\bar{\psi}$  constant (or  $\psi = \text{constant}$ ) gives the equation of a streamline.

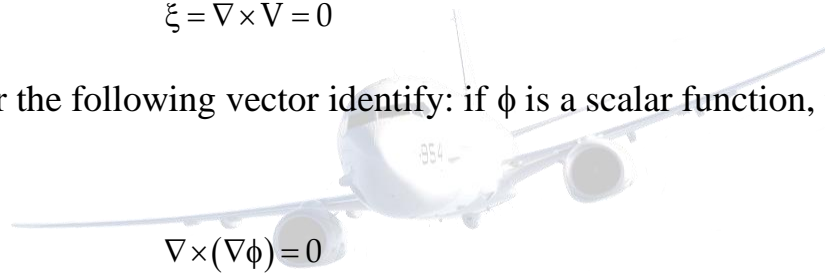
The flow velocity can be obtained by differentiating  $\bar{\psi}$  (or  $\psi$ ), as given by Equations and for compressible flow and Equations and for incompressible flow. We have not yet discussed how  $\bar{\psi}(x,y)$  [or  $\psi(x,y)$ ] can be obtained in the first place; we are assuming that it is known. The actual determination of the stream function for various problems is discussed.

### Velocity Potential.

Recall from section that an irrotational flow is defined as a flow where the vorticity is zero at every point. From Equation, for an irrotational flow,

$$\xi = \nabla \times V = 0$$

Consider the following vector identity: if  $\phi$  is a scalar function, then



$$\nabla \times (\nabla \phi) = 0$$

That is, the curl of the gradient of a scalar function is identically zero. Comparing Equations, we see that

$$\boxed{V = \nabla \phi}$$

Equation states that for an irrotational flow, there exists a scalar function  $\phi$  such that the velocity is given by the gradient of  $\phi$ . We denote  $\phi$  as the velocity potential.  $\phi$  is a function of the spatial coordinates; that is,  $\phi = \phi(x,y,z)$ , or  $\phi = \phi(r,\theta,z)$ , or  $\phi = \phi(r,\theta,\Phi)$ . From the definition of the gradient in Cartesian coordinates given by Equation, we have, from Equation,

$$u\mathbf{i} + v\mathbf{j} + w\mathbf{k} = \frac{\partial \phi}{\partial x}\mathbf{i} + \frac{\partial \phi}{\partial y}\mathbf{j} + \frac{\partial \phi}{\partial z}\mathbf{k}$$

The coefficients of like unit vectors must be the same on both sides of Equation. Thus, in Cartesian coordinates,

$$\boxed{u = \frac{\partial \phi}{\partial x} \quad v = \frac{\partial \phi}{\partial y} \quad w = \frac{\partial \phi}{\partial z}}$$

In a similar fashion, from the definition of the gradient in cylindrical and spherical coordinates given by Equations and, we have, in cylindrical coordinates,

$$V_r = \frac{\partial \phi}{\partial r} \quad V_\theta = \frac{1}{r} \frac{\partial \phi}{\partial \theta} \quad V_z = \frac{\partial \phi}{\partial z}$$

and in spherical coordinates,

$$V_r = \frac{\partial \phi}{\partial r} \quad V_\theta = \frac{1}{r} \frac{\partial \phi}{\partial \theta} \quad V_\Phi = \frac{1}{r \sin \theta} \frac{\partial \phi}{\partial \Phi}$$

The velocity potential is analogous to the stream function in the sense that derivatives of  $\phi$  yield the flow-field velocities. However, there are distinct differences between  $\phi$  and  $\bar{\psi}$  (or  $\psi$ ):

The flow-field velocities are obtained by differentiating  $\phi$  in the same direction as the velocities, whereas  $\bar{\psi}$  (or  $\psi$ ) is differentiated normal to the velocity direction and or Equation.

The velocity potential is defined for irrotational flow only. In contrast, the stream function can be used in either rotational or irrotational flows.

The velocity potential applies to three-dimensional flows, whereas the stream function is defined for two-dimensional flows only.

Where a flow field is irrotational, hence allowing a velocity potential to be defined, there is a tremendous simplification. Instead of dealing with the velocity components (say,  $u$ ,  $v$  and  $w$ ) as unknowns, hence requiring three equations for these three unknowns, we can deal with the velocity potential as one unknown, therefore requiring the solution of only one equation for the flow field. Once  $\phi$  is known for a given problem, the velocities are obtained directly from Equations. This is why, in theoretical

aerodynamics, we make a distinction between irrotational and rotational flows and why the analysis of irrotational flows is simpler than that of rotational flows.

Because irrotational flows can be described by the velocity potential  $\phi$ , such flows are called potential flows.

In this section, we have not yet discussed how  $\phi$  can be obtained in the first place; we are assuming that it is known. The actual determination of  $\phi$  for various problems is discussed.

### Relationship between the stream function and velocity potential

In section we demonstrated that for an irrotational flow  $\mathbf{V} = \nabla\phi$ . At this stage, take a moment and review some of the nomenclature introduced in section for the gradient of a scalar field. We see that a line of constant  $\phi$  is an isoline of  $\phi$  is an isoline of  $\phi$ ; since  $\phi$  is the velocity potential, we give this isoline a specific name, equipotential line. In addition, a line drawn in space such that  $\nabla\phi = \mathbf{V}$ , this gradient line is a streamline. In turn, from section, a streamline is a line of constant  $\psi$  (for a two-dimensional flow). Because gradient lines and isolines are perpendicular, Gradient of a Scalar Field), then equipotential lines ( $\phi=\text{constant}$ ) and streamlines ( $\psi=\text{constant}$ ) are mutually perpendicular.

To illustrate this result more clearly, consider a two-dimensional, irrotational, incompressible flow in Cartesian coordinates. For a streamline,  $\psi(x,y) = \text{constant}$ . Hence, the differential of  $\psi$  along the streamline is zero; that is,

$$d\psi = \frac{\partial\psi}{\partial x}dx + \frac{\partial\psi}{\partial y}dy = 0$$

From Equation (a and b), Equation can be written as

$$d\psi = -dx + udy = 0$$

Solve Equation for  $dy/dx$ , which is the slope of the  $\psi = \text{constant}$  line, that is, the slope of the stream:

$$\left(\frac{dy}{dx}\right)_{\psi=\text{const}} = \frac{v}{u}$$

Similar, for an equipotential line,  $\phi(x,y) = \text{constant}$ . Along this line,

$$d\phi = \frac{\partial\phi}{\partial x}dx + \frac{\partial\phi}{\partial y}dy = 0$$

From Equation, Equation can be written as

$$d\phi = udx + vdy = 0$$

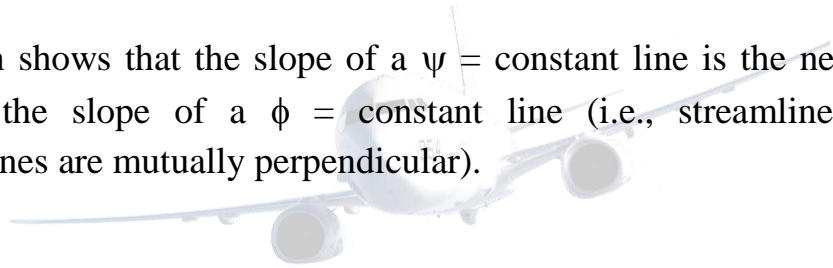
Solving Equation for  $dy/dx$ , which is the slope of the  $\phi = \text{constant}$  line (i.e., the slope of the equipotential line), we obtain

$$\left(\frac{dy}{dx}\right)_{\phi=\text{const}} = -\frac{u}{v}$$

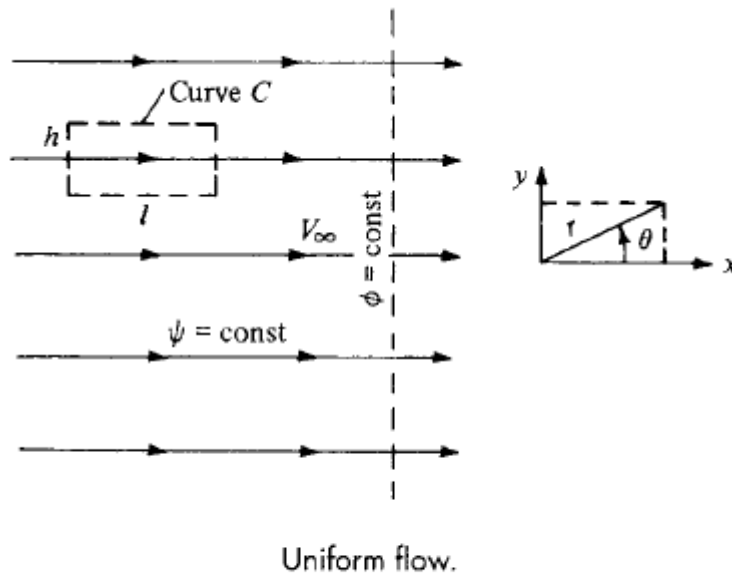
Combining Equation and we have

$$\left(\frac{dy}{dx}\right)_{\psi=\text{const}} = -\frac{1}{(dy/dx)_{\phi=\text{const}}}$$

Equation shows that the slope of a  $\psi = \text{constant}$  line is the negative reciprocal of the slope of a  $\phi = \text{constant}$  line (i.e., streamlines and equipotential lines are mutually perpendicular).



## Uniform Flow



Consider a uniform flow with velocity oriented in the positive X direction, as sketched in Figure. A uniform flow is a physically possible incompressible flow (i.e., it satisfies  $\nabla \cdot \mathbf{V} = 0$ ) and that it is irrotational (i.e., it satisfies  $\nabla \times \mathbf{V} = 0$ ). Hence, a velocity potential for uniform flow can be obtained such that

$$\frac{\partial \phi}{\partial x} = u = V_{\infty}$$

$$\frac{\partial \phi}{\partial y} = v = 0$$

Integrating Equation with respect to x, we have

$$\phi = V_{\infty}x + f(y)$$

Where  $f(y)$  is a function of y only. Integrating Equation with respect to y, we obtain

$$\phi = \text{const} + g(x)$$

Where  $g(x)$  is a function of x only.

Comparing these two equations

$$\phi = V_{\infty}x + \text{const}$$

In a practical aerodynamic problem, the actual value of  $\phi$  is not significant; So we can drop the constant from the equation

$$\phi = V_{\infty}x$$

The velocity potential for a uniform flow with velocity oriented in the positive x direction. Consider the incompressible stream function  $\psi$  From Figure we have

$$\frac{\partial \psi}{\partial y} = u = V_{\infty}$$

$$\frac{\partial \psi}{\partial x} = -v = 0$$

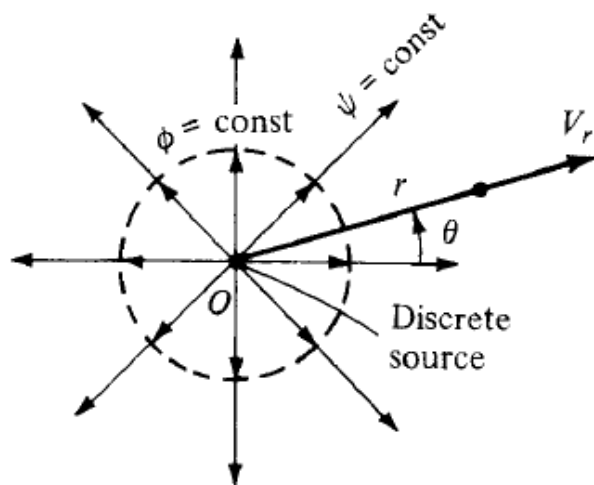
Integrating Equation with respect to y with respect to x, and comparing the results, we obtain

$$\psi = V_{\infty}y$$

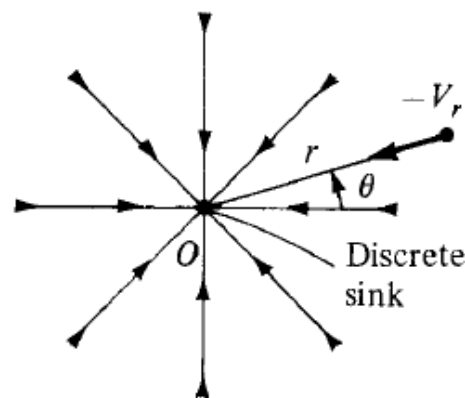
Equation is the stream function for an incompressible uniform flow oriented in the positive x direction.



## Source Flow



Source flow



Sink flow

Source and sink flows.

Consider a two-dimensional, incompressible flow where all the streamlines are straight lines emanating from a central point O. Let the velocity along each of the streamlines vary inversely with distance from point O. Such a flow is called a source flow. The velocity components in the radial and tangential directions are  $V_r$  and  $V_\theta$  respectively. (Note that polar coordinates are simply the cylindrical coordinates  $r$  and  $\theta$  confined to a single plane given by  $z = \text{constant}$ .)

Assumptions

- (1) Source flow is a physically possible incompressible flow, that is,  $\nabla \cdot \mathbf{V} = 0$ , at every point except the origin, where  $\nabla \cdot \mathbf{V}$  becomes infinite, and
- (2) Source flow is irrotational at every point.

In a source flow, the streamlines are directed away from the origin the opposite case is that of a sink flow, where by definition the streamlines are directed toward the origin.

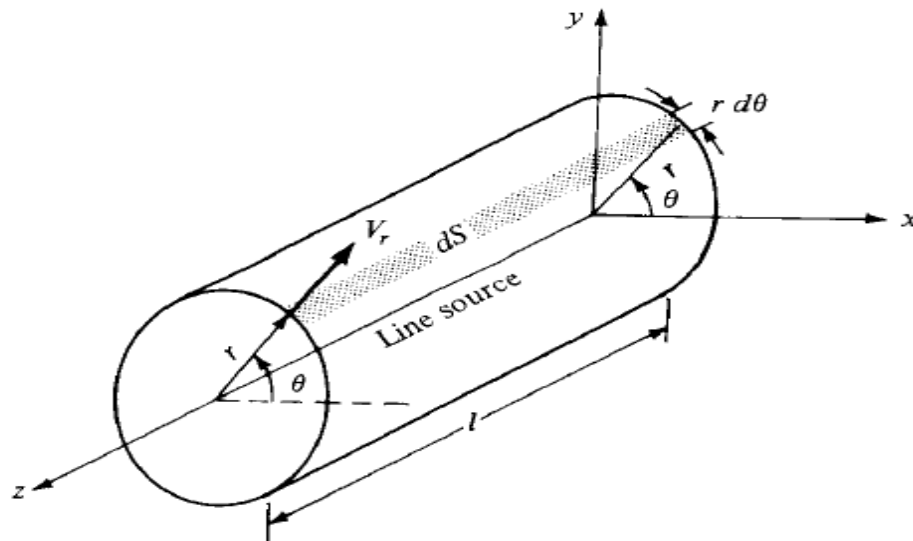
Let us look at the velocity field induced by a source or sink. By definition, the velocity is inversely proportional to the radial distance  $r$ . As stated earlier, this velocity variation is a physically possible flow, because it yields  $\nabla \cdot \mathbf{V} = 0$ . Moreover, it is the *only* such velocity variation for which the relation  $\nabla \cdot \mathbf{V} = 0$  is satisfied for the radial flows shown in Figure

Hence,

$$V_r = \frac{c}{r}$$

$$V_\theta = 0$$

where  $c$  is constant. The value of the constant is related to the volume flow from the source.



Volume flow rate from a line source.

The total mass flow across the surface of the cylinder is

$$\dot{m} = \int_0^{2\pi} \rho V_r (r d\theta) l = \rho r l V_r \int_0^{2\pi} d\theta = 2\pi r l \rho V_r$$

Since  $\rho$  is defined as the mass per unit volume and  $m$  is mass per second, then  $\dot{m}/\rho$  is the volume flow per second. Denote this rate of volume flow by  $\dot{v}$ . Thus, from Equation

$$\dot{v} = \frac{\dot{m}}{\rho} = 2\pi r l V_r$$

Moreover, the rate of volume flow per unit length along the cylinder is  $\dot{v}/l$ . Denote this volume flow rate per unit length. Hence, from Equation we obtain

$$\Lambda = \frac{\dot{v}}{l} = 2\pi r V_r$$

$$V_r = \frac{\Lambda}{2\pi r}$$

$\Lambda$  defines the source length; it is physically the rate of volume flow from the source, per unit depth perpendicular to the page.

The velocity potential for a source can be obtained as follows

$$\frac{\partial \phi}{\partial r} = V_r = \frac{\Lambda}{2\pi r}$$

$$\frac{1}{r} \frac{\partial \phi}{\partial \theta} = V_\theta = 0$$

Integrating Equation with respect to  $r$ , we have

$$\phi = \frac{\Lambda}{2\pi} \ln r + f(\theta)$$

Integrating Equation with respect to  $\theta$ , we have

$$\phi = \text{const} + f(r)$$

Comparing Equations

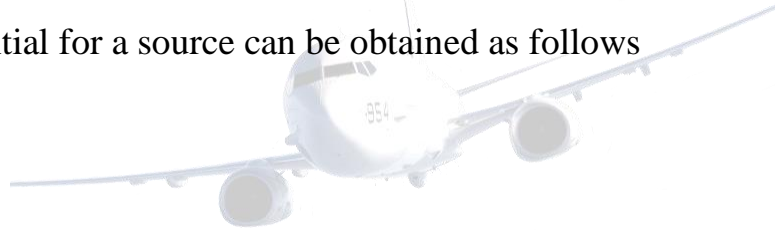
$$\phi = \frac{\Lambda}{2\pi} \ln r$$

The stream function can be obtained as follows

$$\frac{1}{r} \frac{\partial \psi}{\partial \theta} = V_r = \frac{\Lambda}{2\pi r}$$

$$-\frac{\partial \psi}{\partial r} = V_\theta = 0$$

Integrating Equation with respect to  $r$ , we have





$$\psi = \frac{\Lambda}{2\pi}\theta + f(r)$$

Integrating Equation with respect to  $\theta$ , we have

$$\psi = \text{const} + f(\theta)$$

Comparing Equations

$$\psi = \frac{\Lambda}{2\pi}\theta$$

Equation is the stream function for a two-dimensional source flow.

## Combination of a Uniform Flow with a Source and Sink

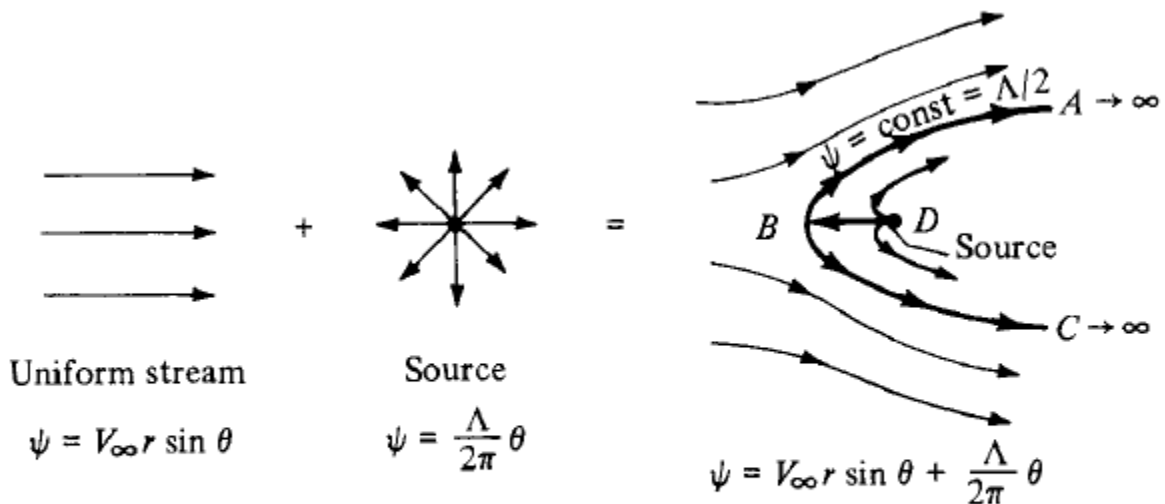
Consider a polar coordinate system with a source of strength  $\Lambda$  located at the origin. Superimpose on this flow a uniform stream with velocity  $V_\infty$  moving from left to right. The stream function for the resulting flow is

$$\psi = V_\infty r \sin \theta + \frac{\Lambda}{2\pi}\theta$$

The streamlines of the combined flow are obtained from Equation

$$\psi = V_\infty r \sin \theta + \frac{\Lambda}{2\pi}\theta = \text{const}$$

The source is located at point D. The velocity field is obtained by differentiating Equations



Superposition of a uniform flow and a source; flow over a semi-infinite body.

$$V_r = \frac{1}{r} \frac{\partial \psi}{\partial \theta} = V_\infty \cos \theta + \frac{\Lambda}{2\pi r}$$

$$V_\theta = -\frac{\partial \psi}{\partial r} = -V_\infty \sin \theta$$

The stagnation points in the flow can be obtained by setting Equations equal to zero

$$\begin{aligned} V_\infty \cos \theta + \frac{\Lambda}{2\pi r} &= 0 \\ V_\infty \sin \theta &= 0 \end{aligned}$$

If the coordinates of the stagnation point at *B* *are* substituted into Equation we obtain

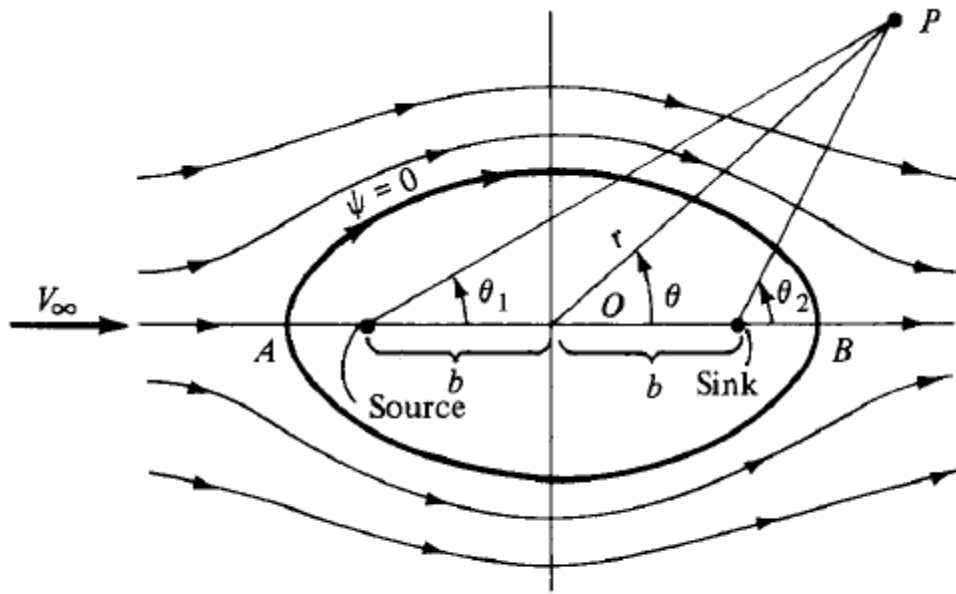
$$\psi = V_\infty \frac{\Lambda}{2\pi V_\infty} \sin \pi + \frac{\Lambda}{2\pi} \pi = \text{const}$$

$$\psi = \frac{\Lambda}{2} = \text{const}$$

Consider a polar coordinate system with a source and sink placed a distance *b* to the left and right of the origin, respectively, The strengths of the source and sink are  $\Lambda$  and  $-\Lambda$ , respectively (equal and opposite). In addition, superimpose a uniform stream with velocity  $V_\infty$ . The stream function for the combined flow at any point *P* with coordinates (*r*,  $\theta$ ) is obtained as

$$\psi = V_\infty r \sin \theta + \frac{\Lambda}{2\pi} \theta_1 - \frac{\Lambda}{2\pi} \theta_2$$

$$\psi = V_\infty r \sin \theta + \frac{\Lambda}{2\pi} (\theta_1 - \theta_2)$$



Superposition of a uniform flow and a source-sink pair; flow over a Rankine oval.

The velocity field is obtained by differentiating Equations. In turn, by setting  $V = 0$ , two stagnation points are found, namely, points A and B in Figure. These stagnation points are located such that

$$OA = OB = \sqrt{b^2 + \frac{\Lambda b}{\pi V_\infty}}$$

The equation of the streamlines is given by Equation as

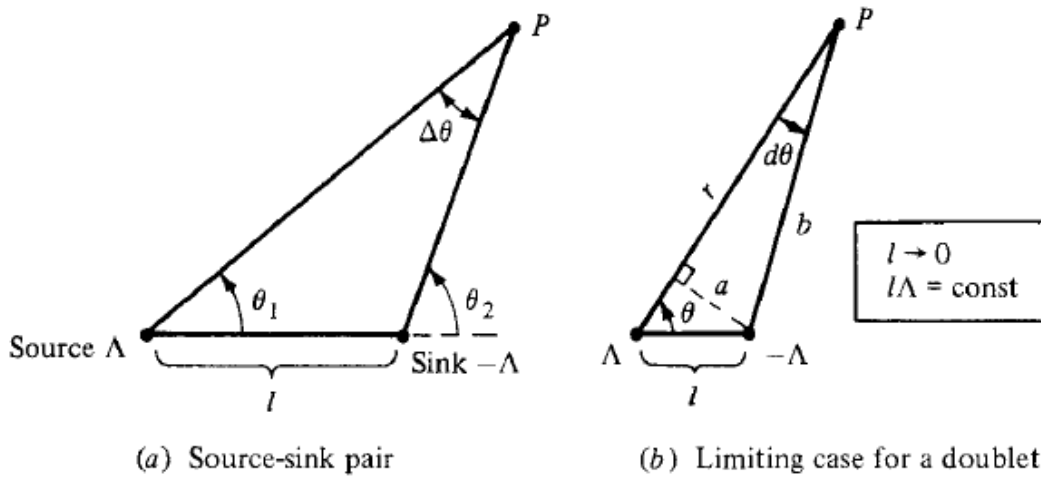
$$\psi = V_\infty r \sin \theta + \frac{\Lambda}{2\pi} (\theta_1 - \theta_2) = \text{const}$$

The equation of the specific streamline going through the stagnation points is obtained from Equation

$$V_\infty r \sin \theta + \frac{\Lambda}{2\pi} (\theta_1 - \theta_2) = 0$$

## Doublet Flow

There is a special, degenerate case of a source-sink pair that leads to a singularity called a doublet. The doublet is frequently used in the theory of incompressible flow;



How a source-sink pair approaches a doublet in the limiting case.

Consider a source of strength  $\Lambda$  and a sink of equal (but opposite) strength  $-\Lambda$  separated by a distance  $l$ , as shown in Figure.

At any point  $P$  in the flow, the stream function is

$$\psi = \frac{\Lambda}{2\pi} (\theta_1 - \theta_2) = -\frac{\Lambda}{2\pi} \Delta\theta$$

In the limit, as  $l \rightarrow 0$  while  $l\Lambda$  remains constant, we obtain a special flow pattern defined as a doublet. The strength of the doublet is denoted by  $k$  and is defined as  $k = l\Lambda$ . The stream function for a doublet is obtained from Equation as follows:

$$\psi = \lim_{\substack{l \rightarrow 0 \\ k = l\Lambda = \text{const}}} \left( -\frac{\Lambda}{2\pi} d\theta \right)$$

For an infinitesimal  $d\theta$ , the geometry yields

$$\begin{aligned} a &= l \sin \theta \\ b &= r - l \cos \theta \\ d\theta &= \frac{a}{b} \\ d\theta &= \frac{a}{b} = \frac{l \sin \theta}{r - l \cos \theta} \end{aligned}$$

Substituting Equation we have

$$\psi = \lim_{\substack{l \rightarrow 0 \\ k = \text{const}}} \left( -\frac{\Lambda}{2\pi} \frac{l \sin \theta}{r - l \cos \theta} \right)$$

$$\psi = \lim_{\substack{l \rightarrow 0 \\ k = \text{const}}} \left( -\frac{\kappa}{2\pi} \frac{\sin \theta}{r - l \cos \theta} \right)$$

$$\boxed{\psi = -\frac{\kappa}{2\pi} \frac{\sin \theta}{r}}$$

Equation is the stream function for a doublet. In a similar fashion, the velocity potential for a doublet is given as

$$\phi = \frac{\kappa}{2\pi} \frac{\cos \theta}{r}$$

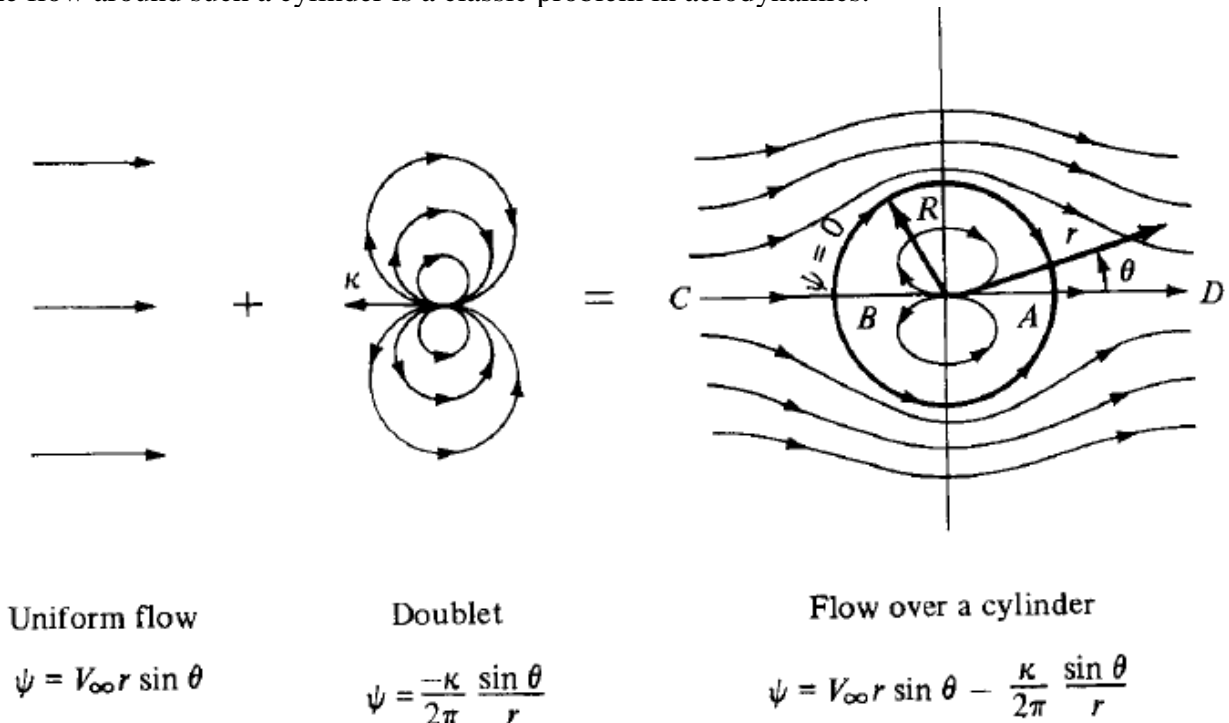
The streamlines of a doublet flow are obtained from Equation

$$\psi = -\frac{\kappa}{2\pi} \frac{\sin \theta}{r} = \text{const} = c$$

$$r = -\frac{\kappa}{2\pi c} \sin \theta$$

## Non lifting Flow over a Circular Cylinder

A circular cylinder is one of the most basic geometric shapes available, and the study of the flow around such a cylinder is a classic problem in aerodynamics.



Superposition of a uniform flow and a doublet; nonlifting flow over a circular cylinder.

Consider the addition of a uniform flow with velocity  $V_{\infty}$  and a doublet of strength  $K$ , as shown in Figure. The direction of the doublet is upstream, facing into the uniform flow. The stream function for the combined flow is

$$\psi = V_{\infty} r \sin \theta - \frac{\kappa}{2\pi} \frac{\sin \theta}{r}$$

$$\psi = V_{\infty} r \sin \theta \left( 1 - \frac{\kappa}{2\pi V_{\infty} r^2} \right)$$

Substituting the value for  $r^2$

$$\psi = (V_{\infty} r \sin \theta) \left(1 - \frac{R^2}{r^2}\right)$$

Equation is the stream function for a uniform flow-doublet combination; it is also the stream function for the flow over a circular cylinder of radius  $R$  as shown in Figure and as demonstrated below.

The velocity field is obtained by differentiating Equation as follows:

$$V_r = \frac{1}{r} \frac{\partial \psi}{\partial \theta} = \frac{1}{r} (V_{\infty} r \cos \theta) \left(1 - \frac{R^2}{r^2}\right)$$

$$V_r = \left(1 - \frac{R^2}{r^2}\right) V_{\infty} \cos \theta$$

$$V_{\theta} = -\frac{\partial \psi}{\partial r} = -\left[(V_{\infty} \sin \theta) \frac{2R^2}{r^3} + \left(1 - \frac{R^2}{r^2}\right) (V_{\infty} \sin \theta)\right]$$

$$V_{\theta} = -\left(1 + \frac{R^2}{r^2}\right) V_{\infty} \sin \theta$$

To locate the stagnation points, set Equations equal to zero:

$$\left(1 - \frac{R^2}{r^2}\right) V_{\infty} \cos \theta = 0$$

$$\left(1 + \frac{R^2}{r^2}\right) V_{\infty} \sin \theta = 0$$



The velocity distribution on the surface of the cylinder is given by Equations with  $r = R$ , resulting in

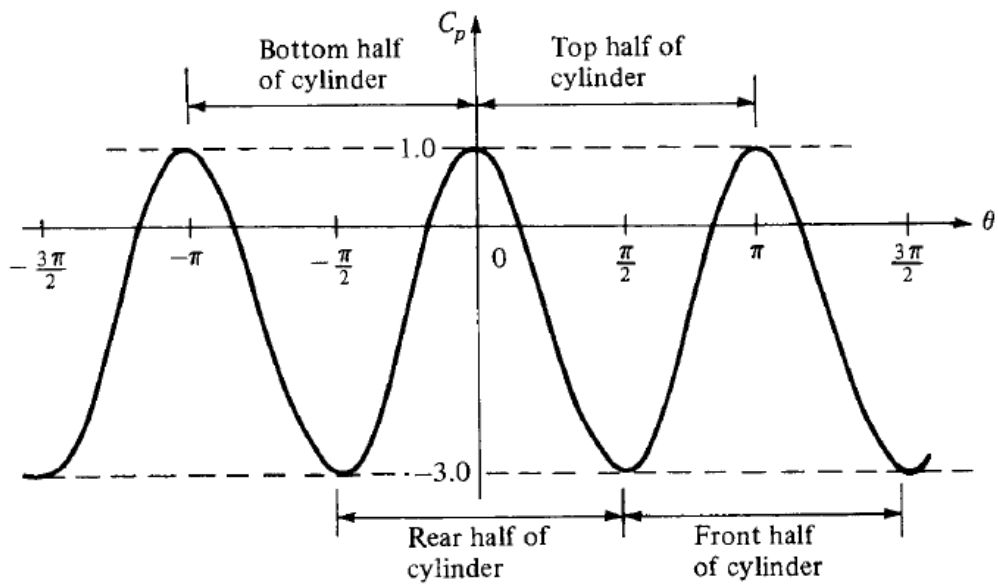
$$V_r = 0$$

$$V_{\theta} = -2V_{\infty} \sin \theta$$

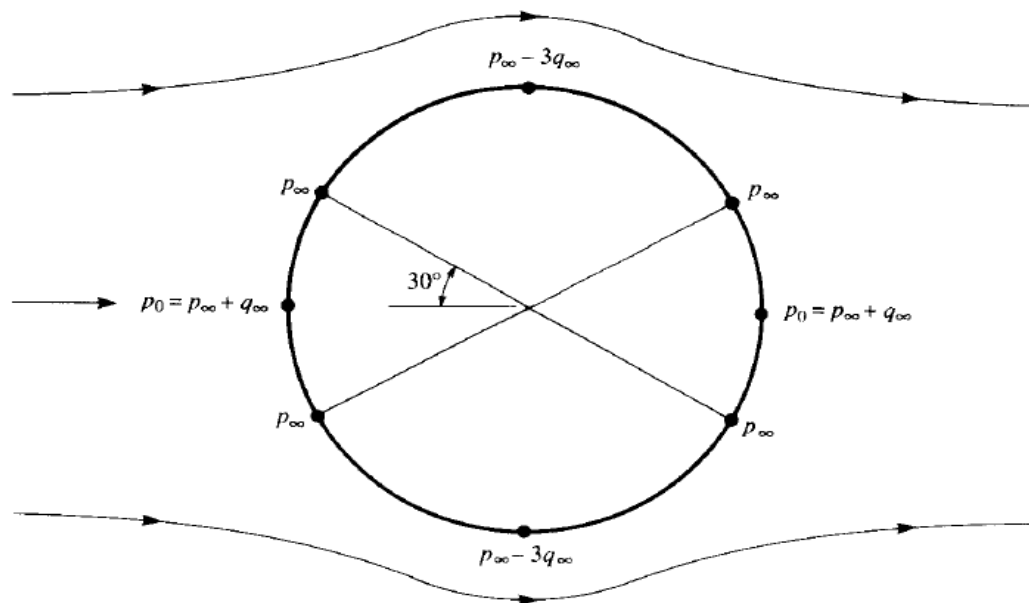
The pressure coefficient is given by Equation  $C_p = 1 - \left(\frac{V}{V_{\infty}}\right)^2$

From this the surface pressure coefficient over a circular cylinder is

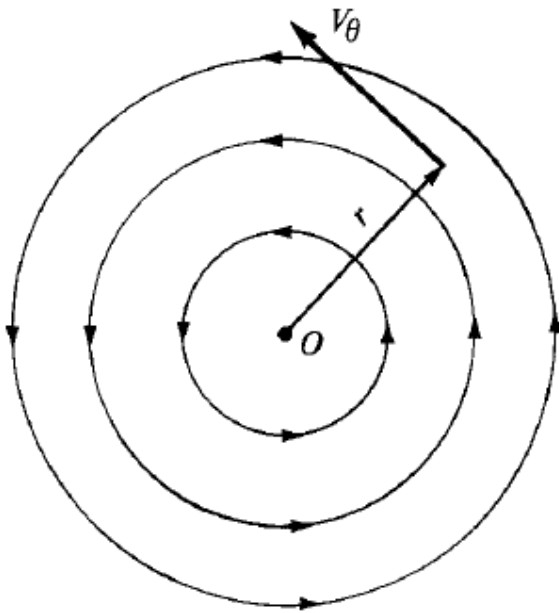
$$C_p = 1 - 4 \sin^2 \theta$$



Pressure coefficient distribution over the surface of a circular cylinder; theoretical results for inviscid, incompressible flow.



Values of pressure at various locations on the surface of a circular cylinder; nonlifting case.



Vortex flow.

Consider a flow where all the streamlines are concentric circles about a given point, as sketched in Figure. , let the velocity along any given circular streamline be constant, but let it vary from one streamline to another inversely with distance from the common center. Such a flow is called a vortex flow.

The velocity components in the radial and tangential directions are  $V_r$  and  $V_\theta$ , respectively

From the definition of vortex flow, we have

$$V_\theta = \frac{\text{const}}{r} = \frac{C}{r}$$

To evaluate the constant  $C$ , take the circulation around a given circular streamline of radius  $r$

$$\Gamma = - \oint_C \mathbf{V} \cdot d\mathbf{s} = -V_\theta(2\pi r)$$

$$V_\theta = -\frac{\Gamma}{2\pi r}$$

Comparing Equations

$$C = -\frac{\Gamma}{2\pi}$$

Relating circulation to vorticity we have:

$$\Gamma = - \iint_S (\nabla \times \mathbf{V}) \cdot d\mathbf{S}$$

Combining Equations



$$2\pi C = \iint_S (\nabla \times \mathbf{V}) \cdot d\mathbf{S}$$

Since we are dealing with two-dimensional flow Equation can be written as

$$2\pi C = \iint_S (\nabla \times \mathbf{V}) \cdot d\mathbf{S} = \iint_S |\nabla \times \mathbf{V}| dS$$

The circulation will still remain  $\Gamma = -2\pi C$ . The area inside this small circle around the origin will become infinitesimally small, and

$$\iint_S |\nabla \times \mathbf{V}| dS \rightarrow |\nabla \times \mathbf{V}| dS$$

Combining Equations

$$2\pi C = |\nabla \times \mathbf{V}| dS$$

$$|\nabla \times \mathbf{V}| = \frac{2\pi C}{dS}$$

However, as  $r \rightarrow 0$ ,  $dS \rightarrow 0$ . Therefore, in the limit as  $r \rightarrow 0$ , from Equation we have

$$|\nabla \times \mathbf{V}| \rightarrow \infty$$

The velocity potential for vortex flow can be obtained as follows:

$$\frac{\partial \phi}{\partial r} = V_r = 0$$

$$\frac{1}{r} \frac{\partial \phi}{\partial \theta} = V_\theta = -\frac{\Gamma}{2\pi r}$$

Integrating Equations

$$\phi = -\frac{\Gamma}{2\pi} \theta$$

Equation is the velocity potential for vortex flow.

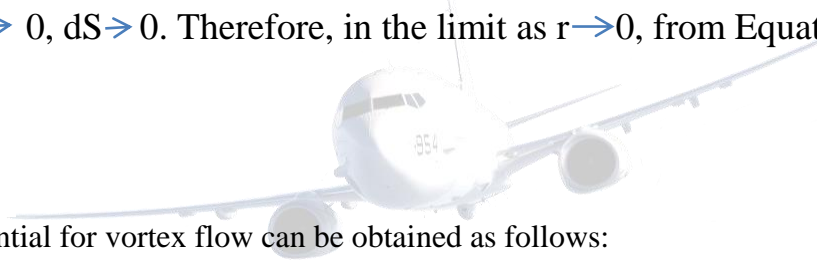
The stream function is determined in a similar manner:

$$\frac{1}{r} \frac{\partial \psi}{\partial \theta} = V_r = 0$$

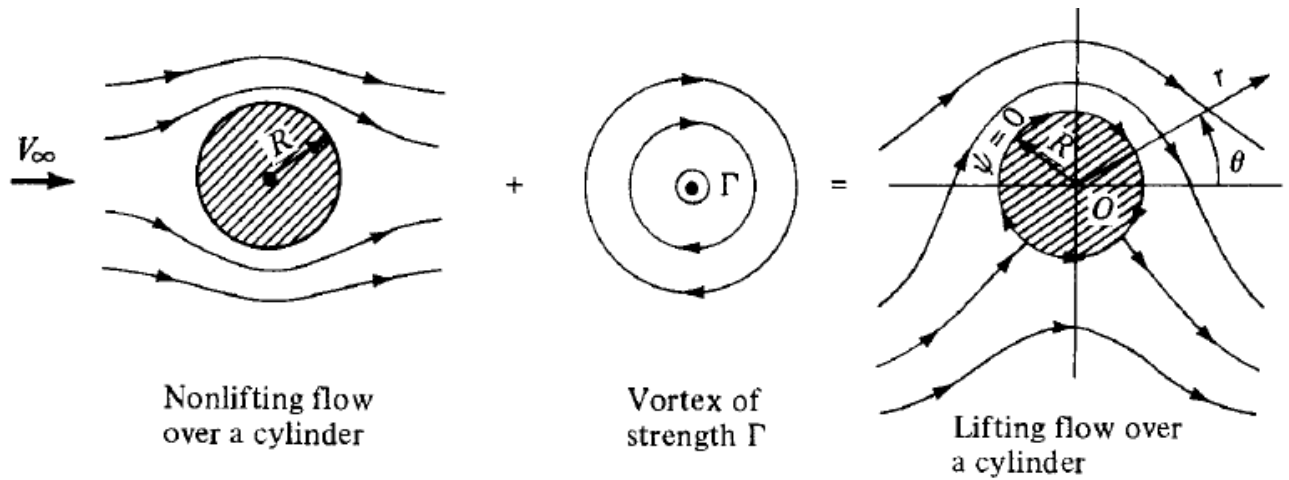
$$-\frac{\partial \psi}{\partial r} = V_\theta = -\frac{\Gamma}{2\pi r}$$

Integrating Equations

$$\psi = \frac{\Gamma}{2\pi} \ln r$$



# LIFTING FLOW OVER A CYLINDER



The synthesis of lifting flow over a circular cylinder.

Consider the flow synthesized by the addition of the nonlifting flow over a cylinder and a vortex of strength  $\Gamma$ , as shown in Figure . The stream function for nonlifting flow over a circular cylinder of radius  $R$  is given by Equation

$$\psi_1 = (V_\infty r \sin \theta) \left( 1 - \frac{R^2}{r^2} \right)$$

Equation can also be written as

$$\psi_2 = \frac{\Gamma}{2\pi} \ln r + \text{const}$$



Since the value of the constant is arbitrary, let

$$\text{Const} = -\frac{\Gamma}{2\pi} \ln R$$

Combining Equations we obtain

$$\psi_2 = \frac{\Gamma}{2\pi} \ln \frac{r}{R}$$

Equation is the stream function for a vortex of strength  $\Gamma$

The resulting stream function for the flow shown at the right of figure is

$$\psi = \psi_1 + \psi_2$$

Or

$$\psi = (V_\infty r \sin \theta) \left( 1 - \frac{R^2}{r^2} \right) + \frac{\Gamma}{2\pi} \ln \frac{r}{R}$$

The velocity field can be obtained by differentiating Equation. An equally direct method of obtaining the velocities is to add the velocity field of a vortex to the velocity field of the nonlifting cylinder.

Hence, from Equations we have, for the lifting flow over a cylinder of radius  $R$ ,

$$V_r = \left(1 - \frac{R^2}{r^2}\right) V_\infty \cos \theta$$

$$V_\theta = -\left(1 + \frac{R^2}{r^2}\right) V_\infty \sin \theta - \frac{\Gamma}{2\pi r}$$

To locate the stagnation points in the flow, set  $V_r = V_\theta = 0$  in Equations and solve for the resulting coordinates  $(r, \theta)$

$$V_r = \left(1 - \frac{R^2}{r^2}\right) V_\infty \cos \theta = 0$$

$$V_\theta = -\left(1 + \frac{R^2}{r^2}\right) V_\infty \sin \theta - \frac{\Gamma}{2\pi r} = 0$$

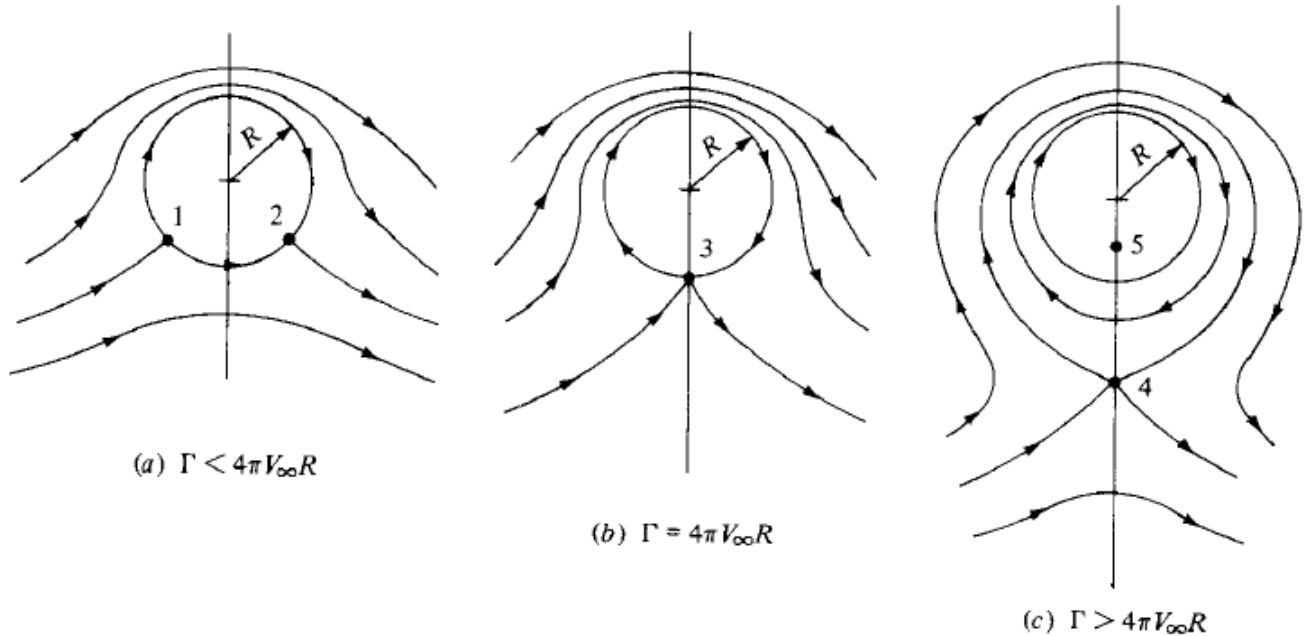
From Equation,  $r = R$ . Substituting this result into Equation and solving for  $\theta$ , we obtain

$$\theta = \arcsin \left( -\frac{\Gamma}{4\pi V_\infty R} \right)$$



Substituting  $\theta = -\pi/2$  into Equation and solving for  $r$ , we have

$$r = \frac{\Gamma}{4\pi V_\infty} \pm \sqrt{\left(\frac{\Gamma}{4\pi V_\infty}\right)^2 - R^2}$$



Stagnation points for the lifting flow over a circular cylinder.

The velocity on the surface of the cylinder is given by Equation with  $r = R$

$$V = V_\theta = -2V_\infty \sin \theta - \frac{\Gamma}{2\pi R}$$

In turn, the pressure coefficient is obtained by

$$C_p = 1 - \left( \frac{V}{V_\infty} \right)^2 = 1 - \left( -2 \sin \theta - \frac{\Gamma}{2\pi R V_\infty} \right)^2$$

$$C_p = 1 - \left[ 4 \sin^2 \theta + \frac{2\Gamma \sin \theta}{\pi R V_\infty} + \left( \frac{\Gamma}{2\pi R V_\infty} \right)^2 \right]$$



## Kutta–Joukowski theorem

The Kutta–Joukowski theorem is a fundamental theorem of aerodynamics, for the calculation of the lift on a rotating cylinder. It is named after the German Martin Wilhelm Kutta and the Russian Nikolai Zhukovsky (or Joukowski) who first developed its key ideas in the early 20th century. The theorem relates the lift generated by a right cylinder to the speed of the cylinder through the fluid, the density of the fluid, and the circulation. The circulation is defined as the line integral, around a closed loop enclosing the cylinder or airfoil, of the component of the velocity of the fluid tangent to the loop.

The magnitude and direction of the fluid velocity change along the path.

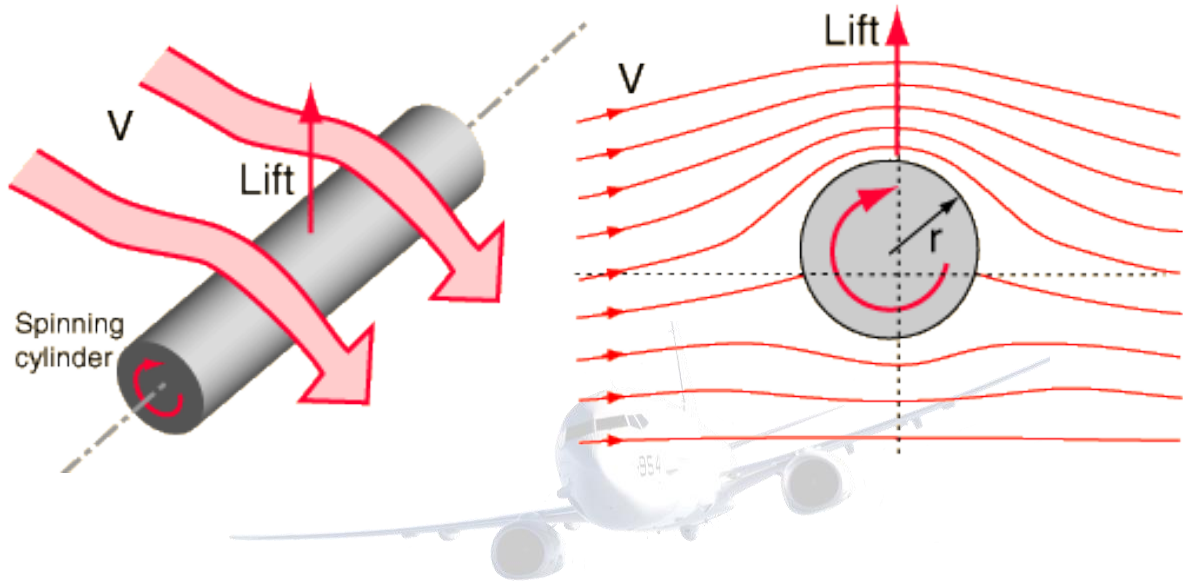
The flow of air in response to the presence of the airfoil can be treated as the superposition of a translational flow and a rotational flow, known as a "vortex". (It is, however, misleading to picture a vortex like a tornado encircling the cylinder or the wing of an airplane in flight. The vortex is defined by the integral's path that encircles the cylinder, and is defined by the mathematical value of the vorticity; not a vortex of air.) In

descriptions of the Kutta–Joukowski theorem the airfoil is usually considered to be a circular cylinder or some other Joukowski airfoil.

The theorem refers to two-dimensional flow around a cylinder (or a cylinder of infinite span) and determines the lift generated by one unit of span. When the circulation  $\Gamma$  is known, the lift  $L$  per unit span (or  $L'$ ) of the cylinder can be calculated using the following equation:

$$L' = -\rho_{\infty} V_{\infty} \Gamma,$$

where  $\rho_{\infty}$  and  $V_{\infty}$  are the fluid density and the fluid velocity far upstream of the cylinder, and  $\Gamma$  is the (anticlockwise positive) circulation defined as the line integral.



The velocity on the surface of the cylinder is given by Equation with  $r = R$ :

$$V = V_{\theta} = -2V_{\infty} \sin \theta - \frac{\Gamma}{2\pi R}$$

In turn, the pressure coefficient is obtained by substituting Equation into Equation:

$$C_p = 1 - \left( \frac{V}{V_{\infty}} \right)^2 = 1 - \left( -2 \sin \theta - \frac{\Gamma}{2\pi R V_{\infty}} \right)^2$$

or

$$C_p = 1 - \left[ 4 \sin^2 \theta + \frac{2\Gamma \sin \theta}{\pi R V_{\infty}} + \left( \frac{\Gamma}{2\pi R V_{\infty}} \right)^2 \right]$$

In Section, we discussed in detail how the aerodynamic force coefficient can be obtained by integrating the pressure coefficient and skin friction coefficient over the surface. For inviscid flow,  $c_f = 0$ . Hence, the drag coefficient  $c_d$  is given by Equation as

$$c_d = c_a = \frac{1}{c} \int_{LE}^{TE} (C_{p,u} - C_{p,l}) dy$$

or 
$$c_d = \frac{1}{c} \int_{LE}^{TE} C_{p,u} dy - \frac{1}{c} \int_{LE}^{TE} C_{p,l} dy$$

Converting Equation to polar coordinates, we note that

$$y = R \sin \theta \quad dy = R \cos \theta d\theta$$

Substituting Equation into, and noting that  $c = 2R$ , we have

$$c_d = \frac{1}{2} \int_{\pi}^0 C_{p,u} \cos \theta d\theta - \frac{1}{2} \int_{\pi}^{2\pi} C_{p,l} \cos \theta d\theta$$

The limits of integration in Equation are explained as follows. In the first integral, we are integrating from the leading edge (the front point of the cylinder), moving over the top surface, decreases to 0 at the trailing edge. In the second integral, we are integrating from the leading edge to the trailing edge while moving over the bottom surface of the cylinder. hence,  $\theta$  is equal to  $\pi$  at the leading edge and, moving over the bottom surface, increases to  $2\pi$  at the trailing edge. In Equation, both  $C_{p,u}$  and  $C_{p,l}$  are given by the same analytic expression for  $C_p$ , namely, Equation. Hence, Equation can be written as

$$c_d = -\frac{1}{2} \int_0^{\pi} C_p \cos \theta d\theta - \frac{1}{2} \int_{\pi}^{2\pi} C_p \cos \theta d\theta$$

or 
$$c_d = -\frac{1}{2} \int_0^{2\pi} C_p \cos \theta d\theta$$

Substituting Equation into, and noting that

$$\int_0^{2\pi} \cos \theta d\theta = 0$$

$$\int_0^{2\pi} \sin^2 \theta \cos \theta d\theta = 0$$

$$\int_0^{2\pi} \sin \theta \cos \theta d\theta = 0$$

we immediately obtain  $\boxed{c_d = 0}$

Equation confirms our intuitive statements made earlier. The drag on a cylinder in an inviscid, incompressible flow is zero, regardless of whether or not the flow has circulation about the cylinder.

The lift on the cylinder can be evaluated in a similar manner as follows. From Equation with  $C_f = 0$ .

$$c_l = c_n = \frac{1}{c} \int_0^c C_{p,l} dx - \frac{1}{c} \int_0^c C_{p,u} dx$$

Converting to polar coordinates, we obtain



$$x = R \cos \theta \quad dx = -R \sin \theta d\theta$$

Substituting Equation into, we have

$$c_l = -\frac{1}{2} \int_{\pi}^{2\pi} C_{p,l} \sin \theta d\theta + \frac{1}{2} \int_{\pi}^0 C_{p,u} \sin \theta d\theta$$

Again, noting that  $C_{p,l}$  and  $C_{p,u}$  are both given by the same analytic expression, namely, Equation, becomes

$$c_l = -\frac{1}{2} \int_0^{2\pi} C_p \sin \theta d\theta$$

Substituting Equation into, and noting that

$$\int_0^{2\pi} \sin \theta d\theta = 0$$

$$\int_0^{2\pi} \sin^3 \theta d\theta = 0$$

$$\int_0^{2\pi} \sin^2 \theta d\theta = \pi$$

we immediately obtain

$$c_l = \frac{\Gamma}{RV_\infty}$$

From the definition of  $c_l$ , the lift per unit span  $L'$  can be obtained from

$$L' = q_\infty S_{cl} = \frac{1}{2} \rho_\infty V_\infty^2 S c_l$$

Here, the planform area  $S = 2R(1)$ . Therefore, combining Equations and we have

$$L' = \frac{1}{2} \rho_\infty V_\infty^2 2R \frac{\Gamma}{RV_\infty}$$

or

$$\boxed{L' = \rho_\infty V_\infty \Gamma}$$

Equation gives the lift per unit span for a circular cylinder with circulation  $\Gamma$ . It is a remarkably simple result, and it states that the lift per unit span is directly proportional to circulation. Equation is a powerful relation in theoretical aerodynamics. It is called the Kutta-Joukowski theorem, named after the German mathematician M. Wilhelm Kutta (1867-1944) and the Russian physicist Nikolai e. Joukowski (1847-1921), who independently obtained it during the first decade of this century. We will have more to say about the Kutta-Joukowski theorem.

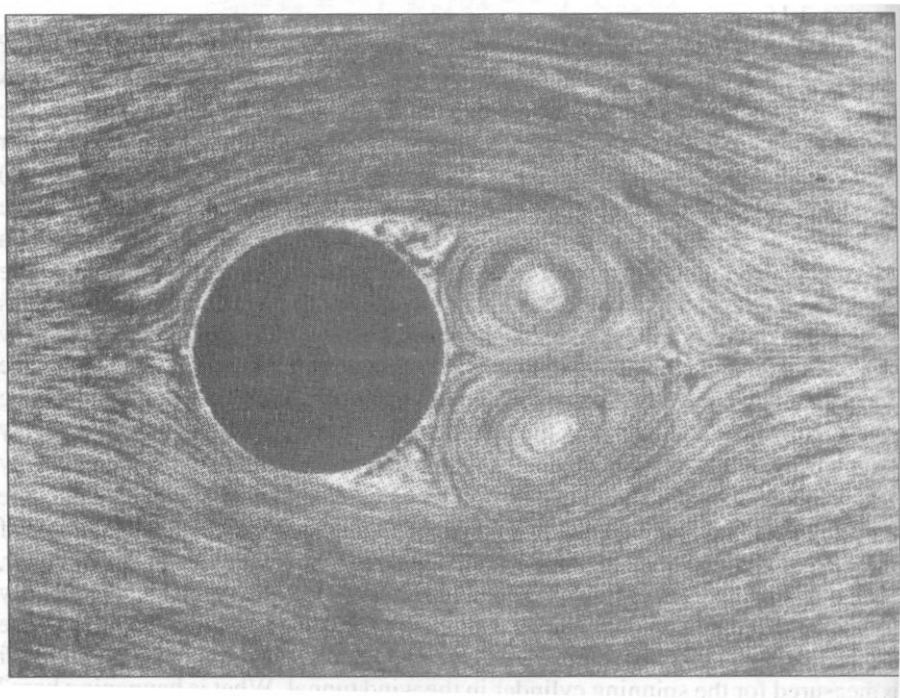


What are the connections between the above theoretical results and real life? As stated earlier, the prediction of zero drag is totally erroneous—viscous effects cause skin friction and flow separation which always produce a finite drag. The inviscid flow treated in this chapter simply does not model the proper physics for drag calculations. On the other hand, the prediction of lift via Equation is quite realistic. Let us return to the wind-tunnel experiments mentioned at the beginning of this chapter. If a stationary, nonspinning cylinder is placed in a low-speed wind tunnel, the flow field will appear as shown in figure a. the streamlines over the front of the cylinder are similar to theoretical predictions, as sketched at the right of Figure. However, because of viscous effects, the flow separates over the rear of the cylinder, creating a recirculating flow in the wake downstream of the body. This separated flow greatly contributes to the finite drag measured for the cylinder. On the other hand, figure a shows a reasonably symmetric flow about the horizontal axis, and the measurement of lift is essentially zero. Now let us spin the cylinder in a clockwise direction about its axis. The resulting flow fields are shown in figure b and c. For a moderate amount of spin b, the stagnation points move to the lower part of the cylinder, increased figure c, the stagnation point lifts off the surface, similar to the theoretical flow sketched in figure c. And what is most important, a finite lift is measured for the spinning cylinder in the wind tunnel. What is happening here? Why does spinning the cylinder produce lift? In actuality, the friction between the fluid and the surface of the cylinder tends to drag the fluid near the surface in the same direction as the rotational motion. Superimposed on top of the usual nonspinning flow, this “extra” velocity contribution creates a higher-than-usual velocity at the top of the cylinder and a lower-than-usual velocity at the bottom, as sketched in figure. These velocities are assumed to be just outside the viscous boundary layer on the surface. Recall from Bernoulli’s equation that as the velocity increases, the pressure decrease. Hence, from figure, the pressure on the top of the cylinder is lower than on the bottom. This pressure imbalance creates a net upward force, that is, a finite lift. Therefore, the theoretical prediction embodied in Equation that the flow over a circular cylinder can produce a finite lift is verified by experimental observation.

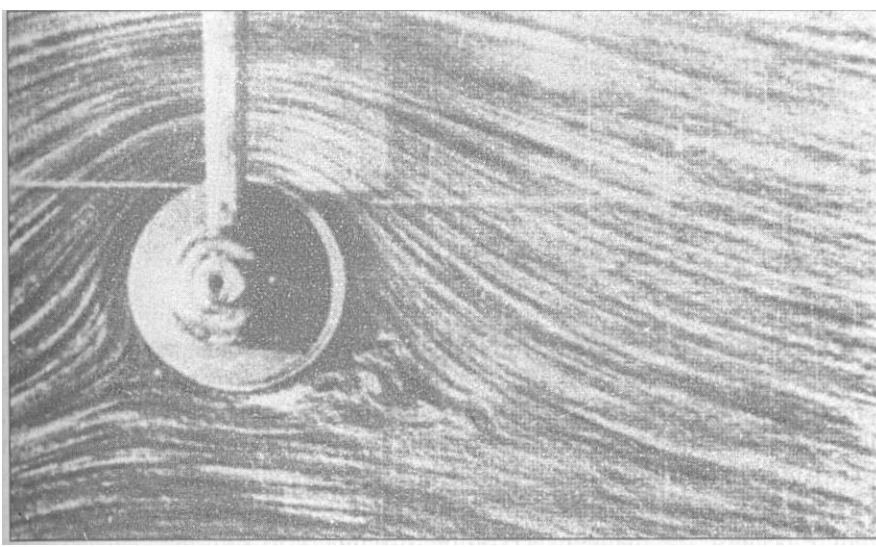
The general ideas discussed above concerning the generation of lift on a spinning circular cylinder in a wind tunnel also apply to a spinning sphere. This explains why a baseball pitcher can throw a curve

and how a golfer can hit a hook or slice—all of which are due to nonsymmetric flows about the spinning bodies, and hence the generation of an aerodynamic force perpendicular to the body's angular velocity vector. This phenomenon is called the Magnus effect, named after the German engineer who first observed and explained it in Berlin in 1852.

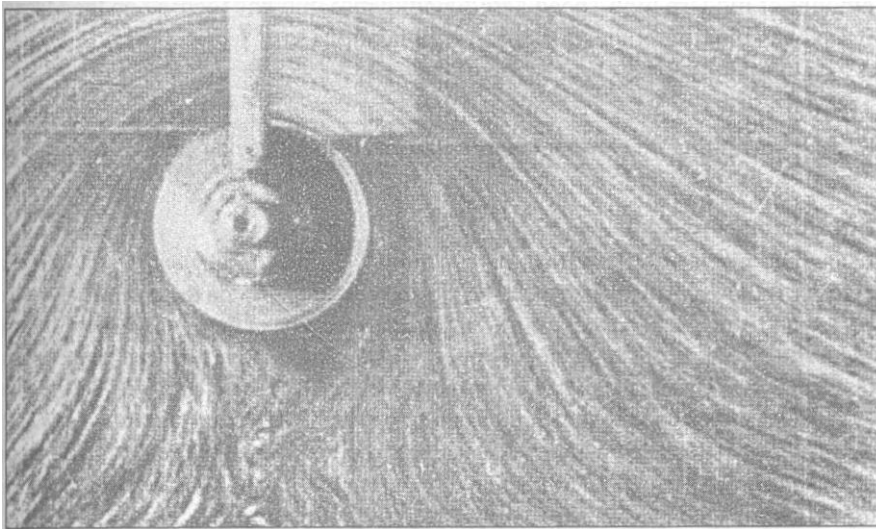
It is interesting to note that a rapidly spinning cylinder can produce a much higher lift than an airplane wing of the same planform area; however, the drag on the cylinder is also much higher than a well-designed wing. As a result, the



(a)



(b)



(c)

Figure: These flow-field pictures were obtained in water, where aluminium filings were scattered on the surface to show the direction of the streamlines. (a) Shown above is the case for the nonspinning cylinder. These flow-field pictures were obtained in water, where aluminium filings were scattered on the surface to show the direction of the streamlines. (b) Spinning cylinder: peripheral velocity of the surface =  $3V_\infty$ . (c) Spinning cylinder: peripheral velocity of the surface =  $6V_\infty$ . (Source: Prandtl and Tietjens,)

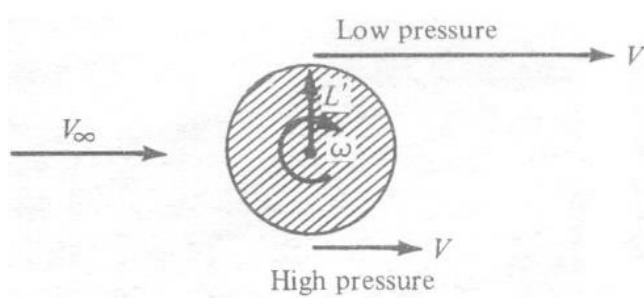


Figure: Creation of lift on a spinning cylinder.

Magnus effect is not employed for powered flight. On the other hand, in the 1920s, the German engineer Anton Flettner replaced the sail on a boat with a rotating circular cylinder with its axis vertical to the deck. In combination with the wind, this spinning cylinder provided propulsion for the boat. Moreover, by the action of two cylinders in tandem and rotating in opposite directions, Flettner was able to turn the boat around. Flettner's device was a technical success, but an economic failure because the maintenance on the machinery to spin the cylinders at the necessary high rotational speeds was too costly. Today, the Magnus effect has an important influence on the performance of spinning missiles; indeed, a certain amount of modern high-speed aerodynamic research has focused on the Magnus forces on spinning bodies for missile applications.

Example:

Consider the lifting flow over a circular cylinder. The lift coefficient is 5. Calculate the peak (negative) pressure coefficient.

Solution:

Examining figure, note that the maximum velocity for the nonlifting flow over a cylinder is  $2V_\infty$  and that it occurs at the top and bottom point on the cylinder. When the vortex in figure is added to the flow field, the direction of the vortex velocity is in the same direction as the flow on the top of the cylinder, but opposes the flow on the bottom of the cylinder. Hence, the maximum velocity for the lifting case occurs at the top of the cylinder and is equal to the sum of the nonlifting value,  $-2V_\infty$ , and the vortex,  $-\Gamma/2\pi R$ . (Note: We are still following the usual sign convention; since the velocity on the top of the cylinder is in the opposite direction of increasing  $\theta$  for the polar coordinate system, the velocity magnitudes here are negative.) Hence,

$$V = -2V_{\infty} - \frac{\Gamma}{2\pi R}$$

The lift coefficient and  $\Gamma$  are related through Equation

$$c_l = \frac{\Gamma}{RV_{\infty}} = 5$$

Hence, 
$$\frac{\Gamma}{R} = 5V_{\infty}$$

Substituting Equation into, we have

$$V = -2V_{\infty} - \frac{5}{2\pi} V_{\infty} = -2.796V_{\infty}$$

Substituting Equation into Equation, we obtain

$$C_p = -1 - \left( \frac{V}{V_{\infty}} \right)^2 = -1 - (2.796)^2 = \boxed{-6.82}$$

This example is designed in part to make the following point. Recall that, for an inviscid, incompressible flow, the distribution of  $C_p$  over the surface of a body depends only on the shape and orientation of the body-the flow properties such as velocity and density are irrelevant here. Recall Equation, which gives  $C_p$  as a function of  $\theta$  only, namely,  $C_p = 1 - 4 \sin^2\theta$ . However, for the case of lifting flow, the distribution of  $C_p$  over the surface is a function of one additional parameter-namely, the lift coefficient. Clearly, in this example, only the value of  $c_l$  is given. However, this is powerful enough to define the flow uniquely; the value of  $C_p$  at any point on the surface follows directly from the value of lift coefficient, as demonstrated in the above problem.

Example:

For the flow field in Example, calculate the location of the stagnation points and the points on the cylinder where the pressure equals freestream static pressure.

Solution:

From Equation, the stagnation points are given by

$$\theta = \arcsin\left(-\frac{\Gamma}{4\pi V_{\infty} R}\right)$$



From Example,

$$\frac{\Gamma}{RV_{\infty}} = 5$$

Thus,  $\theta = \arcsin\left(-\frac{5}{4\pi}\right) = \boxed{203.4^{\circ} \text{ and } 336.6^{\circ}}$

To find the locations where  $p = p_{\infty}$ , first construct a formula for the pressure coefficient on the cylinder surface:

$$C_p = 1 - \left(\frac{V}{V_{\infty}}\right)^2$$

where  $V = -2V_{\infty} \sin \theta - \frac{\Gamma}{2\pi R}$

Thus, 
$$C_p = 1 - \left(-2 \sin \theta - \frac{\Gamma}{2\pi R}\right)^2$$

$$= 1 - 4 \sin^2 \theta - \frac{2\Gamma \sin \theta}{\pi R V_{\infty}} - \left(\frac{\Gamma}{2\pi R V_{\infty}}\right)^2$$

From Example,  $\Gamma / RV_{\infty} = 5$ . thus,

$$C_p = 1 - 4 \sin^2 \theta - \frac{10}{\pi} \sin \theta - \left(\frac{5}{2\pi}\right)^2$$

$$= 0.367 - 3.183 \sin \theta - 4 \sin^2 \theta$$

A check on this equation can be obtained by calculating  $C_p$  at  $\theta = 90^{\circ}$  and seeing if it agrees with the result obtained in Example. For  $\theta = 90^{\circ}$ , we have

$$C_p = 0.367 - 3.183 - 4 = \boxed{-6.82}$$

This is the same result as in Example; the equation checks.

To find the values of  $\theta$  where  $p = p_{\infty}$ , set  $C_p = 0$ :

$$0 = 0.367 - 3.183 \sin \theta - 4 \sin^2 \theta$$

From the quadratic formula,

$$\sin \theta = \frac{3.183 \pm \sqrt{(3.183)^2 + 5.872}}{-8} = \boxed{-0.897 \text{ or } 0.102}$$

Hence,  $\theta = 243.8^\circ$  and  $296.23^\circ$

Also,  $\theta = 5.85^\circ$  and  $174.1^\circ$

There are four points on the circular cylinder where  $p = p_\infty$ . These are sketched in figure, along with the stagnation point locations. As shown in example, the minimum pressure occurs at the top of the cylinder and is equal to  $P_\infty - 6.82q_\infty$ . A local minimum pressure occurs at the bottom of the cylinder, where  $\theta = 3\pi/2$ . This local minimum is given by

$$\begin{aligned} C_p &= 0.367 - 3.183 \sin \frac{3\pi}{2} - 4 \sin^2 \frac{3\pi}{2} \\ &= 0.367 + 3.183 - 4 = \boxed{-0.45} \end{aligned}$$

Hence, at the bottom of the cylinder,  $p = p_\infty - 0.45q_\infty$ .

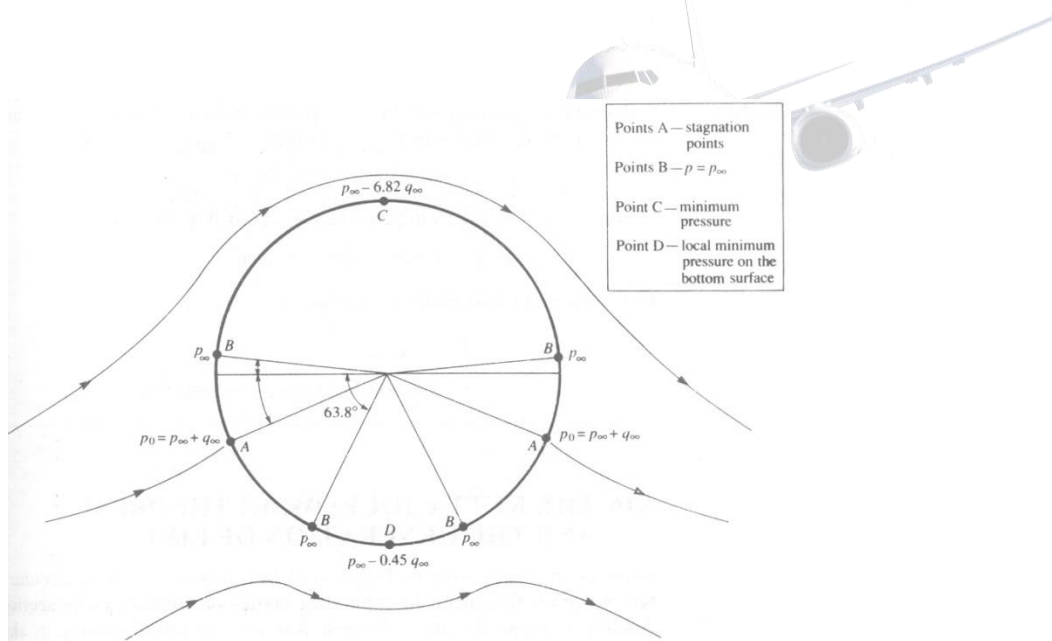


Figure: Value of pressure at various locations on the surface of a circular cylinder, lifting case with finite circulation. The values of pressure correspond to the case discussed in example.

Example:

Consider the lifting flow over a circular cylinder with a diameter of 0.5 m. The freestream velocity is 25 m/s, and the maximum velocity on the

surface of the cylinder is 75 m/s. The freestream conditions are those for a standard attitude of 3 km. Calculate the lift per unit span on the cylinder.

Solution:

From Appendix D, at an altitude of 3 km,  $\rho = 0.90926 \text{ kg/m}^3$ . The maximum velocity occurs at the top of the cylinder, where  $\theta = 90^\circ$ , From Equation.

$$V_\theta = -2V_\infty \sin \theta - \frac{\Gamma}{2\pi R}$$

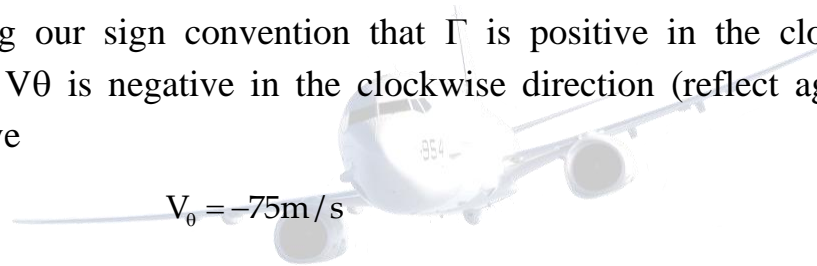
At  $\theta = 90^\circ$

$$V_\theta = -2V_\infty - \frac{\Gamma}{2\pi R}$$

or,

$$\Gamma = -2\pi R(V_\theta + 2V_\infty)$$

Recalling our sign convention that  $\Gamma$  is positive in the clockwise direction, and  $V_\theta$  is negative in the clockwise direction (reflect again on figure), we have



Hence,

$$\Gamma = -2\pi R(V_\theta + 2V_\infty) = -2\pi(0.25)[-75 + 2(25)]$$

$$\Gamma = -2\pi(0.25)(-25) = 39.27 \text{ m}^2/\text{s}$$

From Equation, the lift per unit span is

$$L' = \rho V_\infty \Gamma$$

$$L' = (0.90926)(25)(39.27) = \boxed{892.7 \text{ N}}$$

The Kutta-Joukowski theorem and the generation of lift.

Although the result given by Equation was derived for a circular cylinder, it applies in general to cylindrical bodies of arbitrary cross section. For example, consider the incompressible flow over an airfoil section, as sketched in figure. Let curve A be any curve in the flow enclosing the airfoil. If the airfoil is producing lift, the velocity field around the airfoil will be such that the line integral of velocity around A will be finite, that is, the circulation is finite. In turn, the lift per unit span  $L'$  on the airfoil will be given by the Kutta-Joukowski theorem, as embodied in Equation.



$$\Gamma \equiv \oint_A \mathbf{V} \cdot d\mathbf{s}$$

$$L' = \rho_\infty V_\infty \Gamma$$

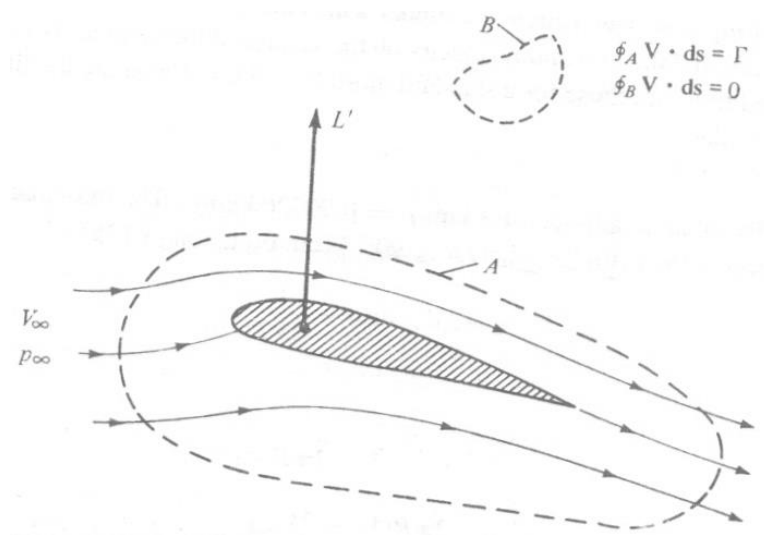


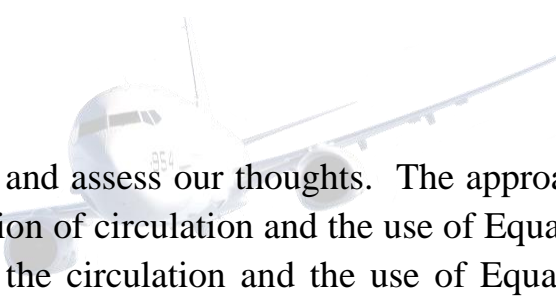
Figure: Circulation around a lifting airfoil.

This result underscores the importance of the concept of circulation, defined in section. The Kutta-Joukowski theorem states that lift per unit span on a two-dimensional body is directly proportional to the circulation around the body. Indeed, the concept of circulation is so important at this stage of our discussion that you should reread section before proceeding further.

The general derivation of Equation for bodies of arbitrary cross section can be carried out using the method of complex variables. Such mathematics is beyond the scope of this book. (It can be shown that arbitrary functions of complex variables are general solutions of Laplace's equation, equation, which in turn governs incompressible potential flow. Hence, more advanced treatments of such flows utilize the mathematics of complex variables as an important tool.

In section the lifting flow over a circular cylinder was synthesized by superimposing a uniform flow, a doublet, and a vortex. Recall that all three elementary flows are irrotational at all points, except for the vortex, which

has infinite vorticity at the origin. Therefore, the lifting flow over a cylinder as shown in Figure is irrotational at every point except at the origin. If we take the circulation around any curve not enclosing the origin, we obtain from equation the result that  $\Gamma = 0$ . It is only when we choose a curve that encloses the origin, where  $\nabla \times \mathbf{V}$  is infinite, that Equation yields a finite  $\Gamma$ , equal to the strength of the vortex. The same can be said about the flow over the airfoil in figure. As we show in chapter, the flow outside the airfoil is irrotational, and the circulation around any closed curve not enclosing the airfoil (such as curve B in figure) is consequently zero. On the other hand, we also show in chapter 4 that the flow over an airfoil is synthesized by distributing vortices either on the surface or inside the airfoil. These vortices have the usual singularities in  $\nabla \times \mathbf{V}$ , and therefore, if we choose a curve that encloses the airfoil (such as curve A in figure), Equation yields a finite value of  $\Gamma$ , equal to the sum of the vortex strengths distributed on or inside the airfoil. The important point here is that, in the Kutta-Joukowski theorem, the value of  $\Gamma$  used in Equation must be evaluated around a closed curve that encloses the body; the curve can be otherwise arbitrary, but it must have the body inside it.



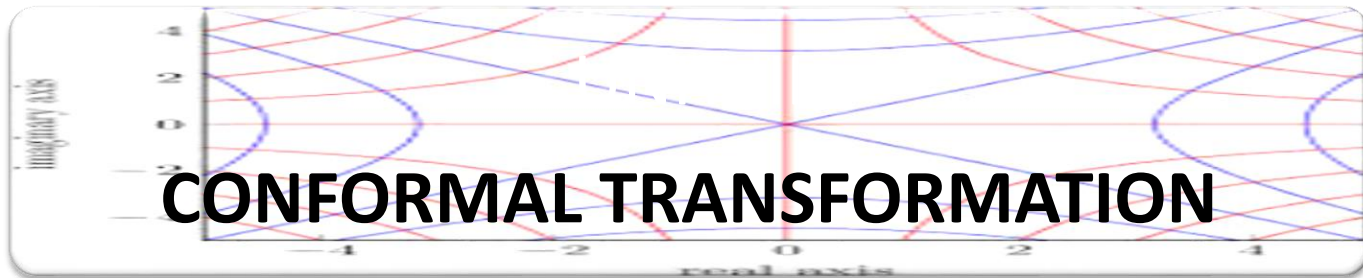
At this stage, let us pause and assess our thoughts. The approach we have discussed above—the definition of circulation and the use of Equation to obtain the lift—is the essence of the circulation theory of lift in aerodynamics. Its development at the turn of the twentieth century created a breakthrough in aerodynamics. However, let us keep things in perspective. The circulation theory of lift is an alternative way of thinking about the generation of lift on an aerodynamics body. Keep in mind that the true physical sources of aerodynamics force on a body are the pressure and shear stress distributions exerted on the surface of the body, as explained in section. The Kutta-Joukowski theorem is simply an alternative way of expressing the consequences of the surface pressure distribution; it is a mathematical expression that is consistent with the special tools we have developed for the analysis of inviscid, incompressible flow. Indeed that equation was derived in section by integrating the pressure distribution over the surface. Therefore it is not quite proper to say that circulation “causes” lift. Rather, lift is “caused” by the net imbalance of the surface pressure distribution, and circulation is simply a defined quantity determined from the same pressures. The relation between the surface pressure distribution (which produces lift  $L'$ ) and circulation is given by Equation. However, in the theory of incompressible, potential flow, it is generally much easier to

determine the circulation around the body rather than calculate the detailed surface pressure distribution. Therein lies the power of the circulation theory of lift.

Consequently, the theoretical analysis of lift on two-dimensional bodies in incompressible, inviscid flow focus on the calculation of the circulation about the body. Once  $\Gamma$  is obtained, then the lift per unit span follows directly from the Kutta-Joukowski theorem.



## UNIT III



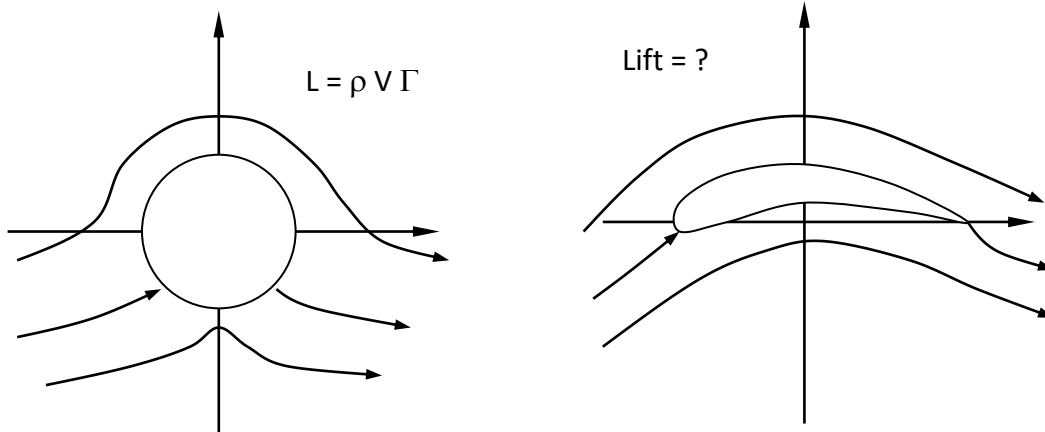
Joukowski transformation and its application to fluid flow problems, Kutta condition, Blasius theorem



# Introduction to Conformal Mapping in Aerodynamics

## Introduction

Conformal mapping is a method used to extend the application of potential flow theory to practical aerodynamics. Standard potential flow theory begins with an ideal flow to show that lift on a body is proportional to the circulation about a closed path encompassing an object. Potential flows start with flows over cylinders since the mathematics is more tractable. However, to use potential flow theory on usable airfoils one must rely on conformal mapping to show a relation between realistic airfoil shapes and the knowledge gained from flow about cylinders.



## Brief review of complex numbers:

Conformal mapping relies entirely on complex mathematics. Therefore, a brief review is undertaken at this point.

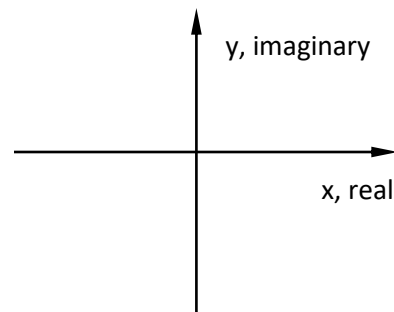
A complex number  $z$  is a sum of a real and imaginary part;  $z = \text{real} + i \cdot \text{imaginary}$

The term  $i$ , refers to the complex number  $i = \sqrt{-1}$

so that;  $i = \sqrt{-1}$ ,  $i^2 = -1$ ,  $i^3 = -i$ ,  $i^4 = 1$

Complex numbers can be presented in a graphical format. If the real portion of a complex number is taken as the abscissa, and the imaginary portion as the ordinate, a two-dimensional plane is formed.

$$z = \text{real} + i \cdot \text{imaginary} = x + i \cdot y$$



A complex number can be written in polar form using Euler's equation;

$$z = x + i \cdot y = r e^{i\theta} = r(\cos\theta + i \cdot \sin\theta)$$

where  $r^2 = x^2 + y^2$

Complex multiplication:  $z_1 \cdot z_2 = (x_1 + i y_1)(x_2 + i y_2) = (x_1 x_2 - y_1 y_2) + i(x_1 y_2 + y_1 x_2)$

$$= r_1 e^{i\theta_1} \cdot r_2 e^{i\theta_2} = r_1 r_2 \cdot e^{i(\theta_1 + \theta_2)}$$

## Complex representation of potential flows

The basic flows used in potential flow theory such as uniform flow, source, sink, doublet and vortex, can all be represented using complex numbers. For example, if a complex number  $w$  with both real and imaginary parts represents a potential flow, then the form of the number is;

$$w(z) = \phi + i\psi = (\text{velocity potential}) + i(\text{stream function})$$

Here, both velocity potential and stream function are themselves complex numbers. As an example, the uniform flow can be written;

$$\text{Uniform flow: } w(z) = V_\infty z = \phi + i\psi = V_\infty(x+iy) = V_\infty x + V_\infty y$$

$$\text{as seen previously, } \phi = V_\infty x = V_\infty r \cos \theta, \psi = V_\infty y = V_\infty r \sin \theta$$

Source flow:

$$w = \frac{\Lambda}{2\pi} \ln(z) = \phi + i\psi = \frac{\Lambda}{2\pi} \ln(re^{i\theta}) = \frac{\Lambda}{2\pi} (\ln(r) + i\theta) = \frac{\Lambda}{2\pi} \ln(r) + i \frac{\Lambda}{2\pi} \theta$$

Vortex flow:

$$w = i \frac{\Gamma}{2\pi} \ln(z) = \phi + i\psi = i \frac{\Gamma}{2\pi} \ln(re^{i\theta}) = i \frac{\Gamma}{2\pi} (\ln(r) + i\theta) = -\frac{\Gamma}{2\pi} \theta + i \frac{\Gamma}{2\pi} \ln(r)$$

Doublet flow:

$$w = \frac{k}{2\pi} \frac{1}{z} = \phi + i\psi = \frac{k}{2\pi} \frac{1}{re^{i\theta}} = \frac{k}{2\pi} \left( \frac{1}{r} e^{-i\theta} \right) = \frac{k}{2\pi} \frac{1}{r} (\cos \theta - i \sin \theta)$$

In complex terms the flow past a cylinder with lift is written:

$$w(z) = V_\infty \left( z + \frac{R^2}{z} \right) + i \frac{\Gamma}{2\pi} \ln(z)$$

### Velocity Components:

When a potential flow is represented in complex form, the velocity components can be found using one of two methods;

1. Re-write the expression from the complex variable  $z$  form into its separate real and complex components. The form of this expression will be  $w = \phi + i\psi$ . The individual velocity components are found by completing the appropriate differentiation on  $\phi$  or  $\psi$  to obtain  $u$  or  $v$ . As an example consider the complex form of the source flow;

$$w = \frac{\Lambda}{2\pi} \ln(z) = \phi + i\psi = \frac{\Lambda}{2\pi} \ln(r) + i \frac{\Lambda}{2\pi} \theta$$

$$V_r = \frac{\partial \phi}{\partial r} = \frac{\Lambda}{2\pi r} \quad V_\theta = \frac{\partial \phi}{\partial \theta} = 0$$

2. An alternative method would be to differentiate on the complex expression directly and then separate the real and complex portions to obtain the velocity components according to;

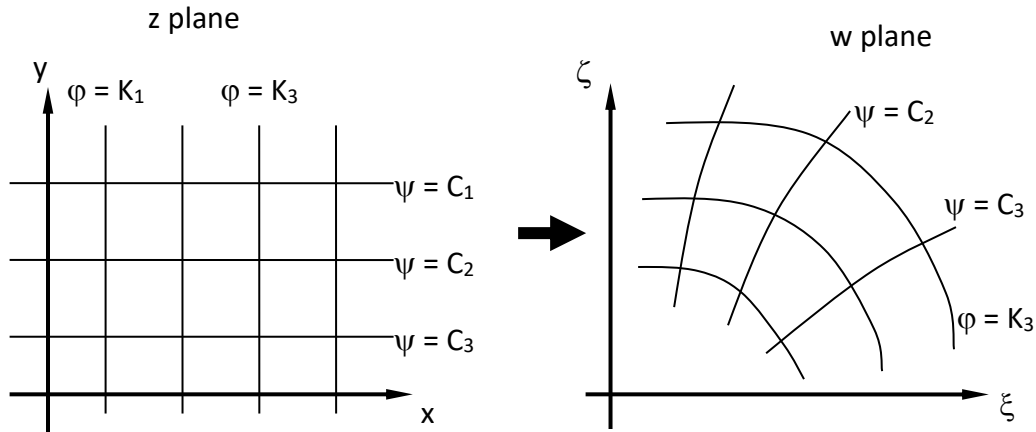
$$\frac{dw}{dz} = u - iv$$

### Conformal Mapping

A conformal mapping is performed through the transformation of a complex function from one coordinate system to another. A transformation function is applied to the original function to perform the mapping. For aerodynamics applications the Joukowski transform is the most commonly used function;

$$w = z + \frac{b^2}{z}$$

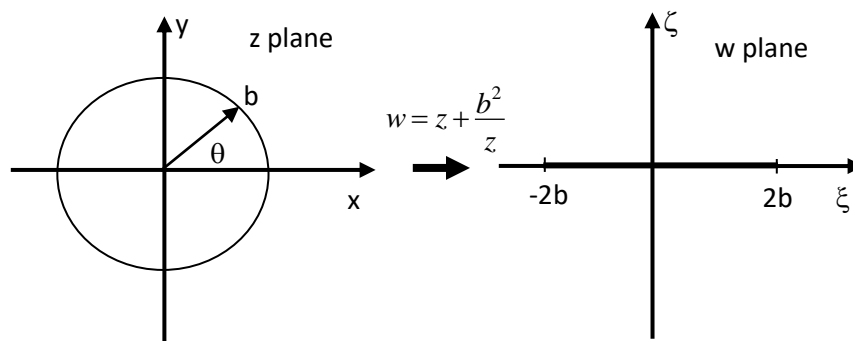
Here,  $b$  is a constant. Graphically, a conformal mapping will transform a complex plane in  $z$  ( $z = x+iy$ ) into a complex plane in a new variable  $w$  ( $w = \xi+i\zeta$ ).



In the diagram a uniform flow in the  $z$  plane is transformed into an equivalent form in the  $w$  plane using a transform of the form  $w = f(z)$ . As an example consider a circle drawn in the  $z$  plane,  $z = be^{i\theta}$ . The Joukowski transform maps the circle into a flat plate,

$$w = z + \frac{b^2}{z}$$

$$w = be^{i\theta} + \frac{b^2}{be^{i\theta}} = be^{i\theta} + be^{-i\theta} = 2b \cos(\theta) + i0$$

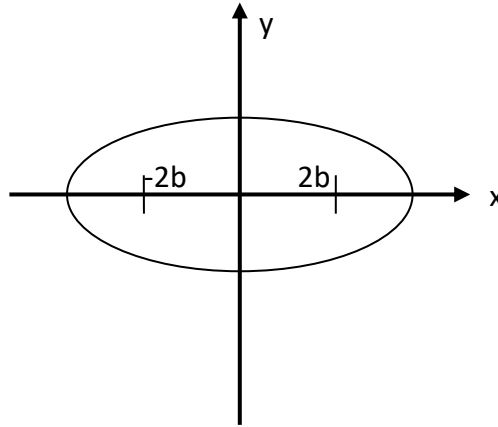


A circle of radius  $b$  is mapped into a straight line in the  $w$  plane entirely on the real axis between  $-2b$  and  $2b$ . If a uniform flow had been drawn over the circle, the transform would have mapped that flow into the flow over a flat plate in the  $w$  plane. If the circle originally had a radius slightly larger than the transform constant  $b$ ,  $z = ae^{i\theta}$ , with  $a > b$ , the circle would have formed an ellipse instead of the flat plate.

$$w = z + \frac{b^2}{z} = ae^{i\theta} + \frac{b^2}{ae^{i\theta}} = \left(a + \frac{b^2}{a}\right) \cos(\theta) + i \left(a - \frac{b^2}{a}\right) \sin(\theta) = x + iy$$

Which can be written,

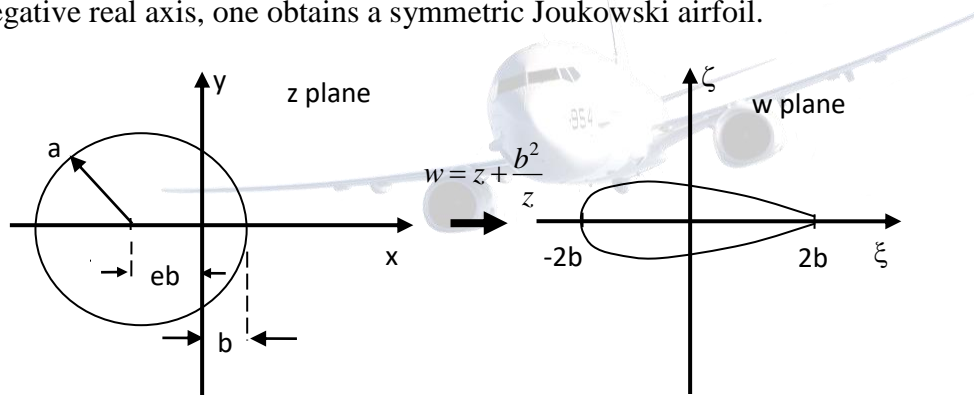
$$\frac{x^2}{\left(a + \frac{b^2}{a}\right)^2} + \frac{y^2}{\left(a - \frac{b^2}{a}\right)^2} = 1$$



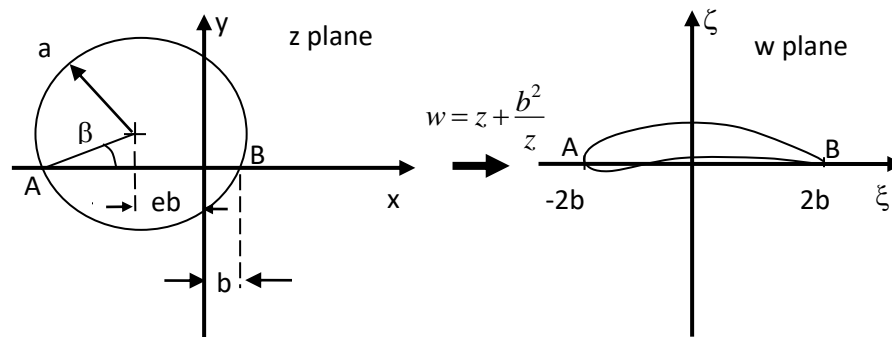
If the flow over a cylinder had been transformed it would have created the flow over an ellipse.

### Joukowski Airfoils

From an aerodynamics point of view, the most interesting application of the Joukowski transform is to an offset circle. If we consider a circle slightly offset from the origin along the negative real axis, one obtains a symmetric Joukowski airfoil.

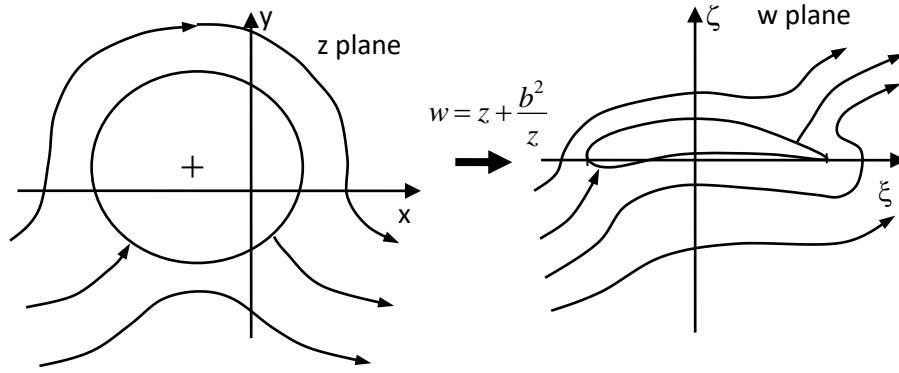


The equation of the offset circle is  $z = ae^{i\theta} - eb$  where the constant  $e$  is a small number. If the cylinder is displaced slightly along the complex axis as well, one obtains a cambered airfoil shape.

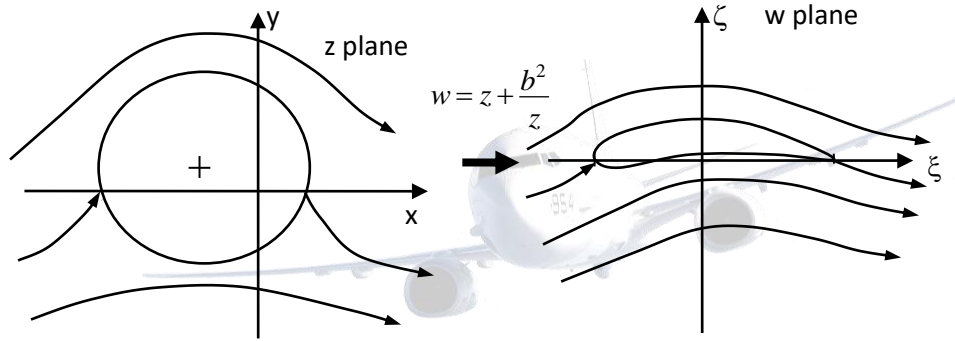


Here, the points  $A$  and  $B$  are the intercepts of the displaced circle on the real axis and their corresponding points in the transformed plane. The angle  $\beta$  is the angle formed by the line joining the point  $A$  (or  $B$ ) and the origin with the real axis. If lifting flow about the original circle had been imposed, the Joukowski transformation would have generated a lifting flow about the Joukowski airfoil;





Although such a flow is mathematically possible, in reality it may not be realistic. The stagnation points on the cylinder map to stagnation points that are not always realistic. For instance the stagnation point on the top surface of the airfoil cannot exist in steady flight since the velocity would tend to infinity as one moves very close to the trailing edge. The only means of making a realistic flow is to impose the Kutta condition where the stagnation point is forced to exist at the trailing edge thus making the streamlines flow smoothly from this point. This is done by adjusting the value of vorticity strength  $\Gamma$ , such that the stagnation points on the cylinder reside at the cylinder's intercepts of the real axis. In this case, when the cylinder is transformed, one stagnation point will be forced to the trailing edge.



The lift force generated by the lifting flow over the cylinder is proportional to the circulation about the cylinder imposed by the added vortex flow according to the Kutta-Joukowski relation,  $L' = \rho V_\infty \Gamma$ . The lifting force on the resulting Joukowski airfoil is not clear. To evaluate the lift, the circulation is needed and therefore the velocity field. The velocity fields in each plane can be related to each other through the chain rule of differentiation. If the lifting flow about the cylinder is defined as function  $Q$  where  $Q = Q(z)$  in the  $z$  plane and  $Q = Q(w)$  in the  $w$  plane, the velocities in each plane are;

$$V_z = \frac{\partial Q}{\partial z} \quad V_w = \frac{\partial Q}{\partial w}$$

By chain rule:

$$\frac{\partial Q}{\partial z} = \frac{\partial Q}{\partial w} \frac{\partial w}{\partial z}$$

$$V_z = V_w \frac{\partial w}{\partial z}$$

Using the Joukowski transformation;

$$\frac{\partial w}{\partial z} = \frac{z^2 - b^2}{z^2}$$

Clearly, the velocity field very close to the cylinder and its transformed counterpart are dissimilar as one would expect. However, farther away from these objects the velocity fields become identical as the magnitude of  $z$  becomes larger than the constant value of  $b$ . Since the circulation can be calculated about any closed path, including paths very far from the object surface, the circulations must be the same in both planes.

$$\rho V_{\infty} \Gamma_{\text{cylinder}} = \rho V_{\infty} \Gamma_{\text{Joukowski}}$$

### Vortex strength

The appropriate vortex strength to impose the Kutta condition must be determined. Consider the lifting flow about a cylinder. The velocity in the  $\theta$  direction is,

$$V_{\theta} = -\left(2V_{\infty} \sin(\theta) + \frac{\Gamma}{2\pi R}\right)$$

Here,  $R$  is the radius of the cylinder surface.

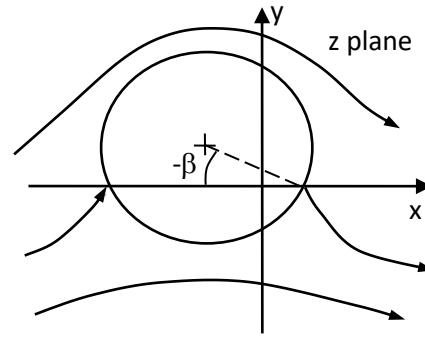
This velocity is zero on the surface of the cylinder at the stagnation points. At these points  $\theta = -\beta$ .

$$0 = 2V_{\infty} \sin(\beta) - \frac{\Gamma}{2\pi R}$$

$$\Gamma = 4\pi V_{\infty} R \sin(\beta)$$

If the field is rotated by  $\alpha$  to simulate an angle of attack,

$$\Gamma = 4\pi V_{\infty} R \sin(\beta + \alpha)$$



Since the chord length of the Joukowski airfoil is  $4b$ , the lift coefficient can be written,

$$C_L = \frac{L'}{\frac{1}{2} \rho V_{\infty}^2 c} = \frac{\rho V \Gamma}{\frac{1}{2} \rho V_{\infty}^2 4b} = \frac{\Gamma}{2V_{\infty}^2 b} = \frac{4\pi V_{\infty}^2 R \sin(\alpha + \beta)}{2V_{\infty}^2 b}$$

Making the assumption that  $b \approx R$ ,

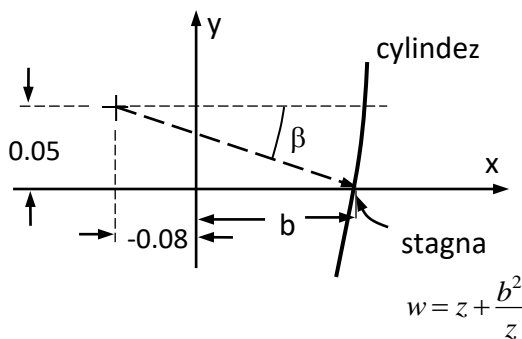
$$C_L = 2\pi \sin(\alpha + \beta) \approx 2\pi(\alpha + \beta)$$

### Example

A Joukowski airfoil is formed by displacing a circle of radius 1 by  $\Delta x = -0.08$  (real axis) and  $\Delta y = 0.05$  (imaginary axis). Find,

a) Vortex strength  $\Gamma$  if  $\alpha = 0^\circ$ , and  $V_{\infty} = 10$  m/s

b)  $C_L$  at  $\alpha = 0^\circ$  and  $\alpha = 10^\circ$



$$\beta = \sin^{-1}\left(\frac{0.05}{1}\right) = 2.87^\circ$$

$$\tan(2.87^\circ) = \frac{0.05}{0.08 + b}$$

$$b = 0.9187$$

$$4\pi(10)(1)\sin(2.87) = 6.2831$$

$$\text{a) } \Gamma = 4\pi V_{\infty} R \sin(\alpha + \beta) =$$

$$\text{b) } C_L = 2\pi\sin(2.87) = 0.31415$$

$$C_L = 2\pi\sin(10 + 2.87) = 1.40$$

Nonlifting flows over arbitrary bodies: The numerical source panel method:

In this section, we return to the consideration of nonlifting flows. Recall that we have already dealt with the nonlifting flows over a semi-infinite body and a Rankine oval and both the nonlifting and the lifting flows over a circular cylinder. For those cases, we added our elementary flows in certain ways and discovered that the dividing streamlines turned out to first the shapes of such special bodies. However, this indirect method of starting with a given combination of elementary flows and seeing what body shape comes out of it can hardly be used in a practical sense for bodies of arbitrary shape. For example, consider the airfoil in figure. Do we know in advance the correct combination of elementary flows to synthesize the flow over this specified body? The purpose of this section is to present such a direct method, limited for the present to nonlifting flows. We consider a numerical method, limited for the present to nonlifting flows. We consider a numerical method appropriate for solution on a high-speed digital computer. The technique is called the source panel method, which, since the late 1960s, has become a standard aerodynamic tool in industry and most research laboratories. In fact, the numerical solution of potential flows by both source and vortex panel techniques has revolutionized the analysis of low-speed flows. We return to various numerical panel techniques in through. As a modern student of aerodynamics, it is necessary for you to become familiar with the fundamentals of such panel methods. The purpose of the present section is to introduce the basic ideas of the source panel method, which is a technique for the numerical solution of nonlifting flows over arbitrary bodies.

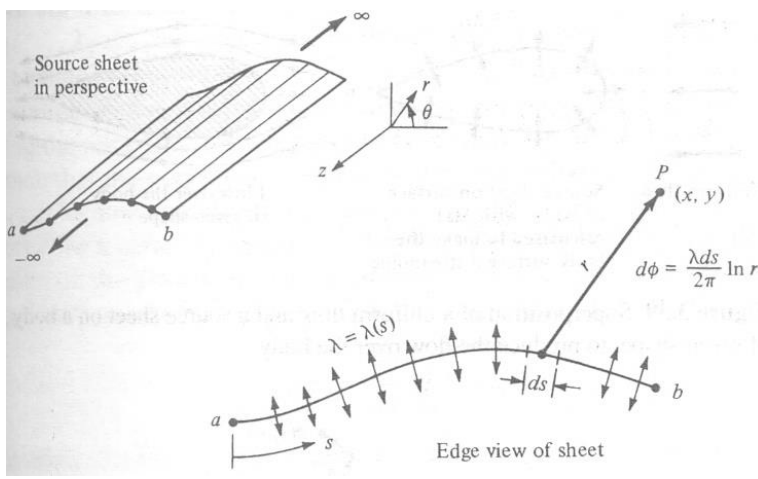


Figure: Source sheet

First, let us extend the concept of a source or sink introduced in section. In that section, we dealt with a single line source, as sketched in figure. Now imagine that we have an infinite number of such line sources side by side, where the strength of each line source is infinitesimally small. These side-by-side line sources form a source sheet, as shown in perspective in the upper left of figure. If we look along the series of line sources (looking along the  $z$  axis in figure. Here, we are looking at an edge view of the sheet; the line sources are all perpendicular to the page. Let  $s$  be the distance measured along the source sheet in the edge view. Define  $\lambda = \lambda(s)$  to be the source strength per unit length along  $s$ . [To keep things in perspective, recall from section that the strength of a single line source  $\Lambda$  was defined as the volume flow rate per unit depth, that is, per unit length in the  $z$  direction. Typically unit for  $\Lambda$  are square meters per second or square feet per second. in turn, the strength of a source sheet  $\lambda(s)$  is the volume flow rate per unit depth (in the  $z$  direction) and per unit length (in the  $s$  direction.) Typical unit for  $\lambda$  are meters per second or feet per second]. Therefore, the strength of an infinitesimal portion  $ds$  of the sheet, as shown in Figure is  $\lambda ds$ . This small section of the source sheet can be treated as a distinct source of strength  $\lambda ds$ . Now consider point  $P$  in the flow, located a distance  $r$  from  $ds$ ; the Cartesian coordinates of  $P$  are  $(x,y)$ . The small section of the source sheet of strength  $\lambda ds$  induces an infinitesimally small potential  $d\phi$  at point  $P$ . From Equation,  $d\phi$  is given by

$$d\phi = \frac{\lambda ds}{2\pi} \ln r$$

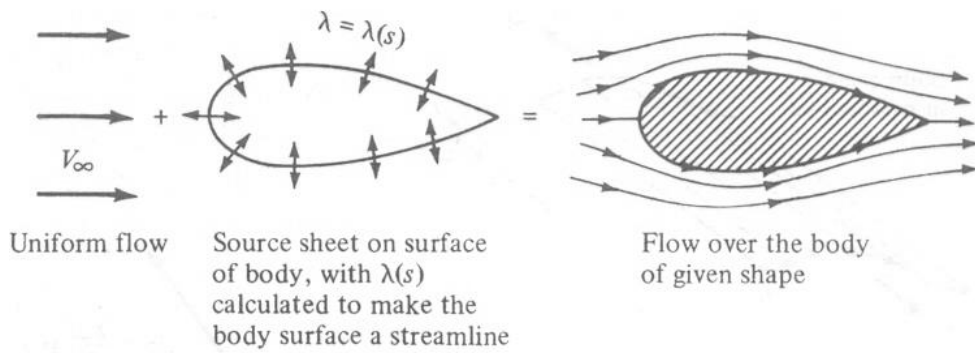


Figure: Superposition of a uniform flow and a source sheet on a body of given shape, to produce the flow over the body.

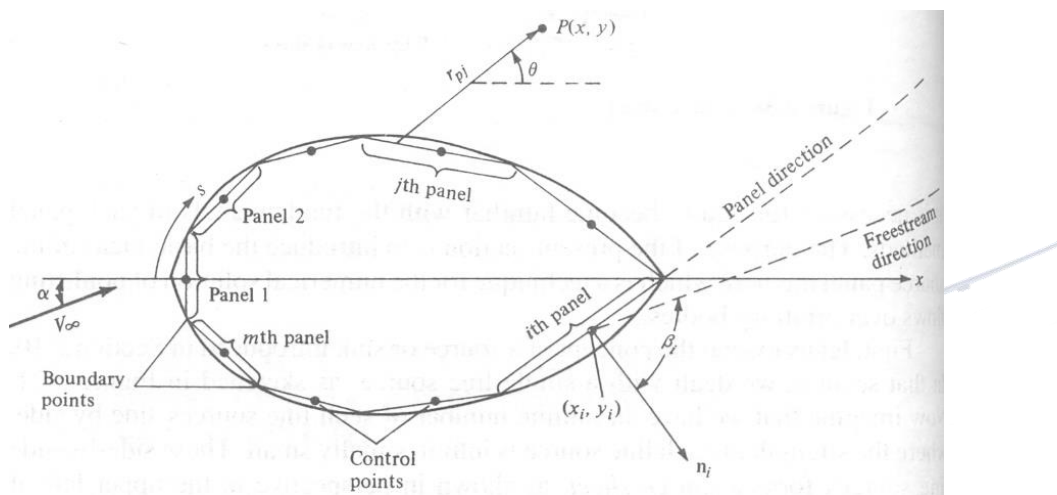


Figure: Source panel distribution over the surface of a body of a arbitrary shape.

The complete velocity potential at point P, induced by the entire source sheet from a to b, is obtained by integrating Equation:

$$\phi(x, y) = \int_a^b \frac{\lambda ds}{2\pi} \ln r$$

Note that, in general,  $\lambda(s)$  can change from positive to negative along the sheet; that is, the “source” sheet is really a combination of line sources and line sinks.

Next, consider a given body of arbitrary shape in a flow with freestream velocity  $V_\infty$ , as shown in figure. Let us cover the surface of the prescribed body with a source sheet, where the strength  $\lambda(s)$  varies in such a fashion that the combined action of the uniform flow and the source sheet makes the airfoil surface a streamline of the flow. Our problem now becomes one of finding the appropriate  $\lambda(s)$ . The solution of this problem is carried out numerically, as follows.

Let us approximate the source sheet by a series of straight panels, as shown in figure. Moreover, let the source strength  $\lambda$  per unit length be constant over a given panel, but allow it to vary from one panel to the next. That is, if there are a total of  $n$  panels, the source panels strengths per unit length are  $\lambda_1, \lambda_2, \dots, \lambda_j, \dots, \lambda_n$ . These panel strengths are unknowns; the main thrust of the panel technique is to solve for  $\lambda_j, j=1$  to  $n$ , such that the body surface becomes a streamline of the flow. This boundary condition is imposed numerically by defining the midpoint of each panel to be a control point and by determining the  $\lambda_j$ 's such that the normal component of the flow velocity is zero at each control point. Let us now quantify this strategy.

Let  $P$  be a point located at  $(x, y)$  in the flow, and let  $r_{pj}$  be the distance from any point on the  $j$ th panel to  $P$ , as shown in figure. The velocity potential induced at  $P$  due to the  $j$ th panel  $\Delta\phi_j$  is, from Equation,

$$\Delta\phi_j = \frac{\lambda_j}{2\pi} \int_j \ln r_{pj} ds_j$$

In Equation,  $\lambda_j$  is constant over the  $j$ th panel, and the integral is taken over the  $j$ th panel only. In turn, the potential at  $P$  due to all the panels is Equation summed over all the panels:

$$\phi(P) = \sum_{j=1}^n \Delta\phi_j = \sum_{j=1}^n \frac{\lambda_j}{2\pi} \int_j \ln r_{pj} ds_j$$

In Equation, the distance  $r_{pj}$  is given by

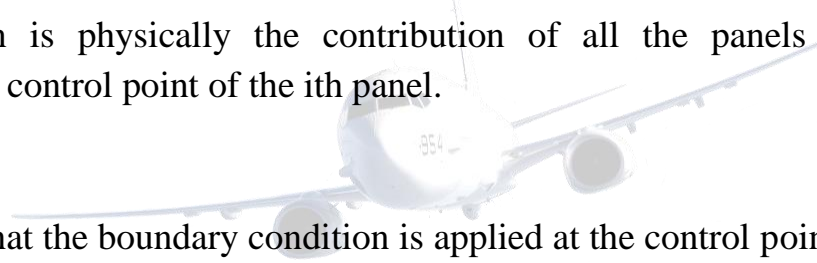
$$r_{pj} = \sqrt{(x - x_j)^2 + (y - y_j)^2}$$

where  $(x_j, y_j)$  are coordinates along the surface of the  $j$ th panel. Since point P is just an arbitrary point in the flow, let us put P at the control point of the  $j$ th panel. Let the coordinates of this control point be given by  $(x_i, y_i)$ , as shown in figure. Then Equations and become

$$\phi(x_i, y_i) = \sum_{j=1}^n \frac{\lambda_j}{2\pi} \int_j \ln r_{ij} ds_j$$

and 
$$r_{ij} = \sqrt{(x_i - x_j)^2 + (y_i - y_j)^2}$$

Equation is physically the contribution of all the panels to the potential at the control point of the  $i$ th panel.



Recall that the boundary condition is applied at the control points; that is, the normal component of the flow velocity is zero at the control points. To evaluate this component, first consider the component of freestream velocity perpendicular to the panel. Let  $n_i$  be unit vector normal to the  $i$ th panel, directed out of the body, as shown in figure. Also, note that the slope of the  $i$ th panel is  $(dy/dx)_i$ . In general, as shown in figure. Therefore, inspection of the geometry of figure reveals that the component of  $V_\infty$  normal to the  $i$ th panel is

$$V_{\infty, n} = V_\infty \cdot n_i = V_\infty \cos \beta_i$$

where  $\beta_i$  is the angle between  $V_\infty$  and  $n_i$ . Note that  $V_{\infty, n}$  is positive when directed away from the body, and negative when directed toward the body.

The normal component of velocity induced at  $(x_i, y_i)$  by the source panels is, from Equation,

$$V_n = \frac{\partial}{\partial n_i} [\phi(x_i, y_i)]$$

Where the derivative is taken in the direction of the outward unit normal vector, and hence, again,  $V_n$  is positive when directed away from the body. When the derivative in Equation is carried out,  $r_{ij}$  appears in the denominator. Consequently, a singular point arises on the  $i$ th panel because when  $j = i$ , at the control point itself  $r_{ij} = 0$ . It can be shown that when  $j = i$ , the contribution to the derivative is itself  $r_{ij} = 0$ . It can be shown that when  $j = i$ , the contribution to the derivative is simply  $\lambda_i / 2$ . Hence, Equation combined with Equation becomes

$$V_n = \frac{\lambda_i}{2} + \sum_{\substack{j=1 \\ (j \neq i)}}^n \frac{\lambda_j}{2\pi} \int_j \frac{\partial}{\partial n_i} (\ln r_{ij}) ds_j$$

In Equation, the first term  $\lambda_i / 2$  is the normal velocity induced at the  $i$ th control point by the  $i$ th panel itself, and the summation is the normal velocity induced at the  $i$ th control point by all the other panels.

The normal component of the flow velocity at the  $i$ th control point is the sum of that due to the freestream [Equation and that due to the source panels equation. The boundary condition states that this sum must be zero:

$$V_{\infty, n} + V_n = 0$$

Substituting Equation and into, we obtain

$$\frac{\lambda_i}{2} + \sum_{\substack{j=1 \\ (j \neq i)}}^n \frac{\lambda_j}{2\pi} \int_j \frac{\partial}{\partial n_i} (\ln r_{ij}) ds_j + V_{\infty} \cos \beta_i = 0$$



Equation is the crux of the source panel method. The values of the integrals in Equation depend simply on the panel geometry; they are not properties of the flow. Let  $I_{i,j}$  be the value of this integral when the control point is on the  $i$ th panel and the integral is over the  $j$ th panel. Then Equation can be written as

$$\frac{\lambda_i}{2} + \sum_{\substack{j=1 \\ (j \neq i)}}^n \frac{\lambda_j}{2\pi} I_{i,j} + V_\infty \cos \beta_i = 0$$

Equation is a linear algebraic equation with  $n$  unknowns  $\lambda_1, \lambda_2, \dots, \lambda_n$ . It represents the flow boundary condition evaluated at the control point of the  $i$ th panel. Now apply the boundary condition to the control points of all the panels; that is, in equation, let  $i = 1, 2, \dots, n$ . The results will be a system of  $n$  linear algebraic equations with  $n$  unknowns  $(\lambda_1, \lambda_2, \dots, \lambda_n)$ , which can be solved simultaneously by conventional numerical methods.

Look what has happened! After solving the system of equation represented by Equation with  $i = 1, 2, \dots, n$ , we now have the distribution of source panel strengths which, in an appropriate fashion, cause the body surface in figure to be a streamline of the flow. This approximation can be made more accurate by increasing the number of panels, hence more closely representing the source sheet of continuously varying strength  $\lambda(s)$  shown in figure. Indeed, the airfoil is accurately represented by as few as 8 panels, and most airfoil shapes, by 50 to 100 panels. (for an airfoil, it is desirable to cover the leading-edge region with a number of small panels to represent accurately the rapid surface curvature and the use larger panels over the relatively flat portions of the body. Note that, in general, all the panels in figure can be different lengths.)

Once the  $\lambda_i$ 's ( $i = 1, 2, \dots, n$ ) are obtained, the velocity tangent to the surface at each control point can be calculated as follows. Let  $s$  be the distance along the body surface, measured positive from front to rear, as shown in figure. The component of freestream velocity tangent to the surface is

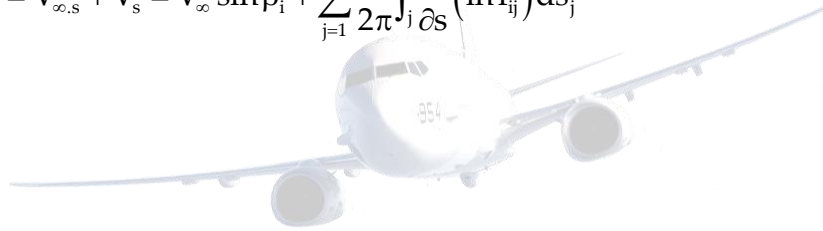
$$V_{\infty, s} = V_\infty \sin \beta_i$$

The tangential velocity  $V_s$  at the control points of the  $i$ th panel induced by all the panels is obtained by differentiating Equation with respect to  $s$ :

$$V_s = \frac{\partial \phi}{\partial s} = \sum_{j=1}^n \frac{\lambda_j}{2\pi} \int_j \frac{\partial}{\partial s} (\ln r_{ij}) ds_j$$

[The tangential velocity on a flat source panel induced by the panel itself is zero; hence, in Equation, the term corresponding to  $j = I$  is zero. This is easily seen by intuition, because the panel can only emit volume flow from its surface in a direction perpendicular to the panel itself]. The total surface velocity at the  $i$ th control point  $V_i$  is the sum of the contribution from the freestream [Equation] and from the source panels [Equation]:

$$V_i = V_{\infty, s} + V_s = V_{\infty} \sin \beta_i + \sum_{j=1}^n \frac{\lambda_j}{2\pi} \int_j \frac{\partial}{\partial s} (\ln r_{ij}) ds_j$$



In turn, the pressure coefficient at the  $i$ th control point is obtained from Equation:

$$C_{p,i} = 1 - \left( \frac{V_i}{V_{\infty}} \right)^2$$

In this fashion, the source panel method gives the pressure distribution over the surface of a nonlifting body of a arbitrary shape.

When you carry out a source panel solution as described above, the accuracy of your results can be tested as follows. Let  $S_j$  be the length of the  $j$ th panel. Recall that  $\lambda_j$  is the strength of the  $j$ th panel per unit length. Hence, the strength of the  $j$ th panel itself is  $\lambda_j S_j$ . For a closed body, such as in figure, the sum of all the source and sink strength must be zero, or else the body itself would be adding or absorbing mass from the flow—an impossible

situation for the case we are considering here. Hence, the values of the  $\lambda_j$  obtained above should obey the relation

$$\sum_{j=1}^n \lambda_j S_j = 0$$

Equation provides an independent check on the accuracy of the numerical results.

Example:

Calculate the pressure coefficient distribution around a circular cylinder using the source panel technique.

Solution:

We choose to cover the body with eight panels of equal length, as shown in figure. This choice is arbitrary; however, experience has shown that, for the case of a circular cylinder, the arrangement shown in figure provides sufficient accuracy. The panels are numbered from 1 to 8, and the control points are shown by the dots in the center of each panel.

Let us evaluate the integrals  $I_{i,j}$  which appear in equation. Consider figure, which illustrates two arbitrary chosen panels. In figure,  $(x_i, y_i)$  are the coordinates of the control point of the  $i$ th panel and  $(x_j, y_j)$  are the running coordinates over the entire  $j$ th panel. The coordinates of the boundary points for the  $i$ th panel are  $(X_i, Y_i)$  and  $(X_{i+1}, Y_{i+1})$ . In this problem,  $V_\infty$  is in the  $x$  direction; hence, the angles between the  $x$  axis and the unit vectors  $n_i$  and  $n_j$  are  $\beta_i$  and  $\beta_j$ , respectively. Note that, in general, both  $\beta_i$  and  $\beta_j$  vary from 0 to  $2\pi$ . Recall that the integral  $I_{i,j}$  is evaluated at the  $i$ th control point and the integral is taken over the complete  $j$ th panel:

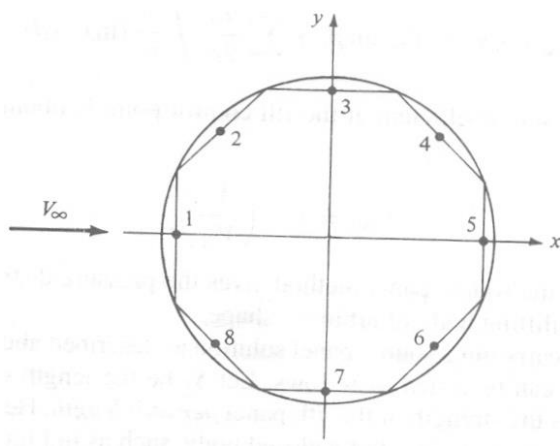


Figure: Source panel distribution around a circular cylinder.

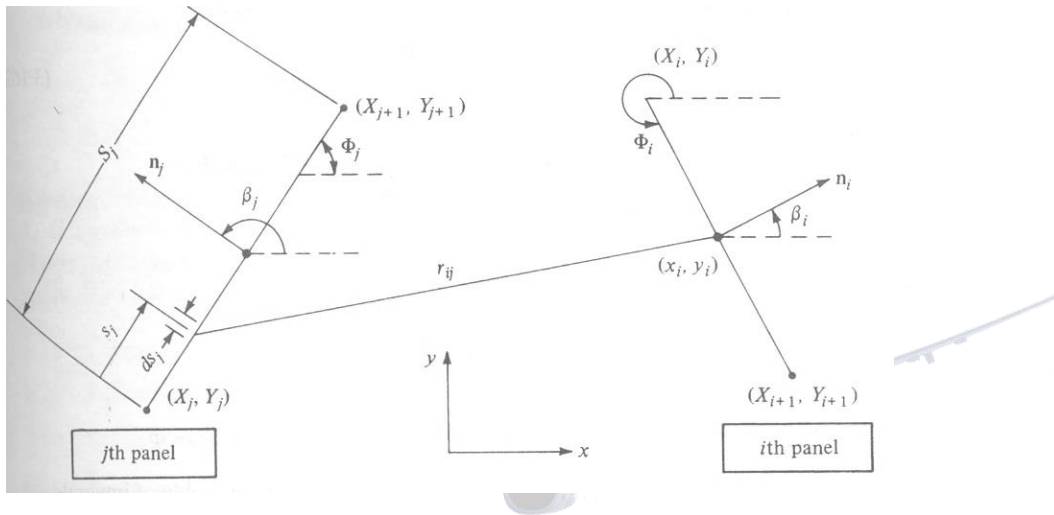


Figure: Geometry required for the evaluation of  $I_{ij}$ .

$$I_{i,j} = \int_j \frac{\partial}{\partial n_i} (\ln r_{ij}) ds_j$$

Since

$$r_{ij} = \sqrt{(x_i - x_j)^2 + (y_i - y_j)^2}$$

then

$$\frac{\partial}{\partial n_i} (\ln r_{ij}) = \frac{1}{r_{ij}} \frac{\partial r_{ij}}{\partial n_i}$$

$$= \frac{1}{r_{ij}} \frac{1}{2} \left[ (x_i - x_j)^2 + (y_i - y_j)^2 \right]^{-1/2} \\ \times \left[ 2(x_i - x_j) \frac{dx_i}{dn_i} + 2(y_i - y_j) \frac{dy_i}{dn_i} \right]$$

or

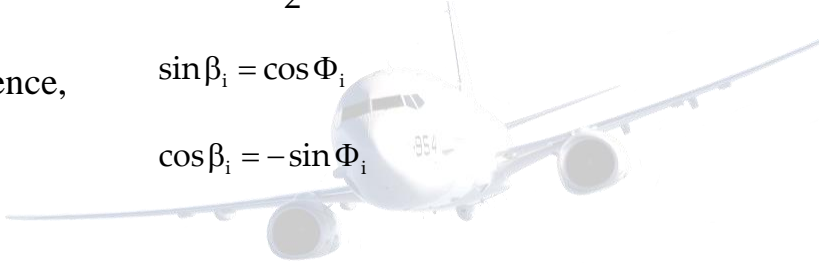
$$\frac{\partial}{\partial n_i} (\ln r_{ij}) = \frac{(x_i - x_j) \cos \beta_i + (y_i - y_j) \sin \beta_i}{(x_i - x_j)^2 + (y_i - y_j)^2}$$

Note in figure that  $\Phi_i$  and  $\Phi_j$  are angles measured in the counter clockwise direction from the x axis to the bottom of each panel. From this geometry.

$$\beta_i = \Phi_i + \frac{\pi}{2}$$

Hence,

$$\sin \beta_i = \cos \Phi_i$$

$$\cos \beta_i = -\sin \Phi_i$$


Also, from the geometry of Figure, we have

$$x_j = X_j + s_j \cos \Phi_j$$

and

$$y_j = Y_j + s_j \sin \Phi_j$$

Substituting Equation to into, we obtain

$$I_{i,j} = \int_0^{s_j} \frac{Cs_j + D}{s_j^2 + 2As_j + B} ds_j$$

where  $A = -(x_i - X_j) \cos \Phi_j - (y_i - y_j) \sin \Phi_j$

$$B = (x_i - X_j)^2 + (y_i - Y_j)^2$$

$$C = \sin(\Phi_i - \Phi_j)$$

$$D = (y_i - Y_j) \cos \Phi_i - (x_i - X_j) \sin \Phi_i$$

$$S_j = \sqrt{(X_{j+1} - X_j)^2 + (Y_{j+1} - Y_j)^2}$$

Letting  $E = \sqrt{B - A^2} = (x_i - X_j) \sin \Phi_j - (y_i - Y_j) \cos \Phi_j$

we obtain an expression for Equation from any standard table of integrals:

$$I_{i,j} = \frac{C}{2} \ln \left( \frac{S_j^2 + 2AS_j + B}{B} \right) + \frac{D - AC}{E} \left( \tan^{-1} \frac{S_j + A}{E} - \tan^{-1} \frac{A}{E} \right)$$

Equation is a general expression for two arbitrarily oriented panel; it is not restricted to the case of a circular cylinder.

We now apply Equation to the circular cylinder shown in figure. For purposes of illustration, let us choose panel 4 as the  $i$ th panel and panel 2 as the  $j$ th panel; that is, let us calculated  $I_{4,2}$ . From the geometry of Figure, assuming a unit radius for the cylinder, we see that

$$\begin{array}{lll} X_j = -0.9239 & X_{j+1} = -0.3827 & Y_j = 0.3827 \\ Y_{j+1} = 0.9239 & \Phi_i = 315^\circ & \Phi_j = 45^\circ \\ x_i = 0.6553 & y_i = 0.6533 & \end{array}$$

Hence, substituting these numbers into the above formulas, we obtain

$$A = -1.3065 \quad B = 2.5607 \quad C = -1 \quad D = 1.3065$$

$$S_j = 0.7654 \quad E = 0.9239$$

Inserting the above values into Equation, we obtain

$$I_{4,2} = 0.4018$$

Return to Figure and. If we now choose panel 1 as the  $j$ th panel, keeping panel 4 as the  $i$ th panel, we obtain, by means of a similar calculation,  $I_{4,1} = 0.4074$ . Similarly,  $I_{4,3} = 0.3528$ ,  $I_{4,5} = 0.3528$ ,  $I_{4,6} = 0.4018$ ,  $I_{4,7} = 0.4074$ , and  $I_{4,8} = 0.4084$ .

Return to Equation, which is evaluated for the  $i$ th panel in Figure and written for panel 4, Equation becomes (after multiplying each term by 2 and noting that  $\beta_i = 45^\circ$  for panel 4)

$$0.4074\lambda_1 + 0.4018\lambda_2 + 0.3528\lambda_3 + \pi\lambda_4 + 0.3528\lambda_5 + 0.4018\lambda_6 + 0.4074\lambda_7 + 0.4084\lambda_8 = -0.70712\pi V_\infty$$

Equation is a linear algebraic equation in terms of the eight unknown,  $\lambda_1, \lambda_2, \dots, \lambda_8$ . If we now evaluate Equation for each of the seven other panels, we obtain a total of eight equations, including Equation, which can be solved simultaneously for the eight unknown  $\lambda$ 's. The result are

$$\begin{aligned} \lambda_1 / 2\pi V_\infty &= 0.3765 & \lambda_2 / 2\pi V_\infty &= 0.2662 & \lambda_3 / 2\pi V_\infty &= 0 \\ \lambda_4 / 2\pi V_\infty &= -0.2662 & \lambda_5 / 2\pi V_\infty &= -0.3765 & \lambda_6 / 2\pi V_\infty &= -0.2662 \\ \lambda_7 / 32\pi V_\infty &= 0 & \lambda_8 / 2\pi V_\infty &= 0.2662 \end{aligned}$$

Note the symmetrical distribution of the  $\lambda$ 's which is to be expected for the nonlifting circular cylinder. Also, as a check on the above solution, return to Equation. Since each panel in Figure has the same length, Equation can be written simply as

$$\sum_{j=1}^n \lambda_j = 0$$

Substituting the value for the  $\lambda$ 's obtained into Equation, we see that the equation is identically satisfied.

The velocity at the control point of the  $i$ th panel can be obtained from Equation. In that equation, the integral over the  $j$ th panel is a geometric quantity that is evaluated in a similar manner as before. The result is

$$\int_j \frac{\partial}{\partial s} (\ln r_{ij}) ds_j = \frac{D - AC}{2E} \ln \frac{S_j^2 + 2AS_j + B}{B} - C \left( \tan^{-1} \frac{S_j + A}{E} - \tan^{-1} \frac{A}{E} \right)$$

With the integrals in Equation evaluated by Equation, and with the values for  $\lambda_1, \lambda_2, \dots, \lambda_8$  obtained above inserted into Equation, we obtain the velocities  $V_1, V_2, \dots, V_8$ . In turn, the pressure coefficients  $C_{p,1}, C_{p,2}, \dots, C_{p,8}$  are obtained directly from

$$C_{p,i} = 1 - \left( \frac{V_i}{V_\infty} \right)^2$$

Result for the pressure coefficients obtained from this calculation are compared with the exact analytical result, Equation in Figure. Amazingly enough, in spite of the relatively crude paneling shown in figure the numerical pressure coefficient results are excellent.



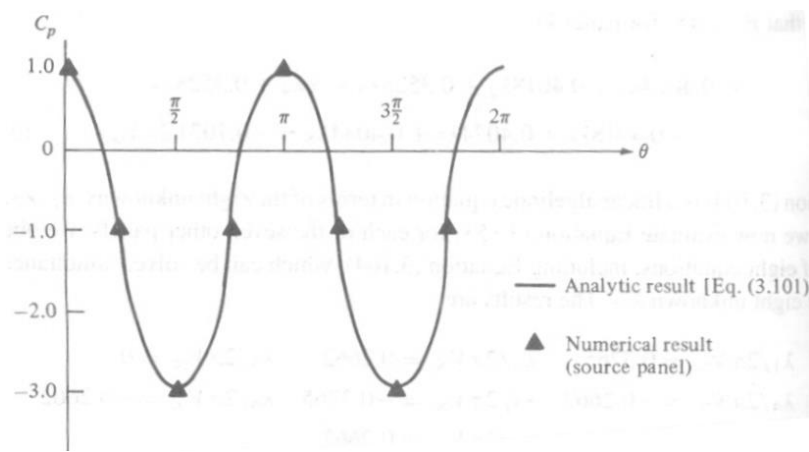


Figure: Pressure distribution over a circular cylinder; comparison of the source panel results and theory.

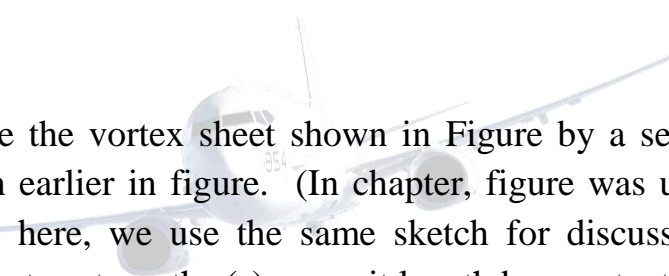
Lifting flows over arbitrary bodies: The vortex panel numerical method:

the thin airfoil theory described in section and is just what it says-it applies only to thin airfoils at small angles of attack. (Make certain that you understand exactly where in the development of thin airfoil theory these assumptions are made and the reasons for making them.) The advantage of thin airfoil theory is that closed-form expressions are obtained for the aerodynamic coefficients. Moreover, the results compare favorably with experimental data for airfoils of about 12 Percent thickness or less. However, the airfoils on many low-speed airplanes are thicker than 12 percent. Moreover, we are frequently interested in high angles of attack, such as occur during takeoff and landing. Finally, we are sometimes concerned with the generation of aerodynamic lift on other body shapes, such as automobiles or submarines. Hence, thin airfoil theory is quite restrictive when we consider the whole spectrum of aerodynamic applications. We need a method that allows us to calculate the aerodynamic characteristics of bodies of arbitrary shape, thickness, and orientation. Such a method is described in this section. Specially, we treat the vortex panel method, which is a numerical technique that has come into widespread use since the early 1970s. In reference to our road map in figure, we now move to the left-hand branch. also, since this chapter deals with airfoils, we limit our attention to two-dimensional bodies.

The vortex panel method is directly analogous to the source panel method described in section. However, because a source has zero

circulation, source panels are useful only for nonlifting cases. In contrast, vortices have circulation, and hence vortex panels can be used for lifting cases. (Because of the similarities between source and vortex panel methods, returns to section and review the basic philosophy of the source panel method before proceeding further.

The philosophy of covering body surface with a vortex sheet of such a strength to make the surface a streamline of the flow was discussed in section. We then went on to simplify this idea by placing the vortex sheet on the camber line of the airfoil as shown in figure, thus establishing the basis for thin airfoil theory. We now return to the original idea of wrapping the vortex sheet over the complete surface of the body, as shown in figure. We wish to find  $\gamma(s)$  such that the body surface becomes a streamline of the flow. There exists no closed-form analytical solution for  $\gamma(s)$ ; rather, the solution must be obtained numerically. This is the purpose of the vortex panel method.



Let us approximate the vortex sheet shown in Figure by a series of straight panels, as shown earlier in figure. (In chapter, figure was used to discussed source panels; here, we use the same sketch for discussion of vortex panels.) Let the vortex strength  $\gamma(s)$  per unit length be constant over a given panel, but allow it to vary from one panel to the next. That is, for the  $n$  panels shown in figure, the vortex panel strengths per unit length are  $\gamma_1, \gamma_2, \dots, \gamma_j, \dots, \gamma_n$ . These panel strengths are unknowns; the main thrust of the panel technique is to solve for  $\gamma_j, j=1$  to  $n$ , such that the body surface becomes a streamline of the flow and such that the Kutta condition is satisfied. As explained in section, the midpoint of each panel is a control point at which the boundary condition is applied; that is, at each control point, the normal component of the flow velocity is zero.

Let  $P$  be a point located at  $(x, y)$  in the flow, and let  $r_{pj}$  be the distance from any point  $o$  the  $j$ th panel to  $P$ , as shown in Figure. The radius  $r_{pj}$  makes the angle  $\theta_{pj}$  with respect to the  $x$  axis. The velocity potential induced at  $P$  due to the  $j$ th panel,  $\Delta\phi_j$ , is, from Equation,

$$\Delta\phi_j = -\frac{1}{2\pi} \int_j \theta_{pj} \gamma_j ds_j$$

In Equation,  $\gamma_j$  is constant over the  $j$ th panel, and the integral is taken over the  $j$ th panel only. The angle  $\theta_{pj}$  is given by

$$\theta_{pj} = \tan^{-1} \frac{y - y_j}{x - x_j}$$

In turn, the potential at P due to all the panels is Equation summed over all the panels:

$$\phi(P) = \sum_{j=1}^n \phi_j = -\sum_{j=1}^n \frac{\gamma_j}{2\pi} \int_j \theta_{pj} ds_j$$

Since point P is just an arbitrary point in the flow, let us put P at the control point of the  $i$ th panel shown in Figure. The coordinates of this control point are  $(x_i, y_i)$ . Then Equation and become

$$\theta_{ij} = \tan^{-1} \frac{y_i - y_j}{x_i - x_j}$$

$$\phi(x_i, y_i) = -\sum_{j=1}^n \frac{\gamma_j}{2\pi} \int_j \theta_{ij} ds_j$$

Equation is physically the contribution of all the panels to the potential at the control point of the  $i$ th panel.

At the control points, the normal components of the velocity is zero; this velocity is the superposition of the uniform flow velocity and the velocity induced by all the vortex panels. The component of  $V_\infty$  normal to the  $i$ th panel is given by Equation:

$$V_{\infty, n} = V_\infty \cos \beta_i$$

The normal component of velocity induced at  $(x_i, y_i)$  by the vortex panel is

$$V_n = \frac{\partial}{\partial n_i} [\phi(x_i, y_i)]$$

Combining Equation and, we have

$$V_n = - \sum_{j=1}^n \frac{\gamma_j}{2\pi} \int_j \frac{\partial \theta_{ij}}{\partial n_i} ds_j$$

where the summation is over all the panels. The normal component of the flow velocity at the  $i$ th control point is the sum of that due to the freestream [Equation and that due to the vortex panels [Equation. The boundary condition states that this sum must be zero:

$$V_{\infty, n} + V_n = 0$$

Substituting Equation and into, we obtain

$$V_{\infty} \cos \beta_i - \sum_{j=1}^n \frac{\gamma_j}{2\pi} \int_j \frac{\partial \theta_{ij}}{\partial n_i} ds_j = 0$$



Equation is the crux of the vortex panel method. The values of the integrals in Equation depend simply on the panel geometry; they are not properties of the flow. Let  $J_{i,j}$  be the value of this integral when the control point is on the  $i$ th panel. Then Equation can be written as

$$V_{\infty} \cos \beta_i - \sum_{j=1}^n \frac{\gamma_j}{2\pi} J_{i,j} = 0$$

Equation is a linear algebraic equation with  $n$  unknowns,  $\gamma_1, \gamma_2, \dots, \gamma_n$ . It represents the flow boundary condition evaluated at the control point of the  $i$ th panel. If Equation is applied to the control points of all the panels, we obtain a system of  $n$  linear equation with  $n$  unknowns.

To this point, we have been deliberately paralleling the discussion of the source panel method given in section; however, the similarity stops here. For the source panel method, the  $n$  equations for the  $n$  unknown source strengths are routinely solved, giving the flow over a nonlifting body. In contrast, for the lifting case with vortex panels, in addition to the  $n$  equations given by Equation applied at all the panels, we must also satisfy the Kutta condition. This can be done in several ways. For example, consider figure, which illustrates a detail of the vortex panel distribution at the trailing edge. Note that the length of each panel can be different; their length and distribution over the body are up to you discretion. Let the two panels at the trailing edge (panels  $i$  and  $i-1$  in figure) be very small. The Kutta condition is applied precisely at the trailing edge and is given by  $\gamma_{(TE)} = 0$ . To approximate this numerically, if points  $i$  and  $i-1$  are close enough to the trailing edge, we can write



Figure: Vortex panels at the trailing edge.

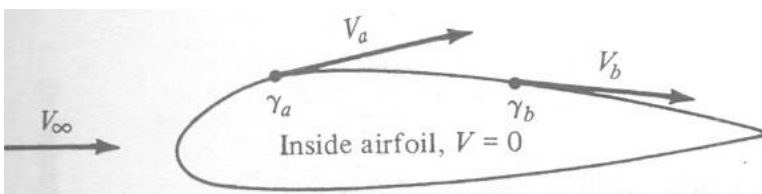


Figure: Airfoil as a solid body, with zero velocity inside the profile.

$$\gamma_i = -\gamma_{i-1} - 1$$

such that the strengths of the two vortex panels  $i$  and  $i - 1$  exactly cancel at the point where they touch at the trailing edge. Thus, in order to impose the Kutta condition on the solution of the flow, Equation (or an equivalent expression) must be included. Note that Equation evaluated at all the panels and Equation constitute an over determined system of  $n$  unknowns with  $n + 1$  equations. Therefore, to obtain a determine system, Equation is not evaluated at one of the control points on the body. That is, we choose to ignore one of the control points, and we evaluate Equation at the other  $n - 1$  control points. This, in combination with Equation, now gives a system of  $n$  linear algebraic equations with  $n$  unknowns, which can be solved by standard techniques.

At this stage, we have conceptually obtained the values of  $\gamma_1, \gamma_2, \dots, \gamma_n$  which make the body surface a streamline of the flow and which also satisfy the Kutta condition. In turn, the flow velocity tangent to the surface can be obtained directly from  $\gamma$ . To see this more clearly, consider the airfoil shown in Figure. We are concerned only with the flow outside the airfoil and on its surface. Therefore, let the velocity be zero at every point inside the body, as shown in Figure. In particular, the velocity just inside the vortex sheet on the surface is zero. This corresponds to  $u_2 = 0$  in Equation. Hence, the velocity just outside the vortex sheet is, from Equation,

$$\gamma = u_1 - u_2 = u_1 - 0 = u_1$$

In Equation,  $u$  denotes the velocity tangential to the vortex sheet. In terms of the picture shown in figure, we obtain  $V_a = \gamma_a$  at point  $a$ ,  $V_b = \gamma_b$  at point  $b$ , etc. Therefore, the local velocities tangential to the airfoil surface are equal to the local values of  $\gamma$ . In turn, the local pressure distribution can be obtained from Bernoulli's equation.

The total circulation and the resulting lift are obtained as follows. Let  $s_j$  be the length of the  $j$ th panel. Then the circulation due to the  $j$ th panel is  $\gamma_{js}$ . In turn, the total circulation due to all the panel is

$$\Gamma = \sum_{j=1}^n \gamma_j s_j$$

Hence, the lift per unit span is obtained from

$$L' = \rho_{\infty} V_{\infty} \sum_{j=1}^n \gamma_j s_j$$

The presentation in this section is intended to give only the general flavor of the vortex panel method. There are many variations of the method in use today, and you are encouraged to read the modern literature, especially as it appears in the AIAA Journal and the Journal of Aircraft since 1970. The vortex panel method as described in this section is termed a “first-order” method because it assumes a constant value of  $\gamma$  over a given panel. Although the method may appear to be straightforward, its numerical implementation can sometimes be frustrating. For example, the results for a given body are sensitive to the number of panels used, their various sizes, and the way they are distributed over the body surface (i.e., it is usually advantageous to place a large number of small panels near the leading and trailing edges of an airfoil and a smaller number of larger panels in the middle). The need to ignore one of the control points in order to have a determined system in  $n$  equations for  $n$  unknowns also introduces some arbitrariness in the numerical solution. Which control point do you ignore? Different choices sometimes yield different numerical answers for the distribution of  $\gamma$  over the surface. Moreover, the resulting numerical distribution for  $\gamma$  are not always smooth, but rather, they have oscillations from one panel to the next as a result of numerical inaccuracies. The problems mentioned above are usually overcome in different ways by different groups who have developed relatively sophisticated panel programs for practical use. For example, what is more common today is to use a combination of both source and vortex panels (source panels to basically simulate the airfoil thickness and vortex panels to introduce circulation) in a panel solution. This combination helps to mitigate some of the practical numerical problems just discussed. Again, you are encouraged to consult the literature for more information.

Such accuracy problems have also encouraged the development of higher order panel techniques. For example, a “section-order” panel method assumes a linear variation of  $\gamma$  over a given panel, as sketched in Figure.

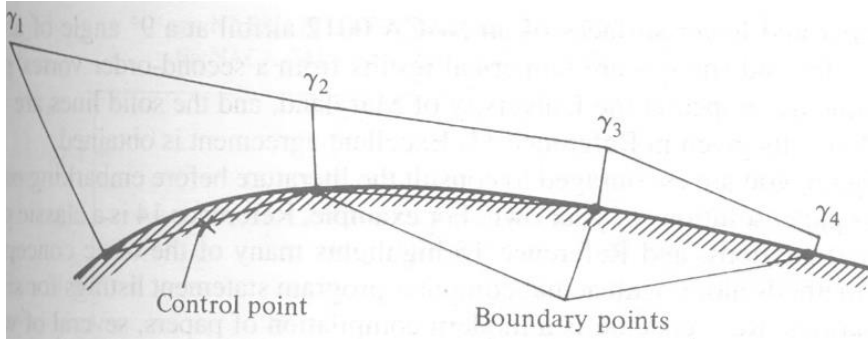


Figure: Linear distribution of  $\gamma$  over each panel-a second-order panel method.

### The Kutta Condition:



The lifting flow over a circular cylinder was discussed in section, where we observed that an infinite number of potential flow solutions were possible, corresponding to the infinite choice of  $\Gamma$ . For example, figure illustrates three different flows over the cylinder, corresponding to three different values of  $\Gamma$ . The same situation applies to the potential flow over an airfoil; for a given airfoil at a given angle of attack, there are an infinite number of valid theoretical solutions, corresponding to an infinite choice of  $\Gamma$ . For example, figure illustrates three different flows over the cylinder, corresponding to three different values of  $\Gamma$ . The same situation applies to the potential flow over the same airfoil at the same angle of attack but with different values of  $\Gamma$ . At first, this may seem to pose a dilemma. We know from experience that a given airfoil at given angle of attack produces a single value of lift. So, although there is an infinite number of possible potential flow solutions, nature knows how to pick a particular solution. Clearly, the philosophy discussed in the previous section is not complete-we need an additional condition that fixes  $\Gamma$  for a given airfoil at a given  $\alpha$ .



To attempt to find this condition, let us examine some experimental results for the development of the flow field around an airfoil which is set into motion from an initial state of rest. Figure shows a series of classic photographs of the flow over an airfoil, taken from Prandtl and Tietjens. In Figure a, the flow has just started, and the flow pattern is just beginning to develop around the airfoil. In these early moments of development of development, the flow tries to curl around the sharp trailing edge from the bottom surface to the top surface, similar to the sketch shown at the left of figure. However, more advanced considerations of inviscid, incompressible flow show the theoretical result that the velocity becomes infinitely large at a sharp corner.

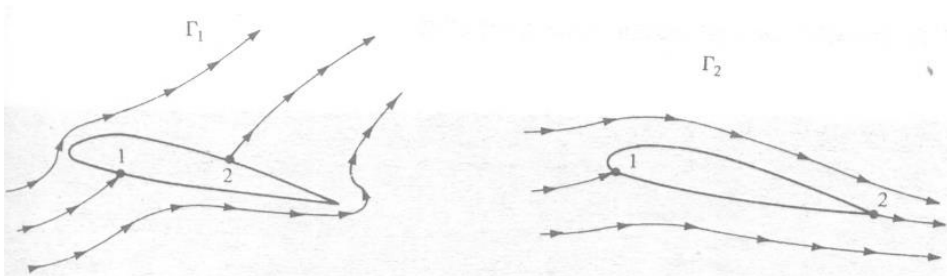
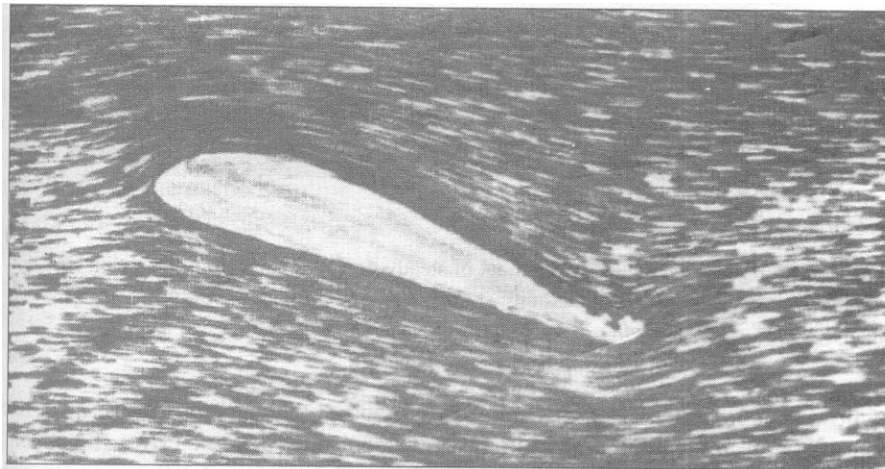
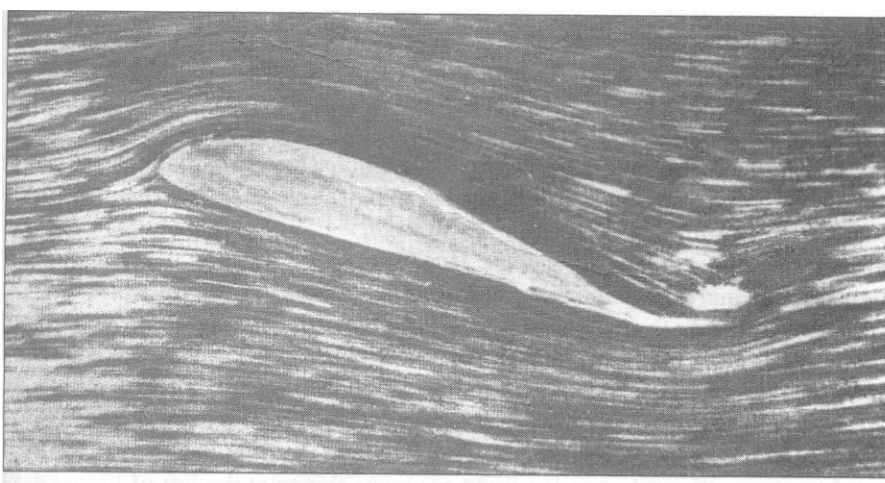


Figure: Effect of different values of circulation on the potential flow over a given airfoil at a given angle of attack. Points 1 and 2 are stagnation points.



(a)



(b)



(c)

Figure: The development of steady flow over an airfoil; the airfoil is impulsively started from rest and attains a steady velocity through the fluid. (a) A moment just after starting. (b) An intermediate time. (c) The final steady flow.

Hence, the type of flow sketched at the left of figure, and shown in figure a, is not tolerated very long by nature. Rather, as the real flow develops over the airfoil, the stagnation point on the upper surface (point 2 in figure) moves toward the trailing edge. Figure b shows this intermediate stage. Finally, after the initial transient process dies out, the steady flow shown in figure c is reached. This photograph demonstrates that the flow is smoothly leaving the top and the bottom surface of the airfoil at the trailing edge. This flow pattern is sketched at the right of figure, and represents the type of pattern to be expected for the steady flow over an airfoil.

Reflecting on figure, and, we emphasize again that in establishing the steady flow over a given airfoil at a given angle of attack, nature adopts that particular value of circulation ( $\Gamma_2$  Figure) which results in the flow leaving smoothly at the trailing edge. This observation was first made and used in a theoretical analysis by the German mathematician M. Wilhelm Kutta in 1902. Therefore, it has become known as the Kutta condition.

In order to apply the Kutta condition in a theoretical analysis, we need to be more precise about the nature of the flow at the trailing edge. The trailing edge can have a finite angle, as shown in figure and as sketched at the left of figure, or it can be cusped, as shown at the right of figure. First, consider the trailing edge with a finite angle, as shown at the left of figure. Denote the velocities along the top surface and the bottom surface as  $V_1$  and  $V_2$ , respectively.  $V_1$  is parallel to the top surface at point  $a$ , and  $V_2$  is parallel to the bottom surface at point  $a$ . For the finite-angle trailing edge, if these velocities were finite at point  $a$ , then we would have two velocities in two different directions at the same point, as shown at the left of Figure. However, this is not physically possible, and the only recourse is for both  $V_1$  and  $V_2$  to be zero at point  $a$ . That is, for the finite trailing edge, point  $a$  is a stagnation point, where  $V_1 = V_2 = 0$ . In contrast, for the cusped trailing edge shown at the right of Figure,  $V_1$  and  $V_2$  are in the same direction at point  $a$ , and hence both  $V_1$  and  $V_2$  can be finite. However, the pressure at point  $a$ ,  $p_2$ , is a single, unique value, and Bernoulli's equation applied at both the top and bottom surface immediately adjacent to point  $a$  yields

$$p_a + \frac{1}{2}\rho V_1^2 = p_a + \frac{1}{2}\rho V_2^2$$

or  $V_1 = V_2$

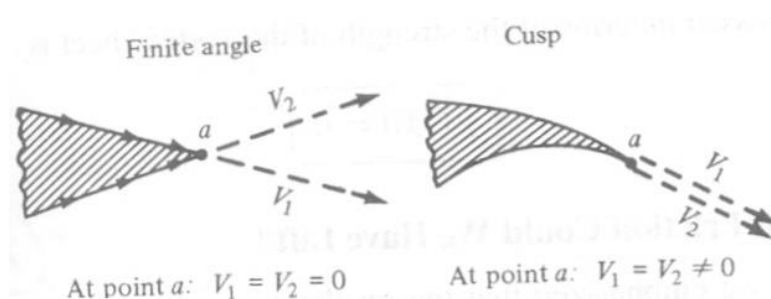


Figure: Different possible shapes of the trailing edge and their relation to the Kutta condition.

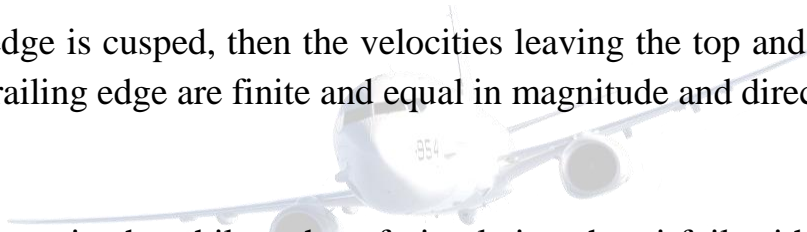
Hence, for the cusped trailing edge, we see that the velocities leaving the top and bottom surfaces of the airfoil at the trailing edge are finite and equal in magnitude and direction.

We can summarize the statement of the Kutta condition as follows:

For a given airfoil at a given angle of attack, the value of  $\Gamma$  around the airfoil is such that the flow leaves the trailing edge smoothly.

If the trailing-edge angle is finite, then the trailing edge is a stagnation point.

If the trailing edge is cusped, then the velocities leaving the top and bottom surface at the trailing edge are finite and equal in magnitude and direction.



Consider again the philosophy of simulating the airfoil with vortex sheets placed either on the surface or on the camber line, as discussed in section. The strength of such a vortex sheet is variable along the sheet and is denoted by  $\gamma(s)$ . The statement of the Kutta condition in terms of the vortex sheet is as follows. At the trailing edge (TE), from Equation, we have

$$\gamma(\text{TE}) = \gamma(a) = V_1 - V_2$$

However, for the finite-angle trailing edge,  $V_1 = V_2 = 0$ ; hence, from Equation,  $\gamma(\text{TE}) = 0$ . For the cusped trailing edge,  $V_1 = V_2 \neq 0$ ; hence, from Equation, we again obtain the result that  $\gamma(\text{TE}) = 0$ . Therefore, the Kutta condition expressed in terms of the strength of the vortex sheet is

$$\boxed{\gamma(\text{TE}) = 0}$$

5. Kelvin's Circulation theorem and the starting vortex:

In this section, we put the finishing touch to the overall philosophy of airfoil theory before developing the quantitative aspects of the theory itself in subsequent sections. This section also ties up a loose end introduced by the Kutta condition described in the previous section. Specially, the Kutta condition states that the circulation around an airfoil is just the right value to ensure that the flow smoothly leaves the trailing edge. Question: How does nature generate this circulation? Does it come from nowhere, or is circulation somehow conserved over the whole flow field? Let us examine these matters more closely.

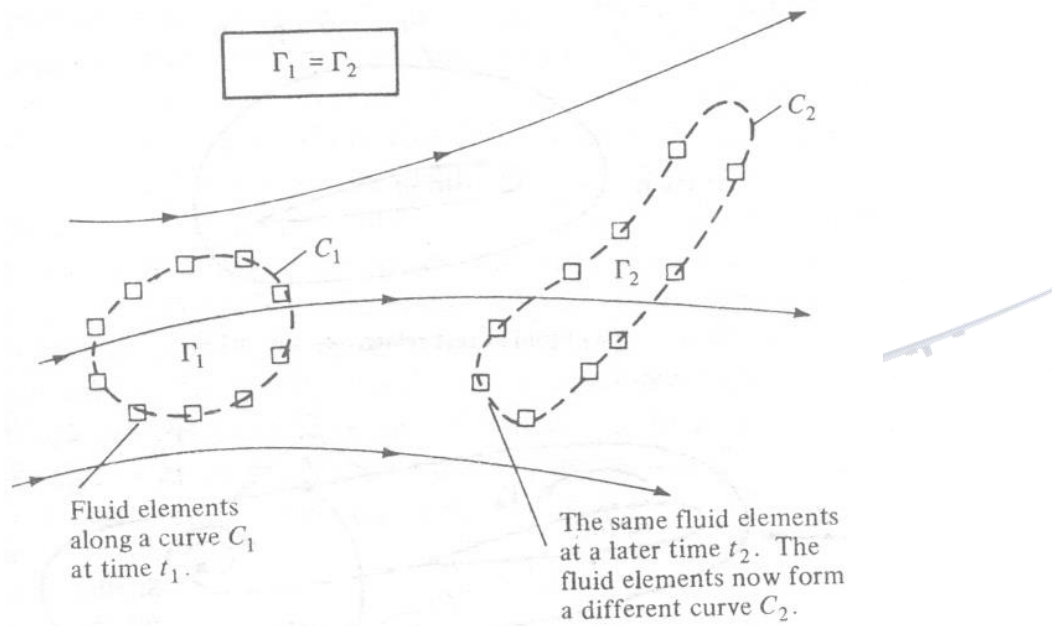


Figure: Kelvin's theorem.

Consider an arbitrary inviscid, incompressible flow as sketched in figure. Assume that all body forces  $f$  are zero. Choose an arbitrary curve  $C_1$  and identify the fluid elements that are on this curve at a given instant in time  $t_1$ . Also, by definition the circulation around curve  $C_1$  is  $\Gamma_1 = -\int_{C_1} \mathbf{V} \cdot d\mathbf{s}$ . Now let these specific fluid elements move downstream. At some later time,  $t_2$ , these same fluid elements will form another curve  $C_2$ , around which the circulation is  $\Gamma_2 = -\int_{C_2} \mathbf{V} \cdot d\mathbf{s}$ . for the conditions stated above, we can readily show that  $\Gamma_1 = \Gamma_2$ . In fact, since we are following a set of specific fluid elements, we can state that circulation around a closed curve formed by a set



of contiguous fluid elements remains constant as the fluid elements move throughout the flow. Recall from section that the substantial derivative gives the time rate of change following a given fluid element. Hence, a mathematical statement of the above discussion is simply

$$\frac{D\Gamma}{Dt} = 0$$

Which says that the time rate of change of circulation around a closed curve consisting of the same fluid elements is zero. Equation along with its supporting discussion is called Kelvin's circulation theorem<sup>4</sup>. Its derivation from first principles is left as Problem. Also, recall our definition and discussion of a vortex sheet in section. An interesting consequence of Kelvin's circulation theorem is proof that a stream surface which is a vortex sheet at some instant in time remains a vortex sheet for all times.

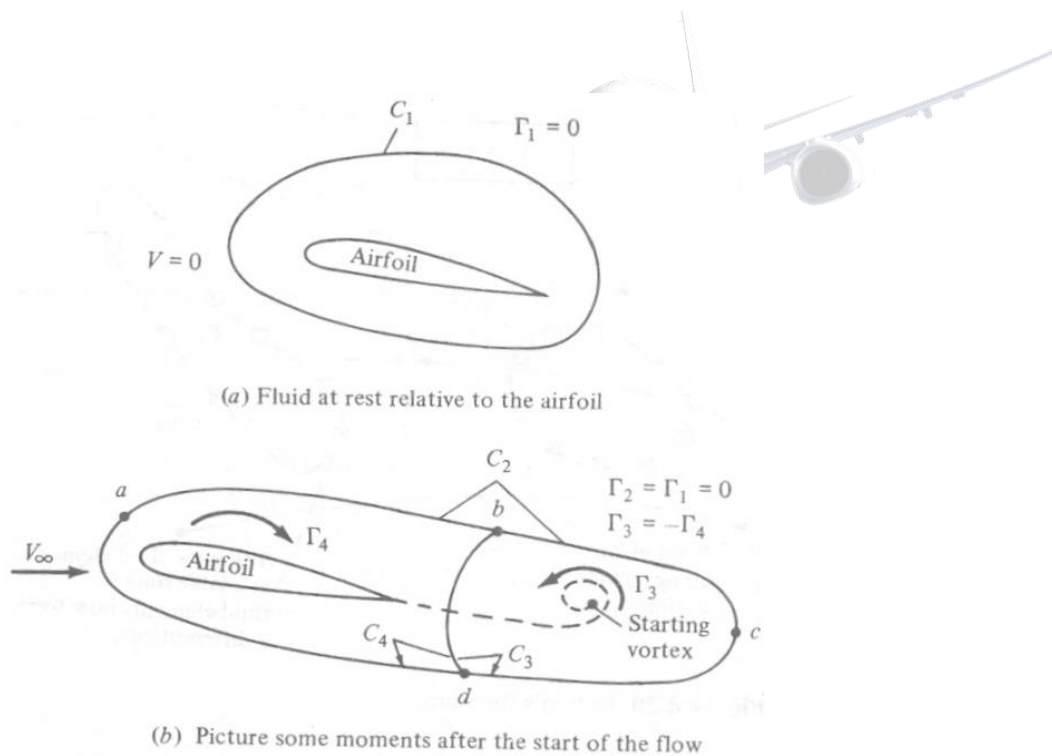


Figure: The creation of the starting vortex and the resulting generation of circulation around the airfoil.

Kelvin's theorem helps to explain the generation of circulation around an airfoil, as follows. consider an airfoil in a fluid at rest, as shown in figure a. Because  $V = 0$  everywhere, the circulation around curve  $C_1$  is zero. Now start the flow in motion over the airfoil. Initially, the flow will tend to curl around the trailing edge, as explained in section and illustrated at the left of

figure. In so doing, the velocity at the trailing edge theoretically becomes infinite. In real life, the velocity tends toward a very large finite number. Consequently, during the very first moments after the flow is started, a thin region of very large velocity gradients (and therefore high vorticity) is started, a thin region of very large velocity region is fixed to the same fluid elements, and consequently it is flushed downstream as the fluid elements begin to move downstream from the trailing edge. As it moves downstream, this thin sheet of intense vorticity is unstable, and it tends to roll up and form a picture similar to a point vortex. This vortex is called the starting vortex and is sketched I figure. After the flow around the airfoil has come to a steady state where the flow leaves the trailing edge smoothly (the Kutta condition), the high velocity gradients at the trailing edge disappear and vorticity is no longer produced at that point. However, the starting vortex has already been formed during the starting process, and it moves steadily downstream with the flow forever after. Figure (b) shows the flow field sometime after steady flow has been achieved over the achieved over the airfoil, with the starting vortex somewhere downstream. The fluid elements that initially made up curve C1 in figure a have moved downstream and now make up curve C2, which is the complete circuit abcd shown in figure b. Thus, from Kelvin's theorem, the circulation  $\Gamma_2$  around curve C2 (which encloses both the airfoil and the starting vortex) is the same as that around curve C1, namely, zero.  $\Gamma_2 = \Gamma_1 = 0$ . Now let us subdivide C2 C4 (circuit abda). Curve C3 encloses the starting vortex, and curve C3 (circuit bcd b) and C4 encloses the airfoil. The circulation  $\Gamma_3$  around C3 is due to the starting vortex; by inspecting Figure b, we see that  $\Gamma_3$  is in the counterclockwise direction (i.e., a negative value). The circulation around curve C4 enclosing the airfoil is  $\Gamma_4$ . Since the cut bd is common to both C3 and C4, the sum of the circulation around C3 and C4 is simply equal to the circulation around C2:

$$\Gamma_3 + \Gamma_4 = \Gamma_2$$

However, we have already established that  $\Gamma_2 = 0$ . Hence,

$$\Gamma_4 = -\Gamma_3$$

that is, the circulation around the airfoil is equal and opposite to the circulation around the starting vortex.

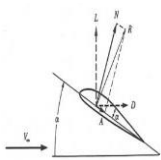
This brings us to the summary as well as the crux of this section. As the flow over an airfoil is started, the large velocity gradients at the sharp trailing edge result in the formation of a region of intense vorticity which rolls up downstream of the trailing edge, forming the starting vortex. This starting vortex has associated with it a counterclockwise circulation around the airfoil is generated. As the starting process continues, vorticity from the trailing edge is constantly fed into the starting vortex, making it stronger with a consequent larger counterclockwise circulation. In turn, the clockwise circulation around the airfoil becomes stronger, making the flow at the trailing edge more closely approach the Kutta condition, thus weakening the vorticity shed from the trailing edge. Finally, the starting vortex builds up to just the right strength such that the equal-and-opposite clockwise circulation around the airfoil leads to smooth flow from the trailing edge (the Kutta condition is exactly satisfied). When this happens, the vorticity shed from the trailing edge becomes zero, the starting vortex no longer grows in strength, and a steady circulation exists around the airfoil.





## UNIT IV

# AIRFOIL AND WING THEORY



Joukowski, Karman - Trefftz, Profiles - Thin aerofoil theory and its applications. Vortex line, Horse shoe vortex, Biot and Savart law, Lifting line theory and its limitations.



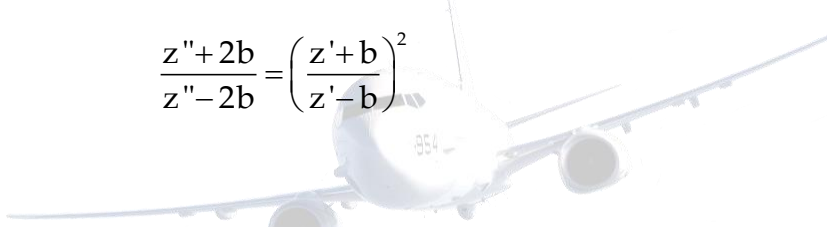
## 1. Karman-Trefftz and Jones-McWilliams Airfoils

There have been several variations of the Joukowski airfoil that add several helpful features. One, proposed by von Karman and Trefftz, eliminates the disadvantage of the thin trailing edge.

Transformation equation can be written in the equivalent forms

$$z''+2b=(z'+b)^2/z', \quad z''-2b=(z'-b)^2/z'.$$

Taking the ratio of these, the Joukowski transformation can therefore be written in the form

$$\frac{z''+2b}{z''-2b}=\left(\frac{z'+b}{z'-b}\right)^2$$


Von Karman and Trefftz suggested replacing the Joukowski transformation with the alternate transformation

$$\frac{z''+2b}{z''-2b}=\left(\frac{z'+b}{z'-b}\right)^n.$$

The trailing edge then has an inside angle of  $(2-n)\pi$ , rather than zero. The details of the shape can be carried out in a manner similar to the Joukowski airfoil, with one more variable ( $n$ ) available to the designer.

A second variation of the Joukowski airfoil was proposed by R. T. Jones and R. McWilliams in a pamphlet distributed at an Oshkosh Air Show. They also start with equation but then follow it with the two transformations

$$z'' = z' - \frac{\varepsilon}{z' - \Delta}$$

and

$$z''' = z'' + \frac{b^2}{z''},$$

where  $\varepsilon$  is a complex number and  $\Delta$  is real. Carrying through an analysis similar to what we did for the Joukowski profile, it can be shown using the same general analysis as for the Joukowski transformation that

$$\varepsilon = (x'_T - b)(x'_T - \Delta) - (y'_T)^2 + iy'_T(2x'_T - \Delta - b),$$

where  $(x'_T, y'_T)$  is the location of the trailing edge in the  $z'$  plane.

It is convenient to set  $b$ , a scale factor, arbitrarily to 1. The parameters  $\Delta, x'_c, y'_c, y'_T$  are then set by the designer. The parameter  $\varepsilon$  is determined by equation subject to the inequality.

$$\left| \Delta - b \pm \sqrt{(\Delta + b)^2 + 4\varepsilon} - 2(x'_c + iy'_c) \right| < 2a,$$

and the parameter  $a$  is determined by

$$a = \sqrt{(x'_T - x'_c)^2 + (y'_T - y'_c)^2}.$$

The circulation is then found from

$$\Gamma = 4\pi a |U| B,$$

with B given by

$$B = \frac{(x'_T - x'_c) \sin \theta - (y'_T - y') \cos \theta}{a}$$

With a careful selection of the parameters, Jones and McWilliams have generated airfoils with the properties of the NACA 6 series, the 747 series, the Clark Y, and the G-387.

## 2. Vortex Line:

Vortex lines can be defined as being lines instantaneously tangent to the vorticity vector, satisfying the equations

$$\frac{dx}{\omega_x} = \frac{dy}{\omega_y} = \frac{dz}{\omega_z}.$$

Vortex sheets are surface of vortex lines lying side by side. Vortex tubes are closed vortex sheets with vorticity entering and leaving through the ends of the tube.

Analogous to the concept of volume flow through an area,  $\iint_s \mathbf{v} \cdot d\mathbf{A}$ , the vorticity flow through an area, termed circulation, is defined as circulation  $\Gamma = \oint_C \mathbf{v} \cdot d\mathbf{s} = \iint_s \boldsymbol{\omega} \cdot d\mathbf{s}$ .

## 3. The Vortex Filament, the biot-savart law, and helmholtz's theorems:

To establish a rational aerodynamic theory for a finite wing, we need to introduce a few additional aerodynamic tools. To begin with, we expand the concept of a vortex filament first introduced in section. In section, we discussed a straight vortex filament extending to  $\pm\infty$ .

In general, a vortex filament can be curved, as shown in figure. Here, only a portion of the filament is illustrated. The filament induces a flow field in the surrounding space. If the circulation is taken about any path enclosing the filament, a constant value  $\Gamma$ . Consider a directed segment of the filament  $d\mathbf{l}$ , as shown in figure. The radius vector from  $d\mathbf{l}$  to an arbitrary point P in space is  $\mathbf{r}$ . The segment  $d\mathbf{l}$  induces a velocity at P equal to

$$d\mathbf{V} = \frac{\Gamma}{4\pi} \frac{d\mathbf{l} \times \mathbf{r}}{|\mathbf{r}|^3}$$

Equation is called the Biot-Savart law and is one of the most fundamental relations in the theory of inviscid, incompressible flow. Its derivation is given in more advanced books. Here, we must accept it without proof. However, you might feel more comfortable if we draw an analogy with electromagnetic theory. If the vortex filament in Figure were instead visualized as a wire carrying an electrical current  $I$ , then the magnetic field strength  $d\mathbf{B}$  induced at point P by a segment of the wire  $d\mathbf{l}$  with the current moving in the direction of  $d\mathbf{l}$  is

$$d\mathbf{B} = \frac{\mu I d\mathbf{l} \times \mathbf{r}}{4\pi |\mathbf{r}|^3}$$

where  $\mu$  is the permeability of the medium surrounding the wire. Equation is identical in form to equation. Indeed, the Biot-Savart law is a general result of potential theory, and potential theory describes electromagnetic fields as well as inviscid, incompressible flows. In fact, our use of the word “induced” in describing velocities generated by the presence of vortices, sources, etc. is a carry-over from the study of electromagnetic fields induced by electrical currents. When developing their finite-wing theory during the period 1911-1918, Prandtl and his colleagues even “induced” drag.

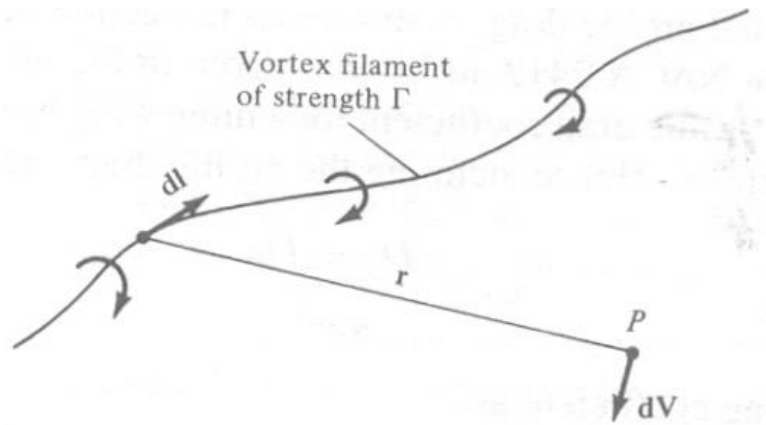


Figure: Vortex filament and illustration of the Bio-Savart law.

Return again to our picture of the vortex filament in figure. Keeping in mind that this single vortex filament and the associated Biot-Savart law [Equation] are simply conceptual aerodynamic tools to be used for synthesizing more complex flows of an inviscid, incompressible fluid. They are, for all practical purposes, a solution of the governing equation for inviscid, incompressible flow-Laplace's equation-and, by themselves, are not of particular value. However, when a number of vortex filaments are used in conjunction with a uniform freestream, it is possible to synthesize a flow which has a practical application. The flow over a finite wing is one such example, as we will soon see.

Let us apply the Biot-Savart law to a straight vortex filament of infinite length, as sketched in figure. The strength of the filament is  $\Gamma$ . The velocity induced at point P by the directed segment of the vortex filament  $dl$  is given by

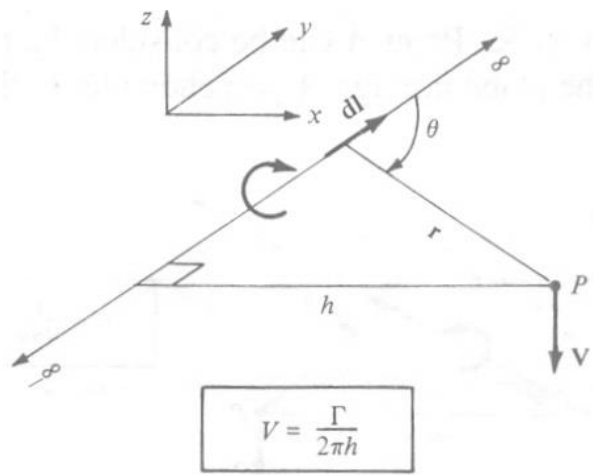


Figure: Velocity induced at point P by an infinite, straight vortex filament.

Equation. Hence, the velocity induced at P by the entire vortex filament is



From the definition of the vector cross product, the direction of  $V$  is downward in figure. The magnitude of the velocity,  $V = |V|$ , is given by

$$V = \frac{\Gamma}{4\pi} \int_{-\infty}^{\infty} \frac{\sin \theta}{r^2} dl$$

In Figure, let  $h$  be the perpendicular distance from point P to the vortex filament. Then, from the geometry shown in Figure,

$$\begin{aligned} r &= \frac{h}{\sin \theta} \\ l &= \frac{h}{\tan \theta} \\ dl &= -\frac{h}{\sin^2 \theta} d\theta \end{aligned}$$

Substituting Equation (a to c) in Equation, we have

$$V = \frac{\Gamma}{4\pi} \int_{-\infty}^{\infty} \frac{\sin \theta}{r^2} dl = -\frac{\Gamma}{4\pi h} \int_{\pi}^0 \sin \theta d\theta$$

or

$$V = \frac{\Gamma}{2\pi h}$$

Thus, the velocity induced at a given point P by an infinite, straight vortex filament at a perpendicular distance h from P is simply  $\Gamma/2\pi h$ , which is precisely the result given by Equation for a point vortex in two-dimensional flow. [Note that the minus sign in Equation does not appear in Equation; this is because V in Equation is simply the absolute magnitude of V, and hence it is positive by definition.]

Consider the semi-infinite vortex filament shown in figure. The filament extends from point A to  $\infty$ . Point A can be considered a boundary of the flow. Let P be a point in the plane through A perpendicular to the filament.

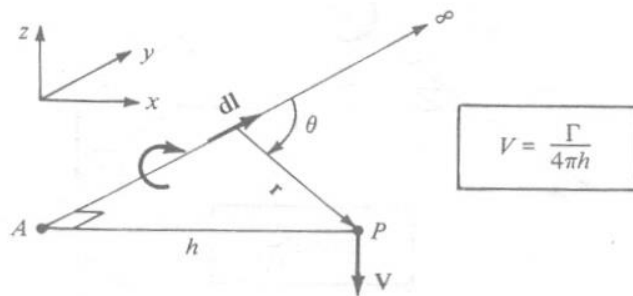


Figure: Velocity induced at point P by a semi-infinite straight vortex filament.

Then, by an integration similar to that above (try it yourself), the velocity induced at P by the semi-infinite vortex filament is



$$V = \frac{\Gamma}{4\pi h}$$

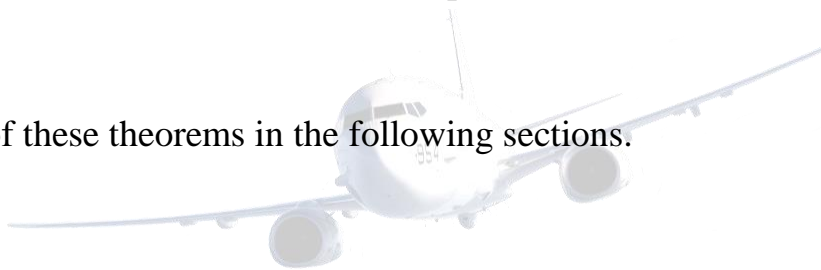
We use Equation in the next section.

The great German mathematician, physicist, and physician Hermann von Helmholtz (1821-1894) was the first to make use of the vortex filament concept in the analysis of inviscid, incompressible flow. In the process, he established several basic principles of vortex behavior which have become known as Helmholtz's vortex theorems:

The strength of a vortex filament is constant along its length.

A vortex filament cannot end in a fluid; it must extend to the boundaries of the fluid (which can be  $\pm\infty$ ) or form a closed path.

We make use of these theorems in the following sections.



Finally, let us introduce the concept of lift distribution along the span of a finite wing. Consider a given spanwise location  $y_1$ , where the local chord is  $c$ , the local geometric angle of attack is  $\alpha$ , and the airfoil section is a given shape. The lift per unit span at this location is  $L'(y_1)$ . Now consider another location  $y_2$  along the span, where  $c$ ,  $\alpha$ , and the airfoil shape may be different. (Most finite wings have a variable chord, with the exception of a simple rectangular wing. Also, many wings are geometrically twisted so that  $\alpha$  is different at different spanwise locations-so-called geometric twist. If the tip is at a lower  $\alpha$  than the root, the wing is said to have washout; if the tip is at a higher  $\alpha$  than the root, the wing has washing. In addition, the wings on a number of modern airplanes have different airfoil sections along the span, with different values of  $\alpha_{L=0}$ ; this is called aerodynamic twist). Consequently, the lift per unit span at this different location,  $L'(y_2)$ , will, in general, be different from  $L'(y_1)$ . Therefore, there is a distribution of lift per unit span along the wing, that is,  $L'=L'(y)$ , as sketched in Figure. In turn, the circulation is also a function of  $\Gamma(y)=L'(y)/\rho_\infty V_\infty$ . Note from Figure that the lift distribution goes to zero at the tips; that is because there is a

pressure equalization from the bottom to the top of the wing precisely at  $y = -b/2$  and  $b/2$ , and hence no lift is created at these points.

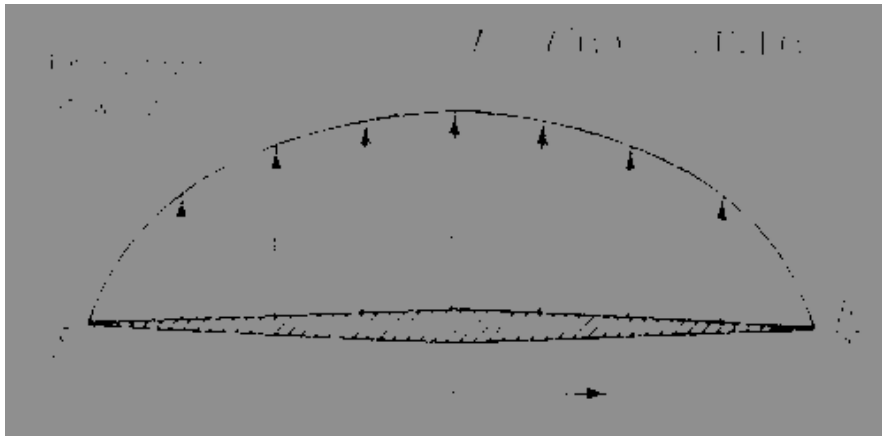


Figure: Sketch of the lift distribution along the span of a wing.

The calculation of the lift distribution  $L(y)$  [or the circulation distribution  $\Gamma(y)$ ] is one of the central problems of finite-wing theory. It is addressed in the following sections.

In summary, we wish to calculate the induce drag, the total lift, and the lift distribution for a finite wing. This is the purpose of the remainder of this chapter.

#### 4. Prandtl's classical lifting-Line Theory:

The first practical theory for predicting the aerodynamics properties of a finite wing was developed by Ludwig Prandtl and his colleagues at Gottingen, Germany, during the period 1911-1918, spanning World War I. The utility of Prandtl's theory is so great that it is still in use today for preliminary calculations of finitewing characteristics. The purpose of this section is to describe Prandtl's theory and to lay the groundwork for the modern numerical methods described in subsequent sections.

Prandtl reasoned as follows. A vortex filament of strength  $\Gamma$  that is somehow bound to a fixed location in a flow—a so-called bound vortex—will experience a force  $L' = \rho_{\infty} V_{\infty} \Gamma$  from the Kutta-Joukowski theorem. This bound vortex is in contrast to a free vortex, which moves with the same fluid elements throughout a flow. Therefore, let us replace a finite wing a span  $b$  with a bound vortex, extending from  $y = -b/2$  to  $y = b/2$ , as sketched in Figure. However, due to Helmholtz's theorem, a vortex filament cannot end in the fluid. Therefore, assume the vortex filament continues as two free vortices trailing downstream from the wing tips to infinity, as also shown in Figure. This vortex (the bounds plus the two free) is in the shape of a horseshoe, and therefore is called a horseshoe vortex.

A single horseshoe vortex is shown in figure. Consider the downwash  $w$  induced along the bound vortex from  $-b/2$  to  $b/2$  by the horseshoe vortex. Examining Figure, we see that the bound vortex induces no velocity along itself; however, the two trailing vortices both contribute to the induced velocity along the bound vortex, and both contributions are in the downward direction.

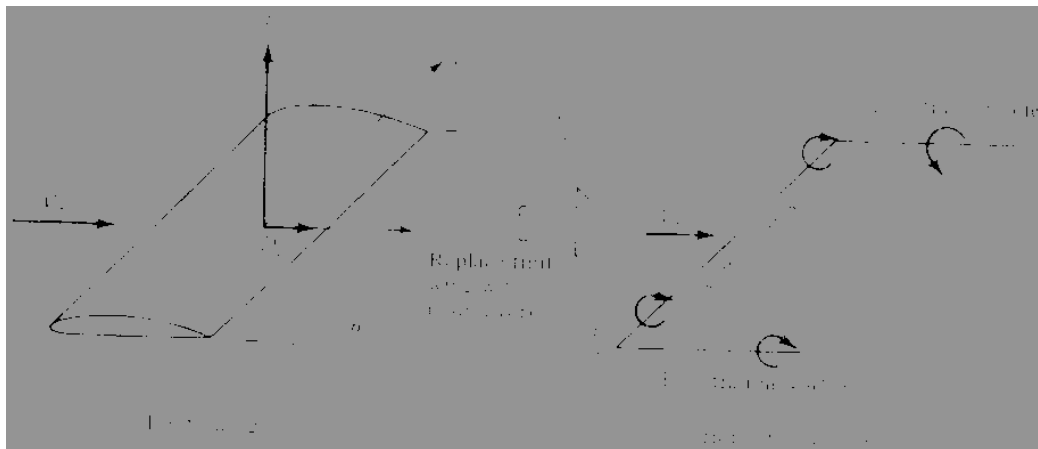


Figure: Replacement of the finite wing with a bound vortex.

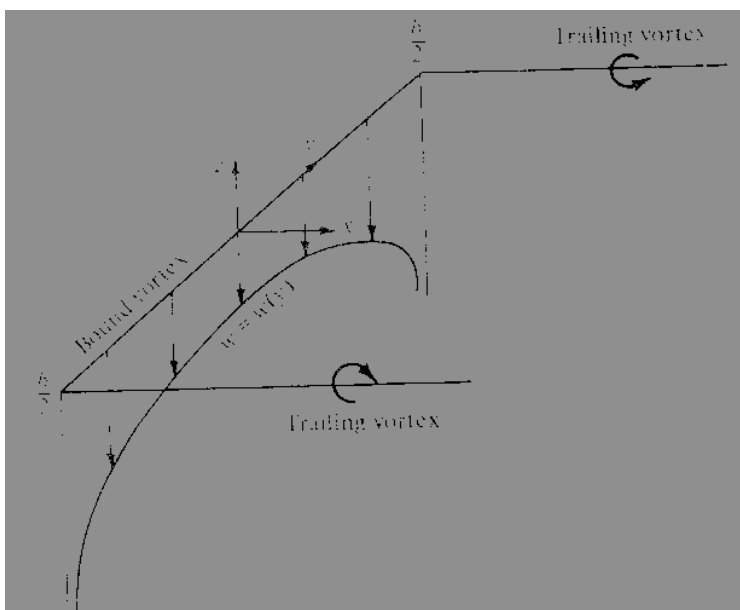


Figure: Downwash distribution along the  $y$  axis for a single horseshoe vortex.

Consider with the  $xyz$  coordinate system in figure, such a downward velocity is negative; that is,  $w$  (which is in the  $z$  direction) is a negative value when directed downward and a positive value when directed upward. If the origin is taken at the center of the bound vortex, then the velocity at any point  $y$  along the bound vortex induced by the trailing-inifinte vortex is, form Equation,

$$w(y) = -\frac{\Gamma}{4\pi(b/2 + y)} - \frac{\Gamma}{4\pi(b/2 - y)}$$

In Equation, the first term on the right-hand side is the contribution from the left trailing vortex (trailing from  $-b/2$ ), and the second term is the contribution from the right trailing vortex (trailing  $b/2$ ). Equation reduces to

$$w(y) = -\frac{\Gamma}{4\pi} \frac{b}{(b/2)^2 - y^2}$$

This variation of  $w(y)$  is sketched in figure. Note that  $w$  approaches  $-\infty$  as  $y$  approaches  $-b/2$  or  $b/2$ .

The downwash distribution due to the single horseshoe vortex shown in Figure does not realistically simulate that of a finite wing; the downwash approaching an infinite value at the tips is especially disconcerting. During the early evolution of finite-wing theory, this problem perplexed Prandtl and his colleagues. After several years of effort, a resolution of this problem was obtained which, in hindsight, was simple and straightforward. Instead of representing the wing by a single horseshoe vortex, let us superimpose a large number of horseshoe vortices, each with a different length of the bound vortex, but with all the bound vortices coincident along a single line, called the lifting line. This concept is illustrated in figure, where only three horseshoe vortices are shown for the sake of clarity. In figure a horseshoe vortex of strength  $d\Gamma_1$  is shown, where the bound vortex spans the entire wing from  $-b/2$  to  $b/2$  (from point A to point F). Super imposed on this is a second horseshoe vortex of strength  $d\Gamma_2$ , where its bound vortex spans only part of the wing, from point B to point E. Finally, superimposed on this is a third horseshoe vortex of strength  $d\Gamma_3$ , where its bound vortex spans only the part of the wing from point C to point D. As a result, the circulation varies along the line of bound vortices-the lifting line defined above. Along AB and EF, where two vortices are superimposed, the circulation is the sum of their strengths  $d\Gamma_1 + d\Gamma_2 + d\Gamma_3$ . This variation of  $\Gamma$  along the lifting line is now have a series of trailing vortices distributed over the span, rather than just two vortices trailing downstream of the tips as shown in figure. The series of trailing vortices in figure represents pairs of vortices, each pair associated with a given horseshoe vortex. Note that the strength of each trailing vortex is equal to the change in circulation along the lifting line.

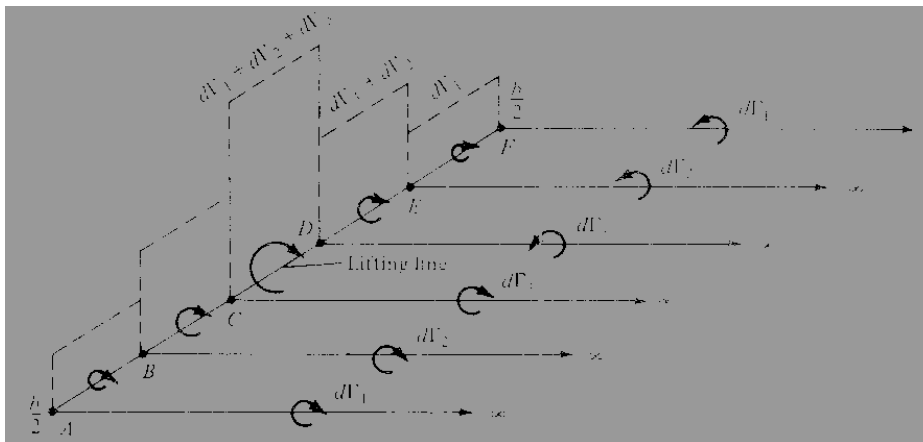


Figure: Superposition of a finite number of horseshoe vortices along the lifting line.

Let us extrapolate Figure to the case where an infinite number of horseshoe vortices are superimposed along the lifting line, each with a vanishingly small strength  $d\Gamma$ . This case is illustrated in figure. Note that the vertical bars in figure have now become a continuous distribution of  $\Gamma(y)$  along the lifting line in figure. The value of the circulation at the origin is  $\Gamma_0$ . Also, note that the finite number of trailing vortices in figure have become a continuous vortex sheet trailing downstream of the lifting line in figure. This vortex sheet is parallel to the direction of  $V_\infty$ . The total strength of the sheet integrated across the span of the wing is zero, because it consists of pairs of trailing vortices of equal strength but in opposite directions.

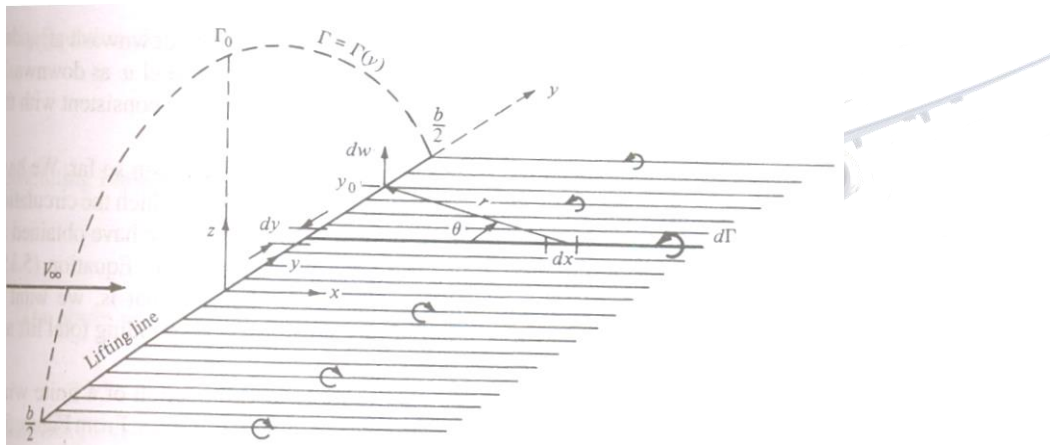


Figure: Superposition of an infinite number of horseshoe vortices along the lifting line.

Let us single out an infinitesimally small segment of the lifting line  $dy$  located at the coordinate  $y$  as shown in Figure. The circulation at  $y$  is  $\Gamma(y)$ , and the change in circulation over the segment  $dy$  is  $d\Gamma = (d\Gamma/dy)dy$ . In turn, the strength of the trailing vortex at  $y$  must equal the change in circulation  $d\Gamma$  along the lifting line; this is simply an extrapolation of our result obtained for the strength of the finite trailing vortices in figure. Consider more closely the trailing vortex of strength  $d\Gamma$  that intersects the lifting line at coordinate  $y$ , as shown in figure. Also consider the arbitrary

location  $y_0$  along the lifting line. Any segment of the trailing vortex  $dx$  will induce a velocity at  $y_0$  with a magnitude and direction given by the Biot-Savart law, Equation. In turn, the velocity  $dw$  at  $y_0$  induced by the entire semi-infinite trailing vortex located at  $y$  is given by Equation, which in terms of the picture given in Figure yields

$$dw = \frac{(d\Gamma/dy)dy}{4\pi(y_0 - y)}$$

The minus sign in equation is needed for consistency with the picture shown in figure; for the trailing vortex shown, the direction of  $dw$  at  $y_0$  is upward and hence is a positive value, whereas  $\Gamma$  is decreasing in the  $y$  direction, making  $d\Gamma/dy$  a negative quantity. The minus sign in Equation makes the positive  $dw$  consistent with the negative  $d\Gamma/dy$ .

The total velocity  $w$  induced at  $y_0$  by the entire trailing vortex sheet is the summation of equation over all the vortex filaments, that is, the integral of equation from  $-b/2$  to  $b/2$ :

$$w(y_0) = -\frac{1}{4\pi} \int_{-b/2}^{b/2} \frac{(d\Gamma/dy)dy}{y_0 - y}$$

Equation is important in that it gives the value of the downwash at  $y_0$  due to all the trailing vortices. (Keep in mind that although we label  $w$  as downwash,  $w$  is treated as positive in the upward direction in order to be consistent with the normal convention in an  $xyz$  rectangular coordinate system.)

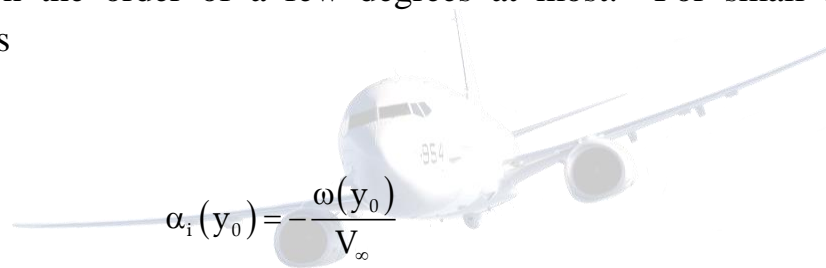
Pause for a moment and assess the status of our discussion so far. We have replaced the finite wing with the model of a lifting line along which the circulation  $\Gamma(y)$  varies continuously, as shown in figure. In turn, we have obtained an expression for the downwash along the lifting line, given by Equation. However, our central problem still remains to be solved; that is,

we want to calculate  $\Gamma(y)$  for a given finite wing, along with its corresponding total lift and induced drag. Therefore, we must press on.

Return to figure, which shows the local airfoil section of a finite wing. Assume this section is located at the arbitrary spanwise station  $y_0$ . From figure, the induced angle of attack  $\alpha_i$  is given by

$$\alpha_i(y_0) = \tan^{-1} \left( \frac{-w(y_0)}{V_\infty} \right)$$

[Note in figure that  $w$  is downward, and hence is a negative quantity. Since  $\alpha_i$  in figure is positive, the negative sign in equation is necessary for consistency.] Generally,  $w$  is much smaller than  $V_\infty$ , and hence  $\alpha_i$  is a small angle, on the order of a few degrees at most. For small angles, Equation yields



$$\alpha_i(y_0) = -\frac{w(y_0)}{V_\infty}$$

Substituting Equation into, we obtain

$$\alpha_i(y_0) = \frac{1}{4\pi V_\infty} \int_{-b/2}^{b/2} \frac{(d\Gamma/dy)dy}{y_0 - y}$$

that is, an expression for the induced angle of attack in terms of the circulation distribution  $\Gamma(y)$  along the wing.

Consider again the effective angle of attack  $\alpha_{\text{eff}}$ , as shown in figure. As explained in section,  $\alpha_{\text{eff}}$  is the angle of attack actually seen by the local airfoil section. Since the downwash varies across the span, then  $\alpha_{\text{eff}}$  is also



variable;  $\alpha_{\text{eff}} = \alpha_{\text{eff}}(y_0)$ . The lift coefficient for the airfoil section located  $y = y_0$  is

$$c_l = a_0 [\alpha_{\text{eff}}(y_0) - \alpha_{L=0}] = 2\pi [\alpha_{\text{eff}}(y_0) - \alpha_{L=0}]$$

In Equation, the local section lift slope  $a_0$  has been replaced by the thin airfoil theoretical value of  $2\pi(\text{rad}^{-1})$ . Also, for a wing with aerodynamic twist, the angle of zero lift  $\alpha_{L=0}$  in equation varies with  $y_0$ . If there is no aerodynamic twist,  $\alpha_{L=0}$  is constant across the span. In any event,  $\alpha_{L=0}$  is a known property of the local airfoil sections. From the definition of lift coefficient and from the Kutta-Joukowski theorem, we have, for the local airfoil section located at  $y_0$ ,

$$L' = \frac{1}{2} \rho_{\infty} V_{\infty}^2 c(y_0) c_l = \rho_{\infty} V_{\infty} \Gamma(y_0)$$

From Equation, we obtain

$$c_l = \frac{2\Gamma(y_0)}{V_{\infty} c(y_0)}$$

Substituting Equation into and solving for  $\alpha_{\text{eff}}$  we have

$$\alpha_{\text{eff}} = \frac{\Gamma(y_0)}{\pi V_{\infty} c(y_0)} + \alpha_{L=0}$$

The above results come into focus if we refer to Equation:

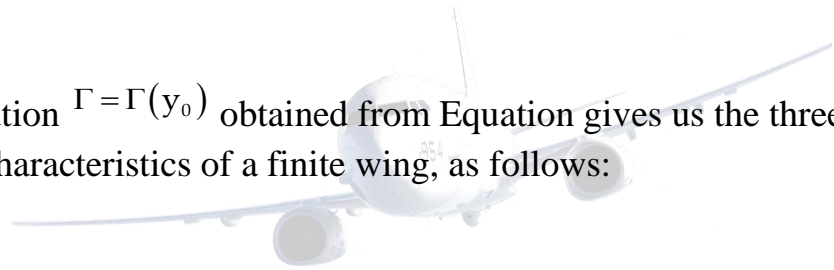
$$\alpha_{\text{eff}} = \alpha - \alpha_i$$

Substituting Equation and into, we obtain

$$\alpha(y_0) = \frac{\Gamma(y_0)}{\pi V_\infty c(y_0)} + \alpha_{L=0}(y_0) + \frac{1}{4\pi V_\infty} \int_{-b/2}^{b/2} \frac{(d\Gamma/dy)dy}{y_0 - y}$$

the fundamental equation of Prandtl's lifting-line theory; it simply states that the geometric angle of attack is equal to the sum of the effective angle plus the induced angle of attack. In Equation,  $\alpha_{\text{eff}}$  is expressed in terms of  $\Gamma$ ; all the other quantities,  $\alpha, c, V_\infty$  and  $\alpha_{L=0}$ , are known for a finite wing of given design at a given geometric angle of attack in a freestream with given velocity. Thus, a solution of Equation yields  $\Gamma = \Gamma(y_0)$ , where  $y_0$  ranges along the span from  $-b/2$  to  $b/2$ .

The solution  $\Gamma = \Gamma(y_0)$  obtained from Equation gives us the three main aerodynamic characteristics of a finite wing, as follows:



1. The lift distribution is obtained from the Kutta-Joukowski theorem:

$$L'(y_0) = \rho_\infty V_\infty \Gamma(y_0)$$

2. The total lift is obtained by integrating Equation over the span:

$$L = \int_{-b/2}^{b/2} L'(y) dy$$

or

$$L = \rho_\infty V_\infty \int_{-b/2}^{b/2} \Gamma(y) dy$$

(Note that we have dropped the subscript on  $y$ , for simplicity.) The lift coefficient follows immediately from Equation.

$$C_L = \frac{L}{q_\infty S} = \frac{2}{V_\infty S} \int_{-b/2}^{b/2} \Gamma(y) dy$$

The induced drag is obtained by inspection of figure. The induced drag per unit span is

$$D'_i = L'_i \sin \alpha_i$$

Since  $\alpha_i$  is small, this relation becomes

$$D'_i = L'_i \alpha_i$$

The total induced drag is obtained by integrating Equation over the span:

$$D_i = \int_{-b/2}^{b/2} L'(y) \alpha_i(y) dy$$

or

$$D_i = \rho_\infty V_\infty \int_{-b/2}^{b/2} \Gamma(y) \alpha_i(y) dy$$

In turn, the induced drag coefficient is

$$C_{D,i} = \frac{D_i}{q_\infty S} = \frac{2}{V_\infty S} \int_{-b/2}^{b/2} \Gamma(y) \alpha_i(y) dy$$

In Equation to  $\alpha_i(y)$  is obtained from Equation. Therefore, in Prndtl's lifting-line theory the solution of Equation for  $\Gamma(y)$  is clearly the key to obtaining the aerodynamic characteristics of a consider a special case, as outlined below.

## Elliptical Lift Distribution

Consider a circulation distribution given by

$$\Gamma(y) = \Gamma_0 \sqrt{1 - \left(\frac{2y}{b}\right)^2}$$

In Equation, note the following:

$\Gamma_0$  is the circulation at the origin, as shown in figure.

The circulation varies elliptically with distance  $y$  along the span; hence, it is designated as an elliptical circulation distribution. Since  $L'(y) = \rho_\infty V_\infty \Gamma(y)$ , we also have

$$L'(y) = \rho_\infty V_\infty \Gamma_0 \sqrt{1 - \left(\frac{2y}{b}\right)^2}$$

Hence, we are dealing with an elliptical lift distribution.

3.  $\Gamma(b/2) = \Gamma(-b/2) = 0$ . Thus, the circulation, hence lift, properly goes to zero at the wing tips, as shown in figure. We have not obtained Equation as a direct solution of Equation; rather we are simply stipulating a lift distribution that is elliptic. We now ask the question, What are the aerodynamic properties of a finite wing with such an elliptic lift distribution?

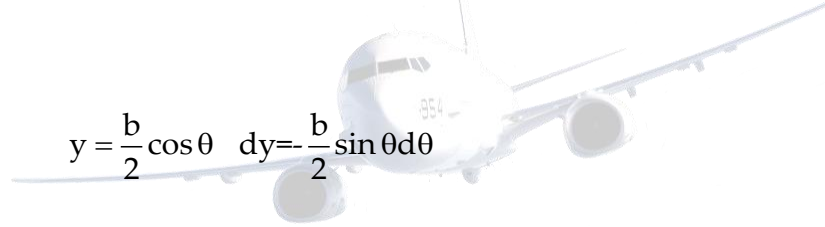
First, let us calculate the downwash. Differentiating Equation, we obtain

$$\frac{d\Gamma}{dy} = -\frac{4\Gamma_0}{b^2} \frac{y}{(1-4y^2/b^2)^{1/2}}$$

Substituting Equation into, we have

$$\omega(y_0) = \frac{\Gamma_0}{\pi b^2} \int_{-b/2}^{b/2} \frac{y}{(1-4y^2/b^2)^{1/2} (y_0 - y)} dy$$

The integral can be evaluated easily by making the substitution

$$y = \frac{b}{2} \cos \theta \quad dy = -\frac{b}{2} \sin \theta d\theta$$


Hence, Equation becomes

$$w(\theta_0) = -\frac{\Gamma_0}{2\pi b} \int_{\pi}^0 \frac{\cos \theta}{\cos \theta_0 - \cos \theta} d\theta$$

$$w(\theta_0) = -\frac{\Gamma_0}{2\pi b} \int_0^{\pi} \frac{\cos \theta}{\cos \theta - \cos \theta_0} d\theta$$

The integral in Equation is the standard form given by Equation for  $n=1$ . Hence, Equation becomes

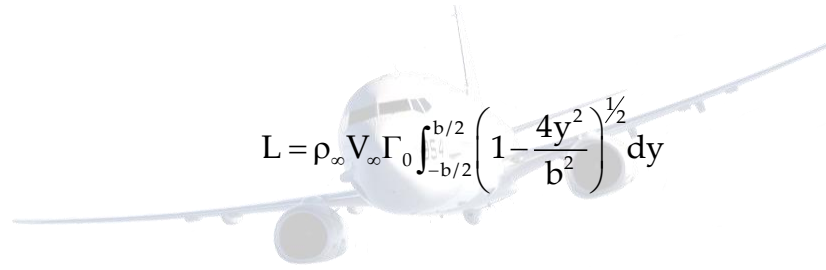
$$\boxed{w(\theta_0) = -\frac{\Gamma_0}{2b}}$$

which states the interesting and important result that that downwash is constant over the span for an elliptical lift distribution. In turn, from Equation, we obtain, for the induced angle of attack,

$$\alpha_i = -\frac{w}{V_\infty} = \frac{\Gamma_0}{2bV_\infty}$$

For an elliptic lift distribution, the induced angle of attack is also constant along the span. Note from Equations and that both the downwash and induced angle of attack go to zero as the wing span becomes infinite- which is consistent with our previous discussions on airfoil theory.

A more useful expression for  $\alpha I$  can be obtained as follows. Substituting Equation, we have



$$L = \rho_\infty V_\infty \Gamma_0 \int_{-b/2}^{b/2} \left(1 - \frac{4y^2}{b^2}\right)^{1/2} dy$$

Again, using the transformation  $y = (b/2)\cos\theta$ , Equation readily integrates to

$$L = \rho_\infty V_\infty \Gamma_0 \frac{b}{2} \int_0^\pi \sin^2 \theta d\theta = \rho_\infty V_\infty \Gamma_0 \frac{b}{4} \pi$$

Solving Equation for  $\Gamma_0$ , we have

$$\Gamma_0 = \frac{4L}{\rho_\infty V_\infty b\pi}$$

However,  $L = \frac{1}{2} \rho_\infty V_\infty^2 S C_L$ . Hence, Equation becomes

$$\alpha_i = \frac{2V_\infty SC_L}{b\pi} \frac{1}{2bV_\infty}$$

or

$$\alpha_i = \frac{SC_L}{\pi b^2}$$

An important geometric property of a finite wing is the aspect ratio, denoted by AR and defined as

$$AR \equiv \frac{b^2}{S}$$

Hence, Equation becomes



Equation is a useful expression for the induced angle of attack, as shown below.

The induced drag coefficient is obtained from, noting that  $\alpha_i$  is constant:

$$C_{D,i} = \frac{2\alpha_i}{V_\infty S} \int_{-b/2}^{b/2} \Gamma(y) dy = \frac{2\alpha_i \Gamma_0}{V_\infty S} \frac{b}{2} \int_0^\pi \sin^2 \theta d\theta = \frac{\pi \alpha_i \Gamma_0 b}{2V_\infty S}$$

Substituting Equations and into, we obtain

$$C_{D,i} = \frac{\pi b}{2V_\infty S} \left( \frac{C_L}{\pi AR} \right) \frac{2V_\infty SC}{b\pi}$$

or

$$C_{D,i} = \frac{C_L^2}{\pi AR}$$

Equation is an important result. It states that the induced drag coefficient is directly proportional to the square of the lift coefficient. The dependence of induced drag on the lift is not surprising, for the following reason. In section, we saw that induced drag is a consequence of the presence of the wing-tip vortices, which in turn are produced by the difference in pressure between the lower and induced drag is intimately related to the production of lift on a finite wing; indeed, induced drag is frequently called the drag due to lift. Equation dramatically illustrates this point. Clearly, an airplane cannot generate lift for free; the induced drag is the price for the generation of lift. The power required to generate the lift of the aircraft. Also, note that because  $C_{D,i} \propto C_L^2$ , the induced drag coefficient increase rapidly as  $C_L$  increases and becomes a substantial part of the total drag coefficient when  $C_L$  is high (e.g., when the airplane is flying slowly such as on takeoff or landing). Even at relatively high cruising speeds, induced drag is typically 25 percent of the total drag.

Another important aspect of induced drag is evident in Equation; that is  $C_{D,i}$  is inversely proportional to aspect ratio. Hence, to reduce the induced drag, we want a finite wing with the highest possible aspect ratio. Wings with high and low aspect ratios are sketched in figure. Unfortunately, the design of very high aspect ratio wings with sufficient structural strength is difficult. Therefore, the aspect ratio of a conventional aircraft is a compromise between conflicting aerodynamic and structural requirements. It is interesting to note that the aspect ratio of the 1903 Wright Flyer was 6 and that today the aspect ratios of conventional subsonic aircraft range typically from 6 to 8. (Exceptions are the Lockheed U-2 high-altitude reconnaissance aircraft with  $AR = 14.3$  and sailplanes with aspect ratios as high as 51. For example, the Schempp-Hirth



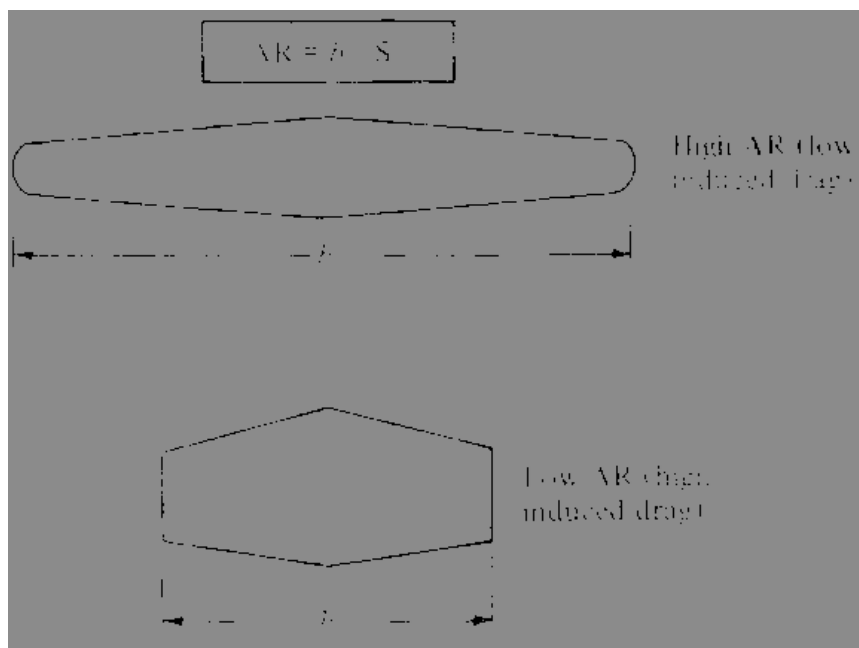


Figure: Schematic of high-and low-aspect-ratio wings.

Nimbus 4 sailplane, designed in 1994 with over 100 built by 2004, has an aspect ratio of 39. The ETA sailplane, designed in 2000 with 6 built by 2004, has an aspect ratio.



Another property of the elliptical lift distribution is as follows. Consider a wing with no geometric twist (i.e.,  $\alpha$  is constant along the span) and no aerodynamic twist (i.e.,  $\alpha_{L=0}$  is constant along the span.) From Equation, we have seen that  $\alpha I$  is constant along the span. Hence,  $\alpha_{\text{eff}} = \alpha - \alpha_i$  is also constant along the span. Since the local section lift coefficient  $c_l$  is given by

$$c_l = a_0 (\alpha_{\text{eff}} - \alpha_{L=0})$$

then assuming that  $a_0$  is the same for each section ( $a_0 = 2\pi$  from thin airfoil theory),  $c_l$  must be constant along the span. The lift per unit span is given by

$$L'(y) = q_{\infty} c_l$$

Solving Equation for the chord, we have

$$c(y) = \frac{L'(y)}{q_{\infty} c_l}$$

In Equation,  $q_{\infty}$  and  $c_l$  are constant along the span. However,  $L'(y)$  varies elliptically along the span. Thus, Equation dictates that for such an elliptic lift distribution, the chord must vary elliptically along the span; that is, for the conditions given above, the wing planform is elliptical.

The related characteristics-the elliptic lift distribution, the elliptic planform, and the constant downwash-are sketched in figure. Although an elliptical lift distribution may appear to be a restricted, isolated case, in reality it gives a reasonable approximation for the induced drag coefficient for an arbitrary finite wing. The form of  $C_{D,i}$  given by Equation is only slightly modified for the general case. Let us now consider the case of a finite wing with a general lift distribution.

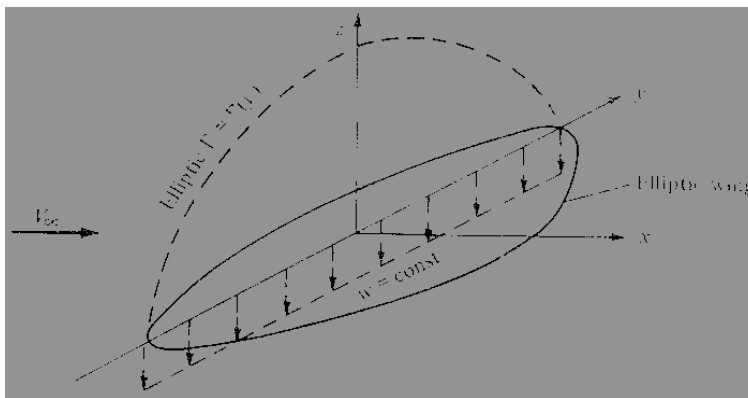


Figure: Illustration of the related quantities: an elliptic lift distribution, elliptic planform, and constant downwash.

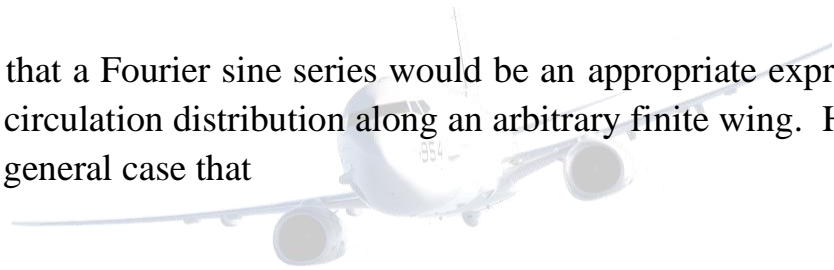
Consider the transformation

$$y = -\frac{b}{2} \cos \theta$$

where the coordinate in the spanwise direction is now given by  $\theta$ , with  $0 \leq \theta \leq \pi$ . In terms of  $\theta$ , the elliptic lift distribution given by Equation is written as

$$\Gamma(\theta) = \Gamma_0 \sin \theta$$

Equation hints that a Fourier sine series would be an appropriate expression for the general circulation distribution along an arbitrary finite wing. Hence, assume for the general case that



$$\Gamma(\theta) = 2bV_\infty \sum_1^N A_n \sin n\theta$$

where as many terms  $N$  in the series can be taken as we desire for accuracy. The coefficients  $A_n$  (where  $n = 1, \dots, N$ ) in Equation are unknowns; however, they must satisfy the fundamental equation of Prandtl's lifting-line theory; that is, the  $A_n$ 's must satisfy Equation. Differentiating Equation, we obtain

$$\frac{d\Gamma}{dy} = \frac{d\Gamma}{d\theta} \frac{d\theta}{dy} = 2bV_\infty \sum_1^N nA_n \cos n\theta \frac{d\theta}{dy}$$

Substituting Equations and into, we obtain

$$\alpha(\theta_0) = \frac{2b}{\pi c(\theta_0)} \sum_1^N A_n \sin n\theta_0 + \alpha_{L=0}(\theta_0) + \frac{1}{\pi} \int_0^\pi \frac{\sum_1^N n A_n \cos n\theta}{\cos \theta - \cos \theta_0} d\theta$$

The integral in Equation is the standard form given by Equation. Hence, Equation becomes

$$\alpha(\theta_0) = \frac{2b}{\pi c(\theta_0)} \sum_1^N A_n \sin n\theta_0 + \alpha_{L=0}(\theta_0) + \sum_1^N n A_n \frac{\sin n\theta_0}{\sin \theta_0}$$

Examine Equation closely. It is evaluated at a given spanwise locating; hence,  $\theta_0$  is specified. In turn,  $b$ ,  $c(\theta_0)$ , and  $\alpha_{L=0}(\theta_0)$  are known quantities from the geometry and airfoil section of the finite wing. The only unknowns in Equations are the  $A_n$ 's. Hence, written at a given spanwise location (a specified  $\theta_0$ ), Equation is one algebraic equation with  $N$  unknowns,  $A_1, A_2, \dots, A_N$ . However, let us choose  $N$  different spanwise stations, and let us evaluate Equation at each of these  $N$  stations. We then obtain a system of  $N$  independent algebraic equations with  $N$  unknowns, namely,  $A_1, A_2, \dots, A_N$ . In this fashion, actual numerical values are obtained for the  $A_n$ 's-numerical values that ensure that the general circulation distribution given by equation satisfies the fundamental equation of finite-wing theory, Equation.

Now that  $\Gamma(\theta)$  is known via Equation, the lift coefficient for the finite wing follows immediately from the substitution of Equation into:

$$C_L = \frac{2}{V_\infty S} \int_{-b/2}^{b/2} \Gamma(y) dy = \frac{2b^2}{S} \sum_1^N A_n \int_0^\pi \sin \theta \sin n\theta d\theta$$

In Equation, the integral is

$$\int_0^\pi \sin n\theta \sin \theta d\theta = \begin{cases} \pi/2 & \text{for } n=1 \\ 0 & \text{for } n \neq 1 \end{cases}$$

Hence, Equation becomes

$$C_L = A_1 \pi \frac{b^2}{S} = A_1 \pi AR$$

Note that  $C_L$  depends only on the leading coefficient of the Fourier series expansion. (However, although  $C_L$  depends on  $A_1$  only, we must solve for all the  $A_n$ 's simultaneously in order to obtain  $A_1$ .)

The induced drag coefficient is obtained from the substitution of Equation into Equation as follows:

$$\begin{aligned} C_{D,i} &= \frac{2}{V_\infty S} \int_{-b/2}^{b/2} \Gamma(y) \alpha_i(y) dy \\ &= \frac{2b^2}{S} \int_0^\pi \left( \sum_1^N A_n \sin n\theta \right) \alpha_i(\theta) \sin \theta d\theta \end{aligned}$$

The induced angle of attack  $\alpha_i(\theta)$  in Equation is obtained from the substitution of Equation and into, which yields

$$\begin{aligned} \alpha_i(y_0) &= \frac{1}{4\pi V_\infty} \int_{-b/2}^{b/2} \frac{(d\Gamma/dy) dy}{y_0 - y} \\ &= \frac{1}{\pi} \sum_1^N n A_n \int_0^\pi \frac{\cos n\theta}{\cos \theta - \cos \theta_0} d\theta \end{aligned}$$

The integral in Equation is the standard form given by Equation. Hence, Equation becomes

$$\alpha_i(\theta_0) = \sum_1^N n A_n \frac{\sin n\theta_0}{\sin \theta_0}$$

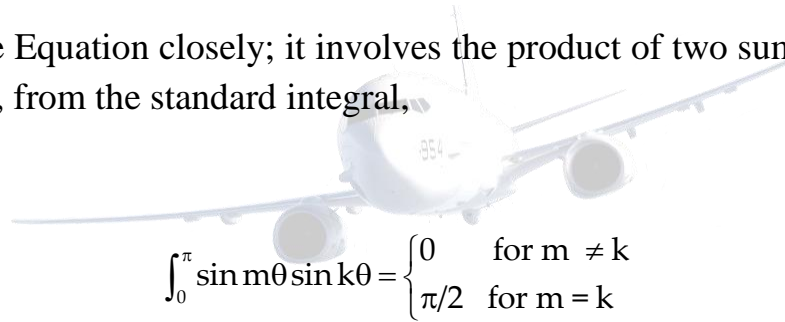
In Equation  $\theta$  is simply a dummy variable which range from 0 to  $\pi$  across the span of the span of the wing; it can therefore be replaced by  $\theta$ , and Equation can be written as

$$\alpha_i(\theta) = \sum_1^N n A_n \frac{\sin n\theta}{\sin \theta}$$

Substituting Equation into, we have

$$C_{D,i} = \frac{2b^2}{S} \int_0^\pi \left( \sum_1^N A_n \sin n\theta \right) \left( \sum_1^N n A_n \sin n\theta \right) d\theta$$

Examine Equation closely; it involves the product of two summations. Also, note that, from the standard integral,



$$\int_0^\pi \sin m\theta \sin k\theta = \begin{cases} 0 & \text{for } m \neq k \\ \pi/2 & \text{for } m = k \end{cases}$$

Hence, in Equation, the mixed product terms involving unequal subscripts (such as  $A_1, A_2, A_2 A_4$ ) are, from Equation, equal to zero. Hence, Equation becomes

$$\begin{aligned} C_{D,i} &= \frac{2b^2}{S} \left( \sum_1^N n A_n^2 \right) \frac{\pi}{2} = \pi A R \sum_1^N n A_n^2 \\ &= \pi A R \left( A_1^2 + \sum_2^N n A_n^2 \right) \\ &= \pi A R A_1^2 \left[ 1 + \sum_2^N n \left( \frac{A_n}{A_1} \right)^2 \right] \end{aligned}$$

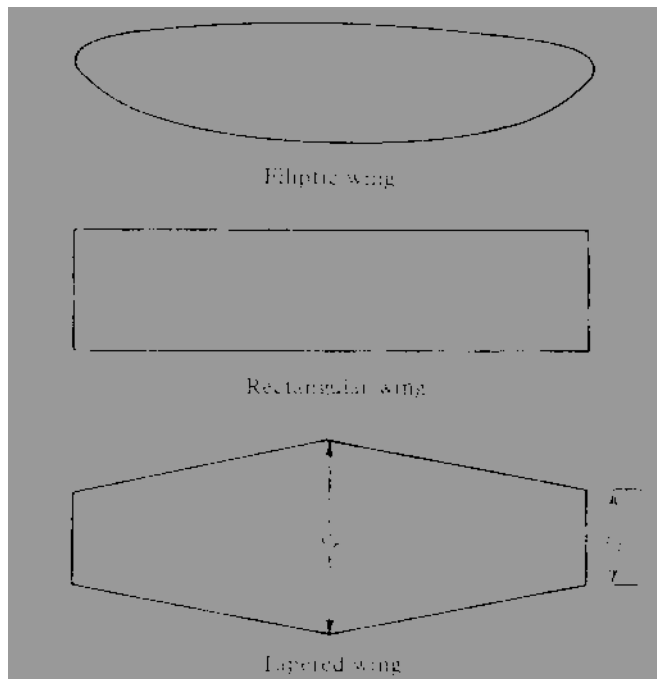
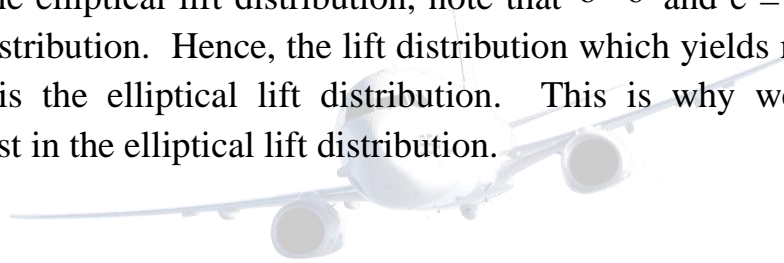
Substituting Equation for CL into Equation, we obtain

$$C_{D,i} = \frac{C_L^2}{\pi AR} (1 + \delta)$$

where  $\delta = \sum_2^N n(A_n / A_1)^2$ . Note that  $\delta \geq 0$ ; hence, the factor  $1 + \delta$  in Equation is either greater than 1 or at least equal to 1. Let us define a span efficiency factor,  $e$ , as  $e = (1 + \delta)^{-1}$ . Then Equation can be written as

$$C_{D,i} = \frac{C_L^2}{\pi e AR}$$

where  $e \leq 1$ . Comparing Equations and for the general lift distribution with Equation for the elliptical lift distribution, note that  $\delta = 0$  and  $e = 1$  for the elliptical lift distribution. Hence, the lift distribution which yields minimum induced drag is the elliptical lift distribution. This is why we have a practical interest in the elliptical lift distribution.



Recall that for a wing with no aerodynamic twist and no geometric twist, an elliptical lift distribution is generated by a wing with an elliptical planform, as sketched at the top of figure. Several aircraft have been designed in the past with elliptical wings; the most famous, perhaps, being the British Spitfire from World War II, shown in Figure. However, elliptic planforms are more expensive to manufacture than, say, a simple rectangular wing as sketched in the middle of Figure. On the other hand, a rectangular wing generates a lift distribution far from optimum. A compromise is the tapered wing shown at the bottom of figure. The tapered wing can be designed with a taper ratio, that is, tip chord/root chord  $\equiv c_t/c_r$ , such that the lift distribution closely approximates the elliptic case. The variation of  $\delta$  as a function of taper ratio for wings of different aspect ratio is illustrated in Figure. Such calculations of  $\delta$  were first performed by the famous English aerodynamicist, Herman Glauert and published in Reference 18 in the year 1926. Note from figure that a tapered wing can be designed with an induced drag coefficient reasonably close to the minimum value. In addition, tapered wings with straight leading and trailing edges are considerably easier to manufacture than elliptical planforms. Therefore, most conventional aircraft employ tapered rather than elliptical wing planforms.

### Effect of Aspect Ratio

Returning of Equations and, note that the induced drag coefficient for a finite wing with a general lift distribution is inversely proportional to the aspect ratio, as was discussed earlier in conjunction with the case of the elliptic lift distribution.



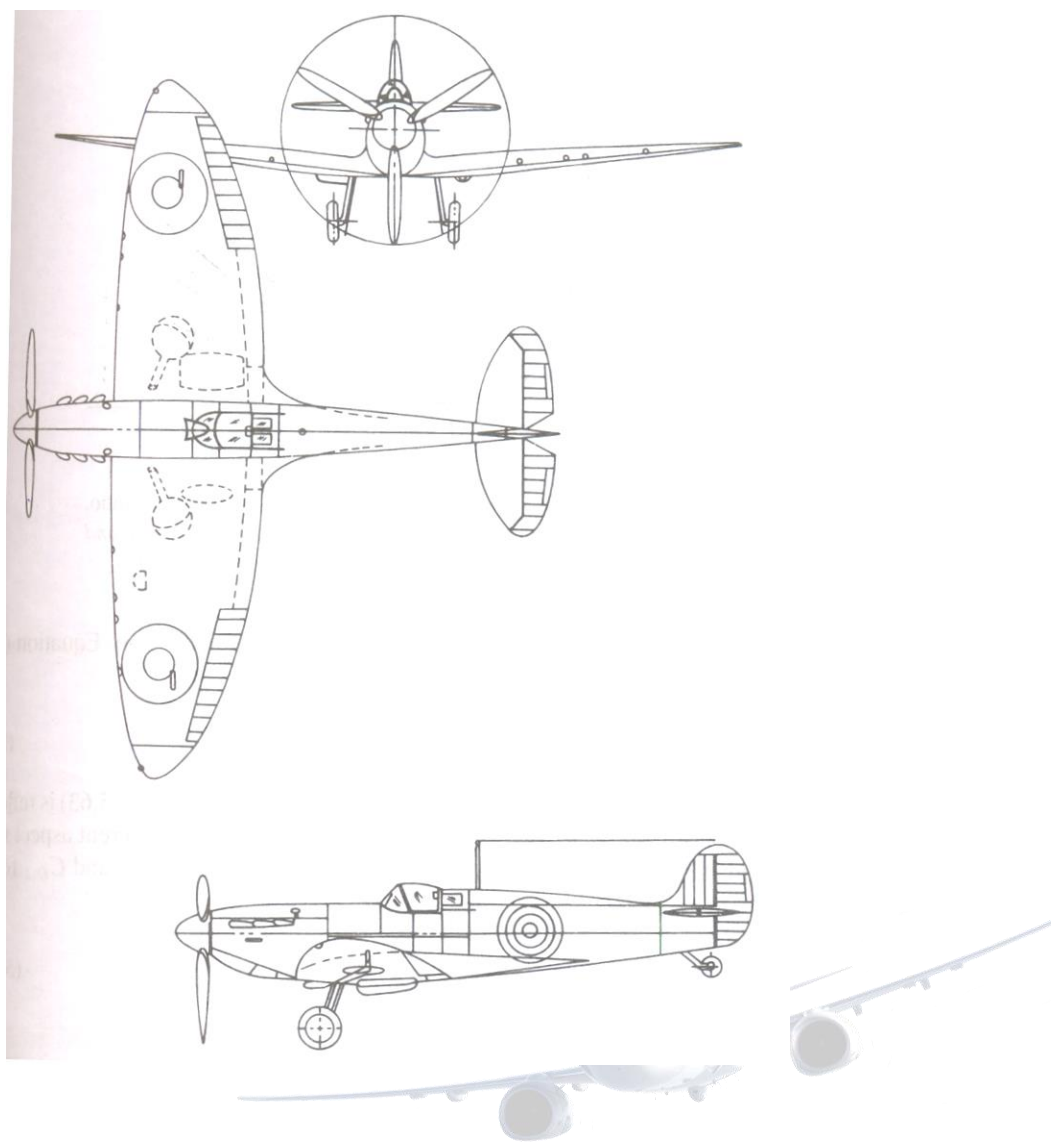


Figure: Three views of the Supermarine Spitfire, a famous British World War II fighter.

Note that  $AR$ , which typically varies from 6 to 22 for standard subsonic airplanes and sailplanes, has a much stronger effect on  $C_{D,I}$  than the value of  $\delta$ , which from Figure varies only by about 10 percent over the practical range of taper ratio. Hence, the primary design factor for minimizing induced drag is not the closeness to an elliptical lift distribution, but rather, the ability to make the aspect ratio as large as possible. The determination that  $C_{D,I}$  is inversely proportional to  $AR$  was one of the great victories of Prandtl's lifting-line theory. In 1915, Prandtl verified this result with a series of classic experiments wherein the lift and drag of seven rectangular wings with different aspect ratios were measured. The data are given in figure. Recall from Equation, that the total drag of a finite wing is given by

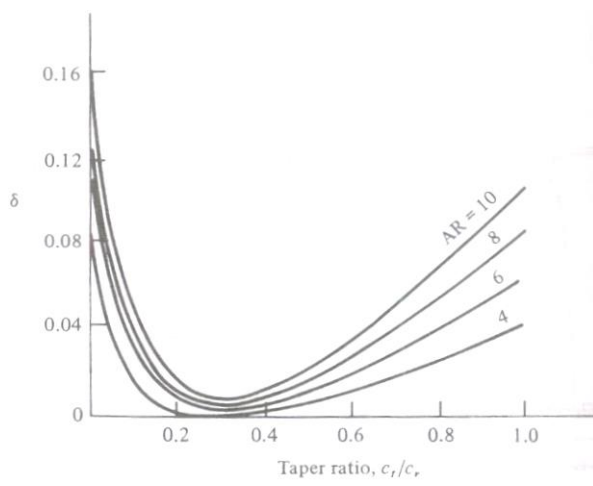


Figure: Induced drag factor  $\delta$  as a function of taper ratio.

$$C_D = c_d + \frac{C_L^2}{\pi e AR}$$

The parabolic variation of  $C_D$  with  $C_L$  as expressed in Equation is reflected in the data of figure. If we consider two wings with different aspect ratios  $AR_1$  and  $AR_2$ , Equation gives the drag coefficients  $C_{D,1}$  and  $C_{D,2}$  for the two wings as

$$C_{D,1} = c_d + \frac{C_L^2}{\pi e AR_1}$$

and

$$C_{D,2} = c_d + \frac{C_L^2}{\pi e AR_2}$$

Assume that the wings are at same  $C_L$ . Also, since the airfoil section is the same for both wings,  $c_d$  is essentially the same. Moreover, the variation of  $e$  between the wings is only a few percent and can be ignored. Hence, subtracting Equation from, we obtain

$$C_{D,1} - C_{D,2} = \frac{C_L^2}{\pi e} \left( \frac{1}{AR_1} - \frac{1}{AR_2} \right)$$

Equation can be used to scale the data of a wing with aspect ratio AR2 to correspond to the case of another aspect ratio AR1. For example, Prandtl Scaled the data of Figure to correspond to a wing with an aspect ratio of 5. For this case, Equation becomes

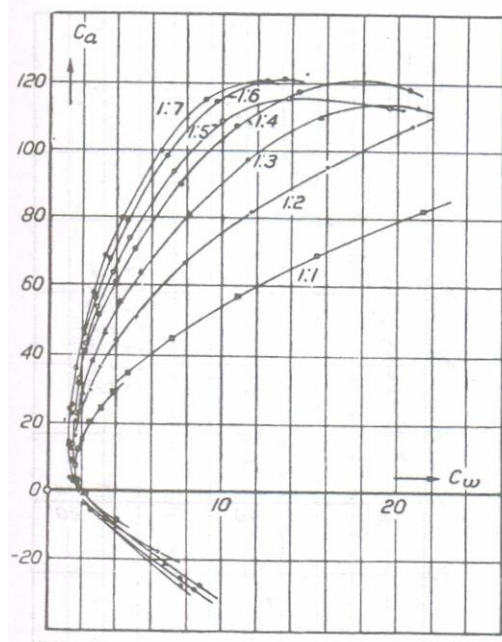


Figure: Prandtl's classic rectangular wing data for seven different aspect ratios from 1 to 7; variation of lift co lift coefficient versus drag coefficient. For historical interest, we reproduce here Prandtl's actual graphs. Note that, in his nomenclature, Ca = lift coefficient and Cw = drag coefficient. Also, the numbers on both the ordinate and abscissa are 100 times the actual values of the coefficients.

$$C_{D,1} = C_{D,2} + \frac{C_L^2}{\pi e} \left( \frac{1}{5} - \frac{1}{AR_2} \right)$$

Inserting the respective values of CD,2 and AR2 from Figure into Equation, Prandtl found that the resulting data for CD,1, versus CL collapsed to essentially the same curve, as shown in Figure. Hence, the inverse dependence of CD,I on AR was substantially verified as early as 1915.

There are two primary differences between airfoil and finite-wing properties. We have discussed one difference, namely, a finite wing generates induced drag. However, a second major difference appears in the lift slope.

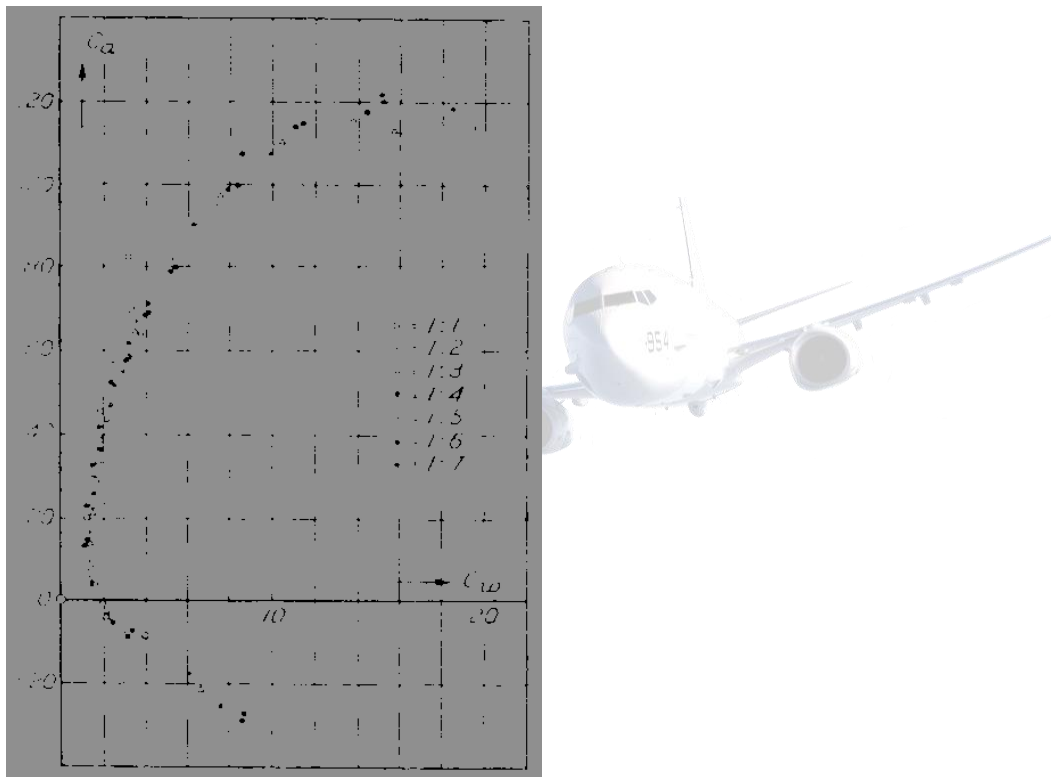


Figure: Data of Figure scaled by Prandtl to an aspect ratio of 5.

In Figure, the lift slope for an airfoil was defined as  $a_0 \equiv dc_l/d\alpha$ . Let us denote the lift slope for a finite wing as  $a \equiv dC_L/d\alpha$ . When the lift slope of a finite wing is compared with that of its airfoil section, we find that  $a < a_0$ . To see this more clearly, return to Figure, which illustrates the influence of downwash on the flow over a local airfoil section of a finite wing. Note that although the geometric angle of attack of the finite wing is  $\alpha$ , the airfoil

section effectively senses a smaller angle of attack, namely,  $\alpha_{\text{eff}}$  where  $\alpha_{\text{eff}} = \alpha - \alpha_i$ . For the time being, consider an elliptic wing with no twist; hence wing versus  $\alpha_{\text{eff}}$ , as shown at the top of figure. Because we are using  $\alpha_{\text{eff}}$  the lift slope corresponds to that for an infinite wing  $a_0$ . However, in real life, our naked eyes cannot see  $\alpha_{\text{eff}}$ , instead, what we actually observe is a finite wing with a certain angle between the chord line and the relative win; that is, in practice, we always observe the geometric angle of attack  $\alpha$ . Hence, CL for a finite wing is generally given as a function of  $\alpha$ , as sketched at the bottom of figure. Since  $\alpha > \alpha_{\text{eff}}$ , the bottom abscissa is stretched, and hence the bottom lift curve is less inclined; it has a slope equal to  $a$ , and figure clearly shows that  $a < a_0$ . The effect of a finite wing is to reduce the lift slope. Also, when  $C_L = 0, \alpha = \alpha_{\text{eff}}$ . As a result,  $\alpha_{L=0}$  is the same for the finite and the infinite wings, as shown in figure.

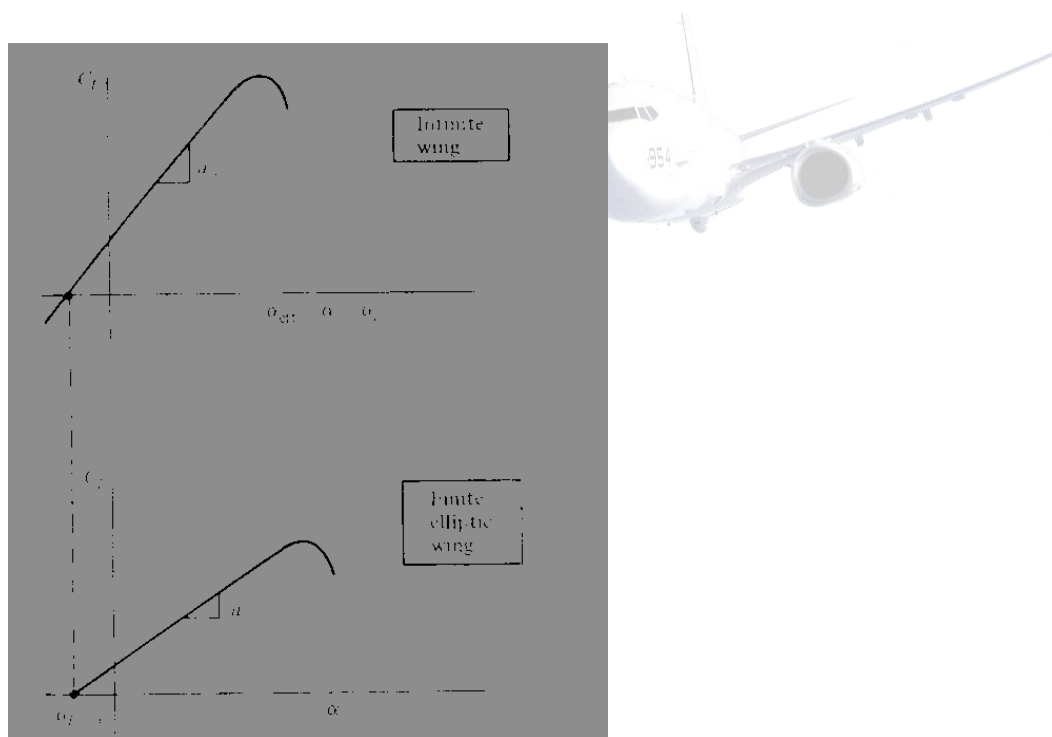


Figure: Lift curves for an infinite wing versus a finite elliptic wing.

The values of  $a_0$  and  $a$  are related as follows. From the top of figure,

$$\frac{dC_L}{d(\alpha - \alpha_i)} = a_0$$

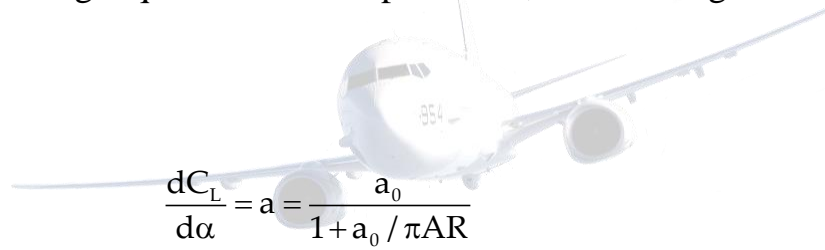
Integrating, we find

$$C_L = a_0 (\alpha - \alpha_i) + \text{const}$$

Substituting Equation into, we obtain

$$C_L = a_0 \left( \alpha - \frac{C_L}{\pi AR} \right) + \text{const}$$

Differentiating Equation with respect to  $\alpha$ , and solving for  $dC_L/d\alpha$ , we obtain



$$\frac{dC_L}{d\alpha} = a = \frac{a_0}{1 + a_0 / \pi AR}$$

Equation gives the desired relation between  $a_0$  and  $a$  for an elliptic finite wing. For a finite wing of general planform, Equation is slightly modified, as given below:

$$a = \frac{a_0}{1 + (a_0 / \pi AR)(1 + \tau)}$$

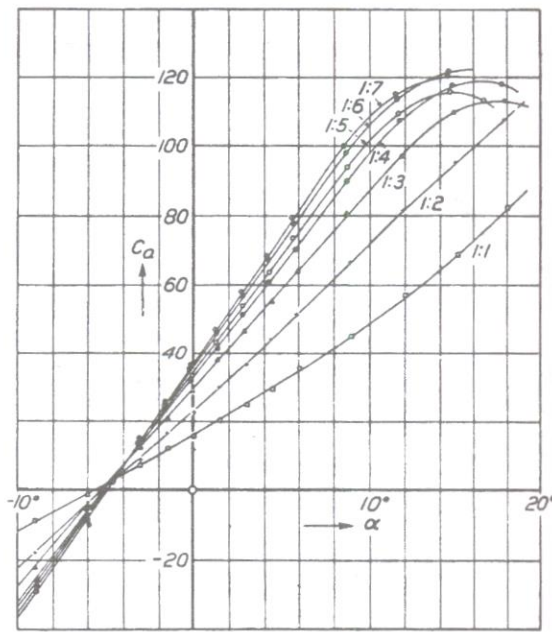


Figure: Prandtl's classic rectangular wing data. Variation of lift coefficient with angle of attack for seven different aspect ratios from 1 to 7. Nomenclature and scale are the same as given in figure.

In Equation,  $\tau$  is a function of the Fourier coefficients  $A_n$ . Values of  $\tau$  were first calculated by Glauert in the early 1920s and were published in Reference 18, which should be consulted for more details. Values of  $\tau$  typically range between 0.005 and 0.25.

Of most importance in Equation and is the aspect-ratio variation. Note that for low-AR wings, a substantial difference can exist between  $a_0$  and  $a$ . However, as  $AR \rightarrow \infty, a \rightarrow a_0$ . The effect of aspect ratio on the lift curve is dramatically shown in figure, which gives classic data obtained on rectangular wings by Prandtl in 1915. Note the reduction in  $dC_L/d\alpha$  as AR is reduced. Moreover, using the equations obtained above, Prandtl scaled the data in figure to correspond to an aspect ratio of 5; his results collapsed to essentially the same curve, as shown in Figure. In this manner, the aspect-ratio variation given in Equation and was confirmed as early as the year 1915.

Consider again the basic model underlying Prandtl's lifting-line theory. Return to figure and study it carefully. An infinite number of infinitesimally weak horseshoe vortices are superimposed in such a fashion as to generate a lifting line which spans the wing, along with a vortex sheet which trails downstream.

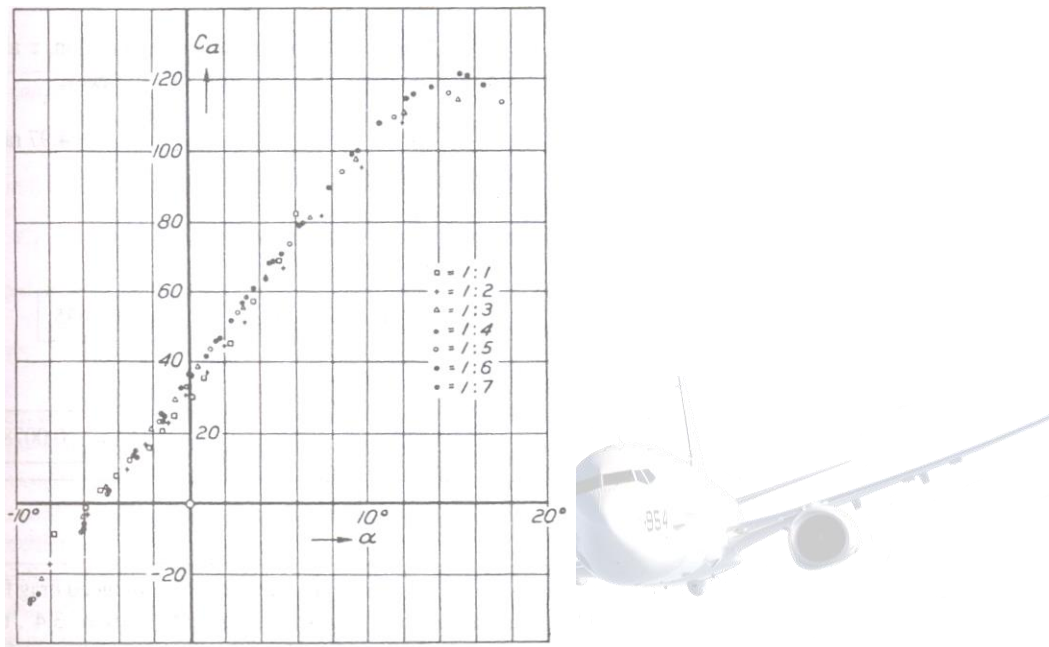


Figure: Data of Figure scaled by Prandtl to an aspect ratio of 5.

This trailing-vortex sheet is the instrument that induces downwash at the lifting line. At first thought, you might consider this model to be somewhat abstract—a mathematical convenience that somehow produces surprisingly useful results. However, to the contrary, the model shown in figure has real physical significance. To see this more clearly, return to figure. Note that in the three-dimensional flow over a finite wing, the streamlines leaving the trailing edge from the top and bottom surfaces are in different directions; that is, there is a discontinuity in the tangential velocity at the trailing edge. We know from that a discontinuous change in tangential velocity is theoretically allowed across a vortex sheet. In real life, such discontinuities do not exist; rather, the different velocities at the trailing edge generate a thin region of large velocity gradients—a thin region of shear flow



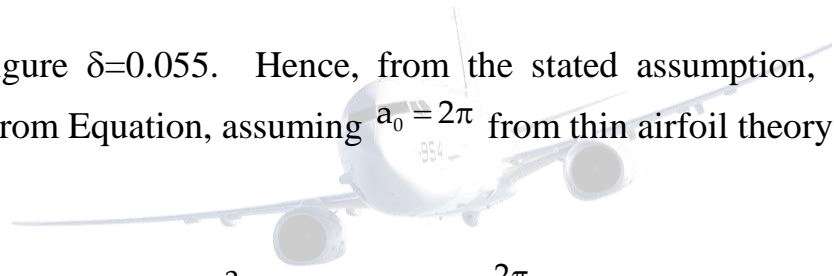
with very large vorticity. Hence, a sheet of vorticity actually trails downstream from the trailing edge of a finite wing. This sheet tends to roll up at the edges and helps to form the wing-tip vortices sketched in figure. Thus, Prandtl's lifting-line model with its trailing-vortex sheet is physically consistent with the actual flow downstream of a finite wing.

Example:

Consider a finite wing with an aspect ratio of 8 and a taper ratio of 0.8. The airfoil section is thin and symmetric. Calculate the lift and induced drag coefficients for the wing when it is at an angle of attack of  $5^\circ$ . Assume that  $\delta = \tau$ .

Solution:

From Figure  $\delta = 0.055$ . Hence, from the stated assumption,  $\tau$  also equal 0.055. From Equation, assuming  $a_0 = 2\pi$  from thin airfoil theory,



$$a = \frac{a_0}{1 + a_0 / \pi AR (1 + \tau)} = \frac{2\pi}{1 + 2\pi(1.055)/8\pi} = 4.97 \text{ rad}^{-1} \\ = 0.0867 \text{ degree}^{-1}$$

Since the airfoil is symmetric,  $\alpha_{L=0} = 0^\circ$ . Thus,

$$C_L = a\alpha = (0.0867 \text{ degree}^{-1} (5^\circ)) = \boxed{0.4335}$$

From Equation,

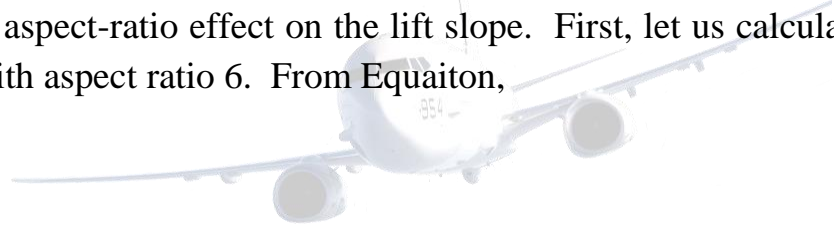
$$C_{D,i} = \frac{C_L^2}{\pi AR} (1 + \delta) = \frac{(0.4335)^2 (1 + 0.055)}{8\pi} = \boxed{0.00789}$$

Example:

Consider a rectangular wing with an aspect ratio of 6, an induced drag factor  $\delta = 0.055$ , and a zero-lift angle of attack of  $-2^\circ$ . At an angle of attack of  $3.4^\circ$ , the induced drag coefficient for this wing is 0.01. Calculate the induced drag coefficient for a similar wing (a rectangular wing with the same airfoil section) at the same angle of attack, but with an aspect ratio of 10. Assume that the induced factors for drag and the lift slope,  $\delta$  and  $\tau$ , respectively, are equal to each other (i.e.,  $\delta = \tau$ ). Also, for  $AR = 10$ ,  $\delta = 0.105$ .

Solution:

We must recall that although the angle of attack is the same for the two cases compared here ( $AR = 6$  and  $10$ ), the value of  $C_L$  is different because of the aspect-ratio effect on the lift slope. First, let us calculate  $C_L$  for the wing with aspect ratio 6. From Equation,



$$C_L^2 = \frac{\pi AR C_{D,i}}{1 + \delta} = \frac{\pi(6)(0.01)}{1 + 0.055} = 0.1787$$

Hence,  $C_L = 0.423$

The lift slope of this wing is therefore

$$\frac{dC_L}{d\alpha} = \frac{0.423}{3.4^\circ - (-2^\circ)} = 0.078 / \text{degree} = 4.485 / \text{rad}$$

The lift slope for the airfoil (the infinite wing) can be obtained from Equation:

$$\frac{dC_L}{d\alpha} = a = \frac{a_0}{1 + (a_0 / \pi AR)(1 + \tau)}$$

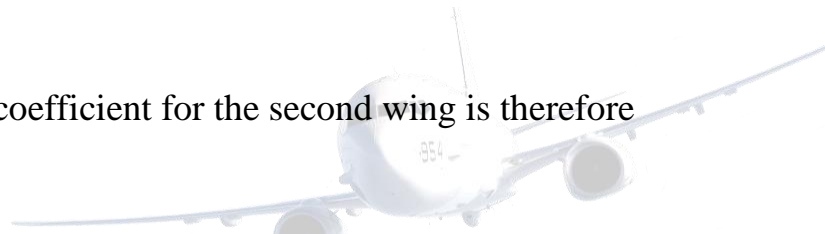
$$4.485 = \frac{a_0}{1 + [(1.055)a_0 / \pi(6)]} = \frac{a_0}{1 + 0.056a_0}$$

Solving for  $a_0$ , we find that this yields  $a_0 = 5.989/\text{rad}$ . Since the second wing (with  $AR = 10$ ) has the same airfoil section, then  $a_0$  is the same. The lift slope of the second wing is given by

$$a = \frac{a_0}{1 + (a_0 / \pi AR)(1 + \tau)} = \frac{5.989}{1 + [(5.989)(1.105) / \pi(10)]} = 4.95 / \text{rad}$$

$$= 0.086 / \text{degree}$$

The lift coefficient for the second wing is therefore



$$C_L = a(\alpha - \alpha_{L=0}) = 0.86[3.4^\circ - (-2^\circ)] = 0.464$$

In turn, the induced drag coefficient is

$$C_{D,i} = \frac{C_L^2}{\pi AR}(1 + \delta) = \frac{(0.464)^2 (1.105)}{\pi(10)} = \boxed{0.0076}$$

Note: This problem would have been more straightforward if the lift coefficients had been stipulated to be the same between the two wings rather than the angle of attack. Then Equation would have yielded the induced drag coefficient directly. A purpose of this example is to reinforce the rationale behind Equation, which readily allows the scaling of drag coefficients from one aspect ratio to another, as long as the lift coefficient is the same. This allows the scaled drag-coefficient data to be plotted versus  $C_L$  (not the angle of attack) as in figure. However, in the present example

where the angle of attack is the same between both cases, the effect of aspect ratio on the lift slope must be explicitly considered, as we have done above.

Example:

Consider the twin-jet executive transport discussed in example. In addition to the information given in Example, for this airplane the zero-lift angle of attack is  $-2^\circ$ , the lift slope of the airfoil section is per degree, the lift efficiency factor  $\tau = 0.04$ , and the wing aspect ratio is 7.96. At the cruising condition treated in Example, calculate the angle of attack of the airplane.

Solution:

The lift slope of the airfoil section in radians is

$$A_0 = 0.1 \text{ per degree} = 0.1(57.3) = 5.73 \text{ rad}$$

From Equation repeated below

$$a = \frac{a_0}{1 + (a_0 / \pi AR)(1 + \tau)}$$

We have

$$a = \frac{5.73}{1 + \left( \frac{5.73}{7.96\pi} \right)(1 + 0.04)} = 4.627 \text{ per rad}$$

or 
$$a = \frac{4.627}{57.3} = 0.0808 \text{ per degree}$$

From Example, the airplane is cruising at a lift coefficient equal to.  
Since

$$C_L = a(\alpha - \alpha_{L=0})$$

We have

$$\alpha = \frac{C_L}{a} + \alpha_{L=0} = \frac{0.21}{0.0808} + (-2) = \boxed{0.6^\circ}$$

Example:

In the Preview Box for this chapter, we considered the Beechcraft Baron. Flying such that the wing is at a 4-degree angle of attack. The wing of this airplane has an NACA 23015 airfoil at the root, tapering to a 23010 airfoil at the tip. The data for the NACA 23105 airfoil is given in Figure. In the Preview Box, we teased you by reading from Figure the airfoil lift and drag coefficients at  $\alpha = 4^\circ$ , namely,  $c_l = 0.54$  and  $c_d = 0.0068$ , and posed the question: Are the lift and drag coefficients of the wing the same values, that is,  $C_L = 0.54(?)$  and  $C_D = 0.0068(?)$  The answer given in the Preview Box was a resounding NO! We now know why. Moreover, we now know how to calculate  $C_L$  and  $C_D$  for the wing. Let us proceed to do just that. Consider the wing of the Beechcraft Baron 58 at a 4-degree angle of attack. The wing has an aspect ratio of 7.61 and a taper ratio of 0.45. Calculate  $C_L$  and  $C_D$  for the wing.

Solution:

From Figure, the zero-lift angle of attack of the airfoil, which is the same for the finite wing, is

$$\alpha_{L=0} = -1^\circ$$

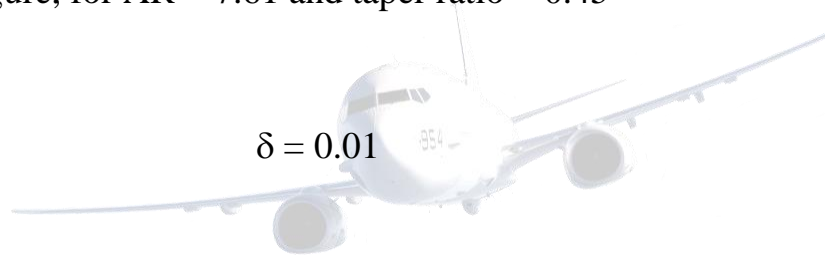
The airfoil lift slope is also obtained from Figure a. Since the lift curve is linear below the stall, we arbitrarily pick two points on this curve:  $\alpha = 7^\circ$  where  $c_l = 0.9$ , and  $\alpha = -1^\circ$  where  $C_l = 0$ . Thus

$$a_0 = \frac{0.9 - 0}{7 - (-1)} = \frac{0.9}{8} = 0.113 \text{ per degree}$$

The lift slope in radians is:

$$a_0 = 0.113(57.3) = 6.47 \text{ per rad}$$

From figure, for  $AR = 7.61$  and taper ratio = 0.45



$$e = \frac{1}{1 + \delta} = \frac{1}{1 + 0.01} = 0.99$$

Hence,

From Equation, assuming  $\tau = \delta$ ,

$$a = \frac{a_0}{1 + \left( \frac{a_0}{\pi AR} \right) (1 + \tau)} \quad (a \text{ and } a_0 \text{ are per rad})$$

where 
$$\frac{a_0}{\pi AR} = \frac{6.47}{\pi(7.61)} = 0.271$$

$$(1 + \tau) = 1 + 0.01 = 1.01$$

we have

$$a = \frac{6.47}{1 + (0.271)(1.01)} = 5.08 \text{ per rad}$$

Converting back to degrees:

$$a = \frac{5.08}{57.3} = 0.0887 \text{ per degree}$$

For the linear lift curve for the finite wing

$$C_L = a(\alpha - \alpha_{L=0})$$

For  $\alpha = 4^\circ$ , we have



$$C_L = 0.0887[4 - (-1)] = 0.0887(5)$$

$$C_L = \boxed{0.443}$$

The drag coefficient is given by Equation;

$$C_D = c_d + \frac{C_L^2}{\pi e AR}$$

Here,  $c_d$  is the section drag coefficient given in Figure. Note that in Figure b,  $c_d$  is plotted versus the section lift coefficient  $c_l$ . To accurately read  $c_d$  from figure, we need to know the value of  $c_l$  actually sensed by the airfoil section on the finite wing, that is, the value of the airfoil  $c_l$  for the airfoil at its effective angle of attack,  $\alpha_{\text{eff}}$ . To estimate  $\alpha_{\text{eff}}$ , we will assume an elliptical lift distribution over the wing. We know this is not quite correct,

but with a value of  $\delta = 0.01$ , it is not very far off. From Equation for an elliptical lift distribution, the induced angle of attack is

$$\alpha_i = \frac{C_L}{\pi AR} = \frac{(0.433)}{\pi(7.61)} = 0.0185 \text{ rad}$$

In degrees

$$\alpha_i = (0.0185)(57.3) = 1.06^\circ$$

From figure,

$$\alpha_{\text{eff}} = \alpha - \alpha_i = 4^\circ - 1.06^\circ = 2.94^\circ \approx 3^\circ$$

The lift coefficient sensed by the airfoil is then

$$\begin{aligned} c_l &= a_0 (\alpha_{\text{eff}} - \alpha_{L=0}) \\ &= 0.113[3 - (-1)] = 0.113(4) = 0.452 \end{aligned}$$

(Note how close this section lift coefficient is to the overall lift coefficient of the wing of 0.433.) From Figure b, taking the data at the highest Reynolds number shows, for  $c_l = 0.452$ , we have

$$C_d = 0.0065$$

Returning to Equation,



$$\begin{aligned}
 C_D &= c_d + \frac{C_L^2}{\pi e AR} \\
 &= 0.0065 + \frac{(0.433)^2}{\pi(0.99)(7.61)} \\
 &= 0.0065 + 0.0083 = \boxed{0.0148}
 \end{aligned}$$



## UNIT - V

# Propeller Theory



## FTOUDE MOMENTUM AND BLADE ELEMENT THEORIES

### Momentum theory

Mathematical model of an ideal propeller or helicopter rotor can be described by The Momentum theory or Disk actuator theory by W.J.M.Rankine, Alfred George Greenhill and R.E. Froude.

In fluid dynamics, the momentum theory describes a mathematical model of an ideal actuator disk, such as a propeller or helicopter rotor. The rotor is modeled as an infinitely thin disk, inducing a constant velocity along the axis of rotation. The basic state of a helicopter is hovering. This disk creates a flow around the rotor. Under certain mathematical premises of the fluid, there can be extracted a mathematical connection between power, radius of the rotor, torque and induced velocity. Friction is not included.

For a stationary rotor, such as a helicopter in hover, the power required to produce a given thrust is:

$$P = \sqrt{\frac{T^3}{2\rho A}}$$

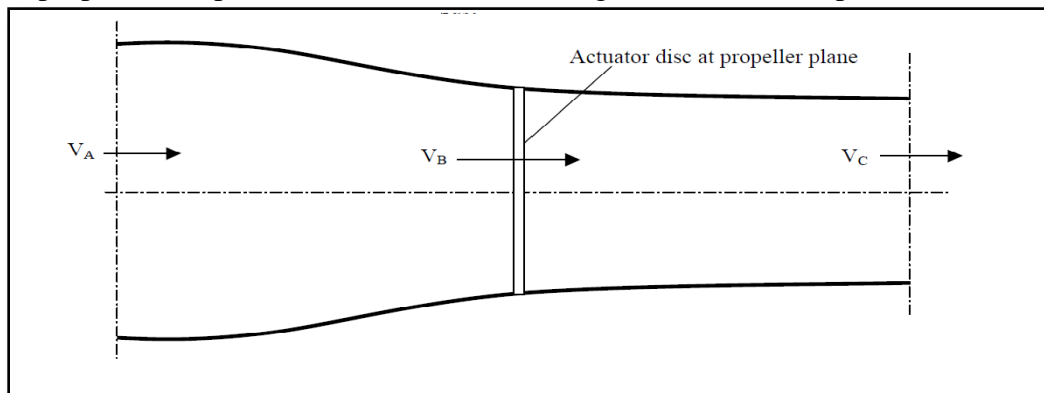
Where:

- $T$  is the thrust
- $\rho$  is the density of air (or other medium)
- $A$  is the area of the rotor disc

A device which converts the translational energy of the fluid into rotational energy of the axis or vice versa is called a Rankine disk actuator.

It was originally intended to provide an analytical means for evaluating ship propellers. Momentum Theory is also well known as Disk Actuator Theory. Momentum Theory assumes that

- The flow is inviscid and steady (ideal flow), therefore the propeller does not experience energy losses due to frictional drag.
- Also the rotor is thought of as an actuator disk with an infinite number of blades, each with an infinite aspect ratio.
- The propeller can produce thrust without causing rotation in the slipstream.



Here the rotor is assumed as an infinitely thin disc, which induces a constant velocity along the axis of rotation.

From the basic thrust equation, we know that the amount of thrust depends on the mass flow rate through the propeller and the velocity change through the propulsion system. In the above figure the flow is proceeding from left to right. Let us denote the subscripts "A and C" for the stations assumed to be far upstream and downstream of the propeller respectively and the location of the actuator disc by the subscript "B". The thrust (T) is equal to the mass flow rate (m) times the difference in velocity (V).

$$T = m(V_C - V_A)$$

There is no pressure-area term because the pressure at the C is equal to the pressure at A.

- The power  $P_D$  absorbed by the propeller is given by:

$$P_D = \frac{1}{2} m (V_C^2 - V_A^2)$$

- Momentum theory thrust is given by,

$$T = \frac{\pi}{4} D^2 (v + \frac{\Delta v}{2}) \rho \Delta v$$



### Blade element theory

Blade element momentum theory is a theory that combines both blade element theory and momentum theory. It is used to describe the flow of fluids round the aerofoils/blades of a rotor of a turbine. Blade element theory is combined with momentum theory to alleviate some of the difficulties in calculating the induced velocities at the rotor.

## Glauert Blade Element Theory

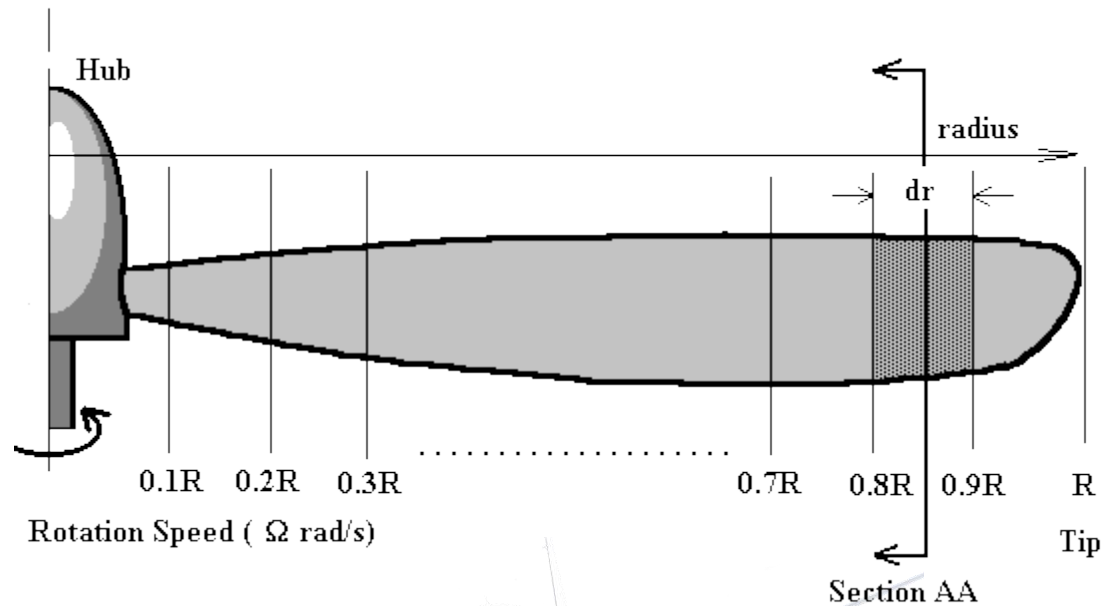
A relatively simple method of predicting the performance of a propeller (as well as fans or windmills) is the use of Blade Element Theory. In this method the propeller is divided into a number of independent sections along the length. At each section a force balance is applied involving 2D section lift and drag with the thrust and torque produced by the section. At the same time a balance of axial and angular momentum is applied. This produces a set of non-linear equations that can be solved by iteration for each blade section. The resulting values of section thrust and torque can be summed to predict the overall performance of the propeller.

The theory does not include secondary effects such as 3-D flow velocities induced on the propeller by the shed tip vortex or radial components of flow induced by angular acceleration due to the rotation of the propeller. In comparison with real propeller results this theory will over-predict thrust and under-predict torque with a resulting increase in theoretical efficiency of 5% to 10% over measured performance. Some of the flow assumptions made also breakdown for extreme conditions when the flow on the blade becomes stalled or there is a significant proportion of the propeller blade in windmilling configuration while other parts are still thrust producing.

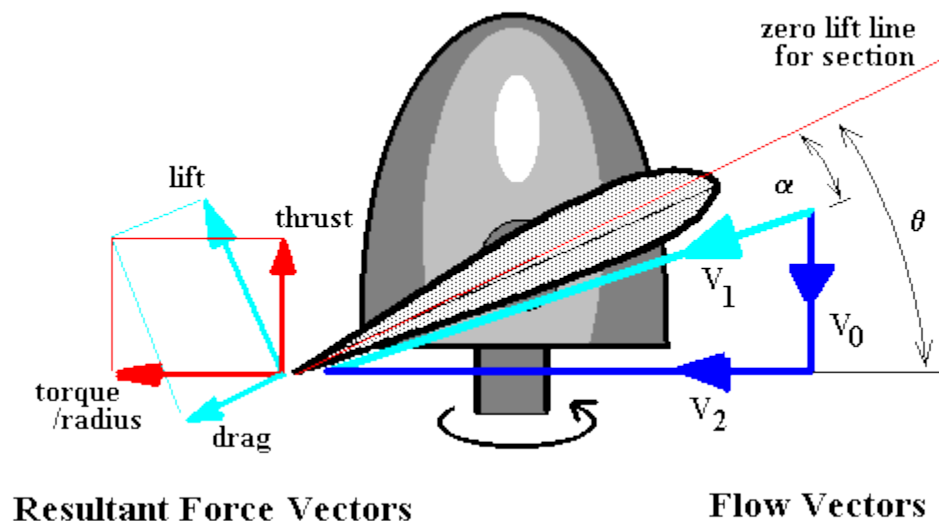
The theory has been found very useful for comparative studies such as optimising blade pitch setting for a given cruise speed or in determining the optimum blade solidity for a propeller. Given the above limitations it is still the best tool available for getting good first order predictions of thrust, torque and efficiency for propellers under a large range of operating conditions.

## Blade Element Subdivision

A propeller blade can be subdivided as shown into a discrete number of sections.



For each section the flow can be analysed independently if the assumption is made that for each there are only axial and angular velocity components and that the induced flow input from other sections is negligible. Thus at section AA (radius =  $r$ ) shown above, the flow on the blade would consist of the following components.



$V_0$  -- axial flow at propeller disk,  $V_2$  -- Angular flow velocity vector

$V_1$  -- section local flow velocity vector, summation of vectors  $V_0$  and  $V_2$

Since the propeller blade will be set at a given geometric pitch angle ( $\theta$ ) the local velocity vector will create a flow angle of attack on the section. Lift and drag of the section can be calculated using standard 2-D aerofoil properties. (Note: change of reference line from chord to zero lift line). The lift and drag

components normal to and parallel to the propeller disk can be calculated so that the contribution to thrust and torque of the complete propeller from this single element can be found.

The difference in angle between thrust and lift directions is defined as

$$\phi = \theta - \alpha$$

The elemental thrust and torque of this blade element can thus be written as

$$\Delta T = \Delta L \cos(\phi) - \Delta D \sin(\phi) \quad , \quad \frac{\Delta Q}{r} = \Delta D \cos(\phi) + \Delta L \sin(\phi)$$

Substituting section data ( $C_L$  and  $C_D$  for the given  $\alpha$ ) leads to the following equations.

$$\Delta L = C_L \frac{1}{2} \rho V_1^2 c \cdot dr \quad , \quad \Delta D = C_D \frac{1}{2} \rho V_1^2 c \cdot dr \text{ per blade}$$

where  $\rho$  is the air density,  $c$  is the blade chord so that the lift producing area of the blade element is  $c \cdot dr$ .

If the number of propeller blades is ( $B$ ) then,

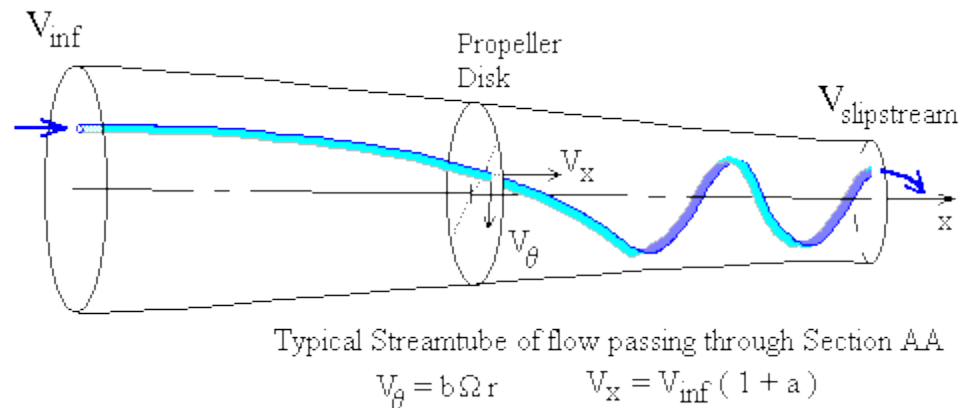
$$\Delta T = \frac{1}{2} \rho V_1^2 c (C_L \cos(\phi) - C_D \sin(\phi)) \cdot B \cdot dr \dots \dots \dots (1)$$

$$\frac{\Delta Q}{r} = \frac{1}{2} \rho V_1^2 c (C_L \sin(\phi) + C_D \cos(\phi)) \cdot B \cdot dr$$

$$\Delta Q = \frac{1}{2} \rho V_1^2 c (C_L \sin(\phi) + C_D \cos(\phi)) \cdot B \cdot r \cdot dr \dots \dots \dots (2)$$

## 2. Inflow Factors

A major complexity in applying this theory arises when trying to determine the magnitude of the two flow components  $V_0$  and  $V_2$ .  $V_0$  is roughly equal to the aircraft's forward velocity ( $V_{inf}$ ) but is increased by the propeller's own induced axial flow into a slipstream.  $V_2$  is roughly equal to the blade section's angular speed ( $\Omega r$ ) but is reduced slightly due to the swirling nature of the flow induced by the propeller. To calculate  $V_0$  and  $V_2$  accurately both axial and angular momentum balances must be applied to predict the induced flow effects on a given blade element. As shown in the following diagram the induced flow components can be defined as factors increasing or decreasing the major flow components.



So for the velocities  $V_0$  and  $V_2$  as shown in the previous section flow diagram,

$$V_o = V_{inf} + a \cdot V_{inf} \text{ where } a \text{ -- axial inflow factor}$$

$$V_2 = \Omega r - b \cdot \Omega r \text{ where } b \text{ -- angular inflow factor (swirl factor)}$$

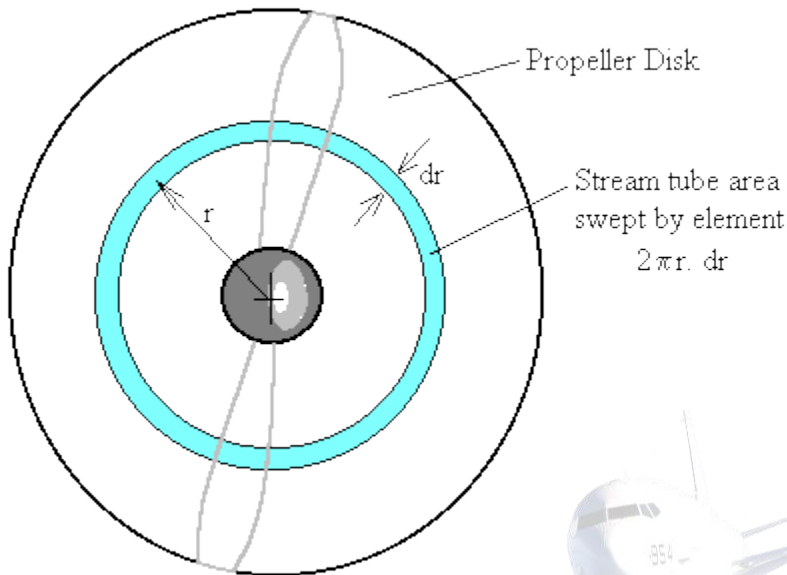
The local flow velocity and the angle of attack for the blade section is thus

$$V_1 = \sqrt{(V_o^2 + V_2^2)} \dots \dots \dots (3)$$

$$\alpha = \theta - \tan^{-1}(V_o/V_2) \dots \dots \dots (4)$$

### 3. Axial and Angular Flow Conservation of Momentum

The governing principle of conservation of flow momentum can be applied for both axial and circumferential directions.



For the axial direction, the change in flow momentum along a stream-tube starting upstream, passing through the propeller at section AA and then moving off into the slipstream, must equal the thrust produced by this element of the blade.

To remove the unsteady effects due to the propeller's rotation, the stream-tube used is one covering the complete area of the propeller disk swept out by the blade element and all variables are assumed to be time averaged values.

$$\Delta T = \text{change in momentum flow rate}$$

$$= \text{mass flow rate in tube} \times \text{change in velocity}$$

$$= \rho 2 \pi r dr V_o (V_{\text{slipstream}} - V_{\text{inf}})$$

By applying Bernoulli's equation and conservation of momentum, for the three separate components of the tube, from freestream to face of disk, from rear of disk to slipstream far downstream and balancing pressure and area versus thrust, it can be shown that the axial velocity at the disk will be the average of the freestream and slipstream velocities.

$$V_0 = (V_{\text{inf}} + V_{\text{slipstream}})/2, \text{ that means } V_{\text{slipstream}} = V_{\text{inf}}(1 + 2a)$$

Thus

$$\Delta T = \rho 2 \pi r V_{\text{inf}}(1+a) \cdot (V_{\text{inf}}(1+2a) - V_{\text{inf}}) \cdot dr$$

$$\Delta T = \rho 2 \pi r V_{\text{inf}}^2 (1+a) \cdot 2a \cdot dr$$

$$\Delta T = \rho 4 \pi r V_{inf}^2 (1+a) \cdot a \cdot dr \dots \dots \dots (5)$$

For angular momentum

$\Delta Q$  = change in angular momentum rate for flow x radius

= mass flow rate in tube x change in circumferential velocity x radius

$$\Delta Q = \rho 2 \pi r dr V_o \cdot (V_{\theta}(\text{slipstream}) - 0(\text{freestream})) \cdot r$$

By considering conservation of angular momentum in conjunction with the axial velocity change, it can be shown that the angular velocity in the slipstream will be twice the value at the propeller disk.

$$V_{\theta}(\text{slipstream}) = 2 b \Omega r$$

Thus

$$\Delta Q = \rho 2 \pi r V_{inf} (1+a) \cdot (2 b \Omega r) \cdot r \cdot dr$$

$$\Delta Q = \rho 4 \pi r^3 V_{inf}^2 (1+a) \cdot b \Omega \cdot dr \dots \dots \dots (6)$$

Because these final forms of the momentum equation balance still contain the variables for element thrust and torque, they cannot be used directly to solve for inflow factors.

However there now exists a nonlinear system of equations (1),(2),(3),(4),(5) and (6) containing the four primary unknown variables  $\Delta T$ ,  $\Delta Q$ , a, b. So an iterative solution to this system is possible.

#### 4. Iterative Solution procedure for Blade Element Theory.

The method of solution for the blade element flow will be to start with some initial guess of inflow factors (a) and (b). Use these to find the flow angle on the blade (equations (3),(4)), then use blade section properties to estimate the element thrust and torque (equations (1),(2)). With these approximate values of thrust and torque equations (5) and (6) can be used to give improved estimates of the inflow factors (a) and (b). This process can be repeated until values for (a) and (b) have converged to within a specified tolerance.

It should be noted that convergence for this nonlinear system of equations is not guaranteed. It is usually a simple matter of applying some convergence enhancing techniques (ie Crank-Nicholson under-relaxation) to get a result when linear aerofoil section properties are used. When non-linear properties are used, ie including stall effects, then obtaining convergence will be significantly more difficult.

For the final values of inflow factor (a) and (b) an accurate prediction of element thrust and torque will be obtained from equations (1) and (2).

#### 5. Propeller Thrust and Torque Coefficients and Efficiency.

The overall propeller thrust and torque will be obtained by summing the results of all the radial blade element values.

$$T = \Sigma \Delta T \text{ (for all elements), and } Q = \Sigma \Delta Q \text{ (for all elements)}$$

The non-dimensional thrust and torque coefficients can then be calculated along with the advance ratio at



which they have been calculated.

$$C_T = T/(\rho n^2 D^4) \text{ and } C_Q = Q/(\rho n^2 D^5) \text{ for } J = V_{inf}/(nD)$$

where  $n$  is the rotation speed of propeller in revs per second and  $D$  is the propeller diameter.

The efficiency of the propeller under these flight conditions will then be

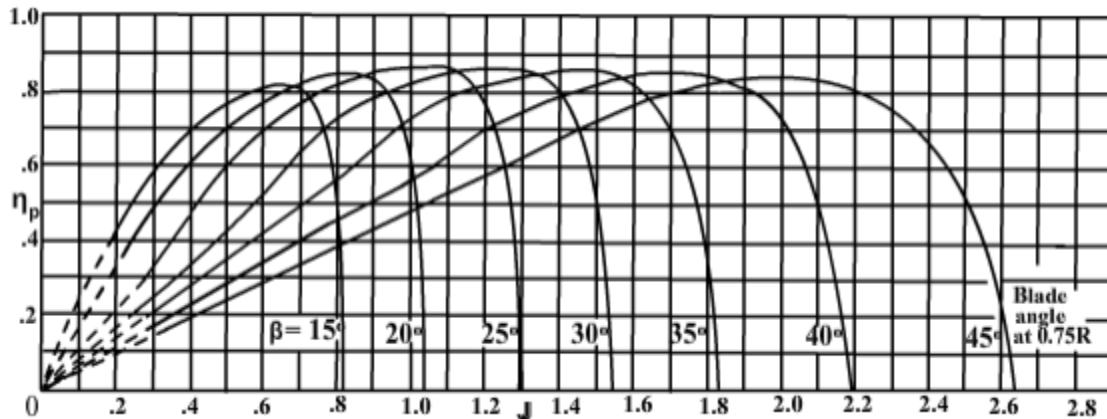
$$\eta(\text{propeller}) = J/(2\pi) \cdot (C_T/C_Q).$$

## 6. Software Implementation of Blade Element Theory

Two programming versions of this propeller analysis technique are available. The first is a demonstration program which can be used to calculate thrust and torque coefficients and efficiency for a relatively simple propeller design using standard linearised aerofoil section data. The blade is assumed to have a constant pitch ( $p$ ) so that the variation of  $\theta$  with radius is calculated from the standard pitch equation.

$$p = 2\pi r \tan(\theta).$$

## PROPELLER COEFFICIENTS



### Propeller efficiency ( $\eta_p$ ) vs advance ( $J$ ) ratio with pitch angle ( $\beta$ ) as parameter

This is because even though the engine is working and producing thrust, no useful work is done when  $V$  is zero.

For a chosen value of  $\beta$ , the efficiency ( $\eta_p$ ) increases as  $J$  increases. It reaches a maximum for a certain value of  $J$  and then decreases.

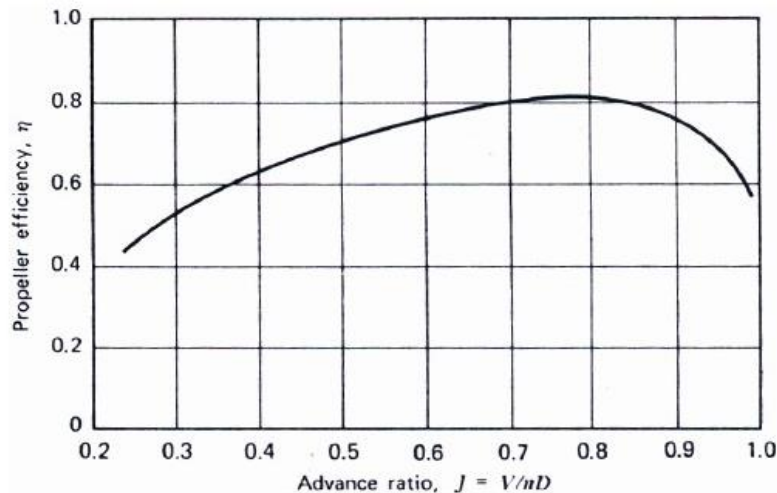
The maximum value of  $\eta_p$  is seen to be around 80 to 85%. However, the value of  $J$  at which the maximum of  $\eta_p$  occurs, depends on the pitch angle  $\beta$ . This indicates that for a single pitch or fixed pitch propeller, the efficiency is high (80 to 85%) only over a narrow range of flight speeds.

Keeping this behavior in view, the commercial airplanes use a variable pitch propeller. In such a propeller the entire blade is rotated through a chosen angle during the flight and the pitch of all blade elements changes. Such propellers have high efficiency over a wide range of speeds.

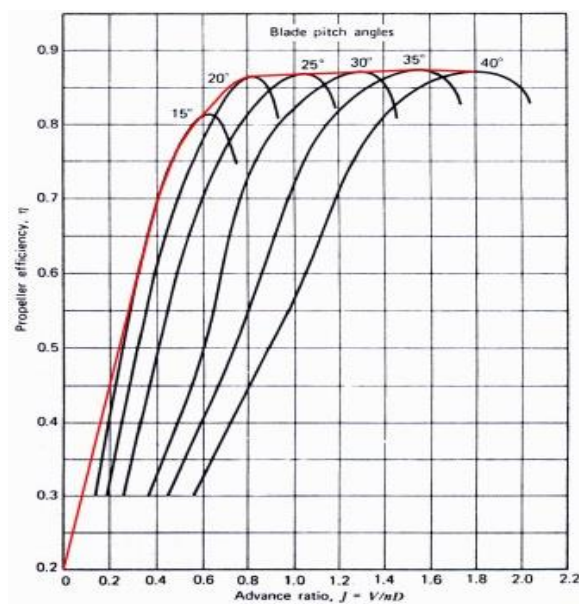
## PERFORMANCE OF FIXED AND VARIABLE PITCH PROPELLERS

The propeller is a twisted airfoil that converts the rotating power of the engine into thrust. For a variable pitch propeller, the device called “propeller governor” changes the propeller pitch to a higher blade angle, as the forward velocity of the aircraft increases. Therefore, maximum efficiency is obtained for a wide range of forward velocities from take-off to cruise. In case of fixed pitch propellers, they are designed to provide optimum efficiency for only one flight phase, either climb or cruise. thus take-off performance is poor with the fixed pitch propellers. which propels the airplane through the air. Sections of the propeller near the center are moving at a slower rate of speed than those near the tip, which is why the blades are twisted.

For a propeller driven aircraft, thrust is produced by a propeller converting the shaft torque into propulsive force, and depends on the propeller efficiency. However, propeller efficiency depends on the propeller angle of attack, consequently on the advance ratio given by where  $V$  is the forward velocity of the aircraft,  $n$  is the rotational speed and  $D$  is the diameter of the propeller. Thus, for a constant RPM, propeller efficiency depends on the forward velocity of the aircraft as shown in Figure.

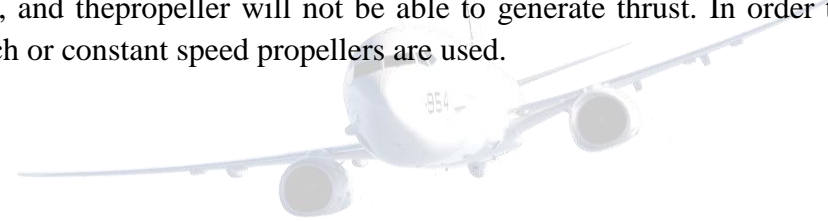


Efficiency versus advance ratio for a fixed pitch propeller



### Efficiency of a variable pitch propeller

If the propeller is a fixed pitch propeller, for a constant RPM, there is only one forward velocity where the efficiency reaches to a maximum. Consider the drawing given in Figure given, where the forward velocity, blade angle, angle of attack, and rotational velocity relations are shown. If the blade angle is fixed, hence the propeller is fixed pitch; angle of attack will decrease as the forward velocity of aircraft increases. Although this will result in an efficiency increase initially, further velocity increase will bring the angle of attack to zero, and the propeller will not be able to generate thrust. In order to avoid this, variable pitch or constant speed propellers are used.



## TWO MARK QUESTION BANK

### UNIT - I REVIEW OF BASIC FLUID MECHANICS

#### 1. Differentiate control volume and control surface.

Control volume has a fixed boundary, Mass, Momentum & energy are allowed to cross the boundary. The boundary of the control volume is referred to as control surface.

#### 2. What is aerodynamics?

Aerodynamics is the study of flow of gases around the solid bodies.

### **3. Differentiate steady and unsteady flow.**

In a steady flow fluid characteristics is velocity, pressure , Density etc at a point do not change with time but for unsteady flow these characteristics will change with repeat to time.

### **4. Differentiate compressible and Incompressible flow.**

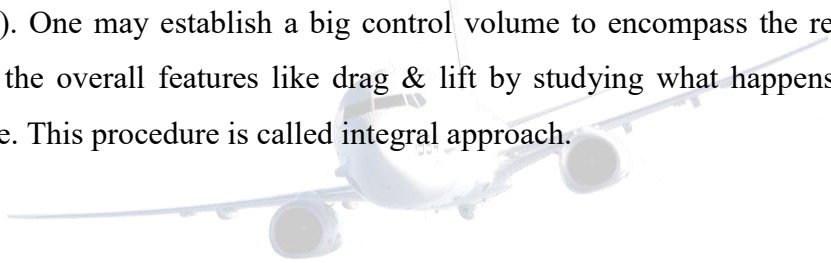
In a compressible flow, Density will change from point to point in a fluid flow, for incompressible flow, density will not change from point to point in a fluid flow.

### **5. Define a system.**

The word system refers to a fixed mass with a boundary, However with time, the boundary of the system may change, but the mass remains the same.

### **6. Differentiate between differential and Integral approach.**

Differential approach aims to calculate flow at every point in a given flow field in the form  $p(x,y,z,t)$ . One may establish a big control volume to encompass the region  $R$  and calculate the overall features like drag & lift by studying what happens at the control surface. This procedure is called integral approach.



**7. What is the principle of conservation of mass?**

Mass can be neither created nor destroyed. This is the basic principle for continuity equation.

**8. Give the continuity equation for a steady flow.**

For a steady flow mass accumulation will not occurs inside the control

volume. So,  $\oint \rho V dA = 0$

Where V is velocity of fluid

**9. Give the continuity equation for a incompressible flow.**

For an incompressible density is constant

$$\frac{\partial u}{\partial x} + \frac{\partial v}{\partial y} + \frac{\partial w}{\partial z} = 0$$

**10. Give the continuity equation for a steady - incompressible flow.**

If the flow is steady & incompressible , then continuity equation is

$$\oint V dA = 0$$

Where V is the velocity of fluid.

**11. Consider a convergent duct with an inlet area  $A_1=5\text{m}^2$ , Air enters this duct with a velocity  $V_1=10\text{m/s}$  and leaves the duct with a velocity  $V_2= 30\text{m/s}$ . what is the area of the duct exit.?**

*Solution:*  $A_1V_1=A_2V_2$ (for in compressible flow = constant)

$$A_2 = \frac{A_1V_1}{V_2} = \frac{5 \times 10}{30} = 1.67\text{m}^2$$

**12. What are the forces that can be experienced by fluid flow in a system?**

1. Body forces like gravity , electromagnetic forces(or)any other forces which act at a distance on a fluid inside volume.
2. Surface forces like pressure and shear stress acting on the control surface S.

**13. What is impulse momentum equation?**

The impulse of a force 'F' acting on a fluid mass 'm' in a short interval of time 'dt' is equal to the change of momentum  $d(mv)$  in the direction of force .

**14. What is meant by streamlining a body?**

Stream lining in a fluid flow to minimize the drag due to skin friction by providing the body with a boundary which permits a gradual divergence of flow with no separation of boundary layer.

**15. What is an ideal fluid?**

Perfect or ideal fluid is one which is friction less and effect of viscosity is negligible. A perfect gas is one which obeys Boyle and Charles law.

**16. What is a rotational flow?**

A fluid flow in which every fluid element rotates about its own centre.

**17. What is vortex line and vortex tube?**

Vortex line is the vector line of the vorticity field.

Vortex tube is a vector tube filled with fluid and famed by vortex lines.

**18. Relate the terms irrotationality and vorticity in fluid flow**

The motion of a fluid is said to be irrotational when vorticity is equal to zero. ie, twice rotation is zero or vorticity is twice rotation.

**UNIT - II TWO DIMENSIONAL FLOWS**

**19. How stream functions may be used to determine the discharge of fluid flow?**

The stream function may be defined as the flux of stream low. Hence difference between adjustment stream functions gives the rate of flow between stream lines.

**20. If stream function or potential function of a flow satisfies Laplace equation, what does it mean?**

If stream function satisfies Laplace equation, then the flow is irrotational. If potential

function satisfies Laplace equation, then the flow is continuous.

**21. How stream function and potential function are related to irrotational flow?**

Stream function exists to both rotational and irrotational flow. Potential function exists only for irrotational flow.

**22. What is a free vortex flow?**

A flow field circular stream lines with absolute value of velocity varying inversely with the distance from centre. The flow is irrotational at every point except of the centre.

**23. What does a free vortex flow mean?**

A flow which is free of vorticity except at the centre.

**24. What is meant by bound vortex of a wing?**

The vortex that represents circulatory flow around the wing is called the bound vortex. This vortex remains stationary with respect to the general flow.

**25. What is a forced vortex flow?**

A flow is which each fluid particle moves in circular path with speed varying directly as the distance from the axis of rotation.

**26. Define velocity vector with respect to a potential line?**

There is no velocity vector tangential to a potential lines, the velocity is perpendicular to the potential line.

**27. Why tornados are highly destructive at or near the centre?**

Tornado is a free vortex flow such that velocity multiplied by distance from centre is constant. Therefore the velocity is maximum at the centre hence it is highly destructive.

**28. Specify the stream and potential lines for a doublet**

Stream lines are circles tangent to X axis ( $\Psi = r/\sin\theta$ )

Potential lines are circles tangent to Y axis ( $\phi = r/\cos\theta$ )

**29. Specify the stream and potential lines for a source and sink.**

Stream lines are radial lines from  
centre Potential lines are circles

**30. Compare the stream lines and potential lines of source/ sink with that of a vortex flow**

The stream lines of source/ sink and potential lines of vortex are similar. The potential lines of source / sink and stream lines of vortex are similar.

**31. State the properties of a stagnation point in a fluid flow**

The sudden change of momentum of fluid from a finite value to stagnant value imparts pressure force at the point of stagnation, thus the velocity gets converted to pressure.

**32. What is Rankine half body?**

The dividing stream line  $y = m/2$  of source, uniform flow combination forms the shape of Rankine half body.



**33. What is Rankine oval?**

The dividing stream line ( $\psi = 0$ ) of doublet, uniform flows combination forms the shape of Rankine oval.

**34. How transverse force can be introduced to a flow around a cylinder?**

Add a circulatory flow along with the uniform flow to get a transverse force. Spin the cylinder about its own axis to get circulatory flow.

**35. How the stream and potential lines act in source vortex combination?**

Stream and potential lines in a source vortex combination are both equiangular, spirals. The change of direction of radial movement of fluid particles will be equal in magnitude while opposite direction to the change in tangential movement so that curves are equiangular spirals.



**36. Compare vortex with source/ sink flow pattern**

The stream lines of source/ sink and potential lines of vortex are similar. The potential lines of source/ sink and stream lines of vortex are similar.

**37. State the stream function for uniform flow of velocity 'U' parallel to positive X-direction**

Stream function  $\psi = -Uy$

**38. State the stream function for uniform flow of velocity V parallel to positive Y direction**

Stream function  $\psi = -Vx$

**39. What is the diameter of a circular cylinder which is obtained by combination of doublet of strength "y" at origin and uniform flow U parallel to X axis ?**

Diameter (a) =  $\sqrt{\mu/2\pi v}$

**40. How a line source differs from a point source?**

A two dimensional source is a point source from which the fluid is assumed to flow out radially in all direction. As this flow is restricted to one plane and to allow for the application of the results to three dimensional flows, the term line source is a sometimes used.

**UNIT - III CONFORMAL TRANSFORMATION**

**41. Define potential flow of a fluid**

The irrotational motion of an incompressible fluid is called potential flows.

**42. Relate vorticity and circulation.**

Vorticity is the circulation around an element divided by its area.

**43. Relate vorticity and angular velocity**

Vorticity is equal to twice angular velocity. Therefore, circulation = 2 x rotation x area.

**44. What is meant by Karmen vortex sheet?**

A body moving in real fluid leaves double row of vortices from the sides of body. These vortices are rotating in opposite directions and gradually dissipated by viscosity as they move down stream. If the vortices are stable, for a distance between vortices 'h' and for pitch 'l' of the vortices,  $h/l = 0.2806$  for Karman vortex sheet.

**45. How are the stream lines in a source sink pair?**

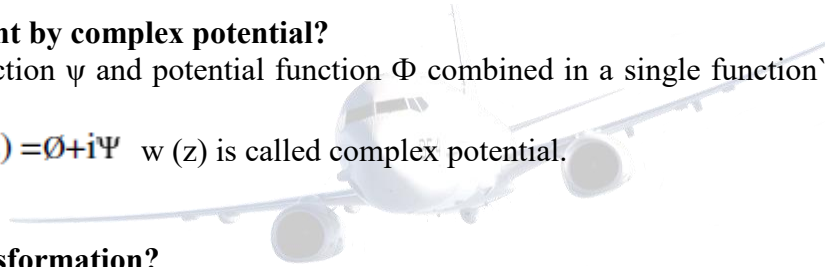
The stream lines are circles with centre on y- axis for a source sink pair. Stream lines are circles with common chord.

**46. What is vortex pair?**

Two vortices of equal strength but of opposite sign or with opposite directions of rotation constitute a vortex pair.

**47. What is meant by complex potential?**

If stream function  $\psi$  and potential function  $\Phi$  combined in a single function 'w' such that then  $w(z) = \Phi + i\psi$  w (z) is called complex potential.



**48. What is transformation?**

A transformation is a mathematical process by which a figure may be distorted or altered in size and shape. This is done by means of algebraic relationship between the original coordinates and co-ordinates of new position, the pair of co- ordinates being represented by complex variables.

**49. When a transformation is said to be conformal?**

The transformation is said to be confirmed if small elements of area are un altered shapes(though they are in general, altered in size, position and orientation).

**50. What is Joukowski transformation?**

Joukowski assumes that relation  $w(z) = z + a^2/z$  so that second term is small when z is large . Thus at great distances from the origin the flow is undisturbed by the transformation.

**51. What is thickness ratio?**

It is the ratio of maximum thickness to chord of a Rankine oval.

**52. Define lift and drag.**

Since the fluid is in motion, we can define a flow direction along the motion. The component of the net force perpendicular (or normal) to the flow direction is called the lift, the component of the net force along the flow but in opposite direction is called the drag.

**53. Define centre of pressure:**

The dynamic forces act in a body through the average location of the pressure variation which is called the centre of pressure.

**54. How velocity varies with radius in a vortex core?**

For viscous flow around a vortex core velocity inversely proportional to the radius

**55. How the down wash of a wing is related down wash of tail plane?**

The down wash on the tail resulting from the wing wake is almost twice as great as the down wash on the wing resulting from wing wake.

**56. What is strength of a vortex and how it is measured?**

It is the magnitude of circulation around it and is equal to the product of vorticity and area.

**57. Brief out how wing tip vortices are formed.**

On account of larger pressure below the wing surface than on the top, some flow is there from bottom to top round the wing tips in case of a finite wing. This produces velocity sideways over most of the wing surface. This causes a surface discontinuity in the air leaving the wing which rolls up to distinct vortices.

## UNIT - IV AIRFOIL AND WING THEORY

### 58. Suggest methods to resolve induced drag of a wing:

- (i) Make lift distribution on wing elliptical
- (ii) increase the aspect ratio.

### 59. State the assumptions made in simplified horseshoe vortex system of a wing:

The wing is replaced by a single bound span wise vortex of constant strength which turns at right angle at each end to trailing vortices which extend to infinity behind the wing. These two trailing vortices.

- i) each of which must provide the same total lift.
- ii) Each must have same magnitude of circulation and same circulation at mid- span

### 60. What is meant by Kutta- Joukowski flow?

Kutta prescribed tangential flow conditional at trailing edge of airfoil, while Joukowski solution permitted a rounded leading edge to have a smooth flow around the leading edge without separation.

### 61. Point out the effect of boundary layer in case of a Kutta- Joukowski flow past an aerofoil:

separation of boundary layer at leading edge can be avoided in a small range of angles of attack due to thin boundary layer formation. The formation of boundary layer caused the flow to leave trailing edge torn and irregularly.

### 62. State the limitations of lifting line theory.

- (i) Straight narrow wings with smooth pressure distribution, theory agrees well.
- (ii) Theory gives correct value of down wash along the centre of pressure of any distribution of lift that is symmetrical ahead and behind a straight line at right angles to the direction.
- (iii) for curved or yawed lifting lines of low aspect ratio, theory is not adequate.

**63. Why a thin aerofoil is considered in subsonic flows?**

The necessity of minimizing the induced drag leads to the choice of high aspect ratio for the wing design at subsonic condition. Hence thin aerofoil is preferred.

With such narrow wings the flow can be approximated to two- dimension of flow around a infinitely long cylindrical wing of same section profile

**64. Define slender body of revolution.**

The radius of body is very small than length is known as slender body of revolution.

**65. Briefly state the limitation of Prandtl -Glauert compressibility correction factor**

(i) The  $M_\infty$  Must be less than unity

(ii) At some Mach number below unity, the value of  $M$  depends on thickness of aerofoil and angle of attack. Aerofoil with finite thickness the perturbation components of velocity cannot be considered small relative to stream velocity ( $u/U$  &  $v/V$  not small)

**66. Why Fourier sine series in the form  $\sum A_n \sin n\theta$  was assumed for distribution of circulation on airplane wings?**

Fourier sine series was chosen to satisfy the end conditions of curve reducing to zero at tips where  $y = \pm s$ . ( $\theta=0$  to  $\theta=\pi$ )

**67. How the sine series was modified for circulation distribution on a symmetrically loaded wing?**

For symmetrical loading maximum or minimum should be at mid- section. This possible only when sine series of odd values of  $(\pi/2)$ . Odd harmonics of sine series are symmetrical.

For any asymmetry due to rolling or side slipping what form of distribution is acceptable.

For any symmetric loading one or more even harmonics of sine series are to be incorporated in the distribution

**68. State Kelvin's circulation theorem**

Circulation and hence vortex strength, does not vary with time if (i) the fluid is nonviscous (ii) the density is either constant or a function of pressure only (iii) body forces such as gravity or magnetic force are single valued potential.

**69. Compare thin aerofoil theory with vortex panel method**

Limitations of thin aerofoil theory (i) it applies only to aerofoil at small of attack (ii) the thickness must be less than 12% of chord. When higher angles of attack aerodynamic lift of other body shape are to be considered vortex panel method finds its own application. Vortex panel method provides the aero dynamic characteristic of bodies of arbitrary shapes, thickness and orientation. This is a numerical method.

**70. List out the application of horseshoe vortex analysis on aerodynamics**

1. Prandtl's lifting line and lifting surface theory of wings.
2. Interference problems of aircraft flying together.
3. On ground effect of aircrafts flying very close to ground.
4. Influence of wing down wash field on flow over other components of aircrafts, especially the tail plane.
5. Interference in wind tunnel.

**71. Why large spacing is to be provided to aircrafts while landing or take –off?**

Wing tip, vortices are essentially like tornadoes that trail down- stream of the wing. These vortices can sometimes cause flow disturbance to aeroplane following closely to it. Hence to avoid any such accidents large spacing is preferred between aircraft performing landing and take- off.

**72. What is the effect of downwash velocity on local free- stream velocity**

Down wash causes the local free- stream to produce relative wind at a slightly higher angle of incidence.

$$\alpha_{\text{eff}} = \alpha - \alpha_i$$

**73. Why geometrical angle of attack of a wing and effective angle of attack of local aerofoil section differs?**

The angle of attack actually seen by local airfoil section is the angle between aerofoil section chord and local relative wind. This is because although the wing is at a geometric angle of attack ' $\alpha$ ' the local aerofoil section will have a smaller value of angle of attack than geometrical.

**74. Show that D' Alembert's paradox is not true to a finite wing.**

D' Alembert's paradox states that there is no drag on bodies submerged in a flow of perfect fluid.

The presence of downwash over a finite wing creates a component of drag- induced drag- even with inviscid incompressible flow of fluid when there is no skin friction or flow separation. Hence paradox is not true in the case of flow over a finite wing.

**75. Can induced drag on a wing be considered as a drag caused by pressure difference. If so Justify.**

The three- dimensional flow induced by wing- tip vortices simply alters the pressure distribution on the finite wing, in such a way that there is a non- balance of pressure in the stream direction. This is induced drag, which may be considered as a type of pressure drag.

**76. How induced drag differs from viscous dominated drag contributions?**

Viscous dominated drags are due to skin friction, pressure drag and boundary layer separation drag. Induced drag is purely due to down- wash induced by vortices and has nothing to do with viscosity of fluid or boundary layer formation.

**77. The profile drag coefficient for a finite wing may be taken equal to that of its aerofoil section. Why?**

Profile drag is the sum of skin friction and pressure drag, which is mainly viscous-dominated part of drag. These depend on the fluid flowing and on the configuration of aerofoil section and not on the extend of the wing.

**78. State analogical electromagnetic theory to Biot- Savart law**

The vortex filament is visualized as a wire carrying current 'I' then the magnetic field strength dB induced at a point P by a segment of wire 'dl' with current in the direction of wire is

$$dB = \frac{\mu I dl \times r}{4\pi |r|^3}$$

Where 'μ' is the permeability of the medium surrounding the wire.

**79. What is meant by geometric twist of a wing? How it differs from aerodynamic twist?**

A small twist is given to the wing so that at different span wise stations are different. This is called geometric twist. The wings of modern aircraft have different aerofoil sections along the span with values of zero lift angle..this is called aerodynamic twist of wing.

**80. Why the lift over the span is not uniform?**

Geometric twist causes angle of incidence variation from root to tip of wing. The wings of air- planes have different aerofoil sections along span with different zero lift incidence (aerodynamic twist). As a result of this, lift per unit span is also different at various locations from centre. There is a distribution of lift per unit span length on long span.

**UNIT - V VISCOUS FLOW**

**81. What is geometric twist? Differentiate “wash out” and “wash in”**

The wings of aircraft are slightly twisted from fuselage towards tip so that the angles of incidence of the individual aerofoil sections are different at different spanwise stations. If the tip of the wing at lower angle of incidence than root the wing is said to have “washout” and if the tip is at higher angle of incidence than root the wing is said to have “washin”.



**82. Why induced drag is named drag due to lift?**

Induced drag is the consequence of the wing tip vortices, which are produced by the difference in pressure between lower and upper surface of the wing. The lift is also produced due to the same pressure difference. Hence the cause of induced drag is closely associated with the production of lift in the finite wing.

**83. When lift is high induced drag is also high and becomes a substantial part of total drag. Why?**

As induced drag coefficient varies as the square of lift coefficient for elliptical load distribution over a wing for higher lift induced drag is also high and becomes a major part of the total drag of the aircraft.

**84. “ Aspect ratio of a conventional aircraft should have a compromise between aerodynamic and structural requirements” - discuss.**

Larger the aspect ratio, smaller will be induced drag coefficient and vice versa. Hence is the induced drag also. In a design of high aspect ratio, wing becomes slender and has poor structural strength. A compromise between these two aspects should be attained in designing the aspect ratio of wing.

**85. How lift distribution, plan form and down wash velocity are related in airplane wings**

For elliptic lift distribution on the span of wing, chord variation from root to tip aerofoil sections may be assumed elliptical or elliptical plan- form may be assumed. In such cases the downwash velocity may be constant through – out span.

**86. Brief out the advantage of a tapered wing.**

Elliptic plan- forms are expensive to manufacture than rectangular plan- forms. Rectangular plan- forms generate lift distribution far from optimum. A compromise is something in between these two plan- forms. Viz, tapered plan- form, so that lift distribution closely approximate elliptical case. Also a tapered wing can be designed with an induced drag reasonably close to minimum value. It is easier to make straight leading and trailing edges to tapered plan- forms. That is why most conventional aircrafts employ tapered rather than elliptical wing plan- forms.

**87. Give range of variation of aspect ratio for subsonic airplanes.**

Aspect ratio is between 6 to 22 for actual wings. For wind tunnel test models it is up to 6.

**88. Specify the design aspect for minimizing induced drag.**

Design factor is not closeness to elliptical plan- form, but to make the aspect ratio as larger as possible.

**89. What is the relation between aspect ratio and lift curve slope?**

For reduction of aspect ratio, lift curve slope reduces for finite wing. An infinite wing large aspect ratio and so larger the lift curve slope ( Aspect Ratio  $\propto a$ )

**90. To which plan forms the lifting line theory and lifting surface theory are applicable.**

Lifting line theory gives a reasonable result for straight wings at moderate and high aspect ratio. At low aspect ratio straight wings, swept wings, and delta wings have a more sophisticated model of lifting line theory, but lifting surface theory is applied.

**91. What is meant by flow tangency condition on every point on wing surface?**

The wing plan- form is assumed as the stream- surface of flow in lifting surface theory. There is no flow velocity component normal to this stream- surface. Hence induced velocity and normal component of free- stream velocity to be zero at all points on the wing. This is called flow tangency condition.

**92. If two wings have same lift coefficient how their aspect ratios and angles of attack are related.**

A wing of low aspect ratio will require a higher angle of attack than a wing of greater aspect ratio in order to produce the same lift coefficient. i.e.,  $C_L \propto AR \cdot \alpha$  ( approximate)

**93. Justify the statement “ the bound vortex strength is reduced to zero at the wing tips”**

The pressure distribution goes to zero at the tips of wings because of pressure equalization from the bottom to the top of wing tips. This causes no discontinuity of velocity between upper and lower surfaces of a wing at the tips. At wing tips single bound vortex of constant strength turns through a right angle at each wing tip to form trailing vortices. This is equivalent to vortex filament of equivalent strength joined at tips. This causes a change in strength at to zero value.

**94. How the span of a simplified vortex system is arrived at from the bound vortex of wing?**

Simplified system may replace the complex vortex system of a wing when considering the influence of the lifting system on distant points in the flow. Wing is replaced by a single bound spanwise vortex of constant strength which is turned at right angles at each tip wing forming trailing vortices which extend to infinite length. When general vortex is simplified following points to be noted (i) bounded vortex and simplified vortex must provide same total lift (ii) must have same magnitude of circulation about trailing edge vortices and hence same circulation at mid span.

**95. What is the length of semi- span of equivalent horseshoe vortex for elliptical distribution of circulation on a wing of span' 2s'**

Equivalent semi span  $s = \frac{\pi}{4} s$

**96. Total downwash for down- stream of the wing is twice that in the vicinity of the wing itself. Why?**

The down- wash near the bound vortex is due to two semi- infinite vortices- trailing vortices

$$w = \frac{\Gamma}{4\pi y} (\cos \theta + \cos \alpha)$$

$$4\pi y$$

$$\text{ie, } w = \frac{\Gamma}{4\pi y} [1 + 1] = \frac{\Gamma}{2\pi y}$$

### 97. State Helmholtz's vortex theorem.

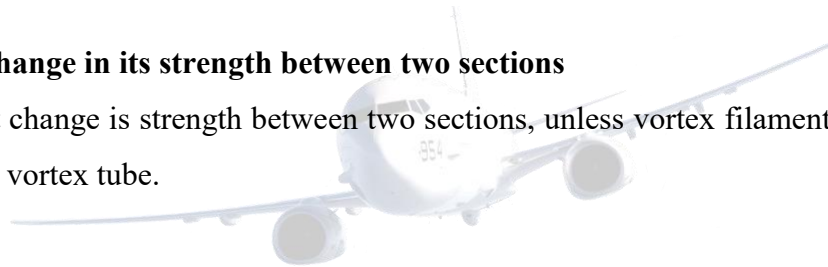
- I. Strength of vortex cannot increase or decrease along its axis or length, the strength being the circulation around it and equal to vorticity. Area. (if section area diminishes vorticity increases and vice versa). Since infinite vorticity is not possible, cross sectional area can not reduce to zero.
- II. Vortex can not end in a fluid. Vortex forms a closed loop, vortex can end only on a solid.
- III. Vortex tube cannot change in strength between two sections unless filaments of equal strength or leave the vortex tube.
- IV. There is no fluid interchange between tube and surrounding fluid and remains constant vortex moves through a fluid.

### 98. Where a vortex can end?

Vortex cannot end in a fluid. It forms a closed loop in a fluid. Vortex can have a discontinuity when there is a solid body against it or where there is a surface of separation.

### 99. Can a vortex tube change in its strength between two sections

A vortex tube cannot change its strength between two sections, unless vortex filaments of equivalent strength join or leave vortex tube.



### 100. State Blasius theorem for 2D incompressible, irrotational flow

This provides a general method of determining the resultant force and moment exerted by a fluid in steady, 2- dimensional flow past a cylinder of any cross- section, provided, that the complex potential  $w = f(z)$  for the flow pattern is known.

If  $x$  and  $y$  components of the resultant force being  $P_x$  and  $P_y$  and moments of the resultant force about origin  $M_z$ .

$$P_x - i P_y = \frac{1}{2} i \rho \int \left( \frac{dw}{dz} \right)^2 dz \text{ and}$$

$$M_x + i M_y = \frac{1}{2} \rho \int z \left( \frac{dw}{dz} \right)^2 dz$$

Where the integrals are taken around the contour of cylinder.

UNIT I

	Questions	opt1	opt2	opt3	opt4	opt5	opt6	Answer
1	The unit for pressure	Newton	Pascal	Joule	Kilogram			Pascal
2	The symbol for mass density	$\rho$	$\mu$	$\psi$	$\Phi$			$\rho$
3	The unit of pressure one bar is	1 Pascal	kilo Pascal	100kpa	1000kpa			100kpa
4	Atmospheric pressure at sea level at 150C is	101.3 N/m2	760mm of mercury	10.33cm of water	7.8 cm of mercury			760mm of mercury
5	Newton’s second law	F=m/a	m=f x a	F=m.a	F = g.a			F=m.a
6	The basic unit for mass is	Newton	kilogram	second	Joule			kilogram
7	Unit for power	Newton	Watt	Joule	second			Watt
8	The unit for energy	Newton	Pascal	Joule	meter			Joule
9	One pascal is	N/m2	N/mm2	KN/m2	KN/mm2			N/m2
10	Which one is not the aerodynamic forces	lift	drag	thrust	sideslip			thrust
11	Continuity equation is	Q1=Q2	$a_1 v_1 = a_2 v_3$	$q_1 / q_2$	$a_1 v_2 = a_2 v_1$			Q1=Q2
12	The expression weight per unit volume is	mass density	Specific weight	Relative density	surface tension			Specific weight
13	_____ is the principle of conservation of mass	Mass can be neither created nor destroyed	Mass can be created	Mass can be destroyed	Energy can be neither created nor destroyed			Mass can be neither created nor destroyed
14	The unit of bulk modulus in SI unit is	N/m2	pa-s	kg/ms	pa			N/m2
15	The unit of mass density in SI unit is	N/m2	pa-s	kg/m3	pa			kg/m3
16	The unit of viscosity in SI unit is	N-S/m2	pa-s	kg/ms	pa			All the other three options are correct
17	In CGS system unit of viscosity is	poise	stokes	mach number	stroke			poise
18	The bulk modulus of the fluid is the reciprocal of	compressibility	viscosity	pressure	surface tension			compressibility
19	It is a product of mass density and volume of the fluid	mass	specific weight	specific volume	specific gravity			mass
20	The expression inverse of mass density is	mass density	specific gravity	specific volume	surface tension			specific volume
21	It is a product of mass density and gravitational acceleration	mass density	specific weight	specific volume	specific gravity			specific gravity
22	Mass flow per unit area is	mass flux	mass	specific volume	mass flow			mass flux
23	Mass can be neither created nor destroyed is a physical principle of	Energy Equation	Momentum Equation	Continuity Equation	Euler Equation			Continuity Equation
24	The momentum Equation for an inviscid flow are called	Euler equation	Navier-Stokes Equation	Momentum Equation	Continuity Equation			Euler equation
25	The momentum Equation for an viscous flow are called	Navier-Stokes Equation	Euler equation	Momentum Equation	Continuity Equation			Navier-Stokes Equation
26	A fixed amount of matter contained within a closed boundary is called	Surroundings	System	Mass	Molecule			System
27	The region outside the system defines	System	Mass	Surroundings	Molecule			Surroundings
28	It is a curve whose tangent at any point is in the direction of the velocity vector at that point is	Stream line	Path line	Streakline	System			Stream line
29	For Steady flow Pathlines and Streakline are	Not Same	equal	zero	constant			equal
30	Vorticity is	$2\omega$	$2\Phi$	$2\Psi$	$2\alpha$			$2\omega$
31	Vorticity is not equal to zero at every point in a flow is	irrotational	rotational	circular	linear			rotational
32	Vorticity is equal to zero at every point in a flow is	irrotational	circular	rotational	linear			irrotational
33	Irrotational flows can be described by	Velocity potential	Stream function	Both velocity and stream function	mathematical functions			Both velocity and stream function
34	Irrotational flows can be described by the velocity potential, such flows are called	Potential flows	Smooth flow	rotational flow	Streamflow			Potential flows
35	Stoke is the unit of	surface tension	viscosity	kinematic viscosity	dynamic viscosity			kinematic viscosity
36	The gases are considered incompressible when Mach Number	is equal to 1.0	is equal to 0.50	is more than 0.3	is less than 0.2			is less than 0.2
37	Pascal’s law states that at a point is equal in all directions	in a liquid at rest	in a fluid at rest	in a laminar flow	in a turbulent flow			in a fluid at rest

38	Using Pitot – Tube we can measure in a pipe.	discharge	average velocity	velocity at a point	pressure at a point			velocity at a point
39	If the fluid particles moving in a zig zag way, the flow is called	Unsteady	Non-uniform	Turbulent	Incompressible			Turbulent
40	If the Reynolds number is less than 2000, the flow in a pipe is	laminar flow	turbulent flow	transition flow	laminar sub flow			laminar flow
41	According to Bernoulli's Principle, the velocity of a moving fluid increases, then the pressure within the fluid	increases	decreases	no change	becomes zero			decreases
42	The property of a fluid or semifluid that causes it to resist flowing is called	velocity	gravity	viscosity	magnitude			viscosity
43	On a swept wing aircraft if both wing tip sections lose lift simultaneously the aircraft will	roll	pitch nose up	pitch nose down	Yaw			pitch nose up
44	Lift on a delta wing aircraft	increases with an increased angle of incidence (angle of attack)	decreases with an increase in angle of incidence (angle of attack)	does not change with a change in angle of incidence (angle of attack)	increases with an increased angle of incidence upto Stall			increases with an increased angle of incidence (angle of attack)
45	On a straight wing aircraft, stall commences at the	root on a low thickness ratio wing	tip on a high thickness ratio wing	tip on a low thickness ratio wing	root on a high thickness ratio wing			root on a high thickness ratio wing
46	For the same angle of attack, the lift on a delta wing	is greater than the lift on a high aspect ratio wing	is lower than the lift on a high aspect ratio wing	is the same as the lift on a high aspect ratio wing	is greater than the lift on a low aspect ratio wing			is lower than the lift on a high aspect ratio wing
47	The ISA	is taken from the equator	is taken from 45 degrees latitude	is taken from 30 degrees latitude	is taken from 60 degrees latitude			is taken from 45 degrees latitude
48	At higher altitudes as altitude increases, pressure	decreases at constant rate	increases exponentially	remains constant	decreases exponentially			decreases exponentially
49	When the pressure is half of that at sea level, what is the altitude?	12,000 ft	8,000 ft	10,000 ft	18,000 ft			18,000 ft
50	During a turn, the stalling angle	increases with AOA	decreases	remains the same	with an increased angle of incidence upto Stall			remains the same
51	The C of G moves in flight. The most likely cause of this is	movement of passengers	movement of the centre of pressure	consumption of fuel and oils	altitude			consumption of fuel and oils
52	The C of P is the point where	all the forces on an aircraft act	the three axis of rotation meet	the lift can be said to act	CG Point			the lift can be said to act
53	The three axis of an aircraft act through the	C of G	C of P	stagnation point	Chord line			C of G
	UNIT II							
54	An inviscid, incompressible fluid is sometimes called	an ideal fluid	a real fluid	a perfect fluid	an ideal or perfect fluid			an ideal or perfect fluid
55	$p + (1/2)\rho V^2 = \text{const}$	Bernoulli's equation	Euler's equation	Navier Stokes equation	Momentum Equation			Bernoulli's equation
56	$dp = -\rho V dV$	Navier Stokes equation	Prandtl's equation	Bernoulli's equation	Euler's equation			Euler's equation
57	$A_1 V_1 = A_2 V_2$ is the quasi-one-dimensional continuity equation for	incompressible flow	compressible flow	low speed flow	low subsonic flow			incompressible flow
58	Pitot tube is the most common device for measure	Velocity	Kinematic Viscosity	Pressure	Dynamic Viscosity			Velocity

59	An airplane is flying at standard sea level. The measurement obtained from Pitot tube mounted on the wing tip reads 104857.2 Pa. What is the velocity of the airplane? 101314.1 Pa at sea level pressure	76.06 m/s	80.32 m/s	70.23 m/s	69.32 m/s			76.06 m/s
60	Consider an airfoil in a flow with a freestream velocity of 45.72 m/s. The velocity at a given point on the airfoil is 68.58 m/s. Calculate the pressure coefficient at this point.	1.25	-1.25	2.3	-2.3			-1.25
61	$\nabla^2 \Phi = 0$	Laplace Equation	Harmonic Function	Homogeneous Equation	Continuity Equation			Laplace Equation
62	Solutions of Laplace's equation are called	Harmonic Function	Non-Harmonic Function	singular function	dynamic function			Harmonic Function
63	$\Psi = V \infty Y$ is the _____ for an incompressible uniform flow	Stream Function	Velocity potential	Angular velocity	Vorticity			Stream Function
64	$\Phi = V \infty X$ is the _____ for an incompressible uniform flow.	Stream Function	Velocity potential	Angular velocity	Vorticity			Velocity potential
65	Circulation around any closed curve in a uniform flow is	0	1	2	3			0
66	Uniform flow is	irrotational	rotational	Both irrotational and rotational	linear			irrotational
67	The streamlines are directed away from the origin is called	source flow	sink flow	rotational flow	doublet flow			source flow
68	Who invented the Pitot tube?	Henri Pitot	Ernest Mach	Prandtl	John Anderson			Henri Pitot
69	The streamlines are directed towards the origin is called	source flow	sink flow	rotational flow	doublet flow			sink flow
70	"When the velocity increases, pressure decreases, and when the velocity decreases, the pressure increases" satisfies	Bernoulli's equation	Euler's equation	Both Bernoulli's equation and Euler's equation	Newtons law			Both Bernoulli's equation and Euler's equation
71	The Quasi-one-dimensional continuity equation is	$\rho_1 A_1 V_1 = \rho_2 A_2 V_2$	$(\rho_1 A_1)/V_2 = (\rho_2 A_2)/V_1$	$\rho_1 A_1 V_2 = \rho_2 A_1 V_2$	$\rho_1 A_1 V_1 = \rho_2 A_2 V_3$			$(\rho_1 A_1)/V_2 = (\rho_2 A_2)/V_1$
72	_____ is the source strength for source flow	$\Psi$	$\Lambda$	$\Omega$	$\epsilon$			$\Lambda$
73	Sorce flow is _____ at every point.	irrotational	rotational	circular	All the other three options are wrong			irrotational
74	Degenerate case of a source-sink pair that leads to a singularity called	doublet flow	sink flow	source flow	uniform flow			doublet flow
75	The strength of the doublet is denoted by	$\kappa$	$\Lambda$	$\epsilon$	$\Omega$			$\kappa$
76	$\kappa$ is defined as	$\Lambda$	$\xi$	$\Omega$	$\eta$			$\Lambda$
77	_____ is called the strength of the vortex flow.	$\Lambda$	$\kappa$	$\Gamma$	$\Omega$			$\Gamma$
78	Source flow of $\Phi =$	$(\Lambda/2\pi) \ln r$	$(\Lambda/2\pi) \theta$	$(\Lambda/3\pi) \ln r$	$(\Phi/2\pi) \ln r$			$(\Lambda/2\pi) \ln r$
79	Source flow of $\Psi =$	$(\Lambda/2\pi) \ln r$	$(\Lambda/2\pi) \theta$	$(\Lambda/3\pi) \ln r$	$(\Phi/2\pi) \ln r$			$(\Lambda/2\pi) \theta$
80	Vortex flow of $\Psi =$	$(\Gamma/2\pi) \ln r$	$(\Gamma/2\pi) \ln r$	$(\Gamma/2\pi) \theta$	$(\Gamma/2\pi) \eta$			$(\Gamma/2\pi) \ln r$
81	Lift per unit span is directly proportional to circulation	Kutta condition	Kutta theorem	Kutta-Joukowski Theorem	Joukowski Theorem			Kutta-Joukowski Theorem
82	$L' = \rho \infty V \infty \Gamma$ is	Kutta-Joukowski Theorem	Prandtl Theorem	Line theory	Joukowski Theorem			Kutta-Joukowski Theorem
83	Bernoulli's equation applies to	an inviscid and incompressible flow	compressible flow	Viscous flow	non viscous flow			an inviscid and incompressible flow
84	Low wing loading	increases stalling speed, landing speed and landing run	increases lift, stalling speed and manoeuvrability	decreases stalling speed, landing speed and landing run	decreases lift, stalling speed and manoeuvrability			decreases stalling speed, landing speed and landing run

85	Due to the change in downwash on an un-tapered wing (i.e. one of constant chord length) it will	not provide any damping effect when rolling	tend to stall first at the root	not suffer adverse yaw effects when turning	provide damping effect when rolling			tend to stall first at the root
86	True stalling speed of an aircraft increases with altitude	because reduced temperature causes compressibility effect	because air density is reduced	because humidity is increased and this increases drag	because increased temperature causes compressibility effect			because air density is reduced
87	As a general rule, if the aerodynamic angle of incidence (angle of attack) of an aerofoil is slightly increased, the centre of pressure will	never move	move towards the root	move towards the tip	move forward towards the leading edge			move forward towards the leading edge
88	On a very humid day, an aircraft taking off would require	a shorter take off run	a longer take off run	humidity does not affect the take off run	high air intake			a longer take off run
89	An aircraft is flying at 350 MPH, into a head wind of 75 MPH, what will its ground speed be?	175 mph	350 mph	200 mph	275 mph			275 mph
90	When does the angle of incidence change?	When the aircraft attitude changes	When the aircraft is descending	It never changes	When the aircraft is ascending			It never changes
91	As the angle of attack decreases, what happens to the centre of pressure?	It moves forward	It moves rearwards	Centre of pressure is not affected by angle of attack decrease	increases			It moves rearwards
92	A decrease in pressure over the upper surface of a wing or aerofoil is responsible for	approximately 2/3 (two thirds) of the lift obtained	approximately 1/3 (one third) of the lift obtained	approximately 1/2 (one half) of the lift obtained	approximately twice of the lift obtained			approximately 2/3 (two thirds) of the lift obtained
93	Pressure decreases	proportionally with a decrease in temperature	inversely proportional to temperature	Pressure and temperature are not related	proportionally with a decrease in temperature			proportionally with a decrease in temperature
94	As air gets colder, the service ceiling of an aircraft	reduces	increases	remains the same	becomes zero			increases
95	When the weight of an aircraft increases, the minimum drag speed	decreases	increases	increases upto stall	remains the same			increases
96	An aircraft will have	less gliding distance if it has more payload	more gliding distance if it has more payload	the same gliding distance if it has more payload	more gliding distance if it has less payload			the same gliding distance if it has more payload
97	When an aircraft experiences induced drag	air flows under the wing span-wise towards the tip and on top of the wing spanwise towards the root	air flows under the wing span-wise towards the root and on top of the wing span-wise towards the tip	air flows under the wing span-wise towards the tip	air flows on top of the wing spanwise towards the root			air flows under the wing span-wise towards the tip and on top of the wing spanwise towards the root



98	At stall, the wingtip stagnation point	moves toward the lower surface of the wing	moves toward the upper surface of the wing	moves toward the lower wing tip	moves toward the upper wing tip			moves toward the lower surface of the wing
99	The rigging angle of incidence of an elevator is	the angle between the mean chord line and the horizontal in the rigging position	the angle between the bottom surface of the elevator and the horizontal in the rigging position	the angle between the bottom surface of the elevator and the longitudinal datum	the angle between the bottom surface of the elevator and the lateral datum			the angle between the mean chord line and the horizontal in the rigging position
100	What is the lapse rate with regard to temperature?	0.98°C per 1000 ft	1.98°F per 1000 ft	4°C per 1000 ft	1.98°C per 1000 ft			1.98°C per 1000 ft
101	What happens to load factor as you decrease turn radius?	It increases	It decreases	It remains constant	load factor is not related to turn radius			It increases
102	If you steepen the angle of a banked turn without increasing airspeed or angle of attack, what will the aircraft do?	It will remain at the same height	It will sideslip with attendant loss of height	It will stall	It will decent			It will sideslip with attendant loss of height
	UNIT III							
103	_____ that provides formulas for finding the force and moment on the airfoil profiler	Blasius theorem	Kutta condition	Joukowski Theorem	Euler theorem			Blasius theorem
104	For a thin uncambered airfoil, the center of pressure $c_p$ is close to the	half-chord point	quarter-chord	chord point	camber			quarter-chord
105	A transformation is conformal when	the figure is altered in size, position, orientation	alter in shape only	altered in size only	altered in orientation only			the figure is altered in size, position, orientation
106	A body with a sharp trailing edge which is moving through a fluid will create about itself a circulation of sufficient strength to hold the rear stagnation point at the trailing edge	Blasius theorem	Kutta condition	Joukowski Theorem	Joukowski condition			Kutta condition
107	Blasius theorem that provides formulas for finding the ____ and ____ on the airfoil profiler	force and moment	force and thrust	moment and drag	thrust and drag			force and moment
108	According to Kutta condition the circulation at the trailing edge of the aerofoil should be	0	1	-1	$\infty$			0
109	Helmholtz's theorem is suitable for the study of	Vortex behavior	airfoil behavior	wing behavior	lift behavior			Vortex behavior
110	Modified Joukowski aerofoil profile	modifies the shape of the aerofoil	modifies the angle at the trailing edge	modifies the position of aerodynamic centre	modifies the maximum thickness			modifies the shape of the aerofoil
111	For a given airfoil at a given angle of attack, the value of $\Gamma$ around the airfoil is such that the flow leaves the trailing edge smoothly.	Kutta condition	Bernoulli's equation	Euler's theorem	Joukowski Theorem			Kutta condition
112	When the trailing edge is finite, then the trailing edge is a	stagnation point	first point	quarter-chord	chord point			stagnation point
113	The _____ are responsible for the component of the downwash.	All the other three options are wrong	leading edge	trailing edge	trailing vortices			trailing vortices
114	The wind tunnel for calculating the lift, drag and accurate aerodynamic measurement was found between the year's	1902-1905	1901-1902	1900-1901	1920-1925			1901-1902
115	Delta wing has a shape of	rectangle	square	pentagon	triangle			triangle
116	The cross sectional shape obtained by the intersection of the wing with perpendicular plane is called	leading edge	wing tip	plane	airfoil			airfoil
117	Some electrical phenomena like aurora borealis occur in	stratosphere	ionosphere	mesosphere	exosphere			ionosphere
118	The portion that meets the air first in an airfoil is	leading edge	upper chamber	lower chamber	trailing edge			leading edge
119	The temperature decreases linearly at the approximation rate of 6.5K per km in	troposphere	stratosphere	ionosphere	mesosphere			troposphere

120	The portion at which the airflow over the upper surface joins the lower surface is the	leading edge	upper chamber	lower chamber	trailing edge			trailing edge
121	The imaginary straight line drawn through the airfoil from its leading edge to its trailing edge is	upper camber	lower camber	mean camber	chord			chord
122	The characteristic curve of its upper or lower surface in an airfoil.	camber	chord	leading curve	trailing curve			camber
123	Which of the following airfoil supports the airplane fly faster?	conventional airfoil	laminar flow airfoil	turbulent flow airfoil	high speed airfoil			laminar flow airfoil
124	Lift is the opposing force of	drag	thrust	gravity	weight			gravity
125	The lift produced without any camber is called	static lift	dynamic lift	normal lift	high lift			dynamic lift
126	The force that propels the aircraft forward is	weight	gravity	lift	thrust			thrust
127	According to newtons law of gravitation, gravity and altitude are	directly proportional	inversely proportional		not equal			inversely proportional
128	The <b>horseshoe vortex</b> model is a simplified representation of the	vortex	wing	aileron	rudder			vortex
129	In horseshoe vortex model the wing vorticity is modelled by a bound vortex of constant	vortex	circulation	angular velocity	stream function			circulation
130	The _____ created as the wing begins to move through the fluid is considered to have been dissipated by the action of viscosity	spiral	bound vortex	circulation	starting vortex			starting vortex
131	The trailing vortices are responsible for the component of the	circulation	downwash	induced drag	starting vortex			downwash
132	The starting vortex created as the wing begins to move through the fluid is considered to have been dissipated by the action of	viscosity	pressure	density	velocity			viscosity
133	the downwash which creates	profile drag	form drag	induced drag	skin friction drag			induced drag
134	The layer of air over the surface of an aerofoil which is slower moving, in relation to the rest of the airflow, is known as	camber layer	boundary layer	chord layer	skin layer			boundary layer
135	What is a controlling factor of turbulence and skin friction?	Aspect ratio	Fineness ratio	Counter-sunk rivets used on engine	Counter-sunk rivets used on skin exterior			Counter-sunk rivets used on skin exterior
136	Changes in aircraft weight	will not affect total drag since it is dependent only upon speed	will not affect total lift since it is dependent only upon speed	will only affect total drag if the lift is kept constant	cause corresponding changes in total drag due to the associated lift change			cause corresponding changes in total drag due to the associated lift change
137	The aircraft stalling speed will	increase with an increase in weight	be unaffected by aircraft weight changes since it is dependent upon the angle of attack	increase with an decrease in weight	decrease with an increase in weight			increase with an increase in weight
138	In a bank and turn	extra lift is not required	lift is not required if thrust is increased	extra thrust is not required	extra lift is required			extra lift is required
139	To achieve the maximum distance in a glide, the recommended air speed is	as close to the stall as practical	as high as possible with VNE	speed where the L/D ratio is maximum	the speed where the L/D ratio is minimum			speed where the L/D ratio is maximum
140	If the C of G is aft of the Centre of Pressure	changes in lift produce a pitching moment which acts to increase the change in lift	when the aircraft sideslips, the C of G causes the nose to turn into the sideslip thus applying a restoring moment	when the aircraft yaws the aerodynamic forces acting forward of the Centre of Pressure	when the aircraft rolls the aerodynamic forces acting forward of the Centre of Pressure			changes in lift produce a pitching moment which acts to increase the change in lift
141	Porpoising is an oscillatory motion in the	pitch plane	roll plane	yaw plane	all three planes			pitch plane

142	Due to the interference effects of the fuselage, when a high wing aeroplane sideslips	the accompanying rolling due to keel surface area is destabilizing	the accompanying lift changes on the wings produces a stabilizing effect	the accompanying rolling due to the fin is destabilizing	the accompanying drag changes on the wings produces a stabilizing effect			the accompanying lift changes on the wings produces a stabilizing effect
143	The power required in a horizontal turn	is greater than that for level flight at the same airspeed	must be the same as that for level flight at the same airspeed	is less than that for level flight at the same airspeed	is less than that for level flight at the same altitude			is greater than that for level flight at the same airspeed
144	A wing mounted stall sensing device is located	usually on the under surface	always at the wing tip	always on the top surface	always on empenna			usually on the under surface
145	For an aircraft in a glide	thrust, drag, lift and weight act on the aircraft	weight, lift and drag act on the aircraft	weight and drag only act on the aircraft	weight, lift and thrust act on the aircraft			weight, lift and drag act on the aircraft
146	The upper part of the wing in comparison to the lower	develops more drag	develops the same lift	develops less lift	develops more lift			develops more lift
147	What effect would a forward CG have on an aircraft on landing?	Increase stalling speed	No effect on landing	Reduce stalling speed	Reduce ground speed			Increase stalling speed
148	An aspect ratio of 8 would mean	span 64, mean chord 8	mean chord 64, span 8	span squared 64, chord 8	span squared 4, chord 8			span 64, mean chord 8
149	If an aircraft in level flight loses engine power it will	pitch nose up	pitch nose down	not change pitch without drag increasing	not change pitch without drag decreasing			pitch nose down
150	The lift /drag ratio at stall	increases	decreases	remains constant	Remains constant upto stalling point			decreases
151	The optimum angle of attack of an aerofoil is the angle at which	the aerofoil produces maximum lift	the aerofoil produces zero lift	the highest lift/drag ratio is produced	the lowest lift/drag ratio is produced			the highest lift/drag ratio is produced
152	A high aspect ratio wing has a	increased induced drag	decreased induced drag	decreased skin friction drag	increased skin friction drag			decreased induced drag
153	Minimum total drag of an aircraft occurs	at the stalling speed	when profile drag equals induced drag	when induced drag is least	when wave drag is least			when profile drag equals induced drag
154	If the weight of an aircraft is increased, the induced drag at a given speed	will increase	will decrease	will remain the same	will remain the same upto 8000 ft			will increase
155	The transition point on a wing is the point where	the flow separates from the wing surface	the boundary layer flow changes from laminar to turbulent	the flow divides to pass above and below the wing	the boundary layer flow changes from turbulent to laminar			the boundary layer flow changes from laminar to turbulent

156	The boundary layer of a body in a moving air stream is	a thin layer of air over the surface where the air is stationary	a layer of separated flow where the air is turbulent	a layer of air over the surface where the airspeed is changing from free stream speed to zero speed	a layer of separated flow where the air is laminar			a layer of air over the surface where the airspeed is changing from free stream speed to zero speed
157	A laminar boundary layer will produce	more skin friction drag than a turbulent one	less skin friction drag than a turbulent one	less pressure drag than a turbulent one	more pressure drag than a turbulent one			less skin friction drag than a turbulent one
UNIT IV								
158	The _____ is the locus of points halfway between the upper and lower surfaces.	mean camber line	chord	camber	chord line			mean camber line
159	The most forward points of the mean camber line is	trailing edge	leading edge	camber line	chord line			leading edge
160	The most rearward points of the mean camber line is	camber line	leading edge	trailing edge	chord line			trailing edge
161	The straight line connecting the leading and trailing edges is	mean camber line	chord	camber	chord line			chord line
162	The _____ is the distance between the upper and lower surfaces.	camber line	leading edge	trailing edge	Thickness			Thickness
163	The _____ is the maximum distance between the mean camber line and the chord line, measured perpendicular to the chord line.	mean camber line	chord	camber	chord line			camber
164	An airfoil with no camber, that is, with the camber line and chord line coincident, is called	symmetric airfoil	cambered airfoil	low speed airfoil	high speed airfoil			symmetric airfoil
165	The lift goes to zero only when the airfoil will pitch to	Negative angle of attack	Positive angle of attack	Neutral	zero			Negative angle of attack
166	The value of $\alpha$ when lift equals zero called	zero lift angle of attack	Negative angle of attack	Positive angle of attack	Neutral			zero lift angle of attack
167	Pressure drag due to flow separation, sometimes called	form drag	wave drag	skin friction drag	surface drag			form drag
168	_____, due to the shear stress acting on the surface	form drag	skin friction drag	wave drag	interference drag			skin friction drag
169	The theoretical results for a symmetric airfoil is	$cl = 2\pi\alpha$	$cl = \pi\alpha$	$cl = 2\alpha$	$cl = \alpha$			$cl = 2\pi\alpha$
170	In symmetric airfoil the center of pressure and the aerodynamics center are both located at the_____	quarter-chord point	half-chord point	chord point	camber			quarter-chord point
171	In cambered airfoil the center of pressure is varies with	lift coefficient	momentum coefficient	drag coefficient	thrust			lift coefficient
172	In cambered airfoil the aerodynamic center is at the	half-chord point	quarter-chord point	chord point	camber			quarter-chord point
173	Lift slope for symmetric and cambered airfoil is	$2\pi$	$\pi$	$4\pi$	$6\pi$			$2\pi$
174	An induced drag is frequently called	drag due to lift	drag due to thrust	drag due to weight	drag due to gravity			drag due to lift
175	The most _____ points of the mean camber line is leading edge.	forward	rearward	negative	positive			forward
176	The most _____ points of the mean camber line is trailing edge.	side	rearward	negative	positive			rearward
177	A form drag is otherwise called	wave drag	skin friction drag	parasite drag	pressure drag			pressure drag
178	The _____ line connecting the leading and trailing edges is chord line	parallel line	diagonal line	perpendicular line	straight line			straight line
179	The _____ vortex created as the wing begins to move through the fluid is considered to have been dissipated by the action of viscosity	point	starting	horse shoe	wing tip			starting
180	In cambered airfoil the _____ is varies with lift coefficient	pressure	aerodynamic pressure	center of pressure	density			center of pressure
181	The value of $\alpha$ when lift equals _____ called zero lift angle of attack	one	zero	two	three			zero
182	The number of wings in monoplane is	1	2	3	4			1
183	The number of wings in biplane is	1	2	3	4			2
184	The number of wings in triplane is	1	2	3	4			3
185	Taper ratio is defined as the ratio of tip chord to	rear chord	mid chord	low chord	front chord			rear chord

186	The gross weight of an aeroplane divided by the square of the span is	aspect ratio	span length	span loading	taper ratio			span loading
187	The ratio between gross weight to gross area is called	aspect ratio	wing loading	span loading	taper ratio			wing loading
188	Drag caused by roughness in the surface is called	induced drag	skin friction drag	position drag	none of the given			skin friction drag
189	The component used to modify lift is called	flaps	rudders	spoilers	engine			flaps
190	If the rear position of the aerofoil moves downwards it is called	plain flap	split flap	zap flap	leading edge flap			split flap
191	Open one or more air passages between the upper and lower surface is called	zap flaps	split flaps	slotted flaps	plain flaps			slotted flaps
192	The flap which moves backwards and increase the effective area of the wing is called	zap flaps	split flaps	slotted flaps	extension flap			extension flap
193	Speed of the aircraft must be gained rapidly in order to	rest	take off	landing	none of the given			take off
194	The principle behind dynamic drag is	newton I law	newton II law	newton III law	newton IV law			newton III law
195	The rotatory motion of the aircraft member about longitudinal axis is called	rolling	pitching	yawing	stalling			rolling
196	The rotatory motion of the aircraft member about lateral axis is called	rolling	pitching	yawing	stalling			pitching
197	The rotatory motion of the aircraft member about normal axis is called	rolling	pitching	yawing	stalling			yawing
198	Transition phase from taxiing to climbing about centre of gravity of an aircraft is called	take off	landing	climbing	taxiing down			take off
199	Transition phase from flying to taxiing in an aircraft is called	take off	landing	climbing	taxiing down			landing
200	The lift and drag increases with angle of attack upto a certain limit called	airplane	pressure	point	end point			point
201	A high aspect ratio wing will give	high profile and low induced drag	low profile and high induced drag	low profile and low induced drag	high profile and high induced drag			high profile and low induced drag
202	Aerofoil efficiency is defined by	lift over drag	drag over lift	lift over weight	drag over weight			lift over drag
203	An aircraft banks into a turn. No change is made to the airspeed or angle of attack. What will happen?	The aircraft enters a sideslip and begins to lose altitude	The aircraft turns with no loss of height	The aircraft yaws and slows down	The aircraft begins to gain altitude			The aircraft enters a sideslip and begins to lose altitude
204	The relationship between induced drag and airspeed is, induced drag is	directly proportional to the square of the speed	inversely proportional to the square of the speed	directly proportional to speed	inversely proportional to speed			inversely proportional to the square of the speed
205	What is Boundary Layer?	Separate d layer of air forming a boundary at the leading edge	Turbulent air moving from the leading edge to trailing edge	low energy air that sticks to the wing surface and gradually gets faster until it joins the free stream flow of air	Separate d layer of air forming a boundary at the trailing edge			low energy air that sticks to the wing surface and gradually gets faster until it joins the free stream flow of air
206	The normal axis of an aircraft passes through	the centre of gravity	at the centre of the wings	at the centre of pressure	Chord line			the centre of gravity
207	On a high winged aircraft, what effect will the fuselage have on the up-going wing?	The up-going wing will have a decrease in angle of attack and therefore a decrease in lift	down-going wing will have a decrease in angle of attack and therefore a decrease in lift	The up-going wing will have an increase in angle of attack and therefore a	The up-going wing will have an decrease in angle of attack and therefore a			The up-going wing will have a decrease in angle of attack and therefore a decrease in lift
208	What is the collective term for the fin and rudder and other surfaces aft of the centre of gravity that helps directional stability?	Effective keel surface	Empennage	Fuselage surfaces	ruddervators			Effective keel surface

209	Temperature above 36,000 feet will	decrease exponentially	remain constant	increase exponentially	Increases at 1 degree for 1000 feet			remain constant
210	A decrease in incidence toward the wing tip may be provided to	prevent adverse yaw in a turn	prevent span-wise flow in manoeuvres	retain lateral control effectiveness at high angles of attack	prevent yaw in a turn			retain lateral control effectiveness at high angles of attack
UNIT V								
211	Boundary layer on a flat plate is called laminar boundary layer if	Reynolds Number is less than 2000	Reynolds number is less than 4000	Reynolds number is less than 5 x 10000	Reynolds number is less than 5000			Reynolds number is less than 5 x 10000
212	Boundary layer thickness is the distance from the surface of the solid body in the direction perpendicular to flow, where the velocity of fluid is equal to	free stream velocity	0.9 times the free stream velocity	0.99 times the free stream velocity	zero			0.99 times the free stream velocity
213	The boundary layer separation takes place if	pressure gradient is zero	Pressure gradient is positive	Pressure gradient is negative	camber is high			Pressure gradient is positive
214	Drag is defined as the force exerted by a flowing fluid on a solid body	in the direction of flow	Perpendicular to the direction of flow	in the direction which is at an angle of 45 degree to the direction of flow	in the direction which is at an angle of 60 degree to the direction of flow			in the direction of flow
215	Lift force is defined as the force exerted by a flowing fluid on a solid body	in the direction of flow	perpendicular to the direction of flow	at an angle of 45 degree to the direction of flow	in the direction which is at an angle of 180 degree to the direction of flow			perpendicular to the direction of flow
216	Euler's number is the ratio of	inertia force to pressure force	Inertia force to elastic force	inertia force to gravity force	inertia force to viscous force			inertia force to pressure force
217	Geometric similarity between model and prototype means	the similarity of discharge	the similarity of linear dimensions	the similarity of motion	the similarity of forces.			the similarity of motion
218	Reynold's number is defined as the	ratio of inertia force to gravity force	ratio of viscous force to gravity force	ratio of viscous force to viscous force	ratio of inertia force to elastic force.			ratio of viscous force to viscous force
219	Froude's number is defined as the ratio of	Inertia force to viscous force.	inertia force to gravity force	inertia force to elastic force .	inertia force to pressure force.			inertia force to gravity force
220	Models are known undistorted model if	the prototype and model are having different scale ratios	the prototype and model are having same scale ratio	model and prototype are kinematically similar	model and prototype are similar			the prototype and model are having same scale ratio
221	Model analysis of aero planes and projectile moving at supersonic speed based on	Reynolds number	Mach number	Froude number	Euler number			Mach number
222	The boundary-layer takes place	for ideal fluids	for real fluids	for pipe flow only	flat plates			for real fluids
223	Laminar sub-layer exists in.	Laminar boundary layer region	Turbulent boundary layer	Transition zone	trailing edge			Turbulent boundary layer

224	The laminar flow is characterised by	existence of eddies	irregular motion of fluid particles	fluid particles moving in layers parallel to the boundary surface	All the other three options are wrong			fluid particles moving in layers parallel to the boundary surface
225	Which of the following is an example of laminar flow?	underground flow	flow past tiny bodies	Flow of oil in measuring instruments	All the other three options are wrong			All the other three options are wrong
226	The pressure gradient in the direction of flow is equal to the shear gradient in the direction	parallel to the direction of flow	normal to the direction of flow	both a & b	All the other three options are wrong			normal to the direction of flow
227	_____ studied the laminar flow through a circular tube experimentally	Prandtl	Pascal	Hagen and Poiseuille	Anderson			Hagen and Poiseuille
228	A flow in which the viscosity of fluid is dominating over the inertia force is called	steady flow	unsteady flow	laminar flow	turbulent flow			laminar flow
229	Laminar flow takes place at	very low velocities	very high velocities	both (a) & (b)	All the other three options are wrong			very low velocities
230	The velocity at which the flow changes from laminar flow to turbulent flow is called	critical velocity	velocity of approach	sub-sonic velocity	supersonic velocity			critical velocity
231	The velocity at which the laminar flow stops is known as	velocity of approach	lower critical velocity	sub-sonic velocity	supersonic velocity			lower critical velocity
232	The velocity at which the laminar flow starts is known as	velocity of approach	higher critical velocity	lower critical velocity	supersonic velocity			higher critical velocity
233	The velocity corresponding to Reynolds number of 2800, is called	velocity of approach	supersonic velocity	lower critical velocity	higher critical velocity			higher critical velocity
234	A flow is called super-sonic if the	velocity of flow is very high	discharge is difficult to measure	Mach number is between 1 and 6	All the other three options are wrong			Mach number is between 1 and 6
235	Whenever a plate is held immersed at some angle with the direction of flow of the liquid, it is subjected to some pressure. The component of this pressure, in the direction of flow of the liquid, is known as	lift	drag	stagnation pressure	thrust			drag
236	Whenever a plate is held immersed at some angle with the direction of flow of the liquid, it is subjected to some pressure. The component of this pressure, at the right angles to the direction of flow of the liquid, is known as	lift	drag	stagnation pressure	thrust			lift
237	Streamlining will reduce	form drag	induced drag	skin friction drag	parasite drag increases			form drag
238	If an aircraft has a gross weight of 3000 kg and is then subjected to a total weight of 6000 kg the load factor will be	2G	3G	9G	15G			2G
239	A constant rate of climb is determined by	weight	wind speed	excess engine power	density			excess engine power
240	Ice formed on the leading edge will cause the aircraft to	stall at the same stall speed and AoA	stall at a lower speed	stall at the same stall speed	stall at a higher speed			stall at a higher speed
241	If both wings lose lift the aircraft	itches nose up	itches nose down	glides on a horizontal plane	glides on a vertical plane			itches nose up
242	Under what conditions will an aircraft create best lift?	Cold dry day at 200 ft	Hot damp day at 1200 ft	Cold wet day at 1200 ft	Cold wet day at 1800 ft			Cold dry day at 200 ft
243	If there were an increase of density, what effect would there be in aerodynamic damping?	None	Decreased	Increased	becomes zero			Increased
244	As Mach number increases, what is the effect on boundary layer?	Becomes more turbulent	Becomes less turbulent	Decreases in thickness	increases in thickness			Becomes more turbulent

245	When a slat is retracted it moves	towards the upper leading edge of the wing	towards the lower leading edge of the wing	towards the centre of the leading edge of the wing	towards the trailing edge			towards the upper leading edge of the wing
246	In a turn the up-going wing causes a	de-stabilising effect due to increased AoA	de-stabilising effect due to decreased AoA	stabilising effect due to decreased AoA	stabilising effect due to increased AoA			stabilising effect due to decreased AoA
247	The stagnation point consists of	dynamic and static air pressure	static air pressure	dynamic air pressure	absolute pressure			dynamic and static air pressure
248	Yawing is a rotation around	the normal axis obtained by the elevator	the lateral axis obtained by the rudder	the normal axis obtained by the aileron	the normal axis obtained by the rudder			the normal axis obtained by the rudder
249	Sweepback of the wings will	not affect lateral stability	increase lateral stability at high speeds only	increase lateral stability at all speeds	increase directional stability			increase lateral stability at all speeds
250	With the flaps lowered, the stalling speed will	increase	become zero	remain the same	decrease			decrease
251	When flying close to the stall speed a pilot applies left rudder the aircraft will	pitch nose up	roll to the left	stall the left wing	pitch nose down			stall the left wing
252	When flaps are down it will	increase AoA and increase slow speed stability	decrease AoA and decrease slow speed stability	the AoA remains the same on both wings	increase AoA and decreases low speed stability			decrease AoA and decrease slow speed stability
253	If you have an aircraft that is more laterally stable then directionally stable it will tend to:	skid	slip	bank	yaw			skid
254	A wing section suitable for high speed would be	thick with high camber	thin with high camber	thin with little or no camber	thick with low camber			thin with little or no camber
255	As the speed of an aircraft increases the profile drag	increases	decreases	decreases at first then increase	remains constant			increases
256	The stagnation point on an aerofoil is the point where	the suction pressure reaches a maximum	the boundary layer changes from laminar to turbulent	the airflow is brought completely to rest	the suction pressure reaches zero			the airflow is brought completely to rest
257	The stalling of an aerofoil is affected by the	airspeed	angle of attack	transition speed	density of air			angle of attack
258	What gives the aircraft directional stability?	aileron	Horizontal stabiliser	Elevators	Vertical stabiliser			Vertical stabiliser
259	The most fuel efficient of the following types of engine is the	rocket	turbo-jet engine	turbo-fan engine	turboprop			turbo-fan engine
260	The quietest of the following types of engine is the	rocket	turbo-jet engine	turbo-fan engine	turboprop			turbo-fan engine
261	Forward motion of a glider is provided by	control surfaces	the weight	the drag	the engine			the weight